IMPROVEMENTS IN LIQUID CHROMATOGRAPHY COUPLED TO MASS SPECTROMETRY METHODS FOR THE DETERMINATION OF LEGISLATED AND EMERGING MARINE TOXINS IN THE NORTHWEST MEDITERRANEAN COAST

María García Altares Pérez

Dipòsit Legal: T 330-2016

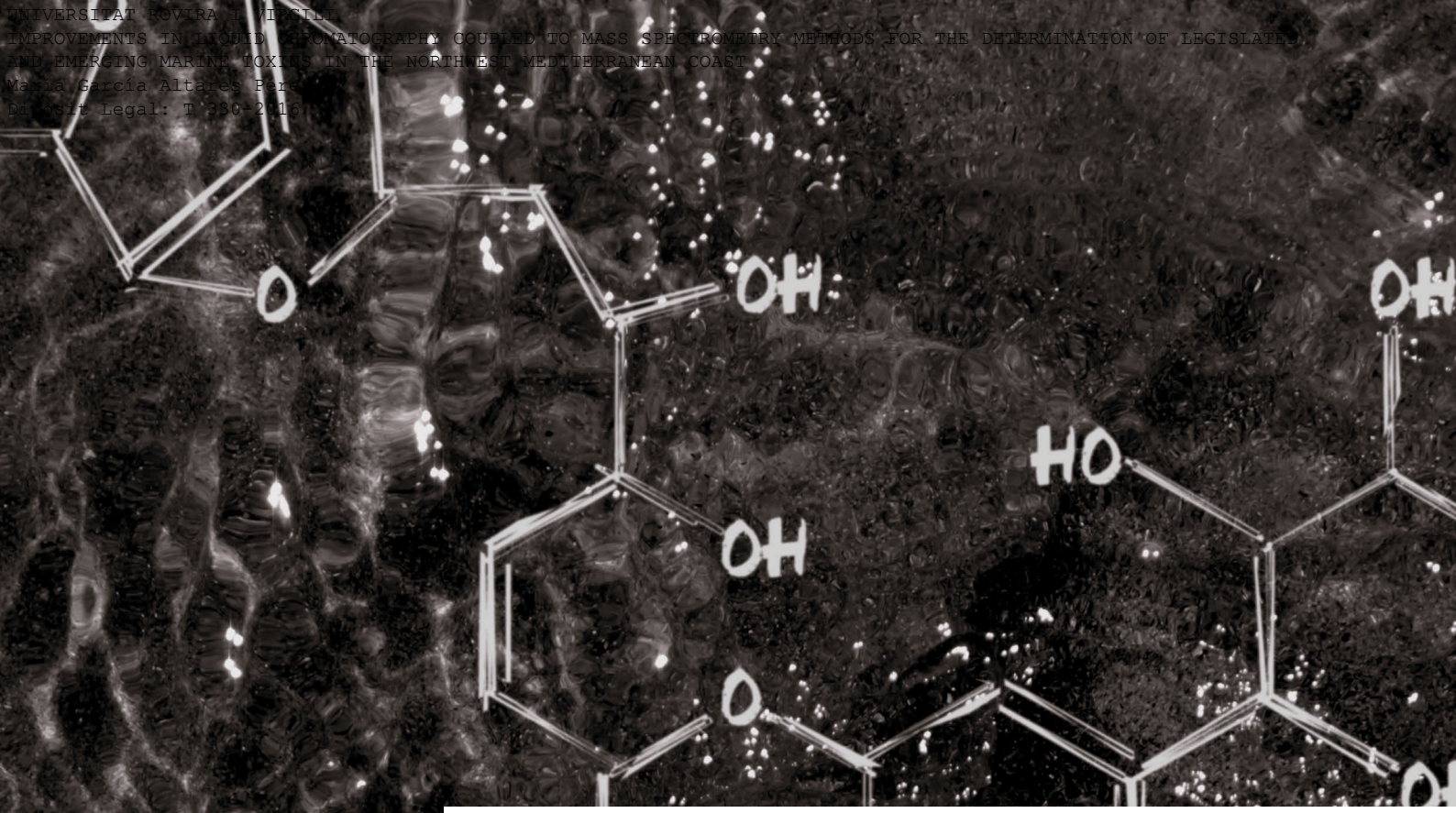

DOCTORAL THESIS

Improvements in Liquid Chromatography Coupled to Mass Spectrometry Methods for the Determination of Legislated and Emerging Marine Toxins in the Northwest Mediterranean Coast

María García Altares Pérez

Supervised by Dr. Jorge Diogène and Dr. Pablo de la Iglesia

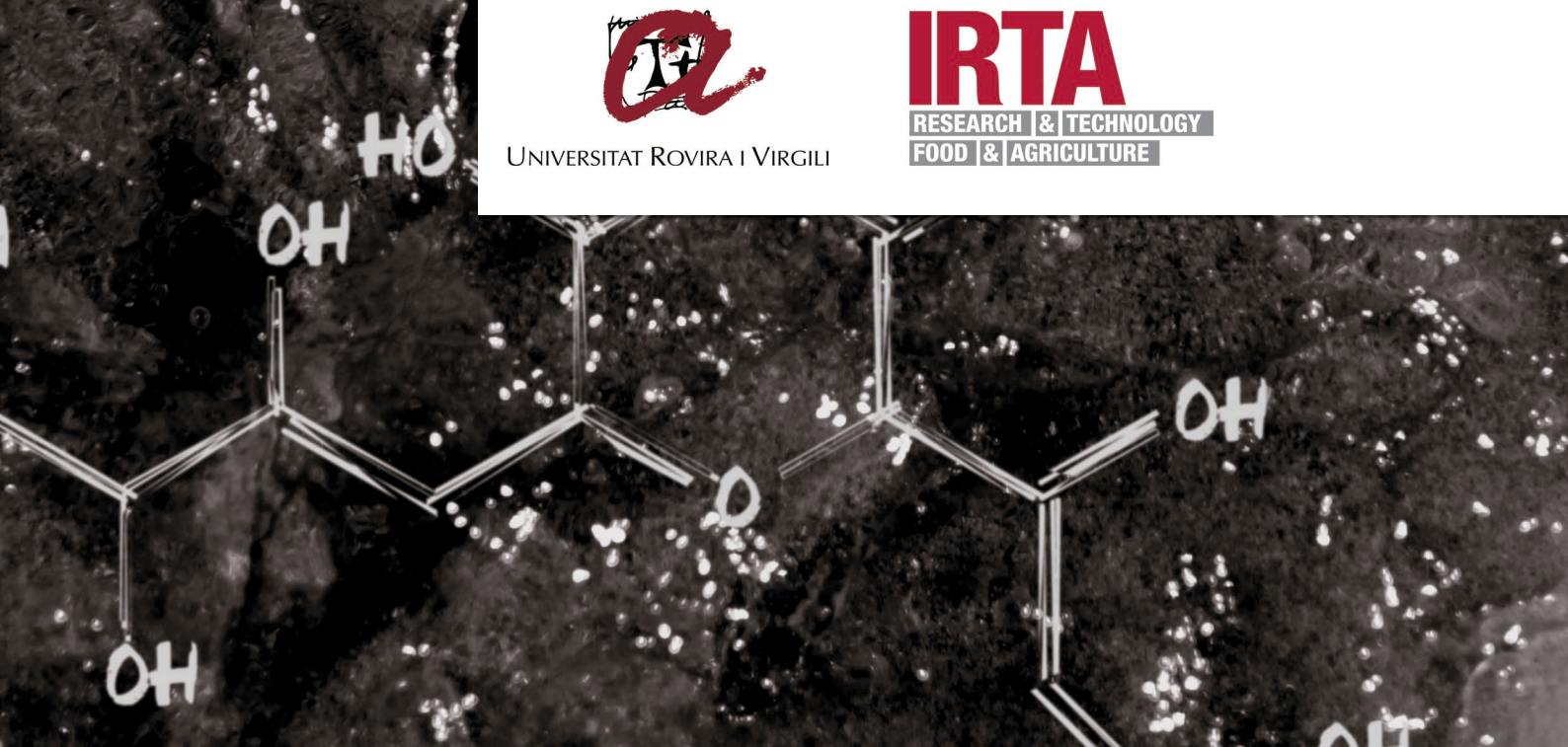

UNIVERSITAT ROVIRA I VIRGILI

IRTA
RESEARCH & TECHNOLOGY
FOOD & AGRICULTURE

UNIVERSITAT ROVIRA I VIRGILI
IMPROVEMENTS IN LIQUID CHROMATOGRAPHY COUPLED TO MASS SPECTROMETRY METHODS FOR THE DETERMINATION OF LEGISLATED AND EMERGING MARINE TOXINS IN THE NORTHWEST MEDITERRANEAN COAST
María García Altares Pérez
Dipòsit Legal: T 330-2016

Photography, cover design and layout by Vicenç Torrent. Reus (2015)

Improvements in Liquid Chromatography coupled to Mass Spectrometry methods for the determination of legislated and emerging marine toxins in the Northwest Mediterranean coast

DOCTORAL THESIS

María García-Altares Pérez

Supervised by Dr. Pablo de la Iglesia and Dr. Jorge Diogène

Sant Carles de la Ràpita – Tarragona
2015

UNIVERSITAT ROVIRA I VIRGILI
IMPROVEMENTS IN LIQUID CHROMATOGRAPHY COUPLED TO MASS SPECTROMETRY METHODS FOR THE DETERMINATION OF LEGISLATED AND EMERGING MARINE TOXINS IN THE NORTHWEST MEDITERRANEAN COAST
María García Altares Pérez
Dipòsit Legal: T 330-2016

FAIG CONSTAR que aquest treball, titulat "Improvements in Liquid Chromatography coupled to Mass Spectrometry methods for the determination of legislated and emerging marine toxins in the Northwest Mediterranean coast", que presenta María García-Altares Pérez per a l'obtenció del títol de Doctor, ha estat realitzat sota la meva direcció al Departament Seguiment del Medi Mari d'IRTA Institut de Recerca i Tecnologia Agroalimentàries i que acompleix els requeriments per poder optar a Menció Internacional.

HAGO CONSTAR que el presente trabajo, titulado "Improvements in Liquid Chromatography coupled to Mass Spectrometry methods for the determination of legislated and emerging marine toxins in the Northwest Mediterranean coast", que presenta María García-Altares Pérez para la obtención del título de Doctor, ha sido realizado bajo mi dirección en el Departamento Seguimiento del Medio Marino de IRTA Instituto de Investigación y Tecnología Agroalimentarias y que cumple los requisitos para poder optar a la Mención Internacional.

I STATE that the present study, entitled "Improvements in Liquid Chromatography coupled to Mass Spectrometry methods for the determination of legislated and emerging marine toxins in the Northwest Mediterranean coast", presented by María García-Altares Pérez for the award of the degree of Doctor, has been carried out under my supervision at the Department Marine Monitoring of this university IRTA Research and Technology in Food and Agriculture, and that it fulfils all the requirements to be eligible for the International Doctorate Award.

Sant Carles de la Ràpita, 27 de Febrer de 2015 / Sant Carles de la Ràpita, 27 de Febrero de 2015 / Sant Carles de la Ràpita, 27th February, 2015

Els directors de la tesi doctoral
Los directores de la tesis doctoral
Doctoral Thesis Supervisors

Dr. Pablo de la Iglesia

Dr. Jorge Diogène

Acknowledgements

This thesis has been funded by the Spanish National Institute for Agriculture and Food Research and Technology (INIA; pre-doctoral FPI-INIA nº 27, 2010) and carried out at the Catalan Institute of Agri-food Research and Technology (IRTA) under the supervision of Dr. Pablo de la Iglesia and Dr. Jorge Diogène. I am very thankful to my supervisors and to the rest of the team of the Marine Monitoring department for their great support. Part of this thesis was performed at two European institutions: the Chemistry department of Cork Institute of Technology (Ireland) and the Natural Products Department of the University Federico II di Napoli (Italy). I am grateful to Dr. Ambrose Furey, Professor Patrizia Ciminiello, and their teams for their warm welcome and invaluable help.

Special thanks to Vicenç Torrent for designing the cover and the layout of the thesis, and for his great support during the writing process.

I owe this work to my family and friends: thank you for your affection and patience.

María García-Altares

Reus, 18th February, 2015

Summary

Catalonia (NW Mediterranean Sea) is the most important region for the aquaculture of shellfish and fish in the Mediterranean coast of Spain. The production areas are mainly located in the Ebro Delta bays (Alfacs and Fangar Bays), where their high concentration of phytoplankton that sustains the shellfish aquaculture sector occasionally leads to one of the most concerning problems of the industry regarding food safety: toxic Harmful Algae Blooms (HABs). In fact, the Ebro Delta bays were proposed as pilot sites for the study of HABs in Stratified Systems within the Global Ecology and Oceanography of Harmful Algal Blooms (GEOHAB) program, and represent a valuable model to study HABs in Mediterranean coastal embayments.

This thesis aimed to improve the application of liquid chromatography coupled to mass spectrometry (LC-MS) methods for the study of lipophilic and emerging toxins related to HABs. More specifically, this work addressed three current challenges of the study of toxic HABs by LC-MS: the implementation of suitable monitoring strategies to protect public health and the shellfish aquaculture sector, the study of the unpredictable nature of toxic HABs, and the role of analytical techniques in the identification and confirmation of marine toxins, especially emerging and new toxic compounds produced by marine microalgae.

Chapter 1 and 2 present a **General Introduction** and the **Objectives** of this work.

The first scientific contribution (published; ***Validation of LC-MS/MS chromatographic conditions for lipophilic toxins*****, Chapter 3**) shows an extensive assessment of the applicability and suitability of four chromatographic conditions for the determination of six groups of marine lipophilic toxins (okadaic acid and dinophysistoxins, pectenotoxins, azaspiracids, yessotoxins, gymnodimines and spirolides) by tandem LC-MS (LC-MS/MS) to select the most appropriate conditions according to the requirements of the European Union Reference Laboratory for Marine Biotoxins. In this study, a single-laboratory validation was performed for the analysis of three relevant matrices for the seafood aquaculture industry (mussels, pacific oysters and clams), and for sea urchins, a poorly studied matrix but relevant in the gastronomy of our study area. Moreover, we compared the performance of the method under alkaline conditions using two quantification strategies: the external standard calibration and the matrix-matched standard calibration. Alkaline conditions with external standard calibration and recovery correction for okadaic acid were selected as the most adequate conditions in the context of our laboratory. This comparative study could help other laboratories to choose the best conditions for the implementation of LC-MS/MS according to their own necessities.

The second scientific contribution (submitted; **Dinophysis *bloom and DSP shellfish toxicity in Alfacs Bay*, Chapter 4**) reports a comprehensive study of a diarrhetic shellfish poisoning (DSP) outbreak in a Mediterranean coastal embayment, Alfacs Bay, integrating phytoplankton data and LC-MS/MS analysis of shellfish samples (mussels and oysters), phytoplankton concentrates in filters and solid phase adsorbing toxin tracking (SPATT) devices. The ban for bivalve harvesting lasted 78 days, from late winter to the end of the spring of 2012, due to a harmful algae bloom of the toxic dinoflagellate *Dinophysis sacculus* that fluctuated in three abundance peaks, reaching maximum abundance of 2220 cell/L. Mussels sampled during the bloom

contained okadaic acid (OA) up to 3.7 times the maximum permitted level set by the European Commission, and pectenotoxin-2 (PTX2) at lower concentrations. Oysters also contained OA and PTX2, but always below the maximum permitted level. Cell toxicity measured from phytoplankton concentrates in filters was most likely overestimated and it did not contain OA-diol esters, but it increased towards the end of the bloom. The applied monitoring strategy, based on the measurement of *Dinophysis* cell abundance in the water column, was effective to protect public health and did not extended the regulatory closure unnecessarily, but may need revision in light of our results. Concentration of DSP in SPATT devices followed *Dinophysis* abundance dynamics, but its potential as early warning systems of the DSP accumulation in shellfish is still under consideration.

The third scientific contribution (published; ***Confirmation of pinnatoxins and spirolides by HRMS*, Chapter 5**) presents the first detection of pinnatoxin G (PnTX-G) in Spain and 13-desmethyl spirolide C (SPX-1) in shellfish from Catalonia. Cyclic imines are lipophilic marine toxins that bioaccumulate in seafood and show acute neurotoxicity in mice. Despite cyclic imines have not been linked yet to human poisonings and are not regulated in Europe, the European Food Safety Authority requires more data to perform a conclusive risk assessment for consumers. Pinnatoxin G and SPX-1 were found at low concentrations in mussels and oysters, and PnTX-G has been also detected in seawater samples using SPATT devices. These cyclic imines were confirmed with both Low and High Resolution MS by comparison of the response with that from reference standards. For other analogs without reference standards, we applied a strategy combining Low Resolution MS with a triple quadrupole mass analyzer for a fast and reliable screening, and high resolution MS for unambiguous confirmation, carefully discarding false positives.

The fourth scientific contribution (published; ***Ovatoxin-g and isomeric palytoxin by LC-HRMS*, Chapter 6**) investigates the toxin profiles in cultures of six new strains of *Ostreopsis* cf. *ovata* isolated from the south of Catalonia. Toxin profile of these strains contained ovatoxin-a, -b, -c, -d and –e, at concentrations per cell remarkably higher than toxin quotas reported for other Mediterranean strains. In addition, our strains produced two minor compounds, ovatoxin-g and an isomer of palytoxin (formerly known as putative palytoxin), whose structures had not been elucidated before. We studied their structures in crude algal extracts through LC-High Resolution MS^n, and as a result, tentative structure was assigned to both compounds: ovatoxin-g (46-dehydroxy ovatoxin-a) and isomeric palytoxin (formerly "putative palytoxin"), which resembles palytoxin but it is hydroxylated at C-42 and in the segment from the A-side terminal to C-8, and dehydroxilated at C-17 and most likely at C-64.

Finally, **General Discussion** can be found in **Chapter 7** and the **General Conclusions** of the thesis are summarized in **Chapter 8**.

Table of contents

1 General Introduction

1.1 The control of marine microalgal toxins in the aquaculture areas of Catalonia

The Mediterranean Sea has shaped the history, culture and way of living in Spain. The Spanish Mediterranean coast hosts about a third of the population of the country, and sustains most part of the successful touristic sector that accounts for 10% of the Gross National Income [1]. However, the exploitation of the Mediterranean ecosystems has not always been sustainable, which leaded to serious degradation in the services provided by the sea [2]. For instance, the total capture production of fish in marine areas of Spain decreased 22% in 30 years (1982-2012) due to the over-exploitation of the wild stock [3]. In fact, Spain cannot cover the internal demand for fish and seafood products, which is almost 40 kg per person per year, one of the highest in the European Union [4, 5]. In consequence, aquaculture has been considered a solution to reduce the pressure on over-exploited wild stocks of fish, potentially guaranteeing food safety and sustainability [6].

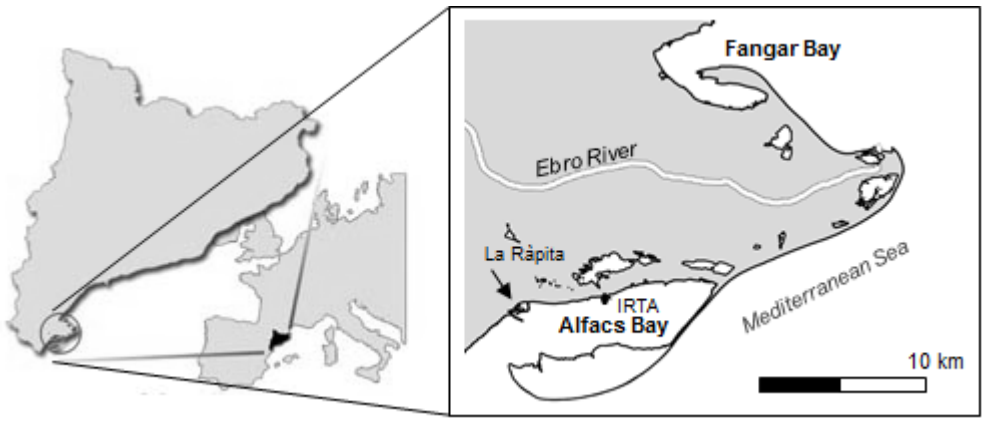

Figure 1-1. Map of the Ebro River Delta bays (NW Mediterranean)

Catalonia is the most important region for the aquaculture of shellfish and fish in the Mediterranean coast of Spain [7]. The production areas are mainly located in the Ebro Delta bays, in the south of the region: Alfacs and Fangar Bays (50 and 12 km^2 respectively, Figure 1-1), which produce about 3,000 tons of bivalves per year [8] thanks to their hydrodynamics and ecological characteristics: they are quite shallow, have relatively long water renewal periods, and regular inputs of fresh water [7]. More importantly, the primary production in the bays is ten times higher than in the surrounding open sea [9], partly due to the high concentration in dissolved inorganic nutrients from the irrigation discharges [10].

The high concentration of phytoplankton that sustains the shellfish aquaculture sector occasionally leads to one of the most concerning problems for this industry [11]: toxic Harmful Algae Blooms (HABs). Proliferations of microalgae causing HABs are a natural, world-wide

problem, whose increasing prevalence in coastal ecosystem gained great scientific attention about twenty years ago [12]. Negative impacts caused by HABs include water discoloration, oxygen depletion from the water column, damage in fish gills, and the production of toxins that are harmless to aquatic organisms but can reach the human food chain [12], which are referred as "toxic HABs" in the present work. Toxic HABs threaten food safety, since the ingestion of contaminated shellfish and fish can cause serious gastrointestinal and neurological illnesses that can be even lethal. Moreover, some phytoplankton blooms produce toxins that may affect humans accidentally exposed by swimming of breathing marine aerosols [13]. The efforts to research this phenomena have resulted in a dramatic increase in the number of microalgae species considered as "toxic" (or toxin producers) in the last two decades: about 40 species were claimed as potentially toxic to humans in 1993 [12], while current databases describe 110 eukaryotic species of toxic marine phytoplankton, mostly dinoflagellates (79 species) and diatoms (15 species) [14].

Toxins from microalgae are secondary metabolites that can bioaccumulate in edible tissues of filter feeding organisms, such as mussels and oysters, the traditional species for shellfish aquaculture in the Mediterranean region [6]. Shellfish toxicity related to toxic HABs has been normally classified (as reviewed in James et al. [15]) in five main syndromes caused by the ingestion of contaminated bivalve molluscs (
Table 1-1): paralytic shellfish poisoning (PSP), amnesic shellfish poisoning (ASP), neurotoxic shellfish poisoning (NSP), azaspiracid shellfish poisoning (AZP) and diarrhetic shellfish poisoning (DSP). With the exception of brevetoxins (causing NSP), the concentration of these marine toxins in shellfish is regulated in the European Union [16]. European regulations have protected public health and permitted the management of shellfish production areas for years, and regulatory levels for okadaic acid (OA), azaspiracids (AZAs), saxitoxins (STXs), domoic acid (DA), and their derivatives, have been generally effective to prevent toxic outbreaks. However, for some toxins the regulations may require revision, since some compounds have been proven not to be related with their original syndrome, such as pectenotoxins (PTXs), no longer considered diarrhetic, or yessotoxins (YTXs), which are even questioned to be toxic for humans [17]. On the other hand, the classification based on toxic syndromes leaves out the heterogeneous group of "emerging toxins" (Table 1-2), that includes recently discovered toxins (such as pinnatoxins, PnTXs), known toxins that have recently appeared in new locations (such as ciguatoxins, CTXs, in Europe), and non-regulated toxins that became a threat to public health (such as palytoxins, PLTXs) [17]. Tetrodotoxins (TTXs), although produced by bacteria instead of microalgae, are usually included in this emerging toxins group, since they cause a potent fish poisoning syndrome that is gaining great concern. In the Mediterranean region, tetrodotoxin poisoning has been confirmed after consumption of *Lagocephalus sceleratus* (elongated puffer fish) [18], which is originally from the Indo-Pacific region but has migrated from the Red Sea to the Mediterranean Sea through the Suez Canal, a phenomenon denominated "Lessepsian migration". Since its first confirmed record in the Mediterranean in Turkey and Greece in 2005 [19, 20], *Lagocephalus sceleratus* has been detected in Israel, Cyprus, Lebanon [18, 21, 22] and recently in Catalonia [23].

A more suitable classification of marine microalgal toxins relies on their chemical characteristics [24]. Marine microalgal toxins belong to three chemical classes: amino acid derivatives (domoic acid, DA), alkaloids (STXs and TTXs) and polyketides (the rest). Microalgal toxins are usually

referred as small compounds (300 to 1500 Da), excluding PLTXs and maitotoxins (MTXs), which are larger than 2000 Da. Most microalgal toxins are lipophilic compounds, except the smallest toxins (STXs and DA), whose acid and basic groups rule their hydrophobicity. Palytoxins and MTXs have long carbon chains and several polar functions, thus they can be considered as amphiphilic. Yessotoxins also show amphiphilic characteristics, but in Europe they are legally considered as lipophilic toxins [25].

European reference control methods for marine toxins in shellfish trend to favor analytical techniques. Methods based on high performance liquid chromatography (HPLC, usually with ultra violet (UV) detection) are the reference control method for ASP toxins, and antibodies based methods (Enzyme-Linked Immunosorbent Assay, ELISA) can be applied as screening tools [26]. For PSP toxins, HPLC with fluorescence detection (FLD, known as the "Lawrence method") is officially accepted, although the reference control method is still the mouse bioassay (MBA) [27, 28]. For lipophilic toxins (AZAs, OA and DTXs, PTXs, and YTXs), the current reference control method is based on liquid chromatography coupled to mass spectrometry (LC-MS) [25]. The adoption of LC-MS as the reference control method for lipophilic toxins was introduced recently in the European Union, on July 1st 2011, to replace MBA as the former reference method[27]. Both methods coexisted until December 31st 2014, when LC-MS became the only reference method for lipophilic toxin control in shellfish in the European Union [25], after being validated in several collaborative (inter-laboratory) exercises [29, 30].

In Catalonia, the toxic phytoplankton species and their related toxins in shellfish are monitored on a routine basis since 1989. the Institute IRTA-Research and Technology-Food and Agriculture, is in charge of this monitoring program since 1999. The strategy of the monitoring program has been proven to be an efficient tool to protect public health in the study area, which is based on the quantification of toxic species of phytoplankton in the water column as an early warning parameter of shellfish toxicity. When a certain abundance threshold is surpassed (adapted for each toxic species or toxic group of species), shellfish samples are analyzed according to their reference control method. The approval of LC-MS in 2011 as a coexisting official method for lipophilic toxins in shellfish was adopted at IRTA as an opportunity to investigate the dynamics of blooms of toxic species and its related toxicity in shellfish. The monitoring of microalgal toxins by LC-MS improves the management of the blooms and the information that the program can provide to the aquaculture industry. Moreover, it enables the study of non-regulated emerging toxins and the discovery of new analogs that may threat the development of the aquaculture industry in the Catalan coast.

Table 1-1. Classification of marine toxins regulated in the European Union and traditionally linked to shellfish poisoning syndromes. Formula and molecular weight of the principal compound of each group (underlined). "European Regulation" includes current regulations applicable in the European Union (in February 2015), maximum permitted levels (in units/kg shellfish meat) and reference monitoring methods. Reviews (Revs) selected as suggested references were published in the last ten years (2005-2015).

Toxic syndrome	Toxins	European Regulation	Chemical class	Formula and molecular weight	Polarity	Vector	Producer	Revs.
Paralytic shellfish poisoning (PSP)	Saxitoxin (STX). neosaxitoxins, gonyautoxin and analogs	800 STX Eq µg/kg [16]. Mouse Bioassay [27]. HPLC-FLD (Lawrence) [28].	Tetrahydropurine alkaloid	$C_{10}H_{17}N_7O_4$ (299)	Hydrophilic	Bivalve shellfish and crustaceans	*Alexandrium* spp., *Gymnodinium catenatum* and *Pyrodinium bahamense*	[31, 32]
Amnesic shellfish poisoning (ASP)	Domoic acid (DA) and analogs	20 DA Eq mg/ kg [16]. HPLC- methods Antibody-methods (ELISA) [26].	Cyclic amino acid	$C_{15}H_{21}NO_6$ (311)	Hydrophilic	Bivalve shellfish and finfish	*Pseudonitzschia* spp.	[33, 34]
Neurotoxic shellfish poisoning (NSP)	Brevetoxin-B and analogs	Not regulated in the EU. Regulated in USA, Australia and New Zealand [35]	Ladder-shaped polyether	$C_{50}H_{70}O_{14}$ (894)	Lipophilic	Bivalve shellfish and marine aerosol inhalation	*Karenia brevis*	[36]
Azaspiracid shellfish poisoning (AZP)	Azaspiracid-1 (AZA) and analogs	160AZA Eq µg/kg [16]. LC-MS methods [25].	Polyether, second amine	$C_{47}H_{71}NO_{12}$ (841)	Lipophilic	Bivalve shellfish	*Azadinium spinosum* and *Protoperidinium crassipes*	[37, 38]
Diarrhetic shellfish poisoning (DSP)	Okadaic acid (OA) and dinophysistoxins (DTXs)	160 OA Eq µg/kg [16]. LC-MS methods[25]	Polyether, spiro-keto assembly	$C_{44}H_{68}O_{13}$ (804)	Lipophilic	Bivalve shellfish	*Dinophysis* spp. and *Prorocentrum* spp.	[30, 39-41]
Currently not associated with human illnesses	Pectenotoxin-2 (PTX) and analogs	Included in the 160 OA Eq µg/kg [16]. LC-MS methods [25].	Polyether, ester macrocycle	$C_{47}H_{70}O_{14}$ (858)	Lipophilic	Bivalve shellfish	*Dinophysis* spp.	[39, 42]
	Yessotoxin (YTX) and analogs	3.75 YTX Eq mg/kg [43]. LC-MS methods [25].	Ladder-shaped polyether	$C_{55}H_{82}O_{21}S_2$ (1140)	Lipophilic	Bivalve shellfish	*Protoceratium reticulatum, Lingulodinium polyedrum, Gonyaulax spinifera*	[39, 44]

Table 1-2. Classification of marine emerging toxins, not regulated in the European Union. Formula and molecular weight of the principal compound of each group (underlined). Reviews (Revs) selected as suggested references were published in the last ten years (2005-2015). Emerging toxins include recently discovered toxins, known toxins that have recently appeared in new locations, and non-regulated toxins that became a threat to public health.

Toxic syndrome	Toxins	Chemical class	Formula and molecular weight	Polarity	Vector	Producer	Revs.
Not associated with human illnesses	13-desmethyl spirolide C (SPX-1), gymnodimines pinnatoxins, and analogs	Cyclic imine, macrocycle	$C_{41}H_{61}NO_7$ (691)	Lipophilic	Bivalve shellfish	*Karenia selliformis, Alexandrium ostenfeldii, A. perivianum,* and *Vulcanodinium rugosum*	[45, 46]
Palytoxin associated syndrome	Palytoxin (PLTX), ostreocins, ovatoxins and mascarenotoxins	Polyol, 2 amide and 1 primary amine	$C_{129}H_{223}N_3O_{54}$ (2678)	Amphiphilic	Bivalve shellfish and marine aerosol inhalation	*Ostreopsis* spp.	[47-49]
Ciguatera fish poisoning	Gambierol	Ladder-shaped polyether	$C_{43}H_{64}O_{11}$ (757)	Lipophilic	Several species of fish ("ciguateric fish")	*Gambierdiscus* spp.	[50, 51]
	Pacific ciguatoxin-4B (CTX) and analogs	Ladder-shaped polyether	$C_{60}H_{85}O_{16}$ (1061)	Lipophilic			
	Maitotoxin (MTX)	Polyol, 4 fused ring system	$C_{164}H_{256}O_{68}S_2Na_2$ (3422)	Amphiphilic			
Tetrodotoxin poisoning	Tetrodotoxin (TTX) and analogs	Guanidinium alkaloid	$C_{11}H_{17}N_3O_8$ (319)	Hydrophilic	Fish, blue-ringed octopus , xanthid crabs, gastropods and amphibians	Bacterial origin: *Vibrio* spp. *Pseudomonas* spp., *Bacillus* spp., *Alteromonas* spp. and others	[52, 53]

1.2 Challenges in the research and monitoring of marine microalgal toxins

This work contributes to expand the theoretical and applied knowledge in the research and monitoring of marine microalgal toxins and shellfish toxicity. This field is experiencing nowadays some contextual changes that require fast adaptations. On one hand, the recent changes in European legislation have a great impact on institutions responsible of shellfish safety control that must adapt their protocols to the new reference method for lipophilic toxins [25]. On the other hand, public health problems related to emerging marine toxins are an increasing concern, due to the lack of exposition data and appropriate methods to monitor them and assess their risk. Therefore, this work focused on the application of LC-MS methods for the study of lipophilic and emerging marine toxins, aiming to shed light on three interesting challenges that this research field has to face:

1.2.1 The implementation of the most suitable monitoring strategy

Shellfish toxicity from microalgal toxins has an enormous economic impact on the aquaculture sector. In Korea, one of the biggest aquaculture producers in the world, marine toxins produce mortalities up to 10% of the total production of fish and shellfish [54]. In Ireland, microalgal toxins are the first factor influencing the productivity of the sector, and the main concern for producers due to the conflicts among stakeholders (producers, processors and regulators) during toxic outbreaks [55]. The economic impact of marine microalgal toxins has not been quantified yet in the Mediterranean coast of Spain, but banning periods for bivalve harvesting are increasingly frequent in Catalonia, while in Andalusia (south of Spain) microalgal toxins already constitute the main constrain for aquaculture [7]. Shellfish safety testing is thus a critical cost for a sector that is considered as "low-cost food industry" (the price per ton at production level is usually below €1,000, except for oysters and scallops [24]), an requires a proper planning of the control systems. The internationalization of shellfish trade has brought new challenges to the monitoring of marine toxins: nowadays, shellfish is imported all year long in several formats (raw, canned, cooked, frozen, and pickled), and the seasonal risks and microalgae species affecting the products can be very different between the importing and the exporting countries, thus control systems must be prepared for the unexpected. Therefore, the ultimate control system must ensure reliability and high throughput (to be economically sustainable), and must be comprehensive to cover all possible scenarios.

For some toxins, such as lipophilic toxins, methods based on LC-MS are the most suitable alternatives to replace animal bioassays and meet the requirements of the shellfish industry, as recommended by expert organizations [56, 57]. These techniques do not pose ethical conflicts and show unequivocal specificity, since they are able to detect, identify and quantify the individual compounds that contribute to toxicity in shellfish samples, avoiding false positives and wrong diagnosis [24]. In addition, they are comprehensive methods able to potentially detect all toxin compounds in a sample, also emerging or unexpected toxins. Moreover, their sensitivity is compatible even with the lower permitted levels in shellfish proposed by EFSA [56] that may be set in the future. Furthermore, these methods can be automated, easily scaled-up if necessary, require small sample quantities and are compatible with simple extraction methods, thus ensuring fast response and high throughput of samples. Nevertheless, the implementation of LC-MS methods requires an important economic investment in instrumentation,

maintenance and qualified personnel. It also needs a stage of method development to adapt the method conditions to every specific instrument, and eventually, a comprehensive in house laboratory validation aimed at providing precise and accurate results (especially regarding matrix effects). The main limitation of these methods is the restricted availability of certified reference standards for marine toxins, in some cases due to economic reasons [58]. Consequently, toxin equivalencies factors for all marine toxin analogs have not been calculated, which complicate the extrapolation from toxin concentrations to actual toxicity in a sample [59].

In the last ten years (2005-2015), advances in LC-MS technologies and validation studies have promoted the research for better LC-MS methods for the determination of marine toxins. Although saxitoxins and domoic acid (and derived compounds) are usually monitored by HPLC with UV and FLD detectors, several scientific contributions have explored the possibilities of analyzing these toxins by LC-MS. For instance, in the case of DA and analogs, the application of LC-MS methods (usually combined with Solid Phase Extraction (SPE) clean-up), permitted the detection of trace concentrations of DA in mussels from the Adriatic Sea (Italy) for the first time [60], and facilitated the study of DA and its analogs dissolved in sea water [61, 62]. Saxitoxins are a complex group of polar compounds without chromophore groups, thus Hydrophilic Interaction Liquid Chromatography (HILIC) coupled to MS methods (also usually combined to SPE clean-up) have been proposed as an alternative to HPLC with FLD detection, which requires derivatization [63-65]. The detection of emerging toxins in shellfish and fish, such as tetrodotoxins in elongated puffer fish [66] and palytoxins in mussels [67], can also be effectively accomplished by LC-MS with low limits of detection and great selectivity. Nevertheless, the influence of recent changes in European legislation [25] focused most attention on lipophilic toxins, and many scientific studies have aimed at investigating the analytical parameters influencing the detection of lipophilic toxins in shellfish by LC-MS. Chromatographic separation of lipophilic toxins is possible under several conditions (i.e. buffers and pH of the mobile phases), being the most used ones the acidic conditions proposed by Quilliam *et al.* in 2001 [68] and further developed by McNabb *et al.* in 2005 [69]; and the alkaline conditions proposed by Gerssen *et al.* in 2009 [70]. Both methodologies have been validated in inter-laboratory collaborative exercises [29, 71]. The influence of chromatographic conditions on method performance for the analysis of lipophilic toxins in shellfish is addressed in this thesis (Chapter 3). Prospect development of LC-MS methods for the detection of marine toxins in shellfish will explore the capabilities of instruments with information dependent acquisition features, such as linear ion traps, which enables the confirmation of toxins by matching the full product ion spectra of a sample with constructed spectral libraries [72]. High resolution mass spectrometry (HRMS) is also a great tool for the study of marine toxins: it enables the screening of an unlimited list of precursor ions in full scan mode, provides great selectivity thanks to its high resolving power and precision in mass accuracy measurements, gives valuable information to support unequivocal confirmation of compounds such as isotopic patterns, and permits retrospectives analysis and data mining for potentially unknown compounds by metabolomics software [73, 74]. In 2014, two studies validated multitoxin methods based on LC-HRMS to determine lipophilic toxins in shellfish, reporting good performance and low limits of detection [75, 76], thus these methods may become more popular, even for monitoring purposes, when HRMS spectrometers become more affordable.

1.2.2 The unpredictability of toxic Harmful Algae Blooms

As explained by Hess [24], the detection of marine algae toxins in shellfish products before they reach the market is essential due to the difficulty to predict its related phenomena. Multiple factors affect microalgae blooms and toxin production, including physical parameters (temperature, light, wind, hydrogeography, etc.), chemical parameters (nutrient types and concentrations, eutrophication, oxygen concentration, pH, anthropogenic pollution, etc.) and biological parameters (algae community and structure, presence of grazing organisms, parasitic bacteria, etc.) [13, 77].

Moreover, the correspondence between one microalgae species and one type of toxin is unusual. In fact, the ability to produce the same toxic compound can be spread across taxa without close phylogenetic relationship. For instance, saxitoxins are produced by cyanobacteria and some species of dinoflagellates [32]. On the other hand, the types of marine toxins produced by one microalgae species can be different among strains. For example, the toxins profiles of the dinoflagellate *Alexandrium ostenfeldii* may include STXs, spirolides (SPXs), or both types of compounds (which are chemically very different,
Table 1-1), depending of their geographical origin [78].

Toxin production and release by dinoflagellates are also complex processes, and usually they depend on the physiological state of the cells [79-81]. Once the toxins are present, the chance that a toxic algal bloom ends up in shellfish toxicity is also difficult to predict, since several factors related to the bivalves also play a role in this phenomenon. For example, each shellfish species may behave differently regarding the accumulation of marine toxins [82, 83], because filtration rates, ability to select which microalga species to feed on, metabolism of toxic compounds and detoxification rates are species-specific. Other factors that can have an impact in toxin accumulation are conditions of shellfish cultures, feeding state, parasites, or the presence of xenobiotics in the environment [84].

Despite of this intrinsic unpredictability, the development of models of HABs and shellfish toxicity may be one of the most promising mitigation tools, since models can give valuable insights on these processes and have the potential to provide short-term forecast [85]. Models that couple physical–biological parameters and hydrodynamics can unravel patterns of phytoplankton distribution, such as the 3D model proposed by Artigas et al. [86] for Alfacs Bay in 2014. This study demonstrated the preferential areas of phytoplankton retention in the bay (NE, inner bay), which will have an impact in the design of sampling points for monitoring and the understanding of the variability of toxicity in shellfish within the bay. Other models have addressed the accumulation of marine toxins in shellfish, in order to predict the time course of the accumulation and detoxification processes, and study other processes such as toxin biotransformations [84], although the complexity of the algae-bivalve system has been in some cases underestimated. The integration of models of phytoplankton dynamics and toxin accumulation kinetics would be of great advantage to allocate monitoring efforts, but it has to be noted that its predicting capacity is limited by the ability to forecast weather conditions (one week in the best case) [87]. Therefore, models can be a valuable complement to confirmatory techniques like LC-MS, reducing the amount of samples that have to be confirmed or quantified, and contextualizing analytical results.

1.2.3 The relevance of analytical techniques in the identification and confirmation of marine toxins

De la Iglesia et al. [88] raised an important concern in the study of harmful algae: the classification of a species as "toxic" or "toxin producer" has to be strongly evidenced by phycologists and analytical chemists, since these labels may can have a significant effect on decision-making processes in monitoring programs. Relevant information about the microalgae strain, its culture, and its harvesting must be provided to contextualize analytical results. Moreover, methods of toxin separation and detection have to be properly described, paying special attention to limits of detection and confirmatory criteria [88]. Analytical methods based on LC-MS, if properly validated, provide enough confidence about the identity of compounds of interest: regarding European guidelines for analytical method performance [89], MS would be the best choice to ensure accurate confirmation, especially when High Resolution MS is applied. Nevertheless, even with the application of LC-MS techniques, the scientific literature of microalgal toxins is fraught with controversies and misidentifications that demonstrate the complexity of developing suitable analytical methods for this type of compounds. Some examples of the potential negative consequences of misidentifications of microalgal toxins are:

- The negative impact on medical treatments when the cause of an acute intoxication is wrongly attributed to a microalgal toxin. For instance, Furey et al. [90] studied how the misidentification of anatoxin-a, a potent cyanobacterial neurotoxin, has obstructed forensic investigations due to its fast decay and the interferences caused by the isobaric and coeluting (in reverse phase LC) amino acid phenylalanine. For anatoxin-a, LC coupled to single MS does not provide reliable confirmation in complex biological samples, thus several strategies, based on derivatization, tandem mass spectrometry, or HRMS, can be applied to unambiguously confirm its presence [90].
- The bias in risk assessments with wrong exposure data. For example, Fassen [91] reviewed the literature on BMAA (β-N-methylamino-L-alanine), a cyanobacterial toxin that is suspected to play a role in chronic neurological diseases (such as amyotrophic lateral sclerosis (ALS), Alzheimer's disease, and Parkinson's disease). This toxin seems to be almost omnipresent in aquatic ecosystems (as reviewed by Fassen [91]), being even pronounced as a cause for the high incidence of ALS among Gulf War veterans [92]. However, scientific literature shows huge variations in BMAA concentrations among cyanobacterial species, and among other aquatic organisms. It has been demonstrated that low-selective analytical methods, such HPLC-FLD with derivatization will result in overestimated BMAA concentrations [93], but incomplete or inaccurate reported methods and results are also common in studies of BMAA with LC-MS techniques, which hinder real estimations of human exposure to BMAA.
- The establishment of unreliable facts by cross-citation. Confirmation of microalgal toxins must be done with either two or more orthogonal separation-detection techniques, or with highly selective methods such as HRMS [88]. Still, high precision in mass accuracy measurements by itself does not exempt HRMS from errors in identification and confirmation. For example, Rossi et al. [94] reported in an Italian strain of *Ostreopsis* cf. *ovata* the presence of mascarenotoxin-a (a palytoxin-like compound produced by the tropical dinoflagellate *O. mascareniensis*). The confirmation was based on the elemental composition computed by the software of a LC/TOF/MS on

the precursor ion ($[M+H]^+$), assuming 57 ppm of mass error. This strategy has been proven to be completely invalid to identify compounds by HRMS: even 1 ppm of mass accuracy is not enough to derive a single solution. Additional orthogonal filters such as isotopic patterns and fragmentation experiments are critical to provide reliable identification by HRMS [95].

Therefore, scientific contributions reporting emerging toxins in new locations, new toxin producer microalgae species, or new toxic compounds, must be extremely cautious and must provide all information regarding strain culture conditions and separation-detection methods [88], but even when HRMS methods are applied, a proper strategy should be designed and communicated to avoid potential false positives or negatives. This strategy may take advantage of the different data provided by HRMS spectrometers: isotopic patterns, MS and MS^2 scans, accurate mass measurements, signal thresholds, data dependent experiments, etc.

This thesis aims to contribute to providing the best analytical solutions based on LC-MS to the study of toxic HABs. Methods based on LC-MS are an excellent tool to monitor and investigate marine toxins, providing reliable and comprehensive information to manage aquaculture industries and ensure food safety. Complementary methods, such as early warning systems and prediction models can optimize the speed of the response and relevance of the results for shellfish producers and policy makers. On the other hand, rigorous and accurate methods enhance the knowledge on bioactive compounds from marine microalgae and complement phycologist studies on this fascinating group of marine organisms.

References

1. INE. *Spanish National Statistics Institute. National Accounts*. 2012; Available from: http://www.ine.es/en/welcome.shtml; 3th January 2015.
2. Royo, L., I. Férriz, and C.M. Duarte, *Ecosistemas Marinos*, in *Ambienta.* . 2012, Spanish Ministry of Agriculture, Food and Environment.
3. Food and Agriculture Organization of the United Nations. *Fishery Statistical Collections. Global Capture Production*. 2012; Available from: http://www.fao.org/fishery/statistics/global-capture-production/; 15th January 2015.
4. Failler, P., *Fish consumption in the European Union in 2015 and 2030. Part 1. European Overview* in *FAO Fisheries Circular No. 972/4, Part 1*. 2007, Food and Agriculture Organization of the United Nations: Rome.
5. Welch, A., et al., *Variability of fish consumption within the 10 European countries participating in the European Investigation into Cancer and Nutrition (EPIC) study*. Public health nutrition, 2002. **5**(6b): p. 1273-1285.
6. Fezzardi, D., et al., *Indicators for sustainable aquaculture in Mediterranean and Black Sea countries: guide for the use of indicators to monitor sustainable development of aquaculture.* Studies and Reviews-General Fisheries Commission for the Mediterranean (FAO), 2013.
7. Ramón, M., et al., *Current status and perspectives of mollusc (bivalves and gastropods) culture in the Spanish Mediterranean.* Bolentín-Instituto Español de Oceanografía, 2005. **21**(1/4): p. 361.
8. IDESCAT. *Catalan Annual Statistics. Fishery and Maritime Issues.* 2013; Available from: http://www.idescat.cat/pub/?id=aec&n=469&lang=es; access data:2015 2nd January.
9. Delgado, M., *Fitoplancton de las bahitas del delta del Ebro.* Scientia Marina, 1987. **51**(4): p. 517-548.
10. Delgado, M. and J. Camp, *Abundancia y distribución de nutrientes inorgánicos disueltos en las bahías del delta del Ebro.* Inv. Pesq, 1987. **51**(3): p. 427-441.
11. Fernández-Tejedor, M., et al., *The Ebro Delta coastal embayments, GEOHAB pilot site for the study of HAB population dynamics.* 12th International Conference on Harmful Algae, Copenhagen, Denmark, 4-8 September 2006., 2008.
12. Hallegraeff, G.M., *A review of harmful algal blooms and their apparent global increase*.* Phycologia, 1993. **32**(2): p. 79-99.
13. Van Dolah, F.M., *Marine algal toxins: Origins, health effects, and their increased occurrence.* Environmental Health Perspectives, 2000. **108**(SUPPL. 1): p. 133-141.
14. IOC-UNESCO. *Taxonomic Reference List of Harmful Micro Algae*. 2009; Available from: http://www.marinespecies.org/hab/; 20th January 2015.
15. James, K.J., et al., *Shellfish toxicity: Human health implications of marine algal toxins.* Epidemiology and Infection, 2010. **138**(7): p. 927-940.
16. European Commission, *Regulation (EC) No 853/2004.* Official Journal of the European Union, 2004. **L 226**(22).
17. Botana, L.M., et al., *The mechanistic complexities of phycotoxins: Toxicology of Azaspiracids and Yessotoxins*, in *Advances in Molecular Toxicology*. 2014. p. 1-33.
18. Bentur, Y., et al., *Lessepsian migration and tetrodotoxin poisoning due to Lagocephalus sceleratus in the eastern Mediterranean.* Toxicon, 2008. **52**(8): p. 964-968.
19. Akyol, O., et al., *First confirmed record of Lagocephalus sceleratus (Gmelin, 1789) in the Mediterranean Sea.* Journal of Fish Biology, 2005. **66**(4): p. 1183-1186.
20. Kasapidis, P., et al., *First record of the Lessepsian migrant Lagocephalus sceleratus (Gmelin 1789) (Osteichthyes: Tetraodontidae) in the Cretan Sea (Aegean, Greece).* Aquatic Invasions, 2007. **2**(1): p. 71-73.

21. Chamandi, S.C., et al., *Human Poisoning after ingestion of puffer fish caught from Mediterranean sea.* Middle East Journal of Anesthesiology, 2009. **20**(2): p. 285-288.
22. Petrou, A., et al. *Fishing yields of lagocephalus sceleratus in Cyprus*. in *Proceedings of the 10th International Conference on the Mediterranean Coastal Environment, MEDCOAST 2011*. 2011.
23. IRTA. *Se confirma la presencia de pez globo en el litoral catalán* 2014; Available from: http://www.irta.cat/es-es/RIT/Noticies/paginas/PezGlobo.aspx; 2nd January 2015.
24. Hess, P., *Requirements for screening and confirmatory methods for the detection and quantification of marine biotoxins in end-product and official control.* Analytical and Bioanalytical Chemistry, 2010. **397**(5): p. 1683-1694.
25. European Commission, *Regulation (EC) No 15/2011.* Official Journal of the European Union, 2011. **L 6**(3).
26. European Commission, *Regulation (EC) No 1244/2007.* Official Journal of the European Union, 2007. **L 281**(22).
27. European Commission, *Regulation (EC) No 2074/2005.* Official Journal of the European Union, 2005. **L 338**(27).
28. European Commission, *Regulation (EC) No 1664/2006.* Official Journal of the European Union, 2006. **L 320**(13).
29. EURLMB, *Interlaboratory Validation Study of the EU-Harmonised SOP LIPO LC MS/MS*. 2011.
30. Suzuki, T. and M.A. Quilliam, *LC-MS/MS analysis of diarrhetic shellfish poisoning (DSP) toxins, okadaic acid and dinophysistoxin analogues, and other lipophilic toxins.* Analytical Sciences, 2011. **27**(6): p. 571-584.
31. Humpage, A.R., V.F. Magalhaes, and S.M. Froscio, *Comparison of analytical tools and biological assays for detection of paralytic shellfish poisoning toxins.* Analytical and Bioanalytical Chemistry, 2010. **397**(5): p. 1655-1671.
32. Wiese, M., et al., *Neurotoxic alkaloids: Saxitoxin and its analogs.* Marine Drugs, 2010. **8**(7): p. 2185-2211.
33. He, Y., et al., *Analytical approaches for an important shellfish poisoning agent: Domoic acid.* Journal of Agricultural and Food Chemistry, 2010. **58**(22): p. 11525-11533.
34. Lefebvre, K.A. and A. Robertson, *Domoic acid and human exposure risks: A review.* Toxicon, 2010. **56**(2): p. 218-230.
35. Alexander, J., et al., *Emerging toxins: Brevetoxin group. Scientific Opinion of the Panel on Contaminants in the Food Chain.* The EFSA Journal, 2010. **1677**(8(7)): p. 1-29.
36. Plakas, S.M. and R.W. Dickey, *Advances in monitoring and toxicity assessment of brevetoxins in molluscan shellfish.* Toxicon, 2010. **56**(2): p. 137-149.
37. Furey, A., et al., *Azaspiracid poisoning (AZP) toxins in shellfish: Toxicological and health considerations.* Toxicon, 2010. **56**(2): p. 173-190.
38. Twiner, M.J., et al., *Azaspiracid shellfish poisoning: A review on the chemistry, ecology, and toxicology with an emphasis on human health impacts.* Marine Drugs, 2008. **6**(2): p. 39-72.
39. Dominguez, H.J., et al., *Dinoflagellate polyether within the yessotoxin, pectenotoxin and okadaic acid toxin groups: Characterization, analysis and human health implications.* Toxicon, 2010. **56**(2): p. 191-217.
40. Reguera, B., et al., *Dinophysis toxins: Causative organisms, distribution and fate in shellfish.* Marine Drugs, 2014. **12**(1): p. 394-461.
41. Vale, C. and L.M. Botana, *Marine toxins and the cytoskeleton: Okadaic acid and dinophysistoxins.* FEBS Journal, 2008. **275**(24): p. 6060-6066.
42. Liu, R. and Y. Liang, *Advances in pectenotoxins studies: A review.* Shengtai Xuebao/ Acta Ecologica Sinica, 2010. **30**(19): p. 5355-5370.
43. European Commission, *Regulation (EC) No 786/2013.* Official Journal of the European Union, 2013. **L 220**(14).

44. Paz, B., et al., *Yessotoxins, a group of marine polyether toxins: An overview.* Marine Drugs, 2008. **6**(2): p. 73-102.
45. Guéret, S.M. and M.A. Brimble, *Spiroimine shellfish poisoning (SSP) and the spirolide family of shellfish toxins: Isolation, structure, biological activity and synthesis.* Natural Product Reports, 2010. **27**(9): p. 1350-1366.
46. Otero, A., et al., *Cyclic imines: chemistry and mechanism of action: a review.* Chemical Research in Toxicology, 2011. **24**: p. 1817-1829.
47. Ciminiello, P., et al., *A 4-decade-long (and still ongoing) hunt for palytoxins chemical architecture.* Toxicon, 2011. **57**(3): p. 362-367.
48. Ciminiello, P., et al., *LC-MS of palytoxin and its analogues: State of the art and future perspectives.* Toxicon, 2011. **57**(3): p. 376-389.
49. Riobó, P. and J.M. Franco, *Palytoxins: Biological and chemical determination.* Toxicon, 2011. **57**(3): p. 368-375.
50. Caillaud, A., et al., *Update on methodologies available for ciguatoxin determination: Perspectives to confront the onset of ciguatera fish poisoning in Europe.* Marine Drugs, 2010. **8**(6): p. 1838-1907.
51. Dickey, R.W. and S.M. Plakas, *Ciguatera: A public health perspective.* Toxicon, 2010. **56**(2): p. 123-136.
52. Bane, V., et al., *Tetrodotoxin: Chemistry, toxicity, source, distribution and detection.* Toxins, 2014. **6**(2): p. 693-755.
53. Noguchi, T. and O. Arakawa, *Tetrodotoxin - Distribution and accumulation in aquatic organisms, and cases of human intoxication.* Marine Drugs, 2008. **6**(2): p. 220-242.
54. Park, T.G., et al., *Economic impact, management and mitigation of red tides in Korea.* Harmful Algae, 2013. **30**: p. S131-S143.
55. Bord Iascaigh Mhara and Enterprise Ireland, *Review of the Irish rope mussel industry, a report jointly commissioned by Board Iascaigh Mhara (BIM) and Entreprise Ireland.* . 2006, Pricewaterhouse Coopers.
56. Alexander, J., et al., *Marine biotoxins in shellfish–Summary on regulated marine biotoxins Scientific Opinion of the Panel on Contaminants in the Food Chain.* The EFSA Journal, 2009. **1306**: p. 1-23.
57. Toyofuku, H., *Joint FAO/WHO/IOC activities to provide scientific advice on marine biotoxins (research report).* Marine pollution bulletin, 2006. **52**(12): p. 1735-1745.
58. Stewart, I. and C. McLeod, *The Laboratory Mouse in Routine Food Safety Testing for Marine Algal Biotoxins and Harmful Algal Bloom Toxin Research: Past, Present and Future.* Journal of AOAC International, 2014. **97**(2): p. 356-372.
59. Botana, L.M., *A perspective on the toxicology of marine toxins.* Chemical research in toxicology, 2012. **25**(9): p. 1800-1804.
60. Ciminiello, P., et al., *Hydrophilic interaction liquid chromatography/mass spectrometry for determination of domoic acid in Adriatic shellfish.* Rapid Communications in Mass Spectrometry, 2005. **19**(14): p. 2030-2038.
61. de la Iglesia, P., G. Giménez, and J. Diogène, *Determination of dissolved domoic acid in seawater with reversed-phase extraction disks and rapid resolution liquid chromatography tandem mass spectrometry with head-column trapping.* Journal of Chromatography A, 2008. **1215**(1-2): p. 116-124.
62. Wang, Z., et al., *Determination of domoic acid in seawater and phytoplankton by liquid chromatography-tandem mass spectrometry.* Journal of Chromatography A, 2007. **1163**(1-2): p. 169-176.
63. Dell'Aversano, C., P. Hess, and M.A. Quilliam, *Hydrophilic interaction liquid chromatography-mass spectrometry for the analysis of paralytic shellfish poisoning (PSP) toxins.* Journal of Chromatography A, 2005. **1081**(2): p. 190-201.

64. Turrell, E., et al., *Optimization of hydrophilic interaction liquid chromatography/mass spectrometry and development of solid-phase extraction for the determination of paralytic shellfish poisoning toxins.* Journal of AOAC International, 2008. **91**(6): p. 1372-1386.
65. Zhuo, L., et al., *Determination of paralytic shellfish poisoning toxins by HILIC-MS/MS coupled with dispersive solid phase extraction.* Food Chemistry, 2013. **137**(1-4): p. 115-121.
66. Rodríguez, P., et al., *Liquid chromatography-mass spectrometry method to detect Tetrodotoxin and Its analogues in the puffer fish Lagocephalus sceleratus (Gmelin, 1789) from European waters.* Food Chemistry, 2012. **132**(2): p. 1103-1111.
67. Ciminiello, P., et al., *Liquid chromatography–high-resolution mass spectrometry for palytoxins in mussels.* Analytical and Bioanalytical Chemistry, 2014.
68. Quilliam, M.A., P. Hess, and C. Dell'Aversano, *No Title*, in *Mycotoxins and Phycotoxins in Perspective at the Turn of the Century*, W.J. DeKoe, et al., Editors. 2001: Wageningen, The Netherlands. p. 383-391.
69. McNabb, P., A. Selwood, and P.T. Holland, *Multiresidue method for determination of algal toxins in shellfish: Single-laboratory validation and interlaboratory study.* Journal of AOAC International, 2005. **88**: p. 761-772.
70. Gerssen, A., et al., *Liquid chromatography-tandem mass spectrometry method for the detection of marine lipophilic toxins under alkaline conditions.* Journal of chromatography A, 2009. **1216**: p. 1421-1430.
71. van den Top, H.J., et al., *Quantitative determination of marine lipophilic toxins in mussels, oysters and cockles using liquid chromatography-mass spectrometry: inter-laboratory validation study.* Food additives & contaminants. Part A, Chemistry, analysis, control, exposure & risk assessment, 2011. **28**(12): p. 1745-57.
72. McCarron, P., E. Wright, and M.A. Quilliam, *Liquid chromatography/mass spectrometry of domoic acid and lipophilic shellfish toxins with selected reaction monitoring and optional confirmation by library searching of product ion spectra.* Journal of AOAC International, 2014. **97**(2): p. 316-324.
73. Kaufmann, A. and S. Walker, *Post-run target screening strategy for ultra high performance liquid chromatography coupled to Orbitrap based veterinary drug residue analysis in animal urine.* Journal of Chromatography A, 2013. **1292**: p. 104-110.
74. Kaufmann, A. and S. Walker, *Evaluation of the interrelationship between mass resolving power and mass error tolerances for targeted bioanalysis using liquid chromatography coupled to high-resolution mass spectrometry.* Rapid Communications in Mass Spectrometry, 2013. **27**(2): p. 347-356.
75. Domènech, A., et al., *Determination of lipophilic marine toxins in mussels. Quantification and confirmation criteria using high resolution mass spectrometry.* Journal of Chromatography A, 2014. **1328**: p. 16-25.
76. Orellana, G., et al., *Validation of a confirmatory method for lipophilic marine toxins in shellfish using UHPLC-HR-Orbitrap MS.* Analytical and Bioanalytical Chemistry, 2014. **406**(22): p. 5303-5312.
77. Anderson, D.M., P.M. Glibert, and J.M. Burkholder, *Harmful algal blooms and eutrophication: Nutrient sources, composition, and consequences.* Estuaries, 2002. **25**(4): p. 704-726.
78. Suikkanen, S., et al., *Paralytic shellfish toxins or spirolides? The role of environmental and genetic factors in toxin production of the Alexandrium ostenfeldii complex.* Harmful Algae, 2013. **26**: p. 52-59.
79. Anderson, D.M., et al., *Dynamics and physiology of saxitoxin production by the dinoflagellates Alexandrium* spp. Marine Biology, 1990. **104**(3): p. 511-524.
80. Hackett, J.D., et al., *DSP toxin production de novo in cultures of Dinophysis acuminata (Dinophyceae) from North America.* Harmful Algae, 2009. **8**(6): p. 873-879.

81. Pizarro, G., et al., *Growth, behaviour and cell toxin quota of Dinophysis acuta during a daily cycle.* Marine Ecology Progress Series, 2008. **353**: p. 89-105.
82. Lindegarth, S., et al., *Differential retention of okadaic acid (OA) group toxins and pectenotoxins (PTX) in the blue mussel, Mytilus Edulis (L.), and European flat oyster, Ostrea Edulis (L.).* Journal of Shellfish Research, 2009. **28**(2): p. 313-323.
83. Skejić, S., et al., *Differences in phytoplankton accumulation between Mediterranean mussel Mytilus galloprovincialis Lamarck, 1819 and European flat oyster Ostrea edulis Linneaus, 1758 after natural exposure to toxic Dinophysis bloom.* Cahiers de biologie marine, 2012. **53**(2): p. 189-195.
84. Blanco, J., *Modelling as a mitigation strategy for harmful algal blooms*, in *Shellfish Safety and Quality*. 2009. p. 200-227.
85. Anderson, D.M., *Approaches to monitoring, control and management of harmful algal blooms (HABs).* Ocean and Coastal Management, 2009. **52**(7): p. 342-347.
86. Artigas, M.L., et al., *Understanding the spatio-temporal variability of phytoplankton biomass distribution in a microtidal Mediterranean estuary.* Deep Sea Research Part II: Topical Studies in Oceanography, 2014. **101**: p. 180-192.
87. Reguera, B., et al., *Harmful Dinophysis species: A review.* Harmful Algae, 2012. **14**: p. 87-106.
88. de la Iglesia, P., et al., *An analytical perspective on detection, screening, and confirmation in phycology, with particular reference to toxins and toxin-producing species.* Journal of Phycology, 2013. **49**(6): p. 1056-1060.
89. European Commission, *Commision Decission 2002/657/EC.* Official Journal of the European Union, 2002. **L 221**(8).
90. Furey, A., et al., *Strategies to avoid the mis-identification of anatoxin-a using mass spectrometry in the forensic investigation of acute neurotoxic poisoning.* Journal of Chromatography A, 2005. **1082**(1 SPEC. ISS.): p. 91-97.
91. Faassen, E.J., *Presence of the neurotoxin BMAA in aquatic ecosystems: What do we really know?* Toxins, 2014. **6**(3): p. 1109-1138.
92. Cox, P.A., et al., *Cyanobacteria and BMAA exposure from desert dust: A possible link to sporadic ALS among Gulf War veterans.* Amyotrophic Lateral Sclerosis, 2009. **10**(SUPPL. 2): p. 109-117.
93. Faassen, E.J., F. Gillissen, and M. Lürling, *A comparative study on three analytical methods for the determination of the neurotoxin BMAA in cyanobacteria.* PLoS ONE, 2012. **7**(5).
94. Rossi, R., et al., *New palytoxin-like molecules in Mediterranean Ostreopsis cf. ovata (dinoflagellates) and in Palythoa tuberculosa detected by liquid chromatography-electrospray ionization time-of-flight mass spectrometry.* Toxicon, 2010. **56**(8): p. 1381-1387.
95. Kind, T. and O. Fiehn, *Metabolomic database annotations via query of elemental compositions: Mass accuracy is insufficient even at less than 1 ppm.* BMC Bioinformatics, 2006. **7**.

2 Objectives of the thesis

According to the exposed background and current challenges in the research and monitoring of marine microalgal toxins, this thesis has the following objectives:

General objective: To expand the knowledge in the application of LC-MS methodologies for the monitoring and research of lipophilic and emerging marine toxins in Mediterranean estuarine system, taking the Ebro Delta (Catalonia, Spain) as the model site.

Specific objectives:

- To assess the selection of the most appropriate set conditions (among the suggested by the European Union Reference Laboratory for Marine Biotoxins) to implement LC-MS/MS methods for the control of lipophilic toxins in shellfish.
- To study the dynamics of diarrhetic shellfish poisoning toxins associated with natural populations of *Dinophysis* spp. in Mediterranean coastal embayments, and evaluate the strategies to monitor them and mitigate their negative impacts.
- To unequivocally confirm the presence of known emerging toxins (such as cyclic imines) in several compartments of marine ecosystems.
- To characterize the toxin profile of novel strains isolated in our study area of dinoflagellates that pose a risk to human health, such as *Ostreopsis* spp, and identify potential new emerging toxins.

CHAPTER 3

The Implementation of Liquid Chromatography Tandem Mass Spectrometry for the Official Control of Lipophilic Toxins in Seafood: Single-laboratory Validation Under Four Chromatographic Conditions

Running Title: **Validation of LC-MS/MS chromatographic conditions for lipophilic toxins**

Published as:

García-Altares, M., J. Diogène, and P. de la Iglesia, *The implementation of liquid chromatography tandem mass spectrometry for the official control of lipophilic toxins in seafood: Single-laboratory validation under four chromatographic conditions*. Journal of Chromatography A, 2013. 1275: p. 48-60.

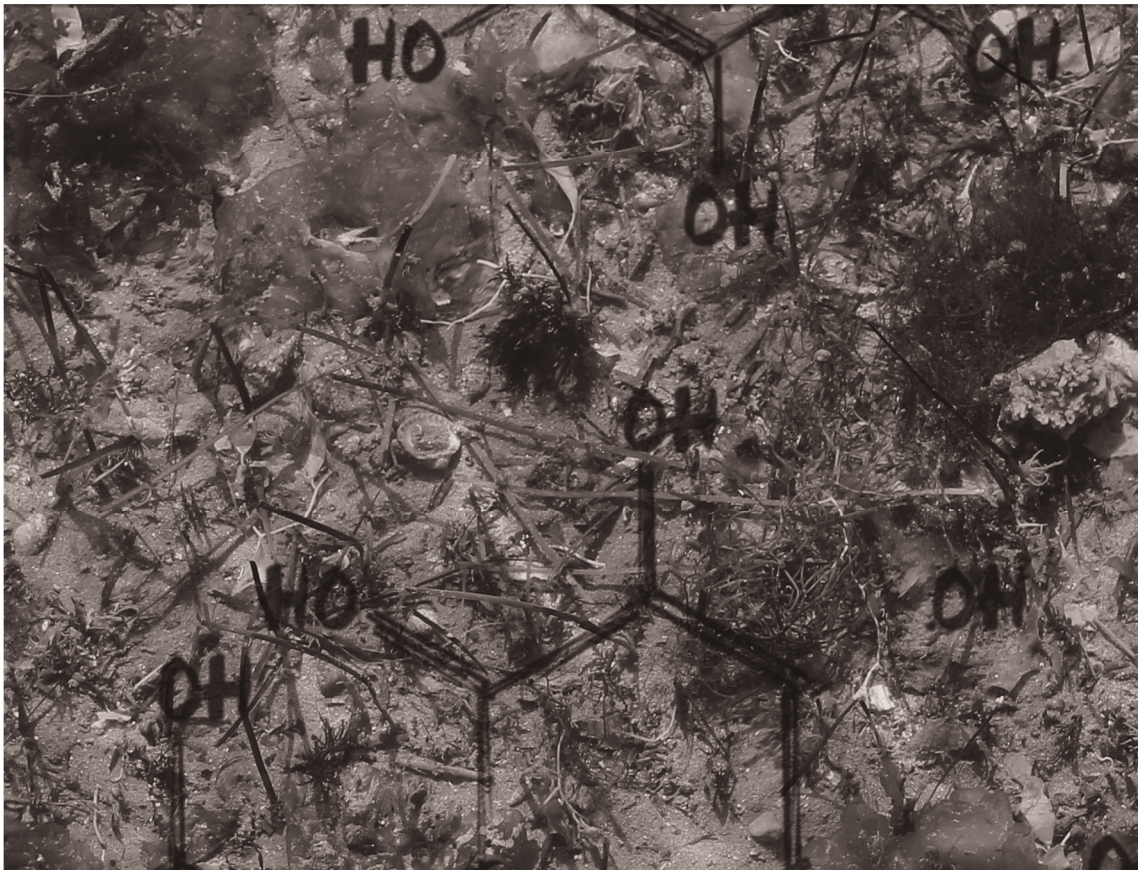

Abstract

We performed a comprehensive study to assess the applicability and suitability of four chromatographic conditions for the determination of six groups of marine lipophilic toxins (okadaic acid and dinophysistoxins, pectenotoxins, azaspiracids, yessotoxins, gymnodimine and spirolides) by LC-MS/MS to select the most appropriate conditions as stated by the European Union Reference Laboratory for Marine Biotoxins (EURLMB). For every case, the elution gradient has been optimized to achieve a total run-time cycle of 12 min. A single-laboratory validation has been performed for the analysis of three relevant matrices for the seafood aquaculture industry (mussels, pacific oysters and clams), and for sea urchins for which no data about lipophilic toxins have been reported before. Moreover, we have compared the performance of the method under alkaline conditions using two quantification strategies: the external standard calibration (EXS) and the matrix-matched standard calibration (MMS). Alkaline conditions were the only scenario that allowed detection windows with polarity switching in a 3200 QTrap mass spectrometer, thus the analysis of all toxins can be accomplished in a single run, increasing sample throughput. The limits of quantification under alkaline conditions met the validation requirements established by the EURLMB for all toxins and matrices, while the rest of conditions failed in some cases. The accuracy of the method and the matrix effects where generally dependent on the mobile phases and the seafood species. The MMS had a moderate positive impact on method accuracy for crude extracts, but it showed poor trueness for other seafood species than mussels when analyzing hydrolyzed extracts. Alkaline conditions with EXS and recovery correction for OA were selected as the most adequate conditions in the context of our laboratory. This comparative study can help other laboratories to choose the best conditions for the implementation of LC-MS/MS according to their own necessities.

Keywords

Lipophilic marine toxins; Liquid Chromatography-Mass Spectrometry; seafood; method validation; matrix effects

3.1 Introduction

Lipophilic marine toxins accumulate in seafood, causing remarkable economic losses in the aquaculture sector [1] and posing a risk to human health. To protect consumers, the European Union demands the monitoring of some lipophilic marine toxins [2] and limits their maximum permitted levels (MPLs) in edible shellfish tissues [3]: 160 μg/kg in okadaic acid (OA) equivalents for OA, dinophysistoxins (DTXs) and pectenotoxins (PTXs) together; 1 mg/kg for yessotoxins (YTXs) and 160 μg/kg for azaspiracids (AZAs). Other lipophilic marine toxins are not yet regulated in the European Union, like cyclic imines mainly comprising spirolides (SPXs) and gymnodimines (GYMs).

The reference method to control lipophilic toxins in the European Union was the bioassay with mice or rats until January of 2011 [2]. The European Food Safety Authority (EFSA) indicated in 2009 the disadvantages of these bioassays [4]: ethical concerns, limited specificity, high variability in results and insufficient detection capability for some toxins. According to the European Commission and the EFSA, the analytical methods based on liquid chromatography tandem mass spectrometry (LC-MS/MS) were a good alternative to replace the bioassays once the methods were validated and proved to be effective to protect consumers.

The LC-MS/MS multi-toxin methods to analyze lipophilic toxins in seafood can work under different chromatographic conditions. Separation of lipophilic toxins under acidic chromatographic conditions was first proposed by Quilliam *et al.* in 2001[5], studied in depth by McNabb *et al.* in 2005 [6] and widely used since then [7-10]. The European Union Reference Laboratory for Marine Biotoxins (EURLMB) also applies acidic conditions and validated its method in-house in 2011 [11]. Gerssen *et al.* proposed in 2009 [12] the alkaline conditions to determine multiple lipophilic toxins in seafood and in-house validated them in 2010 [13]; these conditions gained popularity in the last years [14-16]. Less extreme pH conditions were proposed by Stobo *et al.* [17] using ammonium acetate as buffer (pH 6.8) and by These *et al.* [18] using ammonium bicarbonate (pH 7.9).

Two institutions organized interlaboratory collaborative exercises to validate their LC-MS/MS methods in 2010: the EURLMB and the Dutch Institute of Food Safety (RIKILT). The EURLMB validated its Standardized Operating Procedure (SOP) [11] for OA, PTXs and AZAs (the participants could voluntarily include YTXs). The SOP stipulated the extraction protocol and the alkaline hydrolysis step, recommended a list of MS/MS transitions to monitor and suggested several chromatographic conditions to quantify lipophilic toxins by external standard calibration (EXS). The RIKILT validated its method for all regulated lipophilic toxins under alkaline chromatographic conditions, using matrix-matched standard calibration (MMS) as a quantification strategy [19]. The success of both inter-laboratory studies demonstrated the effectiveness of the methods based on LC-MS/MS to replace the animal bioassays and promoted the approval of the Regulation (EC) No. 15/2011 [2], which settled the method validated under the coordination of the EURLMB as the reference technique for the detection of lipophilic marine toxins in bivalve molluscs in Europe. This regulation applies from July 1st, 2011 and allows the use of mice and rats bioassays for lipophilic toxin determination until December 31st, 2014.

The EURLMB SOP referenced in the Regulation (EC) No. 15/2011 [2] fixes neither the LC-MS/MS conditions nor the recovery correction approach [11], and this may trouble laboratories implementing the methods for control purposes. The EURLMB SOP provides several elution gradients and three possible chromatographic conditions as examples, allowing the analysts to choose the most convenient one: acidic conditions buffered with ammonium formate/formic acid; and basic conditions with ammonia or ammonia and ammonium bicarbonate as buffer. However, the selection of the chromatographic conditions requires a wide-scope study of the alternatives, since the pH and the buffer system of the mobile phases affect many parameters of the method: the selectivity of chromatographic separations, the ionization yields at the electrospray ionization source, the sensitivity of the MS response, the elution order and the matrix effects. Matrix effects can be corrected or compensated by, among other strategies, standard addition to the sample, solid-phase extraction (SPE) clean-up, sample dilution and matrix-matched standard calibration (MMS), the strategy used by RIKILT [17, 20-24].

According to the literature and the conclusions from interlaboratory trials, several chromatographic conditions seem feasible for the analysis of marine toxins. However, neither study compared different elution conditions nor assessed their impact on the methods performance. This paper is a comprehensive comparative study on the suitability of different experimental approaches suggested in the EURLMB SOP. We optimized and in-house validated four chromatographic conditions [6, 13, 17, 18] under the same experimental settings: same instrumentation, chromatographic column, sample preparation protocol, reagents, standards and analyst. We studied the separation and quantification of six groups of lipophilic toxins (all regulated in the EU plus GYMs and SPXs) at three concentration levels (0.5, 1 and 1.5 times the MPLs) with four relevant matrices for the seafood industry (mussels, pacific oysters, clams and sea urchin). We also assessed two quantification strategies (EXS and MMS) under alkaline conditions and studied matrix effects in detail. The aim of the work was to guide other labs in the decision-making process to select the most appropriate conditions for their LC-MS/MS method to analyze lipophilic toxins in seafood.

3.2 Materials and Methods

3.2.1 Standards and chemicals.

Certified reference standard solutions were purchased from the Institute for Marine Bioscience of the National Research Council (NRC) from Halifax (Canada): okadaic acid (OA, 14.3 ± 1.5 µg/mL), yessotoxin (YTX, 5.3 ± 0.3 µg/mL), pectenotoxin-2 (PTX2, 8.6 ± 0.3 µg/mL), azaspiracid-1 (AZA1, 1.24 ± 0.07 µg/mL), 13-desmethyl spirolide-C (SPX1, 7.0 ± 0.4 µg/mL, and gymnodimine-A (GYMA, 5.0 ± 0.2 µg/mL). Certified reference standard solutions for dinophysistoxin-1 (DTX1) and dinophysistoxin-2 (DTX2) were not available, thus a sample of mussel (*Mytilus galloprovincialis*) naturally contaminated with OA, DTX1 and DTX2 from the inter-laboratory proficiency test for lipophilic toxins organized by the EURLMB in 2010 was used to calculate the retention time (t_R) of DTX1 and the chromatographic resolution between OA and DTX2. The samples from the proficiency test for lipophilic toxins organized by the EURLMB in 2011 were used to calculate the relative t_R of AZA2 and AZA3 compared to AZA1; and homo-yessotoxin (homoYTX), 45-hydroxy-yessotoxin (45-OHYTX) and 45-hydroxy-homo-yessotoxin (45-OHhomoYTX) compared to YTX. Unfortunately, none of the samples had PTX1 to be included in the study.

Acetonitrile (ACN) hypergrade for LC-MS, methanol (MeOH) gradient grade for HPLC and formic acid puriss, 98.0% were purchased from Merck (Darmstadt, Germany). Ammonium bicarbonate and ammonium acetate (both elution additive for LC-MS), ammonium hydroxide (28% in water; ≥99.99% trace metals basis), ammonium formate for HPLC ≥99.0% and sodium hydroxide puriss. p.a were purchased from Sigma-Aldrich (Steinheim, Germany). Hydrochloric acid 37% was purchased from Panreac Quimica (Barcelona, Spain). Ultrapure water was obtained through a Milli-Q purification system (resistivity >18 MW·cm) from Millipore (Bedford, MA).

3.2.2 Preparation of extracts

Blue mussels (*Mytilus galloprovincialis*), pacific oysters (*Crassostrea gigas*), clams (*Ruditapes philippinarum*) and sea urchins (*Paracentrotus lividus*) were collected from the seafood harvesting areas of Catalonia, Spain (NW Mediterranean Sea) in 2010 and 2011. A triple-step extraction with MeOH was performed on whole tissues according to the procedure proposed by Gerssen *et al.* [13], but samples were homogenized with a hand blender instead of with an Ultra Turrax homogenizer. We chose this extraction procedure to ensure the recovery of the more lipophilic OA and DTX esters [13]. The protocol used 1 g of tissue (keeping the tissue:extractant volume ratio at 1:10, v/v) saving expensive certificate standards required for spikings. We used an analytical balance Sartorius 1702 (Goettingen, Germany), a vortex-mixer MS2 Minishaker (IKA Labortechnik, Staufen, Germany), and a centrifuge Jouan MR 23i (Thermo Fisher Scientific Inc., Waltham, MA, USA). Crude extracts were filtered through polytetrafluoroethylene (PTFE) 0.2 µm membrane syringe filters.

3.2.3 Alkaline hydrolysis

The alkaline hydrolysis of the samples was performed according to the EURLMB SOP [11] based on the protocol initially developed by Mountfort *et al.* [25].

3.2.4 Chromatographic separation

Toxins were separated on a Waters X-Bridge™ C8 (guard column 2.1 x 10 mm, 3.5 µm particle size, column 2.1 x 50 mm, 3.5 µm particle size; Waters, Milford, MA, USA) in an Agilent 1200 LC system (Agilent Technologies, Santa Clara, CA) consisting of a binary pump (G1312B), four channel degasser (G1379B), thermostated low carry-over autosampler (G1367C + G1330B), and column oven (G1316B). Four elution systems were tested:

• *Mobile phases in acidic conditions (pH 2)* according to McNabb *et al.* [6] and the EURLMB SOP [11]: Mobile phase A consisted of 2 mM of ammonium formate and 50 mM of formic acid in ultrapure Milli-Q water. Mobile phase B consisted of 2 mM of ammonium formate and 50 mM of formic acid in 95/5 v/v ACN/Milli-Q water.

• *Mobile phases in close to neutrality conditions (pH 6.8)* according to Stobo *et al.*[17]. Mobile phase A consisted of 5 mM of ammonium acetate in ultrapure Milli-Q water. Mobile phase B consisted of 5 mM of ammonium acetate in 95/5 v/v ACN/Milli-Q water.

• *Mobile phases in slightly alkaline conditions (pH 7.9)* according to These *et al.*[18]: Mobile phase A consisted of 5 mM of ammonium bicarbonate in ultrapure Milli-Q water. Mobile phase B consisted of 5 mM of ammonium bicarbonate in 95/5 v/v ACN/Milli-Q water. Mobile phase B was kept in the ultrasonic bath for 10 min to dissolve the buffer.

• *Mobile phases in alkaline conditions (pH 11)* according to Gerssen *et al.*[12, 13]: Mobile phase A consisted of 6.7 mM of ammonia in ultrapure Milli-Q water. Mobile phase B consisted of 6.7 mM of ammonia in 90/10 v/v ACN/Milli-Q water.

The mobile phases were filtrated through 0.2 µm nylon-membrane filters and the pH of aqueous mobile phases was measured with a CyberScan pH1100 (EUTECH Instruments, Thermo Fisher Scientific Inc., Waltham, MA, USA).

The column oven temperature was set at 30 °C and the flow rate was 0.5 mL/min. Gradient programs are shown in Table 3-1.We optimized a total run time of 12 min for all gradients, including column conditioning (Table 3-1) and included a step of 100% mobile phase B for 1 min to flush late eluting compounds [23], thus extending the lifespan of the column. The diverter valve was programmed to deliver the eluent from column to waste for the first 1.5 min in all gradients.

Table 3-1. Optimized elution gradients for four chromatographic conditions for the analysis of six groups of lipophilic toxins.

pH 2		pH 6.8 and pH 7.9		pH 11	
Time (min)	% Mobile phase B	Time (min)	% Mobile phase B	Time (min)	% Mobile phase B
0	20	0	20	0	20
6	80	3	40	8	100
7.5	80	5	80	9	100
8	100	7.5	80	9.5	20
9	100	8	100	12	20
9.5	20	9	100		
12	20	9.5	20		
		12	20		

Injection volume was optimized at 10 µL under alkaline conditions and 5 µL for the other conditions after testing the loading capacity of the column. The sample compartment was set at 4 ºC. The outer surface of needle was flushed with MeOH in the autosampler before every injection.

The column used for the whole study was ethylene-bridged hybrid (BEH). This column is designed to work at variable pH from 2 to 11. Before switching mobile phases, the system was purged and the column was washed with mixtures of ACN/Milli-Q water (95% to 0% water) at 0.2 mL/min for 2 h and conditioned with 20% mobile phase B at 0.5 mL/min for 20 min before running gradient five times. Column equilibration was done at the beginning of each batch with the mobile phases used for analysis running the same gradient of analysis five times. At the end

of each batch, the column was washed with mixtures of ACN/Milli-Q water for 25 min to remove lipophilic interferences and buffers.

3.2.5 Mass spectrometry

We used a triple quadrupole 3200 QTRAP® mass spectrometer (MS) equipped with a TurboV electrospray ion source (Applied Biosystems, Foster City, CA). The MS was operated in the multiple reaction monitoring (MRM) mode, selecting two product ions per toxin to allow quantification (the most intense transition) and confirmation (two confirmation ions for GYMA). Table 3-2 shows a summary of the MS/MS settings for lipophilic toxins analysis. The MS/MS conditions were based on the recommended values in the EURLMB SOP [11] for a 3200 QTRAP® MS. The selection of the precursor ions was based on the literature [6, 13, 17, 18]. We chose the double charge precursor ion ($[M-2H]^{2-}$) to monitor YTXs under pH 11 [12] but we decided to maintain the ammonium adduct ($[M+NH_4]^+$) instead of the sodium adduct ($[M+Na]^+$) to monitor PTXs under pH 6.8 since the reference paper [17] only applied single-quadrupole MS analysis, thus it does not provide information about fragmentation or MS/MS parameters from the precursor $[M+Na]^+$ for PTXs.

Table 3-2. Transitions monitored, dwell times, declustering potentials (DP), entrance potentials (EP), collision cell entrance potentials (CEP) and collisions energies (CE) for the detection of six groups of lipophilic toxins.

Toxin	Transitions (m/z)	Time (ms)	DP (V)	EP (V)	CEP (V)	CE (V)	Precursor ion
OA and DTX2	803.5 > 255.2	150	-115	-12	-46	-64	$[M-H]^-$
	803.5 > 113.1	150	-115	-10.5	-41	-68	
DTX1	817.5 > 255.2	150	-115	-12	-46	-64	$[M-H]^-$
	817.5 > 113.1	150	-115	-10.5	-41	-68	
YTX	1141.5 > 855.2	150	-60	-9	-54	-90	$[M-2Na+H]^-$
	1141.5 > 713.2	150	-60	-9	-54	-106	
YTX under pH 11	570.4 > 467.4	150	-75	-9	-54	-30	$[M-2H]^{2-}$
	570.4 > 396.4	150	-75	-9	-54	-30	
45-OHYTX	1157.5 > 855.2	150	-60	-9	-54	-90	$[M-2Na+H]^-$
	1157.5 > 713.2	150	-60	-9	-54	-106	
45-OHYTX under pH 11	578.4 > 467.4	150	-75	-9	-54	-30	$[M-2H]^{2-}$
	578.4 > 396.4	150	-75	-9	-54	-30	
homoYTX	1155.5 > 869.2	150	-60	-9	-54	-90	$[M-2Na+H]^-$
	1155.5 > 727.2	150	-60	-9	-54	-106	
homoYTX under pH 11	577.4 > 474.4	150	-75	-9	-54	-30	$[M-2H]^{2-}$
	577.4 > 403.4	150	-75	-9	-54	-30	
45-OHhomoYTX	1171.5 > 869.2	150	-60	-9	-54	-90	$[M-2Na+H]^-$
	1171.5 > 727.2	150	-60	-9	-54	-106	
45-OHhomoYTX under pH 11	585.4 > 474.4	150	-75	-9	-54	-30	$[M-2H]^{2-}$
	585.4 > 403.4	150	-75	-9	-54	-30	
SPX1	692.5 > 444.2	150	86	7	30	45	$[M+H]^+$
	692.5 > 426.3	150	86	7	30	45	
GYMA	508.4 > 202.4	150	60	8.5	25	55	$[M+H]^+$
	508.4 > 392.4	150	60	8.5	25	55	
	508.4 > 490.4	150	60	8.5	25	55	
PTX2 and 7-epi-PTX2	876.5 > 213.3	150	50	10	35	50	$[M+NH_4]^+$
	876.5 > 823.5	150	50	10	35	50	
PTX-2sa and 7-epi-PTX2sa	894.5 > 213.3	150	50	10	35	50	$[M+NH_4]^+$
	894.5 > 823.5	150	50	10	35	50	
AZA-1	842.5 > 362.3	150	75	12	40	70	$[M+H]^+$
	842.5 > 462.5	150	75	12	40	70	
AZA-2	856.5 > 362.3	150	75	12	40	70	$[M+H]^+$
	856.5 > 462.5	150	75	12	40	70	
AZA-3	828.5 > 362.3	150	75	12	40	70	$[M+H]^+$
	828.5 > 448.5	150	75	12	40	70	

Mass spectrometric detection was performed in both negative (-ESI) and positive polarity (+ESI). Under pH 2, pH 6.8 and pH 7.9, two different injections were needed per sample: the toxins OA, DTX1, DTX2 and YTXs were detected in the -ESI, while the +ESI was used to detect SPX1, GYMA, AZAs and PTXs. The alkaline mobile phase allows polarity switching from negative to positive mode to analyze all toxins in two detection windows during the same run: the first retention time window was programmed during the first 4.5 min in negative ESI mode to detect OA, DTX1, DTX2, and YTXs; the second retention time window lasted 7.5 min in positive ESI mode to analyze SPX1, GYMA, AZAs, PTXs. Resolution of the quadrupoles was set at unit.

3.2.6 Quality requirements posed by the EURLMB

We checked in every batch the quality control criteria stated by the EURLMB SOP [11] regarding resolution, limits of quantification (LOQs) and linearity.

Resolution (*Rs*) between the isomers OA and DTX2 was calculated according to Equation 3.1:

$$R_s = 2\,(t_{R(DTX\text{-}2)} - t_{R(OA)})/(W_{(OA)} + W_{(DTX2)}) \quad \text{Equation 3.1}$$

Where t_R means retention time and W means peak width (both in minutes). The resolution for each chromatographic condition was assessed as the average resolution of six replicates in a reference sample naturally contaminated with OA and DTX2. The EURLMB requests resolution between OA and DTX2 to be greater than one [11].

LOQs were evaluated with three replicate blank samples of each matrix spiked at the theoretical LOQs (calculated with blank homogenized tissues spiked with OA, PTX2, SPX1, GYMA and AZA1 at 80 µg/kg and with YTX at 250 µg/kg), analyzed by triple injection, as the concentration that met a S/N of ten for the most abundant fragment and a S/N greater than three for the transition used for confirmation. Noise was calculated with a blank sample of each matrix at the expected retention times of the toxins. Methods validated under the specification of the EURLMB SOP [11] shall reach LOQs as low as 40 µg/kg for AZA1 and OA, 50 µg/kg for PTX2 and 60 µg/kg for YTX.

Linearity was estimated from the calibration curves analyzed before and after the analysis of a set of samples (six to eight samples). The correlation coefficients of the quantification curves had to be greater than 0.98 to ensure linearity and the deviation of the slopes between consecutive calibration curves has to be lower than 25% to be considered as acceptable, as requested in the EURLMB SOP [11].

Sensitivity of the method was evaluated as the slope of the external standard calibration curves for each toxin.

3.2.7 Validation parameters

The in-house validation study relied on the concepts described in Taverniers *et al.* [26], the guidelines proposed by the Regulation (EC) 657/2002 on performance criteria for analytical methods [27], and the methodology applied in de la Iglesia *et al.* [28].

The accuracy of the methods was assessed by the intermediate precision and the trueness. The spikings were done on blank homogenized tissue instead of on extracts in MeOH to make the validation process as comprehensive as possible.

The intermediate precision was expressed as the relative standard deviation (RSD in %). It was calculated for each matrix (mussels, pacific oysters, clams and sea urchins) at three different concentration levels of OA, PTX2, SPX1, GYMA and AZA1 (80 µg/kg, 160 µg/kg and 240 µg/kg) and two concentration levels of YTX (250 µg/kg and 500 µg/kg) spiked in blank homogenized tissues and quantified using external standard calibration curves. Four replicates spread over four consecutive days were analyzed by single injection using daily fresh mobile phase. The RSD was transformed to HorRat value as the ratio between the experimental RSD and the predicted RSD according to the Horwitz equation [29] (Equation 3.2), which is dependent on the concentration (*C*) spiked for the intermediate precision assessment.

$$\text{HorRat} = \text{RSD}(\%)\ \text{experimental} / 2^{(1-0.5\log C)} \quad \text{Equation 3.2}$$

The Regulation (EC) 657/2002 [27] suggests that for in-house laboratory validation, the experimental RSD should not exceed the expected RSD (HorRat < 1). Intermediate precision was only calculated when at least three out of the four replicates met the quality requirements regarding linearity.

Trueness in terms of recovery was calculated for each sample matrix at the three concentration levels (two concentration levels for YTX) using the four replicates analyzed by single injection in consecutive days and quantified using external standard calibration curves. Recovery in percentage was calculated by comparing the quantifications through external calibration with the theoretical spiked concentration. The Regulation (EC) 657/2002 [27] recommends correcting the quantification with the mean recovery only if trueness falls between 80% and 110%.

We used the same batch sequences for all chromatographic conditions. The matrices were injected always in the same order, grouped by its concentration level (from low to high concentration). Blanks of MeOH were analyzed before and after calibration curves and sets of samples to assess potential carry-over problems.

Chromatographic selectivity was based on t_R of the analytes that have commercial standard solutions (at least one representative for each group of lipophilic toxins). For analogues without standards available, we used the relative retention time (RRT) compared to the representative toxin.

The drift in t_R in the samples compared to those in the standard solutions was acceptable below 3%, as stated in the EURLMB SOP [11]. Mass spectrometric selectivity was assessed with the transitions monitored in the MS/MS system, proposed by the EURLMB SOP [11] and by Gerssen *et al.* [12] for the determination of YTX under alkaline conditions. The maximum permitted tolerances for relative ion intensities were taken from Regulation (EC) 657/2002 [27] and were checked in all matrices analyzed, spiked at the MPL (0.5 times the MPL for YTX) during three consecutive days. The presence of potential interferences was assessed by analyzing blank samples for all matrices.

3.2.8 Calibration strategies and matrix effects assessment

The external standard calibration curves were prepared in MeOH (LC-MS grade) from an initial multi-toxin stock solution of 400 ng/mL of OA, PTX2, SPX1, GYMA and AZA1, and 625 ng/mL of YTX. The calibration curves had six levels in the range of 5 to 60 ng/mL of OA, PTX2, SPX1, GYMA and AZA1 and 8 to 94 ng/mL of YTX.

The in-house validation of the four chromatographic conditions was done using the external standard calibration strategy (EXS) to quantify the spiked samples. This calibration strategy saves the expensive certified standard solutions, assuming the calibration curves prepared in MeOH lasts longer than those involving seafood matrices. Nevertheless, the matrix-matched standard (MMS) calibration strategy has been reported to compensate matrix effects caused by seafood tissues in the determination of lipophilic toxins [13]. The MMS calibration strategy consists on the preparation of the calibration curve in a solvent with the same composition as the matrix of interest, usually in extracts of blank tissues of the same seafood species analyzed [23], thus the influence of the matrix interferences would affect equally to samples and standards.

We performed a comparative study between the External Standard calibration (EXS) and the matrix-matched standard calibration (MMS) prepared with blank mussel extracts. The study tested if matrix effects were species dependent and if MMS improved method accuracy compared to EXS.

We spiked homogenated seafood tissues by adding the standards on the tissues and vortex-mixing them for 1 min. One blank sample of each matrix was spiked at three different concentration levels of OA, PTX2, SPX1, GYMA and AZA1 (80 µg/kg, 160 µg/kg and 240 µg/kg) and two concentration levels of YTX (250 µg/kg and 500 µg/kg), injected in triplicate and quantified with a five level calibration curve (5 to 40 ng/mL) prepared in MeOH to assess the EXS strategy. The same spiked samples were injected in triplicate and quantified against a five level calibration curve (5 to 40 ng/mL) prepared in blank mussel extracts to assess the MMS strategy. The quantification of the hydrolyzed spiked samples was performed by triple injection against an hydrolyzed EXS calibration curve and against an hydrolyzed MMS calibration curve in mussels, both spiked with OA before the hydrolysis (five levels from 5 to 40 ng/mL).

We also studied species dependence in matrix effects for OA (free and total OA after hydrolysis), YTX, PTX2, AZA1, SPX1 and GYMA in mussels, oysters, clams and sea urchins using the four chromatographic conditions. Matrix effects (ME) were estimated as the ratio between the slopes of a five level calibration curve (5 to 40 ng/mL) prepared in extracts of the blank seafood matrices, and the same curve prepared in MeOH. Values of ME lower/higher than one mean the matrix inhibits/enhances the signal of the toxin. If the slope of both calibration curves are equal (ME = 1), the matrix would have no effect on the sensitivity of the method. Each calibration level was analyzed by single injection under pH 2, pH 6.8 and pH 7.9; three injection replicates were analyzed under alkaline conditions.

3.2.9 Statistical analysis.

Statistical calculations were performed using SPSS 17.0. The significance tests used to evaluate the influence of the species in the matrix effect was a One-Way ANOVA (one test per toxin), supported by a Levene Test of Homogeneity of Variances, and a Post Hoc Tukey HSD Test when the ANOVA test showed significant differences in the mean between groups (species). Alpha was set at 0.05 (95% confidence) for all tests and experiments.

3.3 Results and discussion

3.3.1 Implementation of LC-MS/MS methods according to the EURLB-SOP quality requirements

Since the charge state of the toxins is influenced by the pH of the mobile phase, tR and elution order of the toxins were expected to change under different chromatographic conditions [12] (Figure 3-1). Under pH 2, YTX coeluted with PTX2, and the "–ESI toxins" (OA and YTX) eluted in the same time window as the "+ESI toxins" (GYMA, SPX1, PTX2 and AZA1). The shift from acidic to almost neutral conditions reduced OA t_R and slightly alkaline conditions increased the t_R of the cyclic imines. When pH was modified from pH 7.9 to pH 11, t_R of OA, YTX and AZA1 shorted, thus the "–ESI toxins" eluted at the beginning of the chromatogram and "+ESI toxins" eluted afterwards. This change in the elution order enabled to set detection windows with different polarity in our 3200 QTRAP® and analyze all toxins in the same run.

Our results of t_R and elution orders (Figure 3-1 and Table 3-3) agreed with those explained in Gerssen *et al.* [12]. We also appreciated a narrower peak for YTX once the pH was set close to neutrality in relation to acidic conditions. AZA1 t_R was the most shorted by pH changes (3.2 min difference over 9 pH units,) and peaks widened when pH changed from acid to alkaline conditions.

All conditions met the quality requirements for OA-DTX2 resolution. The best resolutions between OA-DTX2 calculated according to Equation 3.1 were 1.67 and 1.55 under pH 6.8 and pH 7.9, respectively. Resolutions achieved with elution at pH 2 and pH 11 were lower (1.09 and 1.01, respectively) though still fulfilled the quality criteria [11].

Table 3-3. Average retention times in minutes (n=6) and average relative retention times (n=2; in brackets and italic) of six groups of lipophilic toxins.

	Retention times (min)			
	pH 2	pH 6.8	pH 7.9	pH 11
AZA1	7.9	6.6	6.3	4.7 *(1.0)*
AZA2				*(0.9)*
AZA3				*(1.1)*
OA-c	6.2	4.8	4.5	3.1
DTX1	7.0	5.9	5.7	3.7
DTX2	6.5	5.2	4.8	3.4
GYMA	4.3	4.4	6.0	5.8
PTX2	6.6	6.5	6.5	6.6 *(1.0)*
PTX2-sa				*(0.5)*
SPX1	4.9	5.5	6.4	6.3
YTX	6.4	6.2	5.9	3.8 *(1.0)*
HomoYTX				*(1.0)*
45-OH-YTX				*(0.84)*
45-OH-homoYTX				*(0.84)*

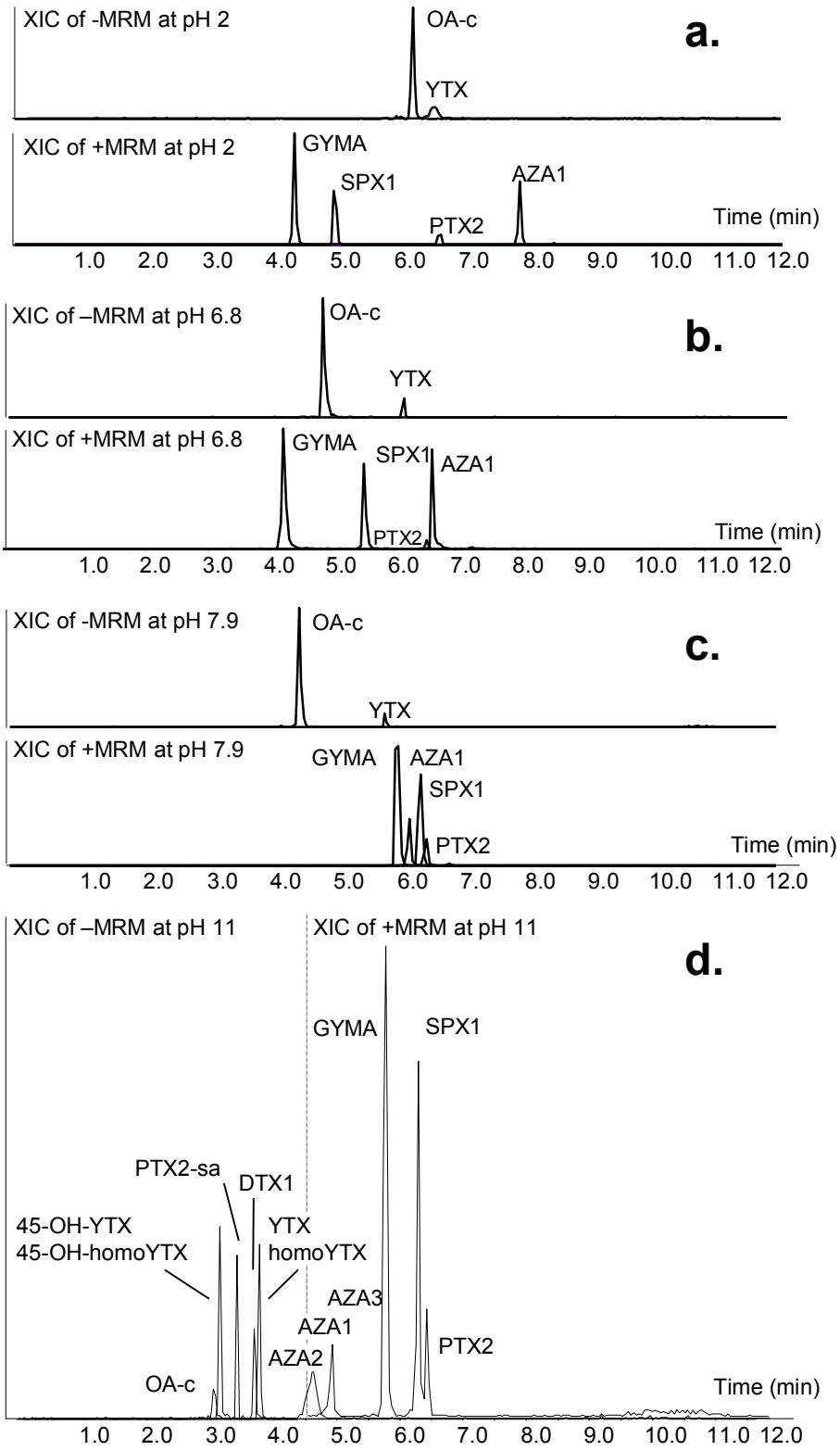

Figure 3-1. Example of chromatograms of NRC CRM standard solution of AZA1, GYMA, OA, PTX2, and SPX1 at 50 ng/mL; YTX at 200 ng/mL, under four chromatographic conditions.

Table 3-4. Sensitivity of six groups of lipophilic toxins (slope of the calibration curve in methanol LCMS) and matrix effects (ME) under four chromatographic conditions, expressed as the ratio between the slopes of a calibration curve in methanolic seafood extracts against the slope of a calibration curve in methanol. MeOH*: Slope of calibration curve in methanol

Sensitivity and matrix effects				
	pH 2 (n=1)	**pH 6.8** (n=1)	**pH 7.9** (n=1)	**pH 11** (n=3)
AZA1				
*MeOH**	*644.38*	*466.11*	*386.35*	*798.85*
Mussel	0.87	0.62	1.03	0.97
Oyster	0.74	0.72	1.00	0.91
Clam	0.96	0.78	0.77	1.18
Sea Urchin	0.94	0.75	0.98	1.00
GYMA				
*MeOH**	*333.81*	*216.09*	*319.44*	*1010.84*
Mussel	0.86	1.19	1.13	0.91
Oyster	0.72	0.87	1.03	0.80
Clam	0.89	0.88	1.12	1.02
Sea Urchin	0.73	1.19	0.96	0.58
OA-c				
*MeOH**	*105.93*	*88.78*	*96.01*	*200.89*
Mussel	1.65	1.92	1.55	2.09
Oyster	1.54	1.10	1.07	2.31
Clam	1.49	1.09	1.01	2.65
Sea Urchin	1.45	1.59	1.16	2.04
PTX2				
*MeOH**	*141.74*	*35.29*	*195.02*	*739.35*
Mussel	0.98	1.27	1.16	0.97
Oyster	0.95	1.10	1.09	1.05
Clam	1.00	1.46	1.27	1.07
Sea Urchin	0.88	1.28	1.08	1.09
SPX1				
*MeOH**	*1157.07*	*607.84*	*957.77*	*2885.69*
Mussel	0.69	1.03	1.22	1.05
Oyster	0.87	1.38	1.17	1.07
Clam	0.81	1.37	0.92	1.21
Sea Urchin	0.77	1.28	1.19	1.19
YTX				
*MeOH**	*32.11*	*13.21*	*9.58*	*335.16*
Mussel	0.94	1.34	1.16	1.80
Oyster	0.90	0.93	1.34	2.57
Clam	0.99	1.13	1.25	3.08
Sea Urchin	1.03	1.18	1.03	2.79

The external calibration curves of the NRC standards confirmed that the elution system does have an effect on sensitivity (Table 3-4) and Figure 3-2). Alkaline conditions showed the highest sensitivity for all toxins but AZA1; the improvements in sensitivity for YTX and PTX2 were remarkable: after normalizing sensitivity data with injection volumes, YTX sensitivity was five times better under alkaline conditions than under acidic conditions, while PTX2 sensitivity increased almost three-fold. Chromatographic conditions under pH 6.8 and 7.9 generally showed lower sensitivities than acidic conditions, especially for PTX2 under pH 6.8 and for YTX in both cases.

In our case and following the EURLMB SOP [11] requirements, only the alkaline conditions could be implemented as a multi-toxin method, since it was the only one proving acceptable LOQs for all regulated toxins (Table 3-4), including YTX (less than 60 µg/kg), with our middle-class 3200 QTRAP® MS. The analysis of YTX under acidic conditions gave high LOQs (Table 3-5), from 272.6 µg/kg (in sea urchin) to 377.1 µg/kg (in mussel), influenced by the poor chromatographic peak shape of YTX under pH 2 (Figure 3-1).

Although more alkaline pH improved YTX peak shape, the detection capability for YTX under pH 6.8 and pH 7.9 was still too low (
Table 3-4) and the theoretical LOQs for YTX under these pH were found over 300 µg/kg, therefore experimental LOQs were not evaluated to save valuable standards. Conditions under pH 6.8 also failed to provide LOQs for PTX2 lower than 50 µg/kg in most of the matrices. The lowest LOQs for AZA1 and GYMA were achieved under pH 7.9 (7.1 µg/kg and 2.3 µg/kg respectively, average for the four matrices), while the lowest LOQs values for OA, PTX2 and SPX1 were found under alkaline conditions (6.5 µg/kg, 11.9 µg/kg and 8.6 µg/kg respectively, average for the four matrices).

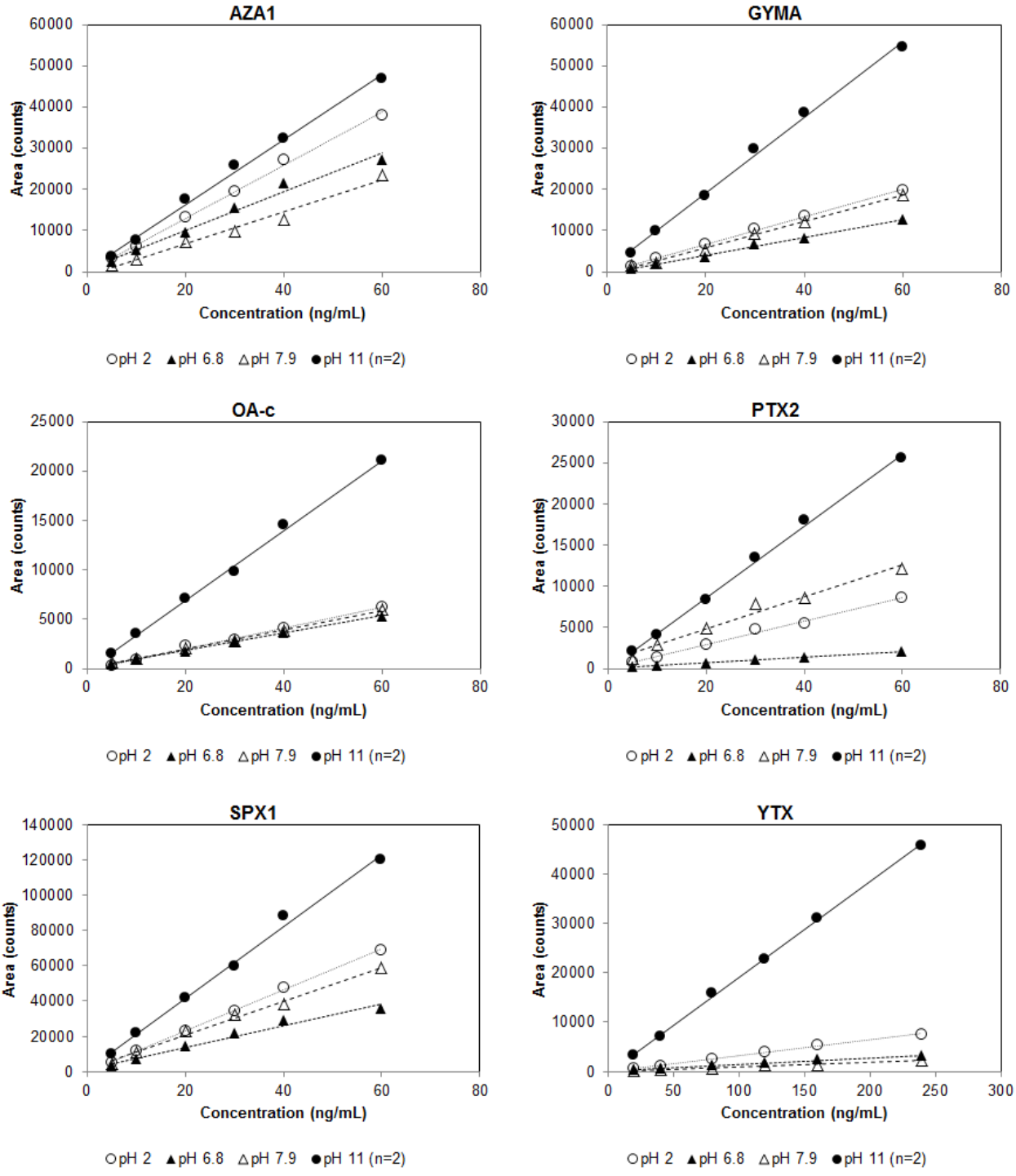

Figure 3-2. Comparison of external calibration curves of six lipophilic toxins under four elution system (different pH and buffer composition). Normalized for 5 ŶL of injection volume for pH 11 (n=2). Slope values are listed in Table 3-4.

Table 3-5. Limits of quantitation (LOQ, Ŷg/kg) evaluated with blank homogenized samples of each matrix spiked at the theoretical LOQs (n=3) for six groups of lipophilic toxins.

	LOQs (µg/kg)			
	pH 2	pH 6.8	pH 7.9	pH 11
AZA1				
Mussel	8.7	12.4	9.2	6.0
Oyster	6.8	13.9	8.3	10.9
Clam	5.6	29.8	7.7	9.7
Sea Urchin	7.6	15.5	3.1	4.6
GYMA				
Mussel	6.1	4.7	1.5	13.2
Oyster	7.0	7.8	3.4	5.7
Clam	11.2	19.2	1.7	10.9
Sea Urchin	18.4	6.4	2.4	3.4
OA-c				
Mussel	14.9	26.9	22.0	3.6
Oyster	15.2	29.2	18.3	6.8
Clam	8.7	21.1	19.1	7.1
Sea Urchin	10.5	25.5	21.7	8.5
PTX2				
Mussel	25.6	71.6	5.3	13.4
Oyster	22.2	52.9	27.2	15.6
Clam	23.3	36.7	11.0	10.2
Sea Urchin	24.8	85.8	13.1	8.7
SPX1				
Mussel	33.7	8.2	55.7	14.7
Oyster	17.4	6.2	15.7	14.3
Clam	5.9	22.8	9.4	3.4
Sea Urchin	7.9	16.4	2.4	1.8
YTX				
Mussel	377.1	> 300.0	> 300.0	36.0
Oyster	340.3	> 300.0	> 300.0	15.8
Clam	312.9	> 300.0	> 300.0	12.4
Sea Urchin	272.6	> 300.0	> 300.0	16.3

This study confirms that the selection of the proper chromatographic condition can contribute to get better LOQs. Alkaline conditions provided better LOQs for YTX because of three reasons: first, they allowed 10 µL of sample injection (instead of 5 µL as in the rest of the conditions) without peak broadening caused by column overloading; second, the double charged species monitored as the precursor ion of YTX were highly selective and sensitive [13]; and finally, alkaline pH seems to reduce secondary interactions between the sulfonic acids of YTX and the stationary phase of the column [12], resulting in narrower peaks with better S/N ratios (Figure 3-1). The ionization yield of YTX at pH 6.8 and 7.9 has not been studied in detail (nor in this study neither in the literature), thus the selection of a different precursor ion might increase YTX sensitivity under these elution systems. Nevertheless, the maximum permitted level for the YTXs is 1 mg/kg, thus other conditions could be also applied and still be efficient to monitor the YTXs according to the Regulation (EC) 853/2004 [3].

Low sensitive instruments may require the reconsideration of the extraction procedure to achieve better LOQs, by reducing the extraction volume or applying pre-concentration steps, but matrix effects and recoveries should be carefully taken into account when applying these strategies.

The correlation of the calibration curves calculated by least-squares adjustment was not always satisfactory. Although all chromatographic conditions had correlation coefficients less than 0.98 in some specific occasions our study proves that some toxins (especially YTX) and chromatographic conditions (particularly pH 7.9) are more prone to have linearity problems.

A major change in the slope (response drift over 25%) of two consecutive calibration curves means the sensitivity of the method for a certain toxin is not stable during the batch, which occurred in 12.5% of the calibration curves of SPX1 and PTX2 analyzed under pH 6.8, and in 25% of the curves of YTX with pH 7.9. Acidic and alkaline conditions kept the sensitivity constant for all toxins in all batches (none of the batches had a slope drift larger than 25%). Changes in sensitivity were unrelated to carry-over problems, since absence of signals were found in control blank samples analyzed after positive control samples or high concentration standards. However, response drifts were more frequent for those toxins with poor sensitivities under certain chromatographic conditions.

3.3.2 Methods performance

The alkaline conditions had the best overall performance in terms of precision (Table 3-6). For AZA1, alkaline conditions provided HorRat values below one in all matrices and concentrations, but the rest of conditions were also precise enough in most cases at medium and high concentrations. The precision in the analysis of GYMA spiked in mussels was only satisfactory under alkaline conditions, but acidic conditions had better precision in sea urchins. The HorRat values for OA (both crude and hydrolyzed) were in general very high (up to 3.4 in mussels spiked at 0.5 times the MPL analyzed under acidic conditions after hydrolysis). The precision for crude OA in mussels under alkaline conditions was good, but in sea urchins the acidic conditions would provide better HorRat values at medium and high concentrations. For PTX2 and SPX1, alkaline conditions resulted in general better than the rest in terms of precision.

Table 3-6. Trueness as recovery (R, in %) and precision as HorRat value (no units) for six groups of lipophilic toxins. Average values of four replicates spread over four consecutive days quantified using an external calibration curve with single injection. n.q.: Not quantified because the batch did not meet the linearity requirements.

	AZA1				GYMA				OA-c				OA Hydrolized				PTX2				SPX1				YTX			
	pH 2	pH 6.8	pH 7.9	pH 11	pH 2	pH 6.8	pH 7.9	pH 11	pH 2	pH 6.8	pH 7.9	pH 11	pH 2	pH 6.8	pH 7.9	pH 11	pH 2	pH 6.8	pH 7.9	pH 11	pH 2	pH 6.8	pH 7.9	pH 11	pH 2	pH 6.8	pH 7.9	pH 11
Mussel																												
80 µg/kg																									*250 µg/kg*			
R (%)	55.3	n.q.	27.4	120.8	41.2	70.8	70.8	73.2	93.3	93.2	73.7	150.5	162.0	96.8	94.7	155.4	67.4	56.0	32.5	93.8	35.8	61.1	50.6	99.0	94.7	113.8	214.9	76.1
HorRat	1.4	n.q.	1.2	0.3	1.7	1.0	1.1	0.8	0.5	0.9	1.5	0.7	3.4	2.2	1.9	1.5	2.5	0.6	1.9	0.5	2.3	1.2	0.8	0.6	1.3	0.5	0.7	1.1
160 µg/kg																									*500 µg/kg*			
R (%)	84.3	23.7	73.7	124.1	73.7	110.1	83.2	82.1	143.7	116.3	94.4	158.4	140.5	100.2	85.5	136.7	96.4	n.q.	n.q.	93.3	71.6	122.0	64.5	111.6	69.0	n.q.	n.q.	42.7
HorRat	1.6	1.3	1.9	0.7	1.5	1.5	1.2	1.4	1.3	1.6	1.2	0.9	1.1	1.6	0.6	1.4	2.4	n.q.	n.q.	1.1	2.2	1.0	0.5	0.4	1.2	n.q.	n.q.	0.9
240 µg/kg																												
R (%)	79.3	30.6	59.1	104.7	55.7	99.0	94.8	74.3	116.3	99.2	96.9	120.7	100.7	77.7	86.0	104.7	89.8	n.q.	n.q.	68.7	68.9	135.0	73.2	94.7				
HorRat	1.1	1.4	1.0	0.7	1.3	1.1	1.4	1.0	1.1	1.0	1.4	0.9	0.7	0.7	0.8	0.9	0.7	n.q.	n.q.	1.1	1.0	1.0	1.4	0.8				
Oyster																												
80 µg/kg																									*250 µg/kg*			
R (%)	58.5	n.q.	33.7	119.5	68.2	67.6	64.2	81.0	97.9	61.8	50.0	134.9	77.1	33.9	42.0	99.4	80.6	90.9	40.9	102.4	51.7	65.2	49.2	94.2	54.3	46.8	131.5	55.0
HorRat	1.6	n.q.	1.3	0.4	1.8	1.3	1.3	0.5	1.3	1.5	2.3	0.5	1.4	1.7	1.7	0.5	0.6	0.6	1.7	0.4	1.6	1.8	0.9	0.9	2.1	2.0	1.4	1.0
160 µg/kg																									*500 µg/kg*			
R (%)	76.7	34.3	60.7	105.9	62.3	90.5	74.2	74.8	104.6	71.5	59.2	119.7	72.1	41.4	45.2	77.1	82.2	96.9	56.2	88.4	73.5	89.3	63.7	102.2	40.8	n.q.	n.q.	37.4
HorRat	1.3	1.8	0.5	0.3	1.4	0.5	0.4	0.6	1.0	1.3	1.7	1.5	2.5	2.5	2.6	1.9	1.2	1.5	1.1	0.5	0.4	0.1	0.4	0.4	1.0	n.q.	n.q.	0.8
240 µg/kg																												
R (%)	78.6	41.2	67.5	100.0	71.6	101.1	87.0	83.9	109.1	78.7	77.0	124.8	82.8	46.5	57.6	89.8	94.1	n.q.	n.q.	77.4	84.1	135.6	78.1	95.5				
HorRat	0.9	0.5	0.4	0.5	1.3	0.9	0.5	0.5	0.9	0.8	0.6	1.0	2.2	2.1	2.9	0.8	0.2	n.q.	n.q.	0.6	1.4	1.7	1.1	0.8				
Clam																												
80 µg/kg																									250 µg/kg			
R (%)	63.4	n.q.	35.8	116.6	51.6	76.2	34.0	79.7	80.9	81.2	51.2	135.6	131.5	74.8	59.4	112.3	53.3	81.6	37.6	95.6	34.1	49.5	46.1	76.5	65.0	73.9	164.1	47.8
HorRat	0.7	n.q.	0.7	0.4	0.5	1.3	1.5	0.3	2.8	1.3	1.7	0.6	2.4	2.4	2.9	0.9	1.7	0.4	1.4	0.5	1.9	1.6	1.4	1.0	2.6	3.4	2.2	0.8
160 µg/kg																									500 µg/kg			
R (%)	101.3	48.7	64.2	104.6	78.4	105.5	65.1	81.7	103.7	107.6	87.0	116.1	106.9	86.1	89.8	92.5	84.8	131.1	76.8	85.8	62.8	131.7	70.7	82.4	61.4	n.q.	n.q.	31.3
HorRat	2.8	1.1	1.3	0.4	1.3	1.0	2.9	0.2	2.5	1.7	2.2	1.3	0.9	1.5	1.8	0.9	2.4	1.5	1.5	0.5	1.0	0.7	1.3	1.0	1.2	n.q.	n.q.	1.1
240 µg/kg																												
R (%)	73.1	45.5	59.4	99.3	67.5	99.1	48.6	91.4	105.9	88.6	75.6	123.3	103.4	60.4	50.8	93.1	75.9	n.q.	n.q.	74.2	66.8	138.1	72.5	82.1				
HorRat	0.9	0.9	1.5	0.3	1.7	1.5	1.3	0.3	1.7	0.9	1.1	1.0	1.0	0.8	0.6	0.8	1.0	n.q.	n.q.	0.4	1.2	0.8	0.8	0.6				
Sea Urchin																												
80 µg/kg																									*250 µg/kg*			
R (%)	63.0	n.q.	37.8	121.3	60.6	72.8	55.5	69.8	83.6	72.2	48.6	140.9	80.5	46.1	44.3	148.0	75.5	43.8	45.3	100.6	59.7	84.4	40.9	74.6	37.5	54.4	106.2	71.1
HorRat	1.3	n.q.	1.6	0.4	1.4	0.5	1.6	1.1	1.2	1.1	2.2	0.9	0.8	1.2	2.4	1.3	0.9	2.2	1.8	0.3	1.0	0.4	0.6	0.6	1.5	1.3	1.1	1.4
160 µg/kg																									*500 µg/kg*			
R (%)	81.7	27.5	58.6	122.9	81.3	84.5	73.7	85.8	112.2	81.5	66.7	150.5	85.2	58.0	56.5	126.6	87.3	n.q.	n.q.	94.6	72.6	109.2	61.9	100.6	43.6	n.q.	n.q.	35.5
HorRat	1.1	1.5	0.3	0.6	0.7	1.0	1.0	1.3	0.4	0.9	0.3	1.6	0.5	1.5	1.4	1.7	0.7	n.q.	n.q.	0.3	0.7	1.1	0.4	1.4	0.6	n.q.	n.q.	0.8
240 µg/kg																												
R (%)	85.9	37.0	62.4	98.8	76.4	83.3	77.8	73.2	118.3	83.6	68.3	107.5	84.4	55.1	58.3	85.2	76.7	n.q.	n.q.	78.0	76.0	133.7	66.5	73.0				
HorRat	0.8	1.4	0.3	0.6	0.9	0.3	0.7	1.4	0.4	0.8	0.4	1.0	1.2	1.3	1.5	0.9	1.0	n.q.	n.q.	0.8	1.0	0.2	0.9	1.2				

The intermediate precision for YTX was generally insufficient under all chromatographic conditions but slightly better under pH 11. Since alkaline conditions were the only one providing LOQs lower than 60 μg/kg for YTX, they were the best choice for the analysis of YTX. Trueness was expressed as recovery (Table 3-6). The recovery of the lipophilic toxins resulted to be dependent on the chromatographic conditions, since the pH and the buffer in the mobile phase can affect the ionization yield of the toxins and the elution of potential interferences present in the matrix.

The recoveries for AZA1 were mostly lower than 70% for all matrices under pH 6.8 and 7.9 and slightly better under pH 2, but the toxin concentration was overestimated under alkaline conditions. The recoveries for GYMA were generally low under all chromatographic conditions (slightly better under pH 6.8), but especially under pH 2, with recoveries below 85%. The recoveries of OA strongly depended on the pH: the overestimation of crude OA under alkaline conditions was remarkable, while the recoveries generally fell in the range of 80% to 120% under pH 2 and were slightly lower under pH 7.9. The hydrolyzed OA also shown overestimation under pH 11, but the recoveries were generally lower than those for the crude OA in all cases. The recoveries for PTX2 were generally low under acidic conditions and under pH 6.8 and 7.9, but they fell between 80% and 110% in most cases under pH 11, thus it would be possible to correct the concentration using the mean recovery [27] Recovery correction can also be applied for SPX1 quantification under alkaline conditions, while SPX1 were under-quantified with pH 2 and pH 7.9 and over-quantified with pH 6.8. The YTX recovery under pH 2, pH 6.8 and pH 7.9 were not reliable since most measurements were imprecise and the LOQs were too high. Under alkaline conditions, recoveries for YTX were always below 80%.

Improvements in precision and trueness enhance accuracy. Precision benefits from replicate injections of the sample and more data points per peak. The EURLMB validated its method using double injection [11], but the SOP allows single injection whenever possible to increase sample throughput and save standards, as aimed in this study, but this approach showed to be sometimes insufficient and double or triple injection is encouraged. The number of acquired points per peak of transitions used for quantitation may also be increased by reducing the dwell time of confirmatory transitions (assuming proper S/N and relative ion intensities ratios). Besides, clustering of "–ESI toxins" and "+ESI toxins" is very useful to increase the sample throughput of instruments with slow polarity switching, but it still provide a benefit even in modern instruments since the less time invested in polarity switches, the more data points acquired per peak. Trueness is improved by correction in recovery with certified reference materials or in-house internal reference materials when the firsts are not available.

The deviation in t_R for all toxins in the spiked samples compared to those in the standards never exceeded 3%. The stability of the pH in the mobile phase is essential to ensure that the retention times remain constant along the analysis: alkaline mobile phase was prone to changes in pH (likely due to the evaporation of the ammonium hydroxide) and we observed AZAs t_R were very sensitive to those slight changes. Thus, alkaline mobile phases should be freshly prepared daily. When there is no available standard to obtain the t_R of a toxin, the relative t_R can provide additional identification points complementary to the MRM transitions. Moreover, it may be interesting to get relative t_R under different elution conditions for toxin analogues for which standards are not commercially available, especially when derivatives are present in samples at

very low concentration and acquisition of a full product ion spectrum is not possible. Changes on retention time can provide additional identification points.

We did not detect interfering peaks in the blank samples for any toxin under any chromatographic conditions, but switching chromatographic conditions can serve as a strategy to get rid of matrix interfering compounds since the pH modifies the selectivity towards the compounds of the matrix, as proposed by Kilcoyne and Fux [23].

The relative ion intensities measured in the samples and in the calibration standards at comparable concentrations fell into the tolerance ranges proposed by the Regulation (EC) 657/2002 [27] in most cases. There were two small deviations out of the tolerance ranges: for PTX2 in sea urchin matrix analyzed under acidic conditions (1% out of the tolerance range) and for YTX in oysters analyzed under alkaline conditions (4% out of the tolerance range). The most important variation was found for YTX in oysters analyzed under acidic conditions (17% out of the tolerance range), probably related to the poor sensitivity and chromatographic peak shape of YTX under pH 2. Nevertheless, the matrix might alter the fragmentation ratios of an analyte [30], although this phenomenon has been barely studied.

3.3.3 Calibration strategies and matrix effects assessment

Matrix effects strongly varied depending on the toxin. Signal enhancement was especially evident for OA in most matrices and chromatographic conditions. Overall positive matrix effects were less important for PTX2, while AZA1 mostly tended to signal suppression. Matrix effects for cyclic imines depended on chromatographic conditions (Table 3-4), and generally suffered from signal suppression under acidic conditions and moderate signal enhancement at more alkaline pH. The use of different chromatographic conditions affects matrix effects by altering the elution order of interferences, but this effect is difficult to assess, and it had not been systematically studied before.

Matrix effects may explain deviations in recovery, a problem often reported in lipophilic toxin determination by LC-MS/MS [12, 17, 20, 22-24]. Signal suppression of AZA1, SPX1 and GYMA under pH 2 could explain the low recovery of these toxins, while OA signal enhancement correlated with the overestimation of OA in mussels and sea urchin. Under pH 6.8 and pH 7.9, the strong signal suppression for AZA1 in all matrices may explain the problems with trueness. Moreover, signal enhancement under pH 6.8 may explain the recoveries over 110% for SPX1, while signal suppression for GYMA in sea urchin and for SPX1 in clams correlated with insufficient recoveries.

The statistical analysis showed that matrix effects were species dependent for YTX and GYMA (Figure 3-3): all seafood matrices enhanced YTX signal in the LC-MS/MS, but the signal promotion was significantly lower ($p < 0.001$) in mussels that in the rest of the matrices tested. GYMA signal suppression was significantly higher ($p = 0.032$) in sea urchin matrix than in mussel matrix.

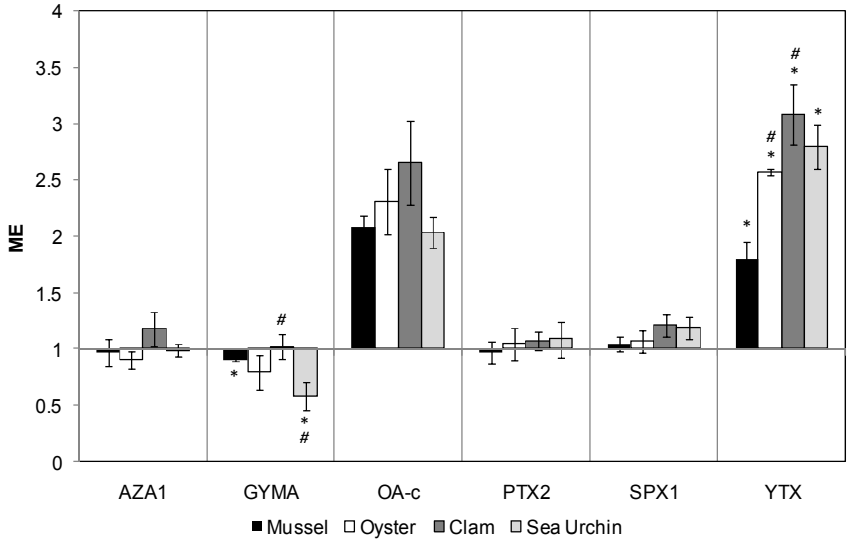

Figure 3-3. Matrix effects (ME) under alkaline conditions, expressed as the ration between the slopes of a calibration curve prepared in methanolic seafood extracts against the slope of a calibration curve prepared in MeOH (n=3). ME > 1 means signal enhancement; ME < 1 means signal suppression; ME =1 means no matrix effect. * and # represent significant differences (Tukey Test, p value < 0.05).

We assessed the accuracy of the method with EXS and MMS (Table 3-7). Precision was evaluated as the HorRat value for intraday precision and trueness was assessed as recovery. We found that the calibration strategy of MMS improved method accuracy for the determination of GYMA and PTX2, since both toxins showed low recoveries (below 80%) when the spiked samples were quantified against an EXS curve. Figure 3-3 shows that GYMA tended to suffer from signal inhibition by seafood matrices, thus MMS would be a suitable approach to obtain satisfactory recovery values for this toxin. The recoveries of AZA1 and SPX1 were slightly higher when the spiked samples were quantified against a MMS curve. However, the use of MMS did not have a great impact in the correction of matrix effects in the determination of these toxins. Okadaic acid tended to show a strong signal enhancement influenced by seafood matrices; this observation agreed with the literature [11, 14, 21, 23]. The recoveries found for OA when the spiked samples were quantified against an EXS curve ranged from 114% (when 80 µg/kg were spiked in clams tissue), to 225% (when 240 µg/kg were spiked in mussels tissue). The use of MMS drastically dropped the recovery values for OA, ranging from 61% (240 µg/kg OA spiked in oyster) to 104% (160 µg/kg spiked in mussel), and being over 70% in most of the cases. In the case of hydrolysed samples, the recovery of OA in hydrolysed extracts decreased following the same trend. However, only hydrolysed mussel samples had good recoveries with MMS, the recoveries for other seafood species were below 80%, although MMS did not noticeably affect precision. Regarding YTX, recoveries drastically decreased with MMS compared to those found with EXS, which were extremely high during this experiment. Nevertheless, only the results for mussels were accurate, since MMS negatively affected precision for YTX and the variation among injections was too high to provide reliable results.

Table 3-7. Trueness as recovery (R, in %) and precision as HorRat value (no units) for the determination of lipophilic toxins under alkaline conditions by triple injection with two calibration strategies: External Standard calibration (EXS) and Matched Standard calibration (MMS).

		AZA1		GYMA		OA		OA Hydrolized		PTX2		SPX1			YTX	
		EXS	MMS	EXS	MMS	EXS	MMS	EXS	MMS	EXS	MMS	EXS	MMS		EXS	MMS
Mussel																
80	R (%)	99.6	110.0	63.8	92.8	175.7	83.0	211.3	81.1	61.8	98.0	98.5	117.0	*250*	232.8	109.1
µg/kg	HorRat	0.4	0.5	0.8	0.4	0.7	1.1	0.3	0.1	0.3	0.2	0.3	0.6	*µg/kg*	0.2	1.3
160	R (%)	104.7	102.8	68.1	83.6	196.9	103.8	222.3	81.5	59.6	88.9	90.8	90.5	*500*	173.3	71.4
µg/kg	HorRat	0.6	0.4	0.4	0.4	0.4	0.3	0.7	0.1	0.3	0.4	0.4	0.5	*µg/kg*	0.7	0.5
240	R (%)	114.3	110.2	69.4	89.4	225.3	84.4	289.7	106.6	66.1	85.0	109.1	98.4			
µg/kg	HorRat	0.5	0.3	0.0	0.5	0.5	0.9	0.8	0.8	0.2	0.5	0.5	1.0			
Oyster																
80	R (%)	108.5	120.4	79.6	108.1	135.7	80.7	159.0	55.4	66.4	103.5	87.4	119.0	*250*	147.2	57.7
µg/kg	HorRat	0.3	0.7	1.0	0.4	1.0	0.2	0.8	0.9	0.5	0.9	0.3	0.6	*µg/kg*	0.3	1.7
160	R (%)	96.1	111.6	75.3	95.2	137.5	66.2	186.2	49.0	56.1	91.4	78.0	105.1	*500*	115.5	40.1
µg/kg	HorRat	0.3	0.3	0.7	0.5	0.1	0.7	0.8	0.8	0.0	0.7	0.4	0.2	*µg/kg*	0.5	1.9
240	R (%)	101.2	100.9	79.3	92.1	154.2	61.5	158.3	49.5	68.4	81.8	81.1	98.6			
µg/kg	HorRat	0.3	0.6	0.2	0.4	0.0	0.5	1.6	0.4	0.1	0.2	0.1	0.2			
Clam																
80	R (%)	92.5	103.1	69.6	90.8	114.5	68.1	143.1	53.8	64.5	89.3	67.9	88.3	*250*	130.8	59.1
µg/kg	HorRat	0.3	0.6	0.8	0.6	0.9	0.3	0.8	0.7	0.1	0.7	0.5	0.2	*µg/kg*	0.6	1.3
160	R (%)	97.9	114.6	77.3	101.3	143.1	70.5	186.2	43.4	78.5	92.9	78.8	93.1	*500*	94.3	39.0
µg/kg	HorRat	0.3	0.4	0.9	0.1	0.3	0.8	0.8	0.6	0.2	0.4	0.8	0.5	*µg/kg*	0.3	1.1
240	R (%)	112.5	101.4	87.2	95.5	173.1	84.3	166.2	40.2	79.5	89.0	90.5	91.0			
µg/kg	HorRat	0.3	0.3	0.3	0.2	0.6	0.1	1.8	0.1	0.7	0.6	0.4	0.7			
Sea Urchin																
80	R (%)	99.7	115.0	55.0	95.9	140.0	69.7	201.8	45.5	74.5	91.9	77.7	82.3	*250*	156.2	64.9
µg/kg	HorRat	0.5	0.5	0.7	0.8	1.0	1.0	1.0	2.0	0.2	0.4	0.4	0.3	*µg/kg*	0.7	1.7
160	R (%)	109.1	108.7	63.1	98.4	138.7	84.8	194.1	39.2	80.6	91.1	81.4	91.6	*500*	136.1	48.1
µg/kg	HorRat	0.5	0.8	1.3	0.2	0.1	0.4	1.3	1.4	0.3	0.5	0.2	0.7	*µg/kg*	0.7	1.1
240	R (%)	117.3	110.0	62.3	93.5	181.6	77.8	160.4	52.6	77.8	96.3	85.9	82.8			
µg/kg	HorRat	0.1	0.6	0.4	0.3	1.0	0.2	1.6	1.2	0.0	0.0	0.6	0.9			

The species dependence of matrix effect may determine if MMS prepared in one species may compensate matrix effects for other species, but the previous studies on the topic did not reach a consensus. Gerssen *et al.* [13] proved that the MMS prepared in blank mussel extract can be used for matrix effect correction even in other seafood matrices, since the influence of the species in the method was negligible. On the other hand, several studies claimed that matrix effects seem to be species dependent. Stobo *et al.* [17] found that matrix effects varied depending on the type of seafood matrix, even for the same toxin. For example, signal suppression for AZA1 was more evident for king scallop than for mussels, cockles and oysters matrices. Kilcoyne and Fux [23] found that the differences in recovery of OA in spiked samples of several seafood tissues were statistically significant. Moreover, the degree of suppression of the AZA1 signal was also species dependent, and the article even warned about the possibility of differences in matrix effects between samples of the same species but collected in different locations due to differences in the diet and physiological state of the organisms. McCarron *et al.* [24] also highlighted the importance of finding a proper matrix to be used as a match in the MMS strategy.

Matrix effects in lipophilic toxins analysis have been extensively studied. Besides MMS, other groups have proposed several techniques to compensate matrix effects: solid phase extraction (SPE) clean-up [12, 23], optimization of the chromatographic method [23], selection of the appropriate instrumentation [20, 23], sample dilution [20], and standard addition [22, 24]. All techniques their disadvantages, mostly related to the additional time and amount of standards needed, thus the selection of a proper strategy to deal with matrix effects is not trivial.

We demonstrated that matrix effects are species dependent for some lipophilic toxins in seafood, thus MMS may not be always suitable to compensate matrix effects under alkaline conditions. Besides, this strategy is more time and standards consuming than the EXS. In our laboratory of shellfish harvesting monitoring, we decided to use EXS as the quantification strategy, since we rarely analyze seafood samples with the toxins that benefit the most from the MMS (GYMA, PTX2 and AZA1). We correct OA recoveries (the most prevalent toxin in our study area) in mussels and oysters with the certified reference material of mussels naturally contaminated with OA, commercially available as CRM-DSP Mus b by the NRC (Canada), since the matrix effects for OA have been proved to be not species-dependent for crude extracts.

In the comparative study between quantification strategies, the low recoveries found for PTX2 using the EXS strategy (Table 3-7) were unexpected, since the in-house validation under pH 11 was performed with the same quantification strategy and the recoveries were satisfactory in that case (Table 3-6). The contradiction between both experiments, which were performed using the exact same method and spiked samples, might be explained by the number of replicates used: the in-house validation experiment assessed intermediate accuracy (four different spiked samples extracted in four days and analyzed by single injection), whereas the EXS strategy experiment evaluated intraday accuracy (one sample analyzed by triple injection in one day). PTX2 is rarely found in seafood matrices, since it is rapidly metabolized into PTX2-sa [31]. The analysis of YTX was very challenging, even under alkaline conditions. The poor precision of the method during the analysis with EXS strategy could explain the overestimation of YTX during this experiment (Table 3-7), which is contradictory with the recoveries found during the in-house validation process (Table 3-6). We expect that the routinely application of the method

and the definition of proper strategies for quality control, such as the participation in collaborative studies and the use of internal reference standards to correct recoveries, will help us to improve the quantitative determination of YTX in seafood samples. As a result of these experiments, we found indispensable to increase the number of replicates to achieve good accuracy in the analysis of YTX.

We highlight the selection of the mobile phase is a crucial step to implement the LC-MS/MS method: it affects chromatographic separation, sensitivity, LOQs, accuracy and matrix effects. We did not investigate the effect of LC conditions on the MS/MS behavior as we follow the recommendations stated in the EURLMB SOP and because the amount of standards needed for that task is unaffordable by our laboratory. The impact of different elution conditions on tandem MS detection should be further investigated. Mobile phase can affect the ionization yield and nature of precursor ions in the ESI source, but it may also alter the MS^2 spectra: ion fragmentation is not always independent of the ionization environment [32, 33]. The next EURLMB SOP shall address this issue.

We consider unlikely that one single set of conditions could work perfectly for all toxin profiles and matrices, thus we would encourage the laboratories to include their priorities regarding toxin and samples types in the decision-making process to implement their methods. This concern has been faced before in marine toxin analysis: the suitability of HPLC methods for paralytic shellfish poisoning (PSP) depending on the toxin profile is already well known as one of the issues that are hindering the adoption of HPLC-FLD methods to replace the bioassays [34, 35]. Nevertheless, the availability of different methods must be seen as a tool for the analyst to gain a better understanding of the marine toxins in environmental matrices.

3.4 Conclusion

The method based on LC-MS/MS for the determination of lipophilic toxins in seafood has been accepted by the European Union as a reliable technique to protect public health and reduce the use of animals for routine analysis. The EURLMB SOP [11] establishes a solid framework for the implementation of the LC-MS/MS method but it is not explicit enough concerning the chromatographic conditions and the matrix effect correction strategy that should be used. The current study is the first work aimed to compare the most common chromatographic alternatives for the determination of lipophilic toxins in seafood by LC-MS/MS in terms of functionality, quality criteria, validation parameters and quantification strategies under the same experimental settings (extraction and hydrolysis procedures, chromatographic column, MS instrument conditions, standards and reagents, and analyst). In our case, we chose the alkaline conditions, External Standard calibration as quantification strategy, and recovery correction for OA with CRM-DSP Mus b to be implemented as the routine method. Alkaline conditions provide higher sample throughput, lower LOQs, and the best overall performance in terms of sensitivity and accuracy in the validation study. The EXS strategy combined with OA recovery correction by CRM-DSP Mus b demanded less time and standard investment and provided satisfactory results. The analysis of YTX was challenging and it is still being improved in our laboratory by increasing the number of injections, participating in collaborative studies and preparing internal reference standards to correct YTXs recoveries.

When selecting the best chromatographic conditions, factors such as the instrumentation available (regarding polarity switching, limits of detection), the number of samples needed to analyze, the toxin profile and the sample matrices should be considered. The matrix effects should be examined carefully, especially when including a new toxin in the method or analyzing a new matrix. A proper selection process may be time and resources demanding, but we hope that this comparative study may serve as starting point to other laboratories implementing their own methods for lipophilic toxins determination in seafood by LC-MS/MS.

References

1. Hoagland, P. and S. Scatasta, *The Economic Effects of Harmful Algal Blooms*, in *Ecology of Harmful Algae*, E. Granéli and J.T. Turner, Editors. 2006, Springer Berlin Heidelberg.
2. European Commission, *Regulation (EC) No 15/2011.* Official Journal of the European Union, 2011. **L 6**(3).
3. European Commission, *Regulation (EC) No 853/2004.* Official Journal of the European Union, 2004. **L 226**(22).
4. Alexander, J., et al., *Marine biotoxins in shellfish–Summary on regulated marine biotoxins Scientific Opinion of the Panel on Contaminants in the Food Chain.* The EFSA Journal, 2009. **1306**: p. 1-23.
5. Quilliam, M.A., P. Hess, and C. Dell'Aversano, *No Title*, in *Mycotoxins and Phycotoxins in Perspective at the Turn of the Century*, W.J. DeKoe, et al., Editors. 2001: Wageningen, The Netherlands. p. 383-391.
6. McNabb, P., A. Selwood, and P.T. Holland, *Multiresidue method for determination of algal toxins in shellfish: Single-laboratory validation and interlaboratory study.* Journal of AOAC International, 2005. **88**: p. 761-772.
7. Chapela, M.-J., et al., *Lipophilic toxins analyzed by liquid chromatography-mass spectrometry and comparison with mouse bioassay in fresh, frozen, and processed molluscs.* Journal of agricultural and food chemistry, 2008. **56**: p. 8979-86.
8. Fux, E., et al., *Development of an ultra-performance liquid chromatography-mass spectrometry method for the detection of lipophilic marine toxins.* Journal of Chromatography A, 2007. **1157**(1-2): p. 273-280.
9. Hess, P., et al., *Tissue distribution, effects of cooking and parameters affecting the extraction of azaspiracids from mussels, Mytilus edulis, prior to analysis by liquid chromatography coupled to mass spectrometry.* Toxicon, 2005. **46**: p. 62-71.
10. Villar-González, A., et al., *Lipophilic toxin profile in Galicia (Spain): 2005 toxic episode.* Toxicon, 2007. **49**: p. 1129-1134.
11. EURLMB, *Interlaboratory Validation Study of the EU-Harmonised SOP LIPO LC MS/MS*. 2011.
12. Gerssen, A., et al., *Liquid chromatography-tandem mass spectrometry method for the detection of marine lipophilic toxins under alkaline conditions.* Journal of chromatography A, 2009. **1216**: p. 1421-1430.
13. Gerssen, A., et al., *In-house validation of a liquid chromatography tandem mass spectrometry method for the analysis of lipophilic marine toxins in shellfish using matrix-matched calibration.* Analytical and Bioanalytical Chemistry, 2010. **397**: p. 3079-3088.
14. Regueiro, J., et al., *Automated on-line solid-phase extraction coupled to liquid chromatography-tandem mass spectrometry for determination of lipophilic marine toxins in shellfish.* Food Chemistry, 2011. **129**(2): p. 533-540.
15. van der Fels-Klerx, H.J., et al., *Monitoring phytoplankton and marine biotoxins in production waters of the Netherlands: results after one decade.* Food additives & contaminants. Part A, Chemistry, analysis, control, exposure & risk assessment, 2012. **29**(10): p. 1616-1629.
16. Rossignoli, A.E., et al., *Esterification of okadaic acid in the mussel Mytilus galloprovincialis.* Toxicon, 2011. **57**(5): p. 712-720.
17. Stobo, L.a., et al., *Liquid chromatography with mass spectrometry--detection of lipophilic shellfish toxins.* Journal of AOAC International, 2005. **88**: p. 1371-82.
18. These, A., J. Scholz, and A. Preiss-Weigert, *Sensitive method for the determination of lipophilic marine biotoxins in extracts of mussels and processed shellfish by high-performance liquid*

chromatography-tandem mass spectrometry based on enrichment by solid-phase extraction. Journal of Chromatography A, 2009. **1216**(21): p. 4529-4538.

19. van den Top, H.J., et al., *Quantitative determination of marine lipophilic toxins in mussels, oysters and cockles using liquid chromatography-mass spectrometry: inter-laboratory validation study.* Food additives & contaminants. Part A, Chemistry, analysis, control, exposure & risk assessment, 2011. **28**(12): p. 1745-57.
20. Fux, E., et al., *Approaches to the evaluation of matrix effects in the liquid chromatography-mass spectrometry (LC-MS) analysis of three regulated lipophilic toxin groups in mussel matrix (Mytilus edulis).* Food additives & contaminants. Part A, Chemistry, analysis, control, exposure & risk assessment, 2008. **25**: p. 1024-32.
21. Gerssen, A., et al., *Solid phase extraction for removal of matrix effects in lipophilic marine toxin analysis by liquid chromatography-tandem mass spectrometry.* Analytical and Bioanalytical Chemistry, 2009. **394**(4): p. 1213-1226.
22. Ito, S. and K. Tsukada, *Matrix effect and correction by standard addition in quantitative liquid chromatographic-mass spectrometric analysis of diarrhetic shellfish poisoning toxins.* Journal of chromatography A, 2002. **943**: p. 39-46.
23. Kilcoyne, J. and E. Fux, *Strategies for the elimination of matrix effects in the liquid chromatography tandem mass spectrometry analysis of the lipophilic toxins okadaic acid and azaspiracid-1 in molluscan shellfish.* Journal of chromatography A, 2010. **1217**: p. 7123-30.
24. McCarron, P., et al., *Identification of pinnatoxins and discovery of their fatty acid ester metabolites in mussels (mytilus edulis) from eastern Canada.* Journal of Agricultural and Food Chemistry, 2012. **60**: p. 1437-1446.
25. Mountfort, D.O., T. Suzuki, and P. Truman, *Protein phosphatase inhibition assay adapted for determination of total DSP in contaminated mussels.* Toxicon, 2000. **39**(2-3): p. 383-390.
26. Taverniers, I., M. De Loose, and E. Van Bockstaele, *Trends in quality in the analytical laboratory. II. Analytical method validation and quality assurance.* TrAC - Trends in Analytical Chemistry, 2004. **23**(8): p. 535-552.
27. European Commission, *Commision Decission 2002/657/EC.* Official Journal of the European Union, 2002. **L 221**(8).
28. de la Iglesia, P., G. Giménez, and J. Diogène, *Determination of dissolved domoic acid in seawater with reversed-phase extraction disks and rapid resolution liquid chromatography tandem mass spectrometry with head-column trapping.* Journal of Chromatography A, 2008. **1215**(1-2): p. 116-124.
29. Horwitz, W. and R. Albert, *The Horwitz ratio (HorRat): A useful index of method performance with respect to precision.* Journal of AOAC International, 2006. **89**: p. 1095-1109.
30. Kaufmann, A., et al., *Are liquid chromatography/electrospray tandem quadrupole fragmentation ratios unequivocal confirmation criteria?* Rapid Communications in Mass Spectrometry, 2009. **23**(7): p. 985-998.
31. Miles, C.O., et al., *Isolation of pectenotoxin-2 from Dinophysis acuta and its conversion to pectenotoxin-2 seco acid, and preliminary assessment of their acute toxicities.* Toxicon, 2004. **43**: p. 1-9.
32. Desaire, H., M.D. Leavell, and J.A. Leary, *Solvent effects in tandem mass spectrometry: Mechanistic studies indicating how a change in solvent conditions and pH can dramatically alter CID spectra.* Journal of Organic Chemistry, 2002. **67**(11): p. 3693-3699.
33. Wang, J., et al., *Effect of mobile phase pH, aqueous-organic ratio, and buffer concentration on electrospray ionization tandem mass spectrometric fragmentation patterns: Implications in liquid chromatography/tandem mass spectrometric bioanalysis.* Rapid Communications in Mass Spectrometry, 2010. **24**(22): p. 3221-3229.

34. Ben-Gigirey, B., et al., *Influence of the sample toxic profile on the suitability of a high performance liquid chromatography method for official paralytic shellfish toxins control.* Journal of chromatography A, 2007. **1140**: p. 78-87.
35. Rodríguez, P., et al., *Comparative analysis of pre- and post-column oxidation methods for detection of paralytic shellfish toxins.* Toxicon, 2010. **56**(3): p. 448-457.

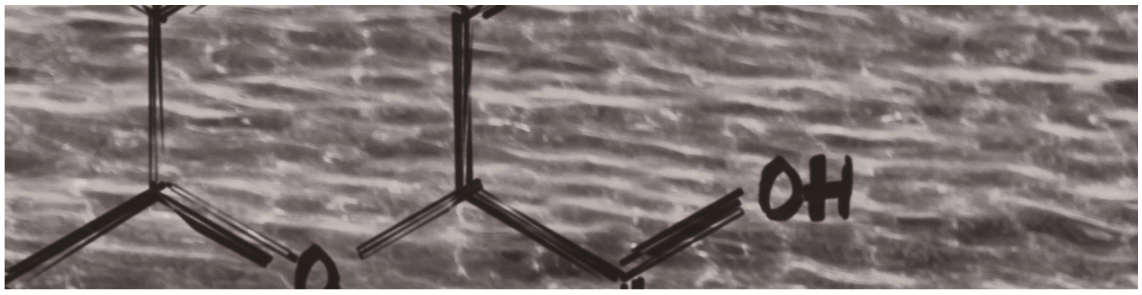

CHAPTER 4

Bloom of *Dinophysis* spp. Dominated by *D. sacculus* and Its Related Diarrheic Shellfish Poisoning (DSP) Outbreak in Alfacs Bay (Catalonia, NW Mediterranean Sea): Identification of DSP Toxins in Phytoplankton, Shellfish and Passive Samplers

Running Title: ***Dinophysis* bloom and DSP shellfish toxicity in Alfacs Bay**

Submitted as:

García-Altares, M., A. Casanova, M. Fernández, J. Diogène, and P. de la Iglesia, *Bloom of* Dinophysis *spp. dominated by* D. sacculus *and its related Diarrheic Shellfish Poisoning (DSP) outbreak in Alfacs Bay (Catalonia, NW Mediterranean Sea): identification of DSP toxins in phytoplankton, shellfish and passive samplers.* Submitted to Harmful Algae in February 2015.

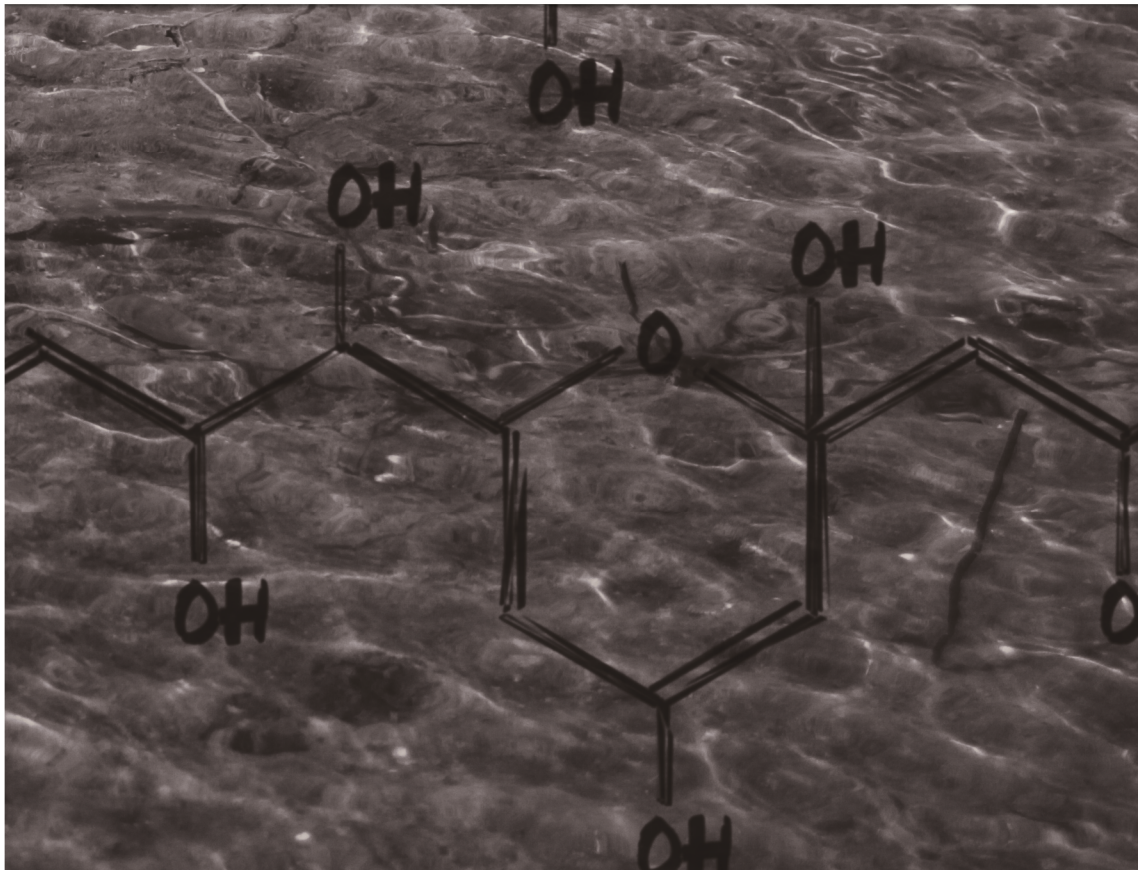

Abstract

We report a comprehensive study of a diarrhetic shellfish poisoning (DSP) outbreak in a Mediterranean coastal embayment, integrating phytoplankton identification and enumeration data, with toxin analysis by LC-MS/MS of shellfish samples (mussels and oysters), phytoplankton concentrates (filters and vertical net-hauls), and solid phase adsorbing toxin tracking (SPATT) devices. Alfacs Bay was proposed as a model for the study of semi-enclosed coastal embayments and it is the most important shellfish farming area in Catalonia (Spain, NW Mediterranean Sea). The bay suffered a ban for bivalve harvesting that lasted 78 days, from late winter to the end of the spring of 2012, due to a harmful algae bloom of the toxic dinoflagellate *Dinophysis sacculus* that fluctuated in three abundance peaks, reaching maximum abundance of 2200 cell/L. Mussels sampled during the bloom contained okadaic acid (OA, maximum 592 μg/kg, 3.7 times the maximum permitted level (MPL) set by the European Commission), and pectenotoxin-2 (PTX2, maximum 61 μg/kg). Oysters also contained OA and PTX2, but always below the MPL. Cell toxin content measured from phytoplankton concentrates in filters and from net-haul samples differed in two orders of magnitude, and it was most likely overestimated in filters (up to 461 pg OA/cell and 668 pg PTX2/cell), but showed an increase of cell toxicity towards the end of the bloom. OA-diol esters were not detected. Concentration of DSP toxins in SPATT devices were up to 94 ng OA/g resine·day, 42 ng PTX2/g resine·day and 7 ng PTX2-sa/g resine·day. The applied monitoring strategy, based on the measurement of *Dinophysis* cell abundance in the water column, was effective to protect public health and did not extended the regulatory closure unnecessarily. Concentration of DSP in SPATT bags followed *Dinophysis* abundance dynamics, thus SPATTs were confirmed as a valuable research tool for *Dinophysis* blooms.

Keywords

Dinophysis; Mediterranean Sea; Liquid Chromatography-Mass Spectrometry; Diarrhetic Shellfish poisoning; Solid Phase Adsorbing Toxin Tracking; phytoplankton concentrates

4.1 Introduction

The accumulation of marine toxins in shellfish is one of the most concerning negative effect of harmful algae blooms in marine environments. Among the several illnesses caused by contaminated bivalves, diarrhetic shellfish poisoning (DSP) is the syndrome that has caused more toxic events in the Mediterranean northwest coast of Spain [1]. The DSP toxin group (comprising okadaic acid (OA), dinophysistoxins (DTXs) and pectenotoxins (PTXs)) is also the one that leads to more banning days for bivalve producers [2] when its concentration in shellfish exceeds the maximum permitted level (MPL) set by the European Union (160 μg/kg of bivalve flesh [3]).

The toxins associated with DSP are produced by dinoflagellates of the genus *Dinophysis* (and *Phalacroma rotundatum*, formerly *D. rotundata*), and *Prorocentrum* spp. In the Mediterranean coasts, the highest abundance of *Dinophysis* cells were recorded between 2003 and 2008 in the eastern Mediterranean (Greece), where *Dinophysis* blooms occurred periodically in late winter and spring, with concentrations over 85,000 cell/L and regulatory closures longer than 150 days [4]. *Dinophysis* populations in the Adriatic Sea are also related to DSP toxicity, mostly in the most eutrophicated regions, and involve six species (*D. acuminata, D. sacculus, D. caudata, D. fortii, P. rotundatum* and *D. tripos*) that bloom consecutively from sprint until winter [5]. *Dinophysis* abundances reached 25,000 cell/L during 2008 in the Mediterranean Bizerte Lagoon (northern Tunisia), where *Dinophysis* blooms comprise three species: *D. sacculus, D. accuminata* and *P. rotundatum* [6]. Similar abundances where found during 1998 in Sicily (western Mediterranean Sea) in a bloom dominated by *D. sacculus*, which seems to be the most common species in this region of the Mediterranean Sea [7]. Blooms of *Dinophysis* are also a recurrent problem in Alfacs Bay [2], the main production area for bivalves in Catalonia (Spain, NW Mediterranean Sea). In spring of 2012, a bloom of *Dinophysis* caused the closure of Alfacs Bay for bivalve extraction during 11 weeks. The MPL in mussels for DSP toxins was exceeded during 78 days which resulted in important economic losses for the Catalan aquaculture sector.

Dinophysis are carefully monitored in the Mediterranean basin, but harmful events of DSP toxicity are very difficult to predict, as it is been reported in several studies that found a weak or even no correlation between cell abundances of *Dinophysis* spp. and toxins levels of DSP [8-14], although other studies found a good correlation between cell abundances and toxicity [15, 16]. Many factors could explain the absence of correlation between cell abundances and toxicity. First, *Dinophysis* spp. blooms are strongly linked to weather conditions: water column stratification (due to warm temperatures and low wind) favor bloom initiation and maintenance, and wind-induced currents influence their transport [17], thus spatio-temporal distribution of the bloom is difficult to predict, which complicates sampling. Second, D*inophysis* spp. blooms present high intra-cell toxin variability during the bloom, and even along the same day [18, 19], thus it is the product of cell abundance and cell toxicity which will influence shellfish toxicity [20].Third, the dynamics of the prey *Mesodinium* spp. is another factor to consider, since its availability is one of the main drivers of *Dinophysis* cell growth, which alters toxin quotas [8, 18, 21]. Filtration rates, accumulation of toxins and availability of alternative food sources for shellfish [8, 16, 22] are factors that also may determine the toxin content in bivalves, and this also complicates the prediction of the toxic events based on cell abundances. A

proper spatio-temporal design of the sampling of the shellfish and the phytoplankton community is the key to provide useful information to managers and aquaculture producers on the presence of toxins and toxin-producing microalgae. The use of solid phase adsorbing toxin tracking (SPATT) devices has been proposed as an early-warning tool to detect lipophilic toxins in bivalves farms [23], but its use as monitoring tool has been questioned, as some authors have found overestimation of the expected toxin levels in shellfish [24].

The toxic phytoplankton species and their related toxins in shellfish are monitored in Catalonia on a routine basis by IRTA-Research and Technology-Food and Agriculture, since 1999. The strategy of the monitoring program has been proven to be an efficient tool to protect public health in the study area, which has been based on the identification and quantification of microalgae in the water column as an early warning parameter and the analysis of shellfish tissue by the mouse bioassay (MBA). The inclusion of Liquid Chromatography coupled to Mass Spectrometry (LC-MS) as coexisting reference method for lipophilic toxins in bivalves [25] was adopted at IRTA in 2012 as an opportunity to investigated the dynamics of *Dinophysis* spp. blooms and its related DSP toxicity in shellfish, and currently it is the method used for the management of shellfish harvesting areas since January 1st 2015.

This work reports a case study that will contribute to better understand the process of bloom development and behavior for *Dinophysis* spp. in Alfacs Bay, which was proposed as a pilot site for comparative studies of HABs in coastal embayments within the Global Ecology and Oceanography of Harmful Algal Blooms (GEOHAB) program [26]. Alfacs Bay and its almost permanent stratification posed a good opportunity to contribute to one of the Core Projects of GEOHABS, the study of HABs in Stratified Systems, which have specific characteristics regarding sampling, modelling and chemically mediated interactions among the thin layers of the stratified water column. Besides, this study will help the assessment of the current monitoring strategies in Catalonia [27].

This study focuses on two consecutive toxic outbreaks of *Dinophysis* spp. occurred in Alfacs Bay during the spring of 2012. We investigated quantitatively and qualitatively the toxins profiles associated with the wild toxic populations of *Dinophysis* spp. in plankton concentrates from sea water (vertical net-hauls and filters concentrates), and studied their relationship with DSP toxin levels in SPATT devices and in two shellfish species (mussels and oysters). The suitability of early warning systems of the monitoring program, such as the use of SPATT devices and the *Dinophysis* spp. abundance current threshold of 500 cell/L, was discussed in light of our results.

4.2 Materials and Methods

4.2.1 Study area

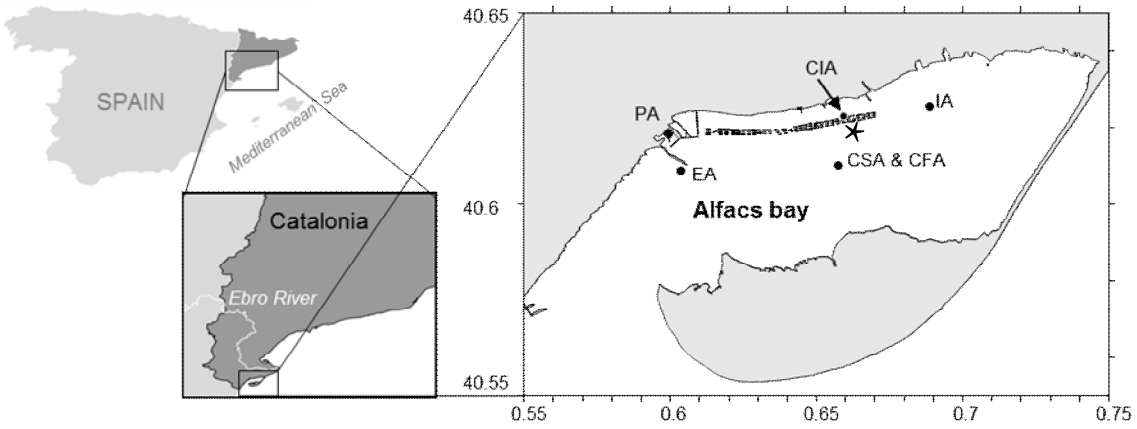

Figure 4-1. Map of Alfacs Bay in the Ebro River Delta (NW Mediterranean). Dots represent sampling stations (PA: Port Alfacs, EA: Exterior Alfacs, CIA: Central Interior Alfacs, CSA & CFA: Central Alfacs, surface (S) and bottom (F), IA: Interior Alfacs, BA: Buoy Alfacs). The star symbol (*) indicates the location of the buoy.

Alfacs Bay is a semi-enclosed water body located in the northeast coast of Catalonia (Spain; Figure 4-1), in the southern part of the Ebro River Delta. It is about 12 km long, 4 km wide, with an average depth of 3 m (maximum depth of 6 m), separated from the Mediterranean Sea by a sand barrier up to the western end, where its mouth of 2.5 km is located [28]. The maximum income of freshwater inputs occurs between April and October each year (approximately $275 \cdot 10^6$ m^3 from its northern edge) according to the seasonal pattern driven by rice cultivation in the region [29, 30]. Alfacs Bay has a Chl *a* concentration higher than other coastal waters in the Mediterranean [31, 32], and this stimulates the shellfish aquaculture in the bays [33]: the annual production of mussels in the Ebro Delta reaches 3000 t per year from the 166 bivalves farms, being 90 of them located in Alfacs Bay [34].

4.2.2 Sampling

Six sampling stations were selected for the study (Figure 4-1): PA: Port Alfacs (N 40º 37.038', E 0º 35.869'), EA: Exterior Alfacs (N 40º 36.456', E 0º 36.148'), CIA: Central Interior Alfacs (N 40º 37.328', E 0º39.491'), CA: Central Alfacs (N 40º36.453', E 0º39.369', CSA: surface; CFA: bottom), IA: Interior Alfacs (N 40º 37.465', E 0º 41.253'), BA: Buoy Alfacs (N 40º 37.152', E 0º 39.757').

Phytoplankton samples were collected for identification and quantification at all sampling stations.

At the buoy sampling station (BA), phytoplankton samples were collected by vertical net hauls (25 cm diameter, 20 µm mesh size) in the upper 5 m to obtain integrated samples of the whole water column. The total volume collected by the vertical net-haul was estimated mathematically (Volume = $\pi \cdot radio^2 \cdot length$; with 25 cm diameter and 5 m length) to be 245.5 L. The total final

volume of filtered seawater collected (400 mL) was filtered under low vacuum through 0.45 µm nylon filters and stored in methanol at -20ºC. In order to estimate toxin content per cell, cell abundances were obtained from integrated water samples.

At Central Alfacs (CSA) and Interior Alfacs (IA) sampling stations, samples of approx. 2.5 L of sea water from 0.5 m depth (surface) were collected with a plastic container. A subsample of approximately 100 mL was kept for phytoplankton identification and quantification, the rest of the volume was filtered under low vacuum through 0.45 µm nylon filters and stored at -80ºC until extraction.

Close to Central Interior Alfacs (CIA), from several surrounding rafts, approximately 1.5 kg per sample of blue mussels (*Mytilus galloprovincialis*) and Pacific oysters (*Crassostrea gigas*) were collected from the shellfish harvesting racks in Alfacs Bay. Shellfish was properly cleaned and opened, and at least 100 g of shellfish tissue per sample was obtained and homogenized with a hand blender.

At buoy sampling station (BA), solid-phase adsorption toxin tracking (SPATT) [23] devices used as passive samplers of dissolved lipophilic toxins in seawater were prepared and desorbed in methanol following the protocol explained in Caillaud et al [35]. Briefly, the SPATT devices were prepared in the laboratory with ~10 g of wet adsorbent styrene-divinylbenzene resin (DIAON® HP20, Mitsubishi Chemical Corporation, Tokyo, Japan). Then, SPATT bags were preserved in water at 4ºC prior to their use. SPATT bags were disposed in the field at a depth of 0,5m and remained immersed in the marine environment for a week.

4.2.3 *Dinophysis* spp. identification and quantification

Phytoplankton cells were counted according to the Utermhöl method [36] with a Nikon or Leica DMIL inverted microscopes settling 50 mL in Hydrobios chambers. The entire bottom of the chamber was counted at 100–200× magnification to quantify *Dinophysis* species.

4.2.4 Preparation of extracts

Cells on filters were extracted with 4 mL of methanol, vortex-mixed for 30 seconds by MS2 Minishaker (IKA Labortechnik, Staufen, Germany) and sonicated for 30 minutes in an ultrasonic bath. The mixture was centrifuged at 3,000 rpm for 10 minutes using a Jouan MR 23i centrifuge (Thermo Fisher Scientific Inc., Waltham, MA, USA) and the supernatant was decanted and then filtered through 0.45 µm nylon membrane syringe filters. This procedure was repeated twice. The extracts were combined, evaporated under nitrogen flow and made up to a final volume of 1 mL with methanol.

For shellfish samples, a triple-step extraction with methanol (10 mL) was performed on whole homogenated tissues (1 g) according to the procedure proposed by Gerssen et al[37] which was also validated intra-laboratory by our group [38]. Analytical balance Sartorius 1702 (Goettingen, Germany), a vortex-mixer MS2 Minishaker (IKA Labortechnik, Staufen, Germany) and a centrifuge Jouan MR 23i (Thermo Fisher Scientific Inc., Waltham, MA, USA) were used. Crude extracts were filtered through polytetrafluoroethylene (PTFE) 0.2 µm membrane syringe filters.

The alkaline hydrolysis of the samples was performed according to the EURLMB SOP [39] based on the protocol developed by Mountfort et al. [40].
For toxin desorption from SPATT devices, the resin was removed, washed with ultrapure water and filtered under vacuum. Then the resin was extracted twice with methanol 100% in a solvent:resin ratio of 8:1 mL/g of resin. Finally, the two methanolic extracts were combined and evaporated, and the dry extract was dissolved in 5 mL of 100% methanol previous to LC-MS analyses.

4.2.5 Standards and chemicals

Certified reference standard solutions were purchased from the Institute for Marine Bioscience of the National Research Council (NRC) from Halifax (Canada): okadaic acid (OA, 14.3 ± 1.5 µg/mL), yessotoxin (YTX, 5.3 ± 0.3 µg/mL), pectenotoxin-2 (PTX2, 8.6 ± 0.3 µg/mL), azaspiracid-1 (AZA1, 1.24 ± 0.07 µg/mL), 13-desmethyl spirolide-C (SPX1, 7.0 ± 0.4 µg/mL, and gymnodimine-A (GYMA, 5.0 ± 0.2 µg/mL).

Certified reference standard solutions for dinophysistoxin-1 (DTX1) and dinophysistoxin-2 (DTX2) were not available, thus a sample of mussel (*Mytilus galloprovincialis*) naturally contaminated with OA, DTX1 and DTX2 from the inter-laboratory proficiency test for lipophilic toxins organized by the EURLMB in 2010 was used as a reference of retention times. Okadaic acid C8 diol ester (CAS 318536-96-8) was purchased from Marbionc (Wilmington, North Carolina, USA).

Acetonitrile (ACN) hypergrade for LC-MS, acetic acid and methanol gradient grade for HPLC were purchased from Merck (Darmstadt, Germany). Ammonium hydroxide solution (≥25% in H_2O, eluent additive for LC-MS) and LC-MS grade water was purchased from Sigma-Aldrich (Steinheim, Germany). Ultrapure water was obtained through a Milli-Q purification system (resistivity >18 MW•cm) from Millipore (Bedford, MA).

4.2.6 Analysis by LC-ESI-MS/MS

Toxins were separated on a Waters X-Bridge™ C8 column (guard column 2.1 x 10 mm^2, 3.5 µm particle size, column 2.1 x 50 mm^2, 3.5 µm particle size; Waters, Milford, MA, USA). This analytical column was ethylene-bridged hybrid (BEH), designed to work on a wide range of pH between 1 and 12.

Chromatographic separation was performed on an Agilent 1200 LC system (Agilent Technologies, Santa Clara, CA) consisting of a binary pump (G1312B), four channel degasser (G1379B), thermostated low carry-over autosampler (G1367C + G1330B), and column oven (G1316B). Alkaline mobile phases (pH 11) were prepared according to Gerssen et al. [37, 41]: mobile phase A consisted of 6.7 mM of ammonia in ultrapure Milli-Q water; mobile phase B consisted of 6.7 mM of ammonia in 90/10 v/v ACN/Milli-Q water. Mobile phases were filtrated through 0.2 µm nylon-membrane. Chromatography of lipophilic toxins under alkaline pH was validated in out laboratory and provided better sensitivity for okadaic acid than other chromatographic conditions tested [38].

The column oven temperature was set at 30 ºC and the flow rate was 0.5 mL/min. The elution gradient was optimized [38] and started at 20% mobile phase B (mpB), reached 100% mpB in 8 minutes, held for one minute, then back to 20% mpB in 0.5 minutes and equilibrated for 2.5 minutes before the next run started. The diverter valve was programmed to deliver the eluent from column to waste for the first 1.5 min and the injection volume 10 µL. The sample compartment was set at 4 ºC. The needle was washed with methanol in the flush port of the autosampler before every injection to avoid carryover.

We used a hybrid triple quadrupole linear ion trap 3200QTrap® mass spectrometer (MS) equipped with a TurboV™ electrospray ion source (Applied Biosystems, Foster City, CA) operating at atmospheric pressure and in negative and positive ionization mode with the following parameters: curtain gas 20 psi, collision gas 4 (arbitrary units), ion spray voltage 5500V, temperature 500 ºC, nebulizer gas 50 psi, heater gas 50 psi, interface heater On. The MS was operated in the multiple reaction monitoring (MRM) mode and resolution of the quadrupoles was set at unit.
Table 4-1 shows a summary of the MS/MS settings for lipophilic toxins quantification, while a more comprehensive MRM list including all regulated lipophilic toxins was used for screening (Sup. Mat. Table 4-1 and García-Altares et al. [38]). The MS/MS conditions were based on the recommended values in the EURLMB SOP (European Union Reference Laboratory for Marine Biotoxins – Standardized Operation Protocol) [39] for a 3200 QTRAP® mass spectrometer. Analyst software v1.4.2 was used for the entire MS tune, instrument control, data acquisition and data analysis.

We checked in every batch the quality control criteria stated by the EURLMB SOP [39] regarding resolution, limits of quantification (LOQs) and linearity. The correlation coefficients of the quantification curves had to be greater than 0.98 to ensure linearity and the deviation of the slopes between consecutive calibration curves has to be lower than 25% to be considered as acceptable, as requested in the EURLMB SOP [39].

The intermediate precision was expressed as the relative standard deviation (RSD in %) and could not exceed 16% among the injection replicates.

The external standard calibration curves were prepared in methanol (LC-MS grade) from an initial multi-toxin stock solution of 200 ng/mL of OA, PTX2, SPX1, GYMA and AZA1, and 1000 ng/mL of YTX. The calibration curves had six levels in the range of 2.5 to 40 ng/mL of OA, PTX2, SPX1, GYMA and AZA1 and 10 to 160 ng/mL of YTX. A preliminary screening was performed before accurate calibration, since concentration of OA and PTXs in several samples was expected to surpass the calibration curve. When the estimated concentration of OA and/or PTX2 in the samples was comprised between 40 ng/mL and 120 ng/mL in the extract, the samples were diluted to fall into the calibration range. On the other hand, samples exceeding three times the concentration of the most concentrated calibration level were diluted and quantified with a different calibration curve with five levels in the range of 10 to 200 ng/mL of OA and PTX2. For quantification, samples were injected in the two polarity modes (+ESI and – ESI): shellfish samples were injected in duplicate, while SPATT samples and phytoplankton concentrated in filters were injected in triplicate. Samples were quantified against the external standard calibration curves (less squared adjustment of the linear regression using peak area).

Table 4-1. Transitions monitored, dwell times, declustering potentials (DP), entrance potentials (EP), collision cell entrance potentials (CEP) and collisions energies (CE) for the detection of marine lipophilic toxins.

Toxin	Transitions (*m/z*)	Time (ms)	DP (V)	EP (V)	CEP (V)	CE (V)	Precursor ion
OA and DTX2	803.5 > 255.2	150	-115	-12	-46	-64	$[M-H]^-$
	803.5 > 113.1	150	-115	-10.5	-41	-68	
DTX1	817.5 > 255.2	150	-115	-12	-46	-64	$[M-H]^-$
	817.5 > 113.1	150	-115	-10.5	-41	-68	
PTX2 and 7-epi-PTX2	876.5 > 213.3	150	50	10	35	50	$[M+NH_4]^+$
	876.5 > 823.5	150	50	10	35	50	
PTX2-sa and 7-epi-PTX2-sa	894.5 > 213.3	150	50	10	35	50	$[M+NH_4]^+$
	894.5 > 823.5	150	50	10	35	50	

4.2.7 Analysis of diol-esters

Analysis of okadaic acid diol esters in plankton net-haul samples devices was performed according to an adapted method based on Fux et al.[42], optimized in our system using (non-certified) OA C8-diol ester reference material. The same chromatographic column (Waters X-Bridge™ C8 2.1 x 50 mm^2, 3.5 µm particle size) without guard column was used for this method, kept at 40 ºC and eluted with 0.25 mL/min of ACN and LC-MS grade water with 0.1% acetic acid in gradient mode as proposed in Fux et al. 2011 (30% ACN in t = 0 min; 100% ACN in t = 9 min and kept until t = 12 min, re-equilibration until t = 21 min). Okadaic acid diol esters were monitored (MRM) in positive mode using their sodium adduct $[M+Na]^+$ as precursor, since it was the most abundant ion in enhance ion scan mode when analyzing OA and OA C8-diol ester reference materials. Transition ions of 723 and 443 *m/z* where selected after analyzing OA and OA C8-diol ester in product ion scan mode, and checking their coherence with the published fragmentation pattern of OA using sodium adduct as precursor [43] (Sup. Mat. Figure 4-1). Precursor ions for the diol-esters of OA were 923, 937, 951, 965 and 979 *m/z*, corresponding to the unsaturated C6 to C10 diols respectively. Nebulizer gas was nitrogen heated at 450 ºC, de-clustering potential was 110 V and collision energy was 80 V.

4.3 Results

4.3.1 Diarrhetic shellfish poisoning (DSP) toxins in phytoplankton samples

4.3.1.1 *Dinophysis* bloom description

Between mid-December 2011 and end-March 2012, a fluctuating *Dinophysis* bloom spread out all across Alfacs Bay (Figure 4-2), reaching maximum abundance in the sampling point located in Interior Alfacs (IA, see Figure 4-1). In this station (Figure 4-3), *Dinophysis* abundance surpassed the alert level (500 cells/L) during 40 days, peaking three times on 27th December 2011 (2200 cell/L), 30th January 2012 (1920 cell/L) and 6th March (1200 cell/L), and returning to

abundances below the alert level between peaks. This station has been chosen as a reference in this study to compare toxins dynamics with *Dinophysis* cell abundances to simplify the analysis.

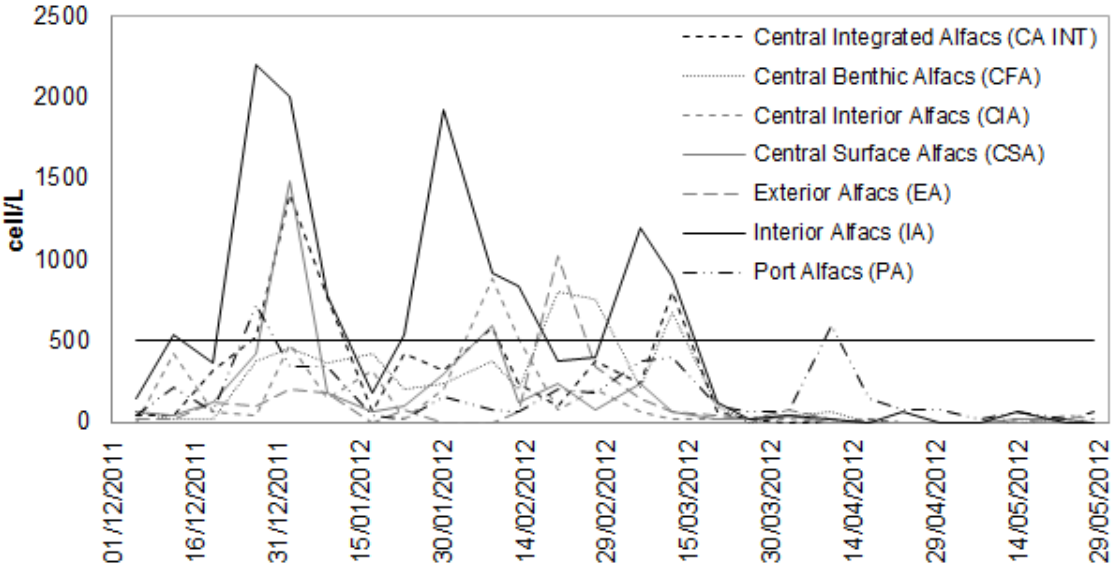

Figure 4-2. Sum of *Dinophysis sacculus* and *D. caudata* in the water column (cell/L) in all sampling stations in Alfacs Bay. Flat black line indicates alert level used for monitoring purpose (500 cell/L).

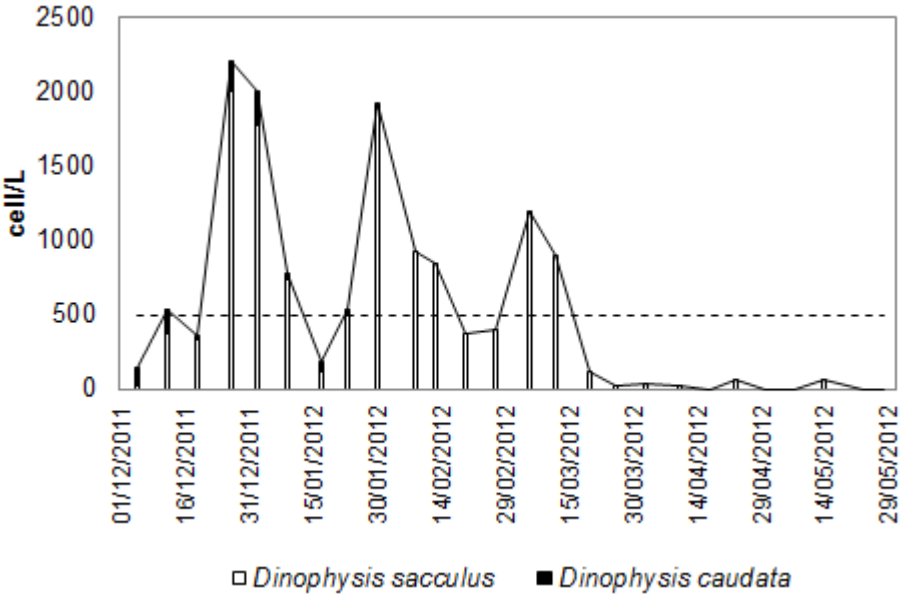

Figure 4-3. Abundance of *Dinophysis* in the water column (cell/L) in the sampling station Interior Alfacs (IA). Discontinuous line indicates alert level used for monitoring purpose (500 cell/L).

The bloom was dominated by *Dinophysis sacculus* in all sampling stations (Sup. Mat. Figure 4-2 A to G), and during some periods it was the only species recorded. In IA sampling station, *D. caudata* accounted for 50% of the *Dinophysis* population at the beginning of the bloom and it made 30% of the population in December 2011, but almost vanished later on. Other *Dinophysis* species investigated were not recorded or found very rarely at very low abundances. In the rest of sampling stations, the species pattern was very similar (Sup. Mat. Figure 4-2 A to G).

4.3.1.2 DSP toxins in net-haul samples

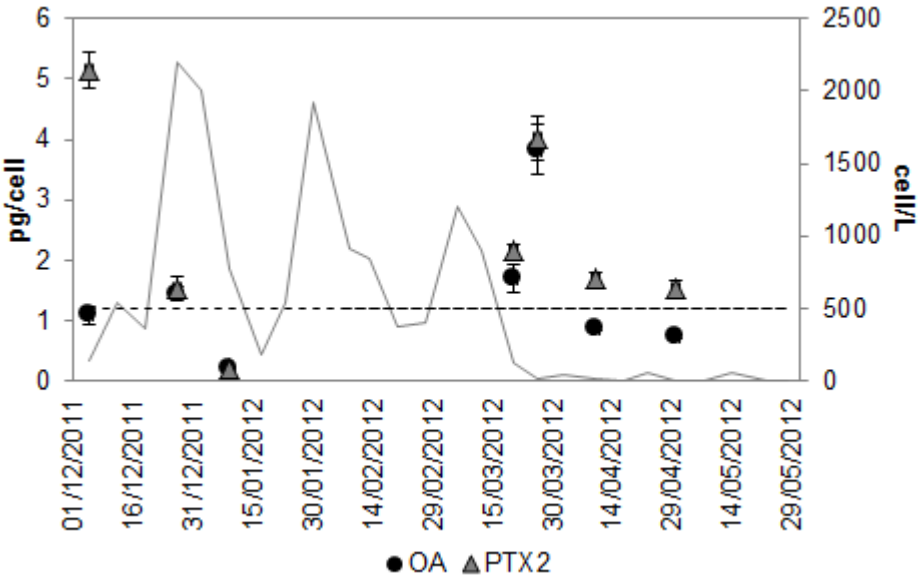

Figure 4-4. Concentration per cell (pg/cell) of okadaic acid (OA) and pectenotoxin-2 (PTX2) in net-haul phytoplankton samples collected at Buoy Alfacs (BA) sampling station. Continuous grey line indicates total abundance of *Dinophysis* in the water column (cell/L) in Interior Alfacs (IA), discontinuous line indicates alert level used for monitoring purpose (500 cell/L).

Samples of *Dinophysis* from vertical net-hauls were used to determine toxin profiles and quantify toxins (Figure 4-4). However, cell toxicity related to most samples could not be calculated because phytoplankton quantification was not always analysed at this station. Net-haul samples only contained OA and PTX2. Concentration of PTX2 (in pg/cell) was higher than OA in most cases, but the ratio between both toxins was not constant. Total toxin content (sum of OA and PTX2 concentration) per cell was always lower than 8 pg/cell.

4.3.1.3 DSP toxins in phytoplankton concentrates in filters

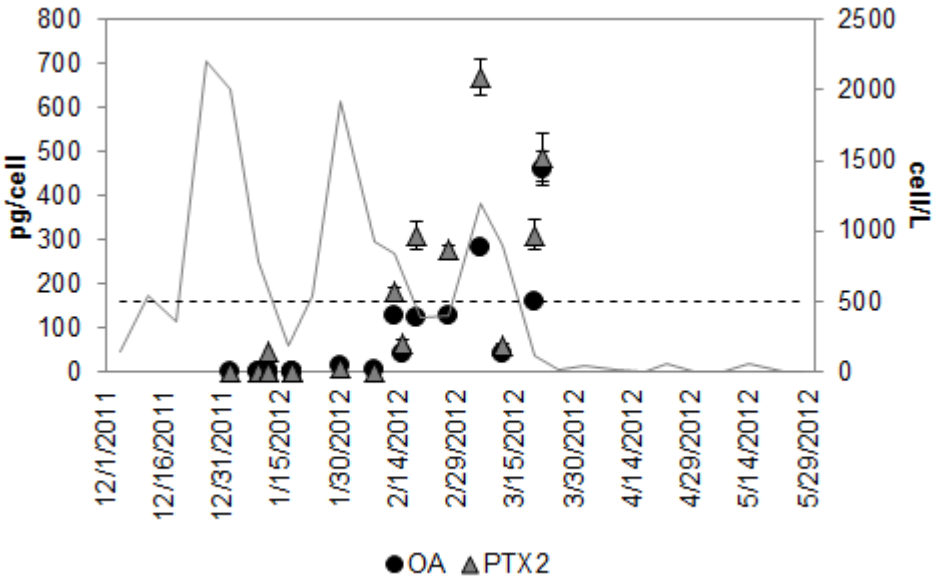

Figure 4-5. Concentration per cell (pg/cell) of okadaic acid (OA) and pectenotoxin-2 (PTX2) for *Dinophysis* from filtered water collected in several locations at Interior Alfacs (IA), Central Alfacs (CA) and the mussel rafts. Samples with concentrations between limit of detection and limit of quantification were represented at 0.01 pg/cell. Continuous grey line indicates total abundance of *Dinophysis* in the water column (cell/L) in Interior Alfacs (IA), discontinuous line indicates alert level used for monitoring purpose (500 cell/L).

Phytoplankton concentrates from filters only contained OA and PTX2. Concentration of DSP toxins per cell during the *Dinophysis* bloom were variable, ranging from 2 to 461 pg OA/cell and 1 to 668 pg PTX2/cell. Cell quotas showed a positive tendency with time, for both OA and PTX2 (Figure 4-5).

4.3.2 Diarrhetic shellfish poisoning (DSP) toxins in shellfish samples

4.3.2.1 DSP toxins in Mediterranean mussels

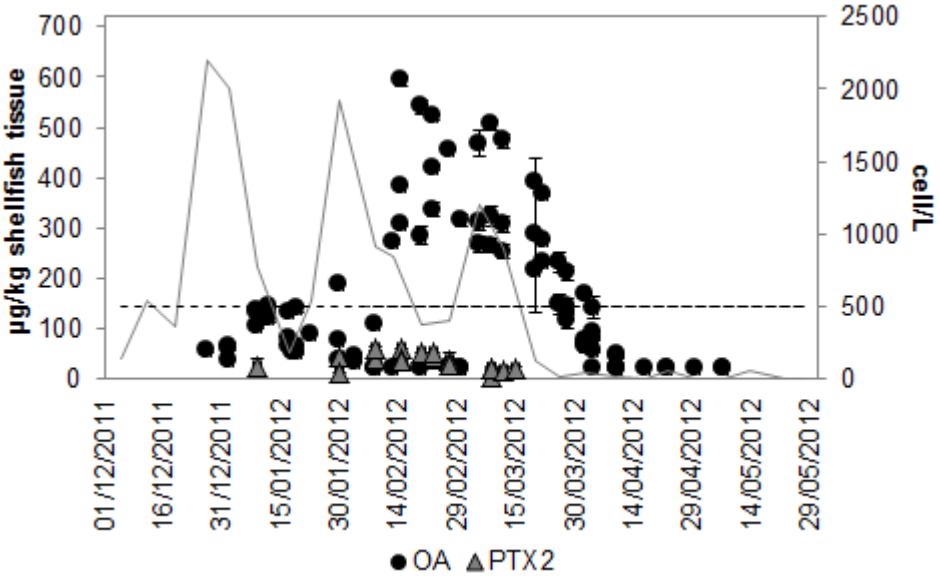

Figure 4-6. Concentration (Ŷg/kg) of total okadaic acid (OA) and pectenotoxin-2 (PTX2) in mussels collected in several racks in Alfacs Bay. Samples with OA concentration between limit of detection and limit of quantification were represented at 25 Ŷg/kg. Grey line indicates total abundance of *Dinophysis* in the water column (cell/L) in Interior Alfacs, discontinuous line indicates alert level used for monitoring purpose (500 cell/L, right y-axis) and maximum permitted level of OA and PTX2 in bivalves (160 Ŷg/kg, left y-axis).

The concentration of total OA (after hydrolysis) in mussels (Figure 4-6) reached 592 µg/kg tissue on 15th February 2012, and surpassed the MPL for 50 days, in two periods: between 19th and 30th January 2012, and between 8th February and 8th April 2012. Pectenotoxin-2 in mussels was detected at low concentration during practically the whole bloom, but never reached concentrations above MPL, with maximum values of 61 µg PTX2 total/kg on 8th February 2012. Pectenotoxin-2sa was not detected.

The first mussel samples showing DSP toxins were collected on 27th December 2011, simultaneously to the maximum of *Dinophysis* cell abundance in the water column, approximately a week after *Dinophysis* abundance surpassed the alert level (500 cell/L). Okadaic acid accumulated in mussels until it overcame the MPL in January 2012, but later it decreased below the MPL. During that period, *Dinophysis* abundance had decreased from 2220 cell/L to less than 100 cell/L.

However, *Dinophysis* abundance peaked again at the end of January 2012, and okadaic acid concentration in mussels increased until its maximum in mid-February 2012, remaining above MPL until April 2012. *Dinophysis* abundance had decreased below the alert level two weeks before, in mid-March 2012. Okadaic acid was still detected in mussels collected in May 2012.

4.3.2.2 DSP toxins in Pacific oysters

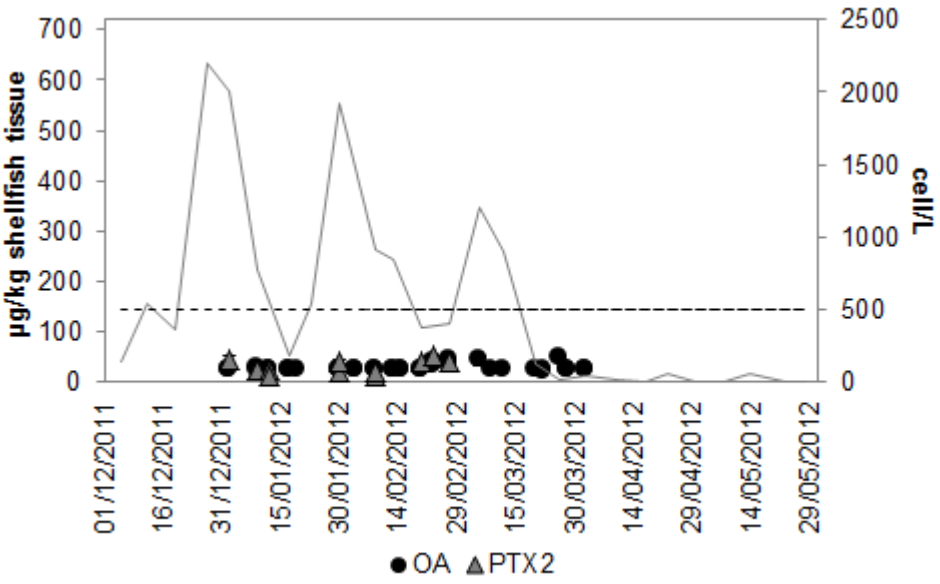

Figure 4-7. Concentration (Ŷg/kg) of total okadaic acid (OA) and pectenotoxin-2 (PTX2) in oysters collected in several racks in Alfacs Bay. Samples with OA concentration between limit of detection and limit of quantification were represented at 5 Ŷg/kg. Grey line indicates total abundance of *Dinophysis* in the water column (cell/L) in Interior Alfacs, discontinuous line indicates alert level used for monitoring purpose (500 cell/L, right y-axis) and maximum permitted level of OA and PTX2 in bivalves (160 Ŷg/kg, left y-axis).

The concentration of DSP in oysters (Figure 4-7) did not surpass the MPL at any point of the bloom. Maximum concentrations of OA and PTX2 were very similar: 49 µg OA/kg on 26th March and 52 µg PTX2/kg on 23rd February 2012.

4.3.3 Diarrhetic shellfish poisoning (DSP) toxins in solid phase adsorbing toxin tracking (SPATT) devices

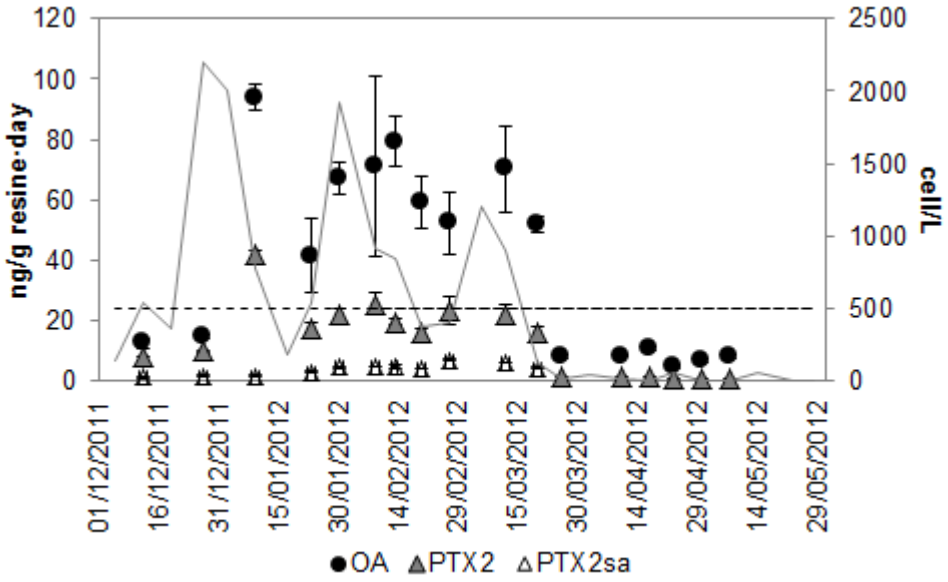

Figure 4-8. Concentration (ng/g resine•day) of okadaic acid (OA), pectenotoxin-2 (PTX2) and pectenotoxin-2 seco-acid (PTX2sa) in SPATT devices collected in in Alfacs Bay (Interior Alfacs sampling station). Grey line indicates total abundance of Dinophysis in the water column (cell/L) in Interior Alfacs, discontinuous line indicates alert level used for monitoring purpose (500 cell/L).

The concentration of DSP toxins in SPATT devices (Figure 4-8) seems to follow the pattern of *Dinophysis* cell abundance. Okadaic acid and PTX2 reached a maximum of 94 ng/g resine·day and 42 ng/g resine·day respectively on the 9th January 2012, approximately two weeks after the maximum of *Dinophysis* cell abundance in the water column. Both toxins peaked twice in the following months, with a similar trend as *Dinophysis* cell abundance but with a two weeks lag. Okadaic acid was always found at a higher concentration than PTX2, as in shellfish samples and contrary to phytoplankton samples. The shellfish metabolite PTX2-sa was also present, always at lower concentration than PTX2 (maximum 7 ng PTX2-sa/g resine·day on 27th February 2012).

4.4 Discussion

The interpretation of data about toxin profiles and toxin concentrations in the different compartments of the ecosystem must be based on a comprehensive methodology [18]. In this work, we applied comparable sampling, extraction protocols and analytical methods to study DSP toxin dynamics in three compartments of the pelagic ecosystem: phytoplankton, bivalve molluscs and the water column.

Quantitative and qualitative toxin profiles in phytoplankton were studied in two types of samples: vertical net-hauls and concentrates in filters. Net-hauls concentrate a great amount of phytoplankton biomass, leaving out dissolved organic matter and particles smaller than 20 µm, and allowing the detection of minor toxins that may be present, although it is a semi-quantitative approach because clogging of the net could be a source of error for phytoplankton

quantification. Phytoplankton concentrates in filters, on the other hand, include all particles larger than 0.45 μm in a precise volume of water. Both approaches are possible when blooms are mono-specific or largely dominated by one species, like in this case, because toxins can be directly linked to the dominant *Dinophysis* species.

The two main species of bivalve molluscs cultured in Alfacs Bay, Mediterranean mussels and Pacific oysters, where included in this study to compare their potential to accumulate DSP toxins, and assess the usefulness of preventive bans on oyster harvesting during *Dinophysis* blooms.

Free toxins in the water column were monitored with SPATT devices, which concentrate toxins *in situ* for a period of time [23, 44]. Thus, SPATT devices do not only give a snapshot of the situation, but integrate information of the whole system during the week previous to the sampling. Lipophilic toxins retained in the resins can come from phytoplankton, from shellfish (released metabolites through pseudo-feces), or from re-suspended solids from the bottom. Also, they may inform about the persistence of toxins in the water column after the bloom has disappeared.

4.4.1 Diarrhetic shellfish poisoning (DSP) toxins in phytoplankton samples

Blooms of *D. sacculus* are a recurrent problem Ebro Delta bays, being the main responsible for DSP toxicity in our seafood production areas [2]. Our results are in line with the qualitative toxin profile determined by LC-MS and with estimations by cell-based assays [2]. In those previous studies on *D. sacculus* from Alfacs Bay, OA concentration in *D. sacculus* cells was estimated (by neuroblastoma cell N2a) to be 17.75 pg/cell, and PTX2 was detected but not quantified. The only toxin profile reported of cultured *D. sacculus*, isolated in Galician Northern Rías (NW Spain), had a similar concentration of OA per cell (7.8 pg/cell), but PTX2 was the main toxin (13.2 pg/cell), and DTX1 was also present at trace amounts [45]. Pectenotoxin-2 is in many cases the most abundant toxin in *Dinophysis* culture profiles [18], although ratios between free OA and PTX2 can be variable and random, as found in net-haul samples of *D. acuta* in a 24-h study during a bloom [46]. Therefore, it has been suggested that OA&DTXs and PTXs production and release mechanisms may be controlled by different regulators, which could imply that they are associated with different biological roles [18]. Dynamic trends of production and excretion of DSP toxins among *Dinophysis* species are still not well known, and they have not been evaluated yet in *D. sacculus* cultures.

Net-haul samples of phytoplankton have the potential to collect a high phytoplankton biomass, which facilitates the detection of complete toxin profiles, including minor toxins. However, in our case, only OA and PTX2 were detected. Total toxin per cell of OA and PTX2 (always below 8 pg/cell) were lower than the toxin quotas estimated previously by neuroblastoma cell N2a during other *D. sacculus* blooms (17.75 pg/cell), although problems in the sampling did not allow us to obtain accurate cell abundances at this station for most of the samples. Nevertheless, according to these preliminary results, toxin content per cell seems to be inversely related to *Dinophysis* cell abundance. Other studies also have reported low toxin content per cell at maximum *Dinophysis* cell abundances, and rising toxin quotas when abundance declines [19, 20]. This inverse relationship between toxin quota and cell abundance has not been definitively

explained yet, but it has been hypothesized to be related to the bacterial "quorum sensing" mechanisms [20], a chemical mediated systems that enable cells to monitor their own population abundance [47]. Higher division rates during blooms, which could lead to decreased accumulation of toxins in cells, could also explain this inverse relationship between toxin quota and cell abundance.

Cell quotas of OA and PTX2 estimated from phytoplankton concentrates were found to be extremely variable, and showed an increasing tendency towards the end of the bloom. This is in line with other studies that claimed that toxin content of *Dinophysis* species may have an important seasonal and interanual variability (up to an order of magnitude), as shown for *D. acuminata*, *D. acuta*, *D. caudata* and *D. rotundata* isolated in Galicia (NW Spain) between 2002 and 2007 [24]. However, other studies comparing toxin quotas estimated in picked cells and phytoplankton concentrates, and model simulations with SPATT devices, suggested that the determination of toxin content per cell from plankton concentrates may be overestimated, since most of the toxins detected in plankton concentrates are those adsorbed by detritus and dissolved organic matter [19, 24]. This hypothesis would explain the estimated cell contents of *Dinophysis* up to 180 pg PTX2/cell found by Pizarro et al. [24] and our results of 668 pg PTX2/cell. According to this explanation, it would be expected that the amount of detritus and organic matter dissolved would be higher at the end of the bloom, when *Dinophysis* cells are decaying. In line with our results, we agree that cell quotas estimated from single picked cells may provide more accurate information about DSP toxins production in *Dinophysis* populations. However, even when toxin content was estimated from picked cells, an inverse relationship between *Dinophysis* abundances and toxin quotas per cell has been reported [19], and our results also show this tendency.

The inverse relationship between total toxin content in cells and *Dinophysis* abundance may have important consequences on monitoring strategies. The decisive factor for DSP toxicity in mussels is the product of cell abundance and cell toxicity [20], thus the alert level of 500 cell/L might be irrelevant for public health protection if the cells produce enough DSP toxins to cause shellfish toxicity at lower abundances. In our case, the *Dinophysis* bloom presented three consecutive peaks that decreased in number of cells per liter, but had increasing cell toxicity (according to phytoplankton concentrates), coincidentally with higher content of DSP toxins in mussels. Therefore, the measurement of toxin content in phytoplankton concentrates may be a better predictor of mussel toxicity than cell abundances. Nevertheless, the monitoring strategy of IRTA, based on the alert threshold of 500 cell/L and toxin evaluation in mussels, has been proven to be protective enough, since no cases of human poisoning have been reported by the local public health administrations.

It is worth noting that cell quotas of OA and PTX2 estimated from phytoplankton concentrates were up to two orders of magnitude higher than estimations from net-haul samples, which did not show overestimation in toxin cell quotas. Net-haul samples do not concentrate dissolved organic matter, and since most toxins are usually found in the dissolved fraction rather than inside the cells in *Dinophysis* cultures [18], this sampling method may be an alternative to estimate more accurate total toxin content per cell in mono-specific blooms.

Okadaic acid diol esters (C6 to C10) were not detected in any net-haul plankton sample or plankton concentrates from filters. These phytoplankton metabolites of OA have never been described in *D. sacculus* samples, so it could be the case that this species does not produce diol esters, or if it does produce them, these could be different metabolites (e.g., different chain length). In fact, it is been suggested that OA diol esters production may be different among *Dinophysis* species [48]. However, we realized that the applied method for OA diol esters was approximately ten times less sensitive than the method based on alkaline mobile phase implemented in our group to determine OA [38], therefore we cannot discard the presence of C6 to C10 diol esters of OA below the limit of detection (approximately 25 ng/mL). Nevertheless, this would be unexpected since OA diol esters were the main toxins in field samples of *D. acuta* [48] and *D. acuminata* from cultures [49]. The determination of OA in negative ionization mode is based on the deprotonation of its carboxylic acid group, which is stimulated by the alkaline pH of the mobile phase. However, the carboxylic acid in OA is involved in the formation of the diol ester, thus these analogs need to be analysed in positive ion mode, even assuming the lost in sensitivity.

4.4.2 Diarrhetic shellfish poisoning (DSP) toxins in shellfish samples

Two regulatory closures of the bay for bivalves harvesting were established for this bloom according to MBA results from 12th January 2012 to 12th April 2012, and were only interrupted during two weeks (20th January to 2nd February 2012). In total, the bay was closed for 78 days for mussels. However, since MBA results were never positive for oyster samples, governmental agents decided to cancel the ban of oysters harvesting in one week, on 16th January and 9th February 2012. Therefore, the oyster harvesting was only prohibited only for 15 days.

The first *Dinophysis* abundance peak leaded to DSP toxin concentration above MPL in mussels about two weeks later, which is coherent with previous research: maximum DSP concentrations in bivalves usually have around two to three weeks lag after a peak of *Dinophysis* abundance, as reported for *D. acuminata* blooms [22] and *D. fortii* [50], although this may depend on the hydrology and meteorology of the site.

Nevertheless, we found the maximum DSP concentration in mussels almost two months after the maximum concentration of *Dinophysis* cells in the water column. We suggest that *Dinophysis* abundance dynamics peaking three consecutive times in four moths made DSP toxin concentration to build up in mussels: the elimination rate of DSP toxins would have been much slower than their accumulation rate, since there was a recurrent input of *Dinophysis* cells in the water available for mussels to feed. Moreover, it is worth noting that most levels of toxins in shellfish above the regulatory level occurred during the period when the highest content of toxins in phytoplankton concentrates in filters occurred (mid-January to end of March) (Figure 4-5 and Figure 4-6). Increasing *D. sacculus* cell toxicity towards the end of the bloom may have caused the delay of the maximum peak of DSP concentration in shellfish.

In our study, oysters and mussels showed a very distinct behavior in the accumulation of DSP toxins, which is in line with common observations that, for the same *Dinophysis*-related toxicity event, DSP concentrations in mussels are much higher than in oysters. This has been proven for blue mussels and European oysters (*Ostrea edulis*) exposed to a *D. acuta* bloom for four weeks

[51], where OA concentration was found to be 10 to 50 times higher in mussels than in oysters. In that study, pectenotoxins concentration was slightly higher in mussels than in oysters, but the elimination rate for PTXs was quite fast for both species. Besides, oysters were found to accumulate OA mainly in esters form, which were eliminated faster than in mussels. However, the authors attributed the differences in toxin profiles between mussels and oysters to differential ingestion and biotransformation processes. In fact, European oysters were shown to ingest and retain less *Dinophysis* cells than blue mussels during a field experiment in the Adriatic Sea [52]: *D. fortii* was the most abundant phytoplankton species in the stomach content of mussels, and also *D. caudata* and *D. rotundata* were present. In oyster stomachs, *D. fortii* was only found in small numbers, and other *Dinophysis* species were not present at all. These results highlight the fact that *C. gigas* does not accumulate DSP toxins; therefore it is not a good sentinel species to study HABs toxic events. Thus, the status of shellfish for human consumption defined by blue mussels is not suitable for other species with different uptake and/or depuration dynamics, which may result in a negative impact for the aquaculture development of a particular shellfish species, such as European oysters.

Pectenotoxin-2 concentration in shellfish samples was in general lower than OA concentration, although we observed the opposite trend in phytoplankton samples. This is probably due to the slower elimination kinetics of OA&DTXs compared to PTXs [22]. Pectenotoxin-2 is metabolized to PTX2-sa in mussels [53], and rapidly eliminated [22]. However, we did not find PTX2-sa in shellfish samples. The causes explaining this fact could be the elimination rate of PTX2-sa being faster than its conversion rate from PTX2, or the possible lowest sensitivity of the analytical method for PTX2-sa than for PTX2.

Moreover, pectenotoxins and OA&DTXs have been observed to have different production/release dynamics [46]. In cultures of *D. acuminata* and *D. fortii*, the excreted cellular OA&DTXs represented about 80% of the total amount, while most PTX2 was found inside *Dinophysis* cells and less than 5% was excreted [54]. This difference in excretion tendencies between OA&DTXs and PTX2 may contribute to explain why PTX2 is very abundant in phytoplankton samples but a minor component of toxin content in bivalves and SPATT devices.

4.4.3 Diarrhetic shellfish poisoning (DSP) toxins in solid phase adsorbing toxin tracking (SPATT) devices

Since SPATT devices were proposed as an early warning system for harmful dinoflagellate blooms [23], several studies have assessed their suitability to become a monitoring tool. Some studies found that SPATT devices forecasted toxicity in mussels in advance [23, 55], but others pointed out that the accumulation in SPATT devices and mussels occurred almost simultaneously or with only a few days of difference [24, 56]. Their suitability may be case specific, depending on the hydrology and meteorology of the monitoring area [44].

In our case, SPATT devices showed that DSP toxins were present in the water column at considerable concentrations from December 2011 to March 2012, and their concentration in SPATTs reflected quite well the fluctuating dynamics of cell abundances. Interestingly, the concentration of OA in resins remained at the baseline until two weeks after the first peak of *Dinophysis* cell abundance, when OA concentrations in resins rose steeply (Figure 4-8). By that point, mussels started to accumulate DSP toxins over the MPL, but their concentration did not

reach its maximum until a month later (Figure 4-7). Thus, although SPATTs would have not provided a much earlier sign of shellfish toxicity as the collected bivalves themselves, abrupt changes in DSP concentrations in SPATTs may inform about the potential magnitude of the toxic bloom. Further studies on the relationship between the accumulation rate of DSP toxins in SPATT devices and mussels in Alfacs Bay may contribute to optimize protocols to use SPATT devices as early warning systems.

The presence of PTX2-sa, a metabolite of mussels, in SPAT devices has been reported before [55, 56]. Its origin may come from mussel feces of surrounding rafts, or from enzymatic transformations of PTX2 released from broken *Dinophysis* cells [46].

4.5 Conclusions

The current work provides a comprehensive study on *Dinophysis sacculus* blooms in a Mediterranean enclosed bay. It included the analysis by LC-MS/MS of field samples of shellfish, plankton aggregates and SPATT devices, to understand the dynamics of DSP toxins from its production and release by *D. sacculus* until its excretion and depuration by mussels and oysters. Our results confirmed previous studies about toxin profiles of *D. sacculus* in our study area, and showed that PTX2 is usually the main toxin produced by *D. sacculus* in Alfacs Bay. Cell toxicity quotas measured in phytoplankton concentrates in filters were largely overestimated, likely due to the DSP toxins adsorbed to organic matter, while estimations from net-haul samples are comparable to those reported in other studies for *D. sacculus*. Mussels accumulated DSP toxins, mostly OA, with concentration values above the maximum permitted levels for more than 78 days, and reaching maximum concentrations of 592 µg of OA equivalents/kg tissue (3.7 times the MPL [3]). Pectenotoxins were also accumulated but at much lower concentrations. Oysters, on the contrary, did not accumulate toxins over the maximum permitted level set by the European Union. The accumulation of DSP toxins in SPATT devices followed the *Dinophysis* abundance trends in the water column and kept the same qualitative toxin profile as shellfish samples, thus the use of passive samplers has been confirmed in this study as a valuable qualitative research tool to study toxins during *Dinophysis* blooms.
A better knowledge about *Dinophysis* blooms helps to optimize the monitoring programs to protect public health. The suitability of the strategy at IRTA, based on the cell counting of *Dinophysis* in the water column to raise an "alert" protocol when abundance surpasses 500 cell/L, has been proven to be an effective method to protect public health. However, in agreement with other studies, our results suggest that total toxin content may increase at the end of the bloom when *Dinophysis* abundance decline, thus the risk of shellfish toxicity can persist even when cell abundance is below the 500 cell/L threshold. This work set the basis for further investigation aimed at linking phytoplankton monitoring and toxicity in shellfish, which will improve monitoring efforts and eventually will provide dynamic forecasting models, relevant for stakeholders of the aquaculture sector.

References

1. Martín Granado, A., et al., *Brotes de intoxicación alimentaria por biotoxinas marinas debidos al consumo de pescado y marisco en España. 2003-2006.* Bol Epidemiol Sem, 2007. **15**(12): p. 133-44.
2. Cañete, E., et al., *Dinophysis sacculus from Alfacs Bay, NW Mediterranean. Toxin profiles and cytotoxic potential*, in *Source of the Document International Conference on Harmful Algae*. 2008. p. 279-281.
3. INE. *Spanish National Statistics Institute. National Accounts*. 2012; Available from: http://www.ine.es/en/welcome.shtml; 3th January 2015.
4. Vlamis, A. and P. Katikou, *Climate influence on* Dinophysis *spp. spatial and temporal distributions in Greek coastal water.* Plankton and Benthos Research, 2014. **9**(1): p. 15-31.
5. Ninčević-Gladan, Ž., et al., *Seasonal variability in* Dinophysis *spp. abundances and diarrhetic shellfish poisoning outbreaks along the eastern Adriatic coast.* Botanica Marina, 2008. **51**(6): p. 449-463.
6. Turki, S., et al., *Harmful algal blooms (HABs) associated with phycotoxins in shellfish: What can be learned from five years of monitoring in Bizerte Lagoon (Southern Mediterranean Sea)?* Ecological Engineering, 2014. **67**: p. 39-47.
7. Giacobbe, M.G., et al., *Toxicity and ribosomal DNA of the dinoflagellate Dinophysis sacculus (Dinophylta).* Phycologia, 2000. **39**(3): p. 177-182.
8. Alves-de-Souza, C., et al., *Seasonal variability of* Dinophysis *spp. and Protoceratium reticulatum associated to lipophilic shellfish toxins in a strongly stratified Chilean fjord.* Deep-Sea Research Part II: Topical Studies in Oceanography, 2014. **101**: p. 152-162.
9. Dahl, E. and T. Johannessen, *Relationship between occurrence of Dinophysis species (Dinophyceae) and shellfish toxicity.* Phycologia, 2001. **40**(3): p. 223-227.
10. Holmes, M.J., et al., *Persistent low concentrations of diarrhetic shellfish toxins in green mussels Perna viridis from the Johor Strait, Singapore: First record of diarrhetic shellfish toxins from South-East Asia.* Marine Ecology Progress Series, 1999. **181**: p. 257-268.
11. Hoshiai, G.I., et al., *A Case of Non-toxic Mussels under the Presence of High Concentrations of Toxic Dinoflagellate Dinophysis acuminata that Occurred in Kesennuma Bay, Northern Japan.* Fisheries Science, 1997. **63**(2): p. 317-318.
12. Rao, D.V.S., et al., *Diarrhetic shellfish poisoning (DSP) associated with a subsurface bloom of Dinophysis norvegica in Bedford Basin, eastern Canada.* Marine Ecology Progress Series, 1993. **97**(2): p. 117-126.
13. Sidari, L., et al., *Phytoplankton selection by mussels, and diarrhetic shellfish poisoning.* Marine Biology, 1998. **131**(1): p. 103-111.
14. Takahashi, E., et al., *Occurrence and seasonal variations of algal toxins in water, phytoplankton and shellfish from North Stradbroke Island, Queensland, Australia.* Marine Environmental Research, 2007. **64**(4): p. 429-442.
15. Godhe, A., S. Svensson, and A.S. Rehnstam-Holm, *Oceanographic settings explain fluctuations in* Dinophysis *spp. and concentrations of diarrhetic shellfish toxin in the plankton community within a mussel farm area on the Swedish west coast.* Marine Ecology Progress Series, 2002. **240**: p. 71-83.
16. Jørgensen, K. and P. Andersen, *Relation between the concentration of Dinophysis acuminata and diarrheic shellfish poisoning toxins in blue mussels (Mytilus edulis) during a toxic episode in the Limfjord (Denmark), 2006.* Journal of Shellfish Research, 2007. **26**(4): p. 1081-1087.
17. Reguera, B., et al., *Harmful Dinophysis species: A review.* Harmful Algae, 2012. **14**: p. 87-106.
18. Reguera, B., et al., *Dinophysis toxins: Causative organisms, distribution and fate in shellfish.* Marine Drugs, 2014. **12**(1): p. 394-461.

19. Pizarro, G., et al., *Seasonal variability of lipophilic toxins during a Dinophysis acuta bloom in Western Iberia: Differences between picked cells and plankton concentrates.* Harmful Algae, 2009. **8**(6): p. 926-937.
20. Lindahl, O., B. Lundve, and M. Johansen, *Toxicity of* Dinophysis *spp. in relation to population density and environmental conditions on the Swedish west coast.* Harmful Algae, 2007. **6**(2): p. 218-231.
21. Kamiyama, T. and T. Suzuki, *Production of dinophysistoxin-1 and pectenotoxin-2 by a culture of Dinophysis acuminata (Dinophyceae).* Harmful Algae, 2009. **8**(2): p. 312-317.
22. Moroño, A., et al., *Accumulation and transformation of DSP toxins in mussels Mytilus galloprovincialis during a toxic episode caused by Dinophysis acuminata.* Aquatic toxicology, 2003. **62**(4): p. 269-280.
23. MacKenzie, L., et al., *Solid phase adsorption toxin tracking (SPATT): A new monitoring tool that simulates the biotoxin contamination of filter feeding bivalves.* Toxicon, 2004. **44**(8): p. 901-918.
24. Pizarro, G., et al., *Evaluation of passive samplers as a monitoring tool for early warning of Dinophysis toxins in shellfish.* Marine drugs, 2013. **11**: p. 3823-45.
25. European Commission, *Regulation (EC) No 15/2011.* Official Journal of the European Union, 2011. **L 6**(3).
26. Fernández-Tejedor, M., et al., *The Ebro Delta coastal embayments, GEOHAB pilot site for the study of HAB population dynamics.* 12th International Conference on Harmful Algae, Copenhagen, Denmark, 4-8 September 2006., 2008.
27. GEOHAB. *HABs in Stratified Systems*. 2008; Available from: http://www.geohab.info/research-activities/core-research-projects/habs-in-stratified-systems; 19th February 2015.
28. Artigas, M.L., et al., *Understanding the spatio-temporal variability of phytoplankton biomass distribution in a microtidal Mediterranean estuary.* Deep Sea Research Part II: Topical Studies in Oceanography, 2014. **101**: p. 180-192.
29. Camp, J. and M. Delgado, *Hidrografía de las bahías del delta del Ebro.* Inv. Pesq, 1987. **51**(3): p. 351-369.
30. Satta, C.T., et al., *Studies on dinoflagellate cyst assemblages in two estuarine Mediterranean bays: A useful tool for the discovery and mapping of harmful algal species.* Harmful Algae, 2013. **24**: p. 65-79.
31. Delgado, M. and J. Camp, *Abundancia y distribución de nutrientes inorgánicos disueltos en las bahías del delta del Ebro.* Inv. Pesq, 1987. **51**(3): p. 427-441.
32. Llebot, C., et al., *Hydrographical forcing and phytoplankton variability in two semi-enclosed estuarine bays.* Journal of Marine Systems, 2011. **86**(3-4): p. 69-86.
33. Galimany, E., M. Ramón, and I. Ibarrola, *Feeding behavior of the mussel Mytilus galloprovincialis (L.) in a Mediterranean estuary: A field study.* Aquaculture, 2011. **314**(1-4): p. 236-243.
34. Ramón, M., et al., *Current status and perspectives of mollusc (bivalves and gastropods) culture in the Spanish Mediterranean.* Bolentín-Instituto Español de Oceanografía, 2005. **21**(1/4): p. 361.
35. Caillaud, A., et al., *Monitoring of dissolved ciguatoxin and maitotoxin using solid-phase adsorption toxin tracking devices: Application to Gambierdiscus pacificus in culture.* Harmful Algae, 2011. **10**(5): p. 433-446.
36. Utermöhl, H., *Zur vervollkommnung der quantitativen phytoplankton-methodik.* Mitt. int. Ver. theor. angew. Limnol., 1958. **9**: p. 1-38.
37. Gerssen, A., et al., *Liquid chromatography-tandem mass spectrometry method for the detection of marine lipophilic toxins under alkaline conditions.* Journal of chromatography A, 2009. **1216**: p. 1421-1430.
38. García-Altares, M., J. Diogène, and P. de la Iglesia, *The implementation of liquid chromatography tandem mass spectrometry for the official control of lipophilic toxins in seafood: Single-laboratory validation under four chromatographic conditions.* Journal of Chromatography A, 2013. **1275**: p. 48-60.

39. EURLMB, *Interlaboratory Validation Study of the EU-Harmonised SOP LIPO LC MS/MS*. 2011.
40. Mountfort, D.O., T. Suzuki, and P. Truman, *Protein phosphatase inhibition assay adapted for determination of total DSP in contaminated mussels.* Toxicon, 2000. **39**(2-3): p. 383-390.
41. Gerssen, A., et al., *In-house validation of a liquid chromatography tandem mass spectrometry method for the analysis of lipophilic marine toxins in shellfish using matrix-matched calibration.* Analytical and Bioanalytical Chemistry, 2010. **397**: p. 3079-3088.
42. Fux, E., et al., *Toxin profiles of five geographical isolates of* Dinophysis *spp. from North and South America.* Toxicon, 2011. **57**: p. 275-287.
43. Carey, B., et al., *Elucidation of the mass fragmentation pathways of the polyether marine toxins, dinophysistoxins, and identification of isomer discrimination processes.* Rapid Communications in Mass Spectrometry, 2012. **26**(16): p. 1793-1802.
44. MacKenzie, L.a. and L. McKenzie, *In situ passive solid-phase adsorption of micro-algal biotoxins as a monitoring tool.* Current opinion in biotechnology, 2010. **21**: p. 326-31.
45. Riobó, P., et al., *First report of the toxin profile of Dinophysis sacculus Stein from LC-MS analysis of laboratory cultures.* Toxicon : official journal of the International Society on Toxinology, 2013. **76**: p. 221-4.
46. Pizarro, G., et al., *Growth, behaviour and cell toxin quota of Dinophysis acuta during a daily cycle.* Marine Ecology Progress Series, 2008. **353**: p. 89-105.
47. Brelles-Marino, G. and E.J. Bedmar, *Detection, purification and characterisation of quorum-sensing signal molecules in plant-associated bacteria.* Journal of biotechnology, 2001. **91**(2): p. 197-209.
48. Suzuki, T., et al., *Discovery of okadaic acid esters in the toxic dinoflagellate Dinophysis acuta from New Zealand using liquid chromatography/tandem mass spectrometry.* Rapid Communications in Mass Spectrometry, 2004. **18**: p. 1131-1138.
49. Hackett, J.D., et al., *DSP toxin production de novo in cultures of Dinophysis acuminata (Dinophyceae) from North America.* Harmful Algae, 2009. **8**(6): p. 873-879.
50. Gladan, Z.N., et al., *Lipophilic toxin profile in Mytilus galloprovincialis during episodes of diarrhetic shellfish poisoning (DSP) in the N.E. Adriatic Sea in 2006.* Molecules, 2011. **16**(1): p. 888-899.
51. Lindegarth, S., et al., *Differential retention of okadaic acid (OA) group toxins and pectenotoxins (PTX) in the blue mussel, Mytilus Edulis (L.), and European flat oyster, Ostrea Edulis (L.).* Journal of Shellfish Research, 2009. **28**(2): p. 313-323.
52. Skejić, S., et al., *Differences in phytoplankton accumulation between Mediterranean mussel Mytilus galloprovincialis Lamarck, 1819 and European flat oyster Ostrea edulis Linneaus, 1758 after natural exposure to toxic Dinophysis bloom.* Cahiers de biologie marine, 2012. **53**(2): p. 189-195.
53. Suzuki, T., et al., *Conversion of pectenotoxin-2 to pectenotoxin-2 seco acid in the New Zealand scallop, Pecten novaezelandiae.* Fisheries Science, 2001. **67**(3): p. 506-510.
54. Nagai, S., et al., *Differences in the Production and Excretion Kinetics of Okadaic Acid, Dinophysistoxin-1, and Pectenotoxin-2 Between Cultures of Dinophysis Acuminata and Dinophysis Fortii Isolated From Western Japan1.* Journal of Phycology, 2011. **47**: p. 1326-1337.
55. Rundberget, T., et al., *A convenient and cost-effective method for monitoring marine algal toxins with passive samplers.* Toxicon, 2009. **53**(5): p. 543-550.
56. Fux, E., R. Bire, and P. Hess, *Comparative accumulation and composition of lipophilic marine biotoxins in passive samplers and in mussels (M. edulis) on the West Coast of Ireland.* Harmful Algae, 2009. **8**: p. 523-537.

Supplementary Materials

Sup. Mat. Table 4-1. Transitions monitored, dwell times, declustering potentials (DP), entrance potentials (EP), collision cell entrance potentials (CEP) and collisions energies (CE) for the screening of marine lipophilic toxins.

Toxin	Transitions (m/z)	Time (ms)	DP (V)	EP (V)	CEP (V)	CE (V)	Precursor ion
OA and DTX2	803.5 > 255.2	150	-115	-12	-46	-64	$[M-H]^-$
	803.5 > 113.1	150	-115	-10.5	-41	-68	
DTX1	817.5 > 255.2	150	-115	-12	-46	-64	$[M-H]^-$
	817.5 > 113.1	150	-115	-10.5	-41	-68	
YTX	1141.5 > 855.2	150	-60	-9	-54	-90	$[M-H]^-$
	1141.5 > 713.2	150	-60	-9	-54	-106	
YTX under pH 11	570.4 > 467.4	150	-75	-9	-54	-30	$[M-2H]^{2-}$
	570.4 > 396.4	150	-75	-9	-54	-30	
45-OHYTX	1157.5 > 855.2	150	-60	-9	-54	-90	$[M-H]^-$
	1157.5 > 713.2	150	-60	-9	-54	-106	
45-OHYTX under pH 11	578.4 > 467.4	150	-75	-9	-54	-30	$[M-2H]^{2-}$
	578.4 > 396.4	150	-75	-9	-54	-30	
homoYTX	1155.5 > 869.2	150	-60	-9	-54	-90	$[M-H]^-$
	1155.5 > 727.2	150	-60	-9	-54	-106	
homoYTX under pH 11	577.4 > 474.4	150	-75	-9	-54	-30	$[M-2H]^{2-}$
	577.4 > 403.4	150	-75	-9	-54	-30	
45-OHhomoYTX	1171.5 > 869.2	150	-60	-9	-54	-90	$[M-H]^-$
	1171.5 > 727.2	150	-60	-9	-54	-106	
45-OHhomoYTX under pH 11	585.4 > 474.4	150	-75	-9	-54	-30	$[M-2H]^{2-}$
	585.4 > 403.4	150	-75	-9	-54	-30	
SPX1	692.5 > 444.2	150	86	7	30	45	$[M+H]^+$
	692.5 > 426.3	150	86	7	30	45	
GYMA	508.4 > 202.4	150	60	8.5	25	55	$[M+H]^+$
	508.4 > 392.4	150	60	8.5	25	55	
	508.4 > 490.4	150	60	8.5	25	55	
PTX2 and 7-epi-PTX2	876.5 > 213.3	150	50	10	35	50	$[M+NH_4]^+$
	876.5 > 823.5	150	50	10	35	50	
PTX1	892.5 > 213.3	150	50	10	35	50	$[M+NH_4]^+$
	892.5 > 821.5	150	50	10	35	50	
PTX-2sa and 7-epi-PTX2sa	894.5 > 213.3	150	50	10	35	50	$[M+NH_4]^+$
	894.5 > 823.5	150	50	10	35	50	
AZA-1	842.5 > 362.3	150	75	12	40	70	$[M+H]^+$
	842.5 > 462.5	150	75	12	40	70	
AZA-2	856.5 > 362.3	150	75	12	40	70	$[M+H]^+$
	856.5 > 462.5	150	75	12	40	70	
AZA-3	828.5 > 362.3	150	75	12	40	70	$[M+H]^+$
	828.5 > 448.5	150	75	12	40	70	

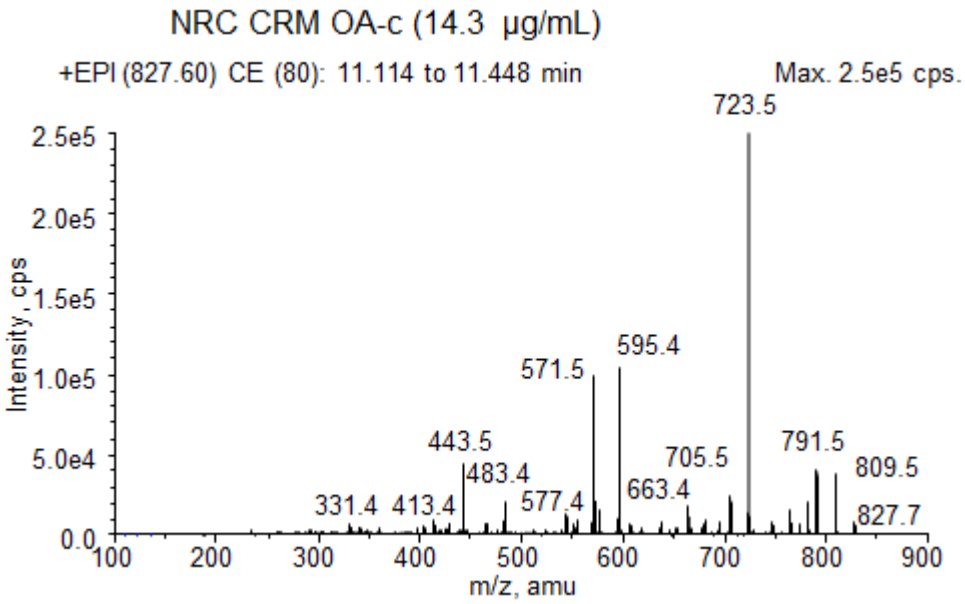

A)

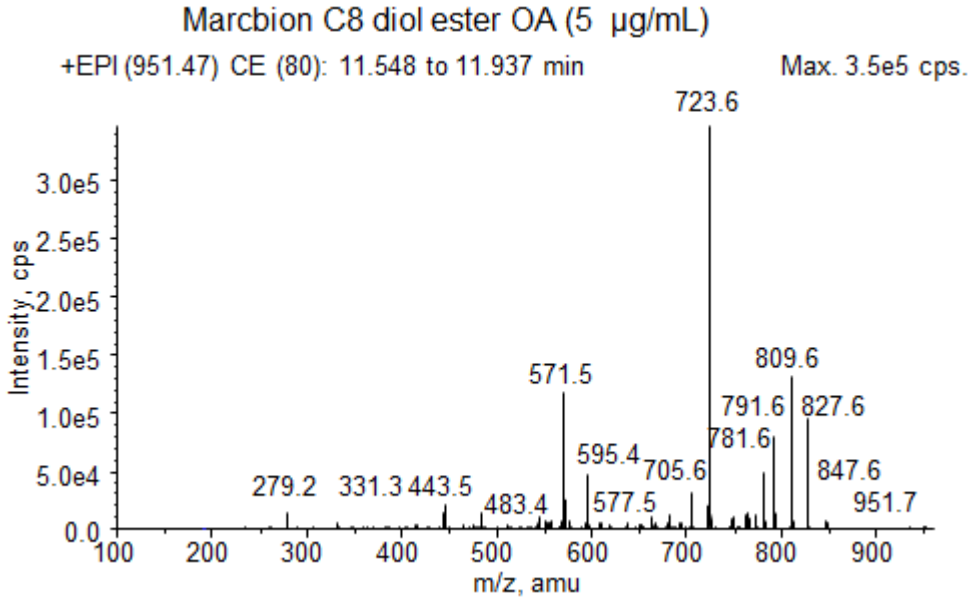

Sup. Mat. Figure 4-1. Product ion spectra of certified standard of A) okadaic acid (NRC) and B) C8-diol ester of okadaic acid (non-certified, Marcbion). Precursor ions were 827.6 *m/z* (OA) and 951.47 (C8-OA). Nebulizer gas was nitrogen heated at 450 ºC, de-clustering potential was 110 V and collision energy was 80 V.

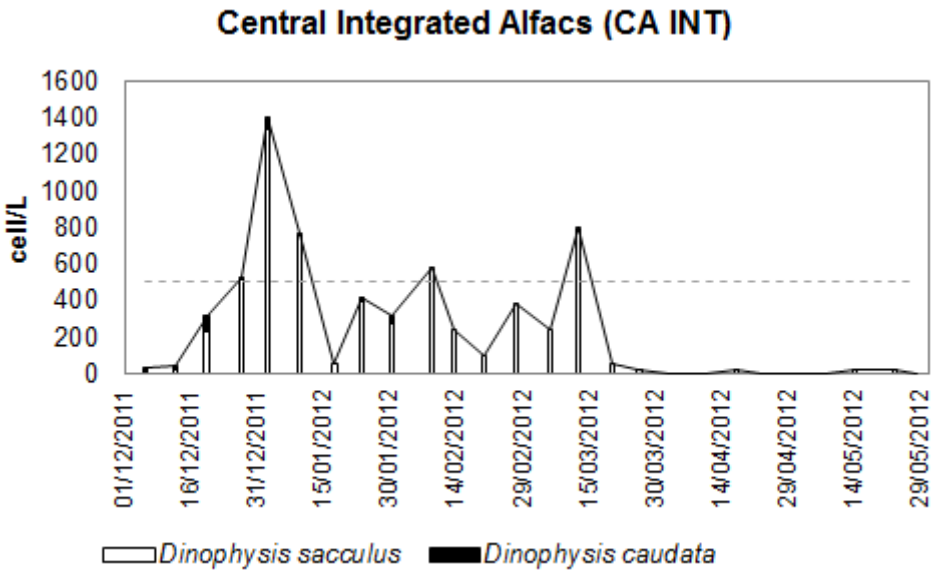

A)

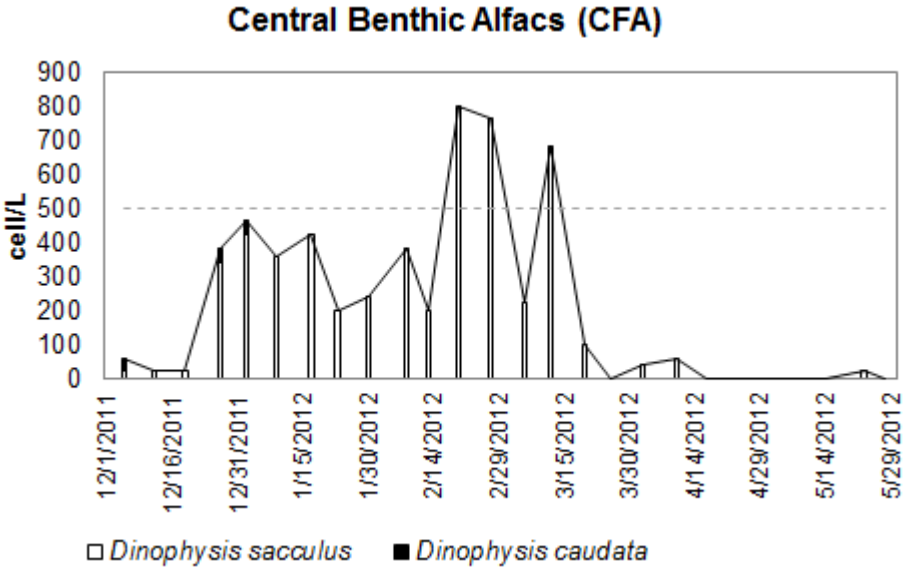

B)

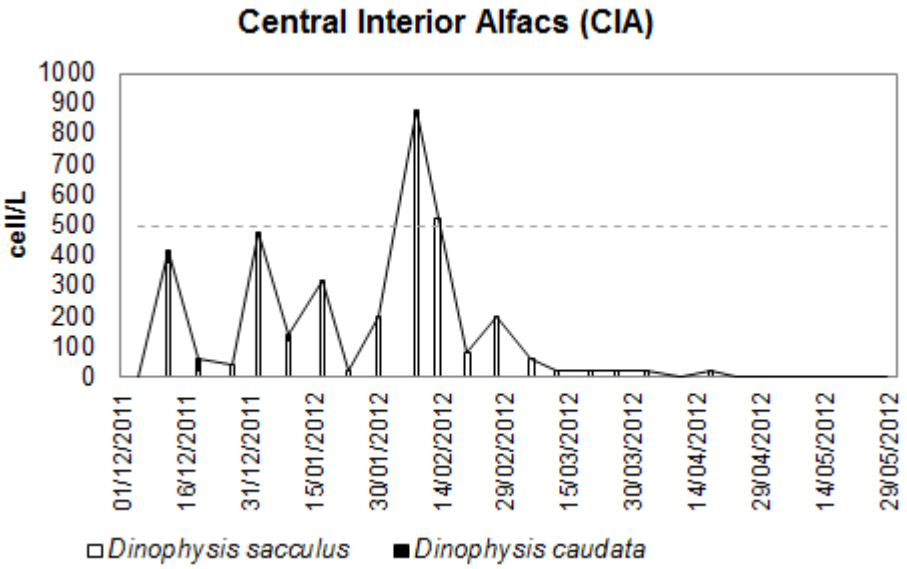

C)

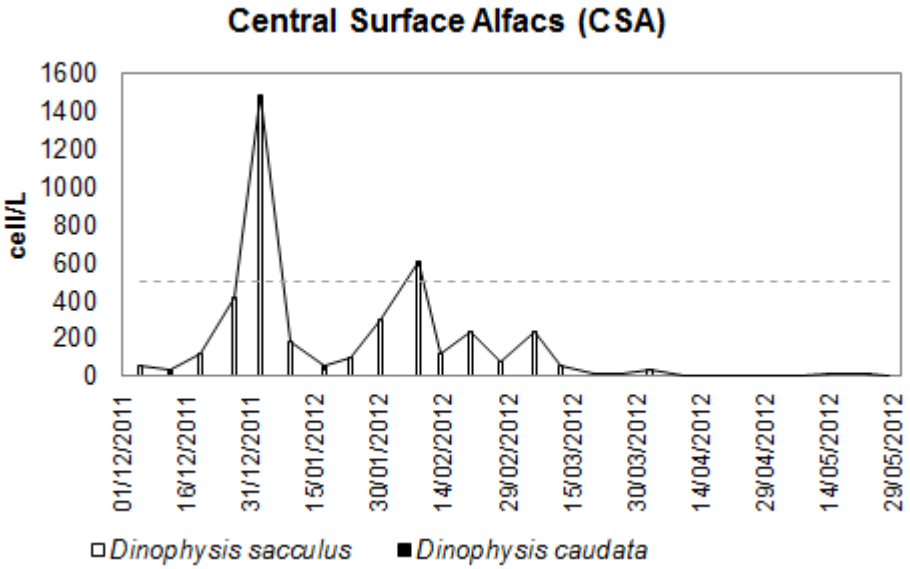

D)

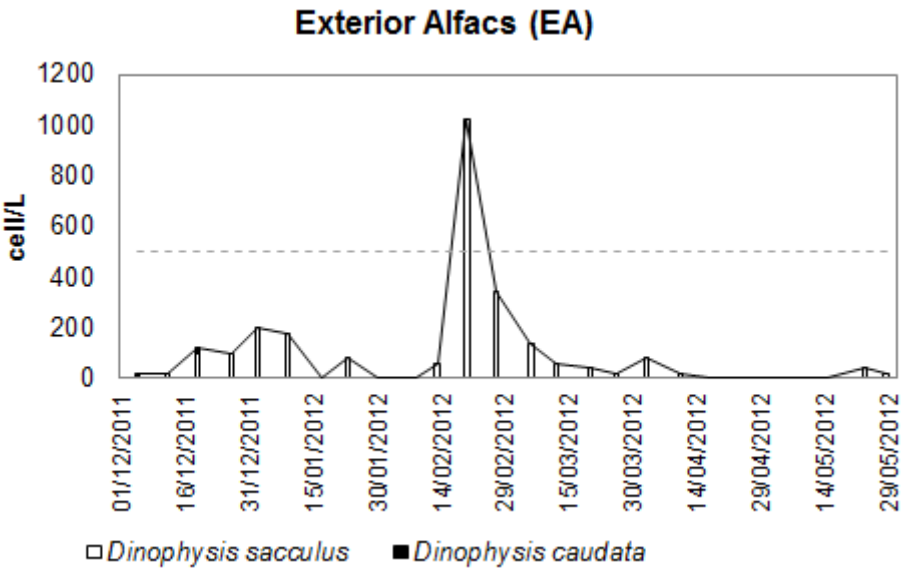

E)

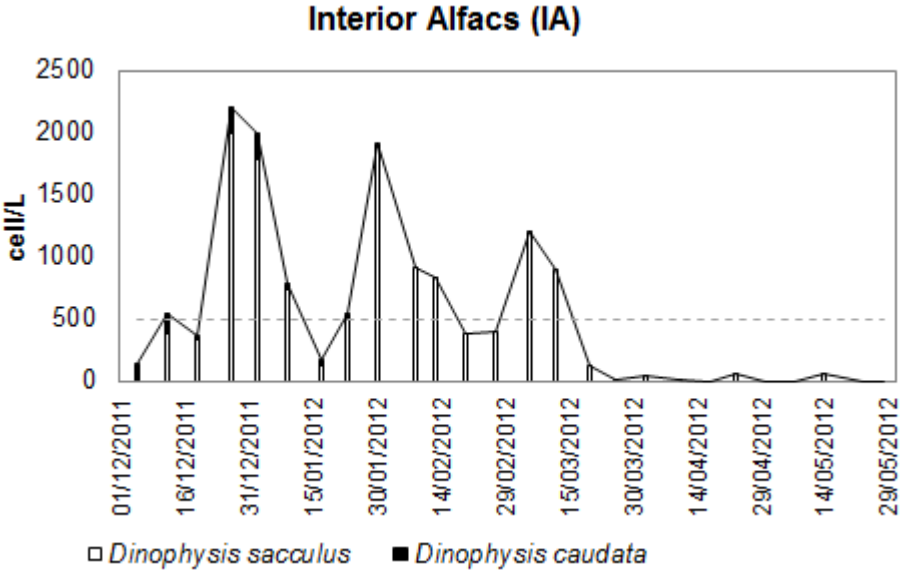

F)

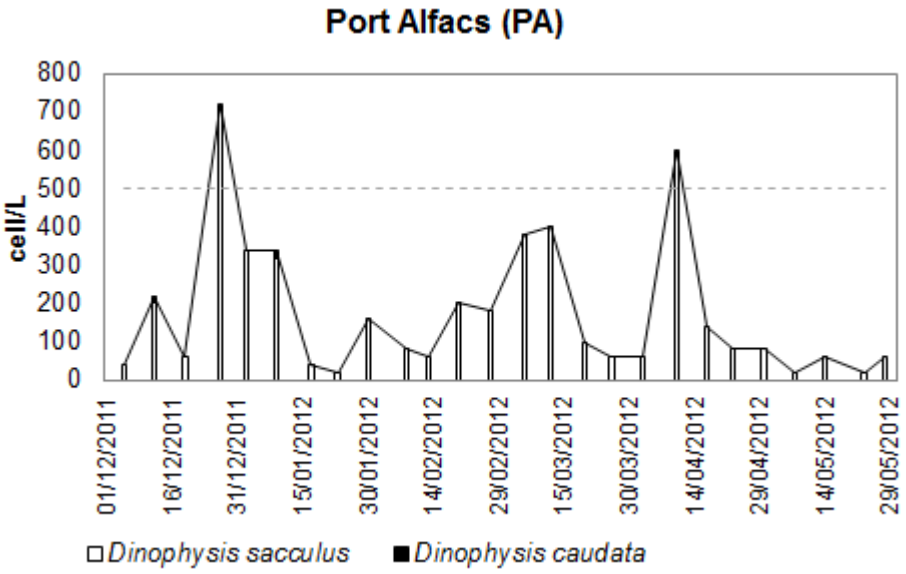

G)

Sup. Mat. Figure 4-2. A-G) Abundance of *Dinophysis* by species in the water column (cell/L) in all sampling stations in Alfacs Bay. Discontinuous line indicates alert level used for monitoring purpose (500 cell/L). Sampling stations are: A) Central Integrated Alfacs, B) Central Benthic Alfacs, C) Central Interior Alfacs, D) Central Surface Alfacs, E) Exterior Alfacs, F) Interior Alfacs, G) Port Alfacs.

CHAPTER 5

Confirmation of Pinnatoxins and Spirolides in Shellfish and Passive Samplers from Catalonia (Spain) by Liquid Chromatography Coupled with Triple Quadrupole and High-Resolution Hybrid Tandem Mass Spectrometry

Running Title: **Confirmation of pinnatoxins and spirolides by HRMS**

Published as:

García-Altares, M., A. Casanova, V. Bane, J. Diogène, A. Furey, and P. de la Iglesia, *Confirmation of pinnatoxins and spirolides in shellfish and passive samplers from Catalonia (Spain) by Liquid Chromatography coupled with triple quadrupole and High-Resolution hybrid tandem Mass Spectrometry.* Marine Drugs, 2014. 12(6): p. 3706-3732.

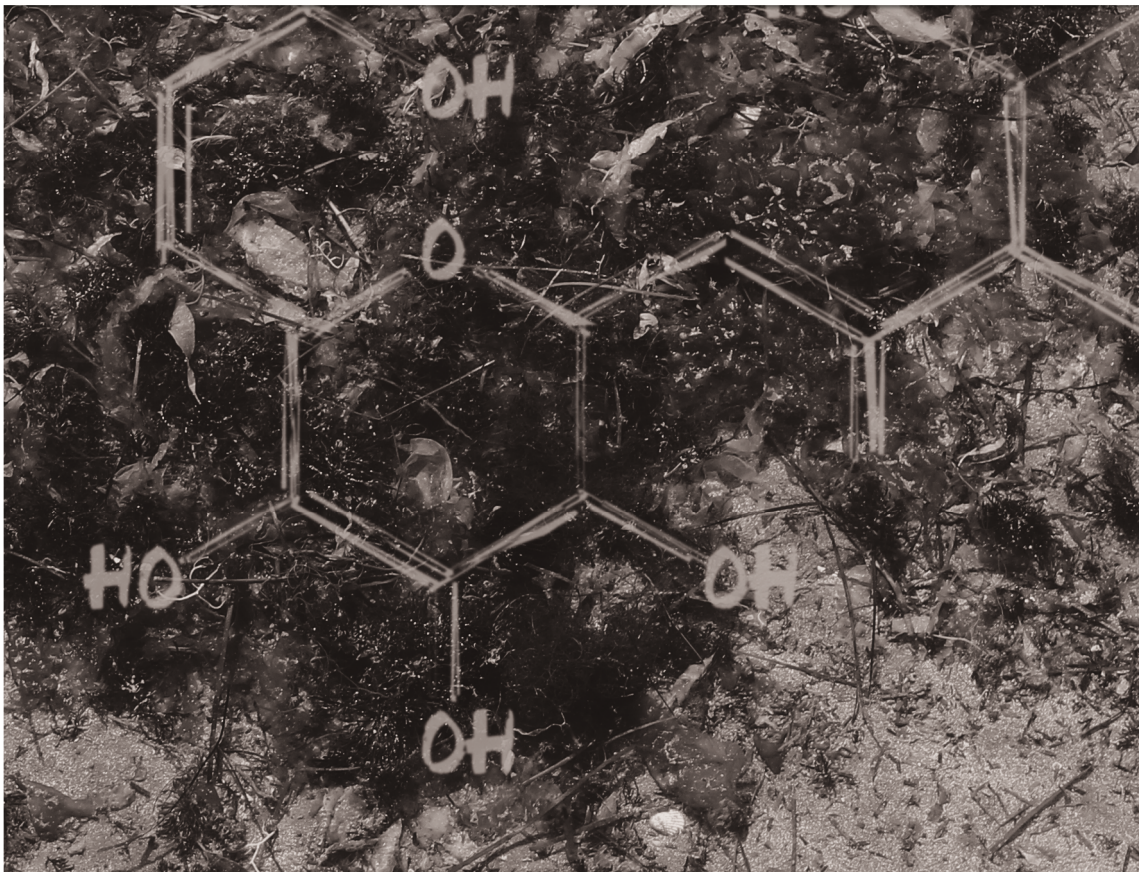

Abstract

Cyclic imines are lipophilic marine toxins that bioaccumulate in seafood. Their structure comprises a cyclic-imino moiety, responsible for acute neurotoxicity in mice. Cyclic imines have not been linked yet to human poisonings and are not regulated in Europe, although the European Food Safety Authority requires more data to perform a conclusive risk assessment for consumers. This work presents the first detection of pinnatoxin G (PnTX-G) in Spain and 13-desmethyl spirolide C (SPX-1) in shellfish from Catalonia (Spain, NW Mediterranean Sea). Cyclic imines were found at low concentrations (2 to 60 μg/kg) in 13 samples of mussels and oysters (22 samples analyzed). Pinnatoxin G has been also detected in 17 seawater samples (out of 34) using solid phase adsorption toxin tracking devices (0.3 to 0.9 μg/kg-resin). Pinnatoxin G and SPX-1 were confirmed with both low and high resolution (<2 ppm) mass spectrometry by comparison of the response with that from reference standards. For other analogs without reference standards, we applied a strategy combining low resolution MS with a triple quadrupole mass analyzer for a fast and reliable screening, and high resolution MS LTQ Orbitrap® for unambiguous confirmation. The advantages and limitations of using high resolution MS without reference standards were discussed.

Keywords

Spirolides; Pinnatoxins; Mediterranean Sea; Triple Quadrupole Mass Spectrometry; High Resolution Mass Spectrometry; Orbitrap FT-MS.

5.1 Introduction

The group of emerging toxins called cyclic imines includes eight types of compounds produced by marine dinoflagellates: spirolides (SPXs, 13 desmethyl SPX-C, also known as SPX-1, being the reference toxin for this group), pinnatoxins (PnTXs, reference compound PnTX-G), gymnodimines (GYMs, reference compound GYMA), pteriatoxins (PtTXs), prorocentrolides, spiro-prorocentrimine[1, 2], symbioimines[3] and portimine [4]. They all share a cyclic imine group, which is extremely rare, that works as the pharmacophore [1, 2], as confirmed for the 6,6-spiroimine in GYM-A [5]. Spirolides and pinnatoxins comprise more than twenty different analogs (Table 5-1) with a similar structure (Figure 5-1) characterized by the 6,7-spiro ring with an imine group and a spiro-linked polyether moiety [6].

Cyclic imines display a fast acute neurotoxicity in mice (by intraperitoneal injection) with an all-or-nothing response (they cause death in less than 20 minutes, or no symptoms at all). They affect the central nervous system as a very potent and non selective antagonist of nicotinic receptors [1, 2]. The SPXs lacking the cyclic imine moiety and having a keto-amine instead (SPX-E and -F, Figure 5-1) do not trigger toxic responses in the mouse bioassay, therefore the spiroimine most likely drives the toxicity of the molecule. Moreover, the mechanism of action is the same for all studied cyclic imines [1, 2, 7] and the affinity of GYM-A and SPX-1 to bind several nicotinic receptors was proven to be comparable [8]. Nevertheless, other parts of the molecule also play a role in toxicity, since not all PnTXs and SPXs with a closed cyclic imine are equally potent [1, 2]. Besides, both reversible (for GYMs) and permanent binding (for SPXs) have been reported for different sub-classes of cyclic imines [9]. To date, there is still a lack of information on the chronic toxicity of cyclic imines.

Until 2011, it was accepted that structurally related cyclic imines originated from different and genetically distant species of dinoflagelates: two species of the genera *Alexandrium* (*A. ostenfeldii* and *A. peruvianum*) produce SPXs [10, 11], *Karenia selliformis* produces GYMs [12], and *Vulcanodinium rugosum* produces PnTXs [13] and portimine [4]. In 2011, a culture of *A. peruvianum* isolated in North Carolina (USA) was found to produce SPX-1 and the novel gymnodimine analog 12-methyl GYMA [14]. This was the first time that a single strain was proved to produce two types of cyclic imines, but the biogenetic implications of this finding have not yet been established [15].

Pinnatoxins were isolated for the first time from shellfish samples in Japan [16] in 1990. Recently, they have been found in Australia and New Zealand (up to 87 pg PnTX-G/cell of *V. rugosum*) [13, 17], and in Canada[18]. In Europe, the presence of PnTXs have been confirmed in shellfish and sea water samples from Norway (up to 115 μg/kg in shellfish tissue), together with SPXs [18]; and in shellfish and culture samples in France [19].

Spirolides were detected for the first time in 1995 in Canada in shellfish [6, 20] and plankton samples (54 pg SPX-1/cell on average) [10]. As explained in the last two comprehensive reviews on cyclic imines [1, 2], SPXs have been found in shellfish, plankton, and sea water samples in different parts of the world. In Europe, SPXs have been reported in Scotland [20], Norway and Denmark [21], France [22], Ireland [11], and Italy (3.7 pg/cell in *A. ostenfeldii* [23]). In 2006,

SPX-1 was detected and quantified (13 to 20 μg/kg) for the first time on the Atlantic coast of Spain, in samples from shellfish harvesting areas in the NW of the country [24]. Spirolides have also been found in Chile (over 6.78 μg/kg of shellfish tissue) [25], and in the USA (up to 195 pg/cell of *A. ostenfeldii* in field samples and 78 pg/cell in cultures) [26].

The presence of cyclic imines in the Mediterranean Sea was confirmed in 2002, when GYM-A was found for the first time in clams from Tunisia [27]. Tunisian shellfish contaminated with gymnodimines was further studied, and the presence of its analogs (GYM-B and -C) was reported in 2010 (up to 1.29 mg GYM-A/kg [28]) and 2012 (over 2 mg GYMs/kg [29]).

Spirolides were reported for the first time in the Mediterranean area in 2007 in mussels from the Italian coasts of the Northern Adriatic Sea, where they were the main contributor to toxicity and shown a very complex profile, including 13-desmethyl SPX-C, 13,19-didesmethyl SPX-C, 27-hydroxy-13,19-didesmethyl SPX-C (unreported until then) and several new minor spirolides from which two of them (27-hydroxy-13-desmethyl SPX-C and 27-oxo-13,19-didesmethyl SPX-C) where isolated and structurally described [30-32]. In 2012, very high concentrations of PnTX-G and traces of PnTX-A were found, mussels and clams from Ingril lagoon, in the SE of France (up to 600 μg PnTX-G /kg of shellfish tissue and 4.7 pg /cell of *V. rugosum*) [19]. The recent discovery of cyst of *V. rugosum* in Fangar Bay (Catalonia, Spain) suggested that PnTXs might be also present in our study area [33].

Cyclic imines have not been directly linked to human intoxications, but the European Food Safety Authority requested more exposure data to properly assess the risk that cyclic imines pose to shellfish consumers [9]. This paper shows the results of a preliminary survey conducted in Catalonia (Spain), NW Mediterranean Sea, to assess the presence of cyclic imines in shellfish and seawater samples from solid phase adsorption toxin tracking (SPATTs) devices. Our aim was to develop a strategy to detect trace amounts of cyclic imines in marine samples guaranteeing their correct identification. Thus we discuss the complementation of two liquid chromatography coupled with mass spectrometry (LC-MS) techniques (low and high resolution MS (HRMS)) to quickly screen the samples, unambiguously confirm the presence of cyclic imines, quantify them and ensuring one avoids false positives.

13-desmethyl SPX-C and derivates

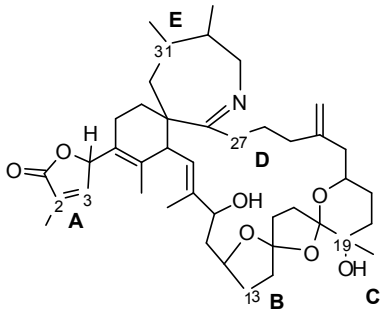

	A	B	C	D	E
SPX-A	$\Delta^{2,3}$	Me	Me	H	H
SPX-B		Me	Me	H	H
SPX-C	$\Delta^{2,3}$	Me	Me	H	Me
SPX-D		Me	Me	H	Me
13-desmethyl SPX-D		H	Me	H	Me
13,19-didesmethyl SPX-C	$\Delta^{2,3}$	H	H	H	Me
27-hydroxy-13-desmethyl SPX-C	$\Delta^{2,3}$	H	Me	OH	Me
27-hydroxy-13,19-didesmethyl SPX-C	$\Delta^{2,3}$	H	H	OH	Me
27-oxo-13,19-didesmethyl SPX-C	$\Delta^{2,3}$	H	H	O=	Me

SPX-E
SPX-F ($\Delta^{2,3}$)

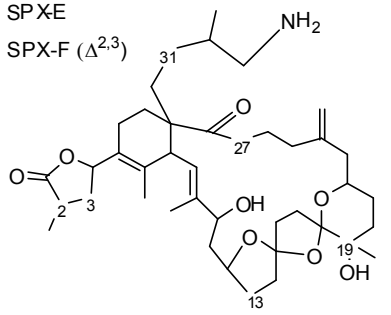

SPX-G

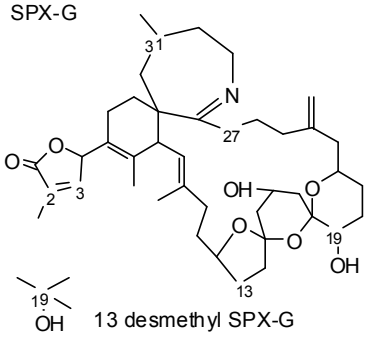

13 desmethyl SPX-G

SPX-H
SPX-I ($\Delta^{2,3}$)

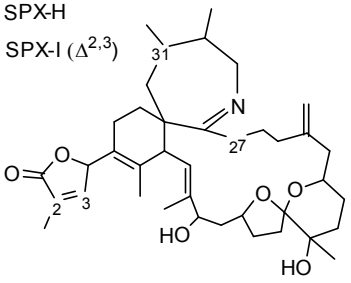

HO_2C–$_{33}$ PnTX-A

HO_2C / H_2N $_{33}$ PnTX-B/C

$_{33}$ PnTX-G

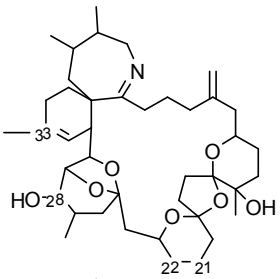

HO_2C O $_{33}$ PnTX-D

O O $_{33}$ PnTX-E

H_3CO_2C HO $_{33}$ PnTX-F

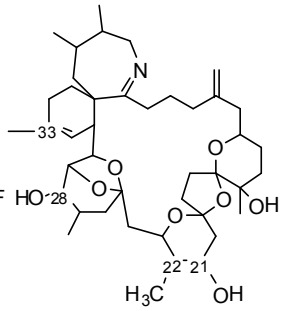

GYM-A

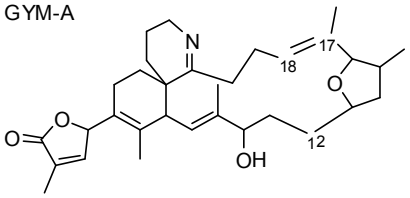

12-methyl GYM-A

GYM-B/C
(epimers in C18)

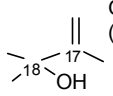

Figure 5-1. Structures of spirolides (13-desmethyl SPX-C type, SPX-E type, SPX-G type and SPX-H type), pinnatoxins (PnTX-A type and PnTX-D type) and gymnodimines (GYM-A type).

Table 5-1. List of spirolides and pinnatoxins analogs reported to date (reference compound of each group in italics). Retention times (RT) and relative retention times in brackets, exact mass and elemental formula of the molecular ions and diagnostic fragments. Relative retention times were calculated from literature by approximation from a chromatogram (a) or by calculation from retention time data (b). The mass of the electron is 1/1837 amu.

		$[M+H]^+$	Fragments		
Toxin	RT (min)	Exact mass (*m/z*)	Formula	Exact mass (*m/z*)	Formula
13 desmethyl Spirolide C[34, 35] *(SPX-1)*	1.00	692.4521	$C_{42}H_{62}NO_7$	674.4415	$C_{42}H_{60}NO_6$
				444.3108	$C_{27}H_{42}NO_4$
				164.1434	$C_{11}H_{18}N$
Spirolide A [34]	(0.90) a.	692.4521	$C_{42}H_{62}NO_7$	150.1277	$C_{10}H_{16}N$
Spirolide B [6, 34]	(1.00) a.	694.4677	$C_{42}H_{64}NO_7$	150.1278	$C_{10}H_{16}N$
Spirolide C [34]	(1.05) a.	706.4677	$C_{43}H_{64}NO_7$	458.3265	$C_{28}H_{44}NO_4$
				164.1434	$C_{11}H_{18}N$
Spirolide D [6]	(1.10) a.	708.4834	$C_{43}H_{66}NO_7$	608.4310	$C_{38}H_{58}NO_5$
				458.3265	$C_{28}H_{44}NO_4$
				164.1434	$C_{11}H_{18}N$
Spirolide E [20]	(1.30) a.	710.4637	$C_{42}H_{64}NO_8$	444.3108	$C_{27}H_{42}NO_4$
Spirolide F [20]		712.4794	$C_{42}H_{66}NO_8$	444.3108	$C_{27}H_{42}NO_4$
Spirolide G [36]	(1.60) a.	692.4521	$C_{42}H_{62}NO_7$	378.2639	$C_{22}H_{36}NO_4$
				164.1434	$C_{11}H_{18}N$
Spirolide H [37]	Not reported	650.4415	$C_{40}H_{60}NO_6$	402.3003	$C_{25}H_{40}NO_3$
				164.1422	$C_{11}H_{18}N$
Spirolide I [37]	Not reported	652.4572	$C_{40}H_{62}NO_6$	402.3003	$C_{25}H_{40}NO_3$
				164.1434	$C_{11}H_{18}N$
13 desmethyl Spirolide D [30, 38]	(1.06) a.	694.4677	$C_{42}H_{64}NO_7$	676.4572	$C_{42}H_{62}NO_6$
				444.3108	$C_{27}H_{42}NO_4$
				164.1434	$C_{11}H_{18}N$
13, 19 didesmethyl Spirolide C [30, 36]	(0.94) b.	678.4364	$C_{41}H_{60}NO_7$	430.2952	$C_{26}H_{40}NO_4$
				164.1434	$C_{11}H_{18}N$
27 hydroxy 13, 19 didesmethyl Spirolide C [30, 32]	(0.91) b.	694.4313	$C_{41}H_{60}NO_8$	464.3007	$C_{26}H_{42}NO_6$
				180.1383	$C_{11}H_{18}NO$
27 hydroxy 13 desmethyl Spirolide C [32]	(0.92) b.	708.4470	$C_{42}H_{62}NO_8$	478.3163	$C_{27}H_{44}NO_6$
				180.1383	$C_{11}H_{18}NO$
27 oxo 13, 19 didesmethyl Spirolide C [32]	(0.99) b.	692.4157	$C_{41}H_{58}NO_8$	444.2745	$C_{26}H_{38}NO_5$
				178.1226	$C_{11}H_{16}NO$
20 methyl Spirolide G [18, 39]	(1.06) b.	706.4677	$C_{43}H_{64}NO_7$	392.2795	$C_{23}H_{38}NO_4$
				164.1434	$C_{11}H_{18}N$
Pinnatoxin G [40]	1.00	694.4677	$C_{42}H_{64}NO_7$	676.4572	$C_{42}H_{62}NO_6$
				458.3265	$C_{28}H_{44}NO_4$
				164.1434	$C_{11}H_{18}N$
Pinnatoxin A [40-42]	(0.77) a.	712.4419	$C_{41}H_{62}NO_9$	458.3265	$C_{28}H_{44}NO_4$
				164.1434	$C_{11}H_{18}N$
Pinnatoxin B/C (epimers) [42, 43]	Not reported	741.4685	$C_{42}H_{65}N_2O_9$	458.3265	$C_{28}H_{44}NO_4$
				164.1434	$C_{11}H_{18}N$
Pinnatoxin D [40]	Not reported	782.4838	$C_{45}H_{68}NO_{10}$	446.3265	$C_{27}H_{44}NO_4$
				164.1434	$C_{11}H_{18}N$
Pinnatoxin E [40]	(0.83) a.	784.4994	$C_{45}H_{70}NO_{10}$	446.3265	$C_{27}H_{44}NO_4$
				164.1434	$C_{11}H_{18}N$
Pinnatoxin F [40]	(0.97) a.	766.4889	$C_{45}H_{68}NO_9$	446.3265	$C_{27}H_{44}NO_4$
				164.1434	$C_{11}H_{18}N$

5.2 Materials and Methods

5.2.1 Standards and chemicals

Certified reference standard solution of 13-desmethyl SPX-C was purchased from the Institute for Marine Bioscience of the National Research Council (NRC) from Halifax (Canada) (SPX-1, 7.0 ± 0.4 µg/mL). Certified reference standard solution of PnTX-G was not commercially available, but a pre-released material (sealed ampoules not yet certified) was kindly donated by the NRC for the purpose of this study (non-certified concentration ~1.9 µg/mL).

For LC-MS/MS analysis in low resolution, we used acetonitrile (ACN) hypergrade for LC-MS, and methanol gradient grade for HPLC were purchased from Merck (Darmstadt, Germany). Ammonium hydroxide (28% in water; ≥99.99% trace metals basis), was purchased from Sigma-Aldrich (Steinheim, Germany). Ultrapure water was obtained through a Milli-Q purification system (resistivity >18 MW•cm) from Millipore (Bedford, MA). For high resolution LC-MS/MS, HPLC grade methanol, ultrapure water and acetonitrile were purchased from LAB-SCAN (Dublin, Ireland) and ammonium hydroxide (28% in water; ≥99.99% trace metals basis), was purchased from Sigma-Aldrich (Dublin, Ireland).

5.2.2 Preparation of extracts

Blue mussels (*Mytilus galloprovincialis*) and pacific oysters (*Crassostrea gigas*) were collected from the shellfish harvesting areas of Catalonia, Spain (NW Mediterranean Sea). A triple-step extraction with methanol (10 mL) was performed on whole homogenated tissues (1 g) according to the procedure proposed by Gerssen et al.[44] which was also validated intra-laboratory by our group [45]. Analytical balance Sartorius 1702 (Goettingen, Germany), a vortex-mixer MS2 Minishaker (IKA Labortechnik, Staufen, Germany) and a centrifuge Jouan MR 23i (Thermo Fisher Scientific Inc., Waltham, MA, USA) were used. Crude extracts were filtered through polytetrafluoroethylene (PTFE) 0.2 µm membrane syringe filters. The alkaline hydrolysis of the samples was performed according to the EURLMB SOP [46] based on the protocol developed by Mountfort et al. [47]. Solid-phase adsorption toxin tracking (SPATTs) [48] devices used as passive samplers of dissolved lipophilic toxins in seawater were prepared and desorbed in methanol following the protocol explained in Caillaud et al [49]. Briefly, the SPATTs were prepared with ~10 g of wet adsorbent styrene-divinylbenzene resin (DIAON® HP20, Mitsubishi Chemical Corporation, Tokyo, Japan) and remained immersed in the marine environment for a week. For toxin desorption, the resin was removed, washed with ultrapure water and filtered under vacuum. Then the resin was extracted twice with methanol 100% in a solvent:resin ratio of 8:1 mL/g of resin. Finally, the methanolic extracts were combined and evaporated, and the dry extract was dissolved in 5 mL of 100% methanol for LC-MS analyses.

5.2.3 Chromatographic separation

Toxins were separated on a Waters X-Bridge™ C8 column (guard column 2.1 x 10 mm^2, 3.5 µm particle size, column 2.1 x 50 mm^2, 3.5 µm particle size; Waters, Milford, MA, USA). This analytical column was ethylene-bridged hybrid (BEH), designed to work on a wide range of pH between 1 and 12.

For low resolution LC-MS/MS, the chromatographic separation was performed on an Agilent 1200 LC system (Agilent Technologies, Santa Clara, CA) consisting of a binary pump (G1312B), four channel degasser (G1379B), thermostated low carry-over autosampler (G1367C + G1330B), and column oven (G1316B). For high resolution LC-MS/MS, chromatography was performed with an Accela LC system (Thermo Fisher Scientific, Hemel Hempstead, UK). Alkaline mobile phases (pH 11) were prepared according to Gerssen et al. [44, 50]: mobile phase A consisted of 6.7 mM of ammonia in ultrapure Milli-Q water; mobile phase B consisted of 6.7 mM of ammonia in 90/10 v/v ACN/Milli-Q water. Mobile phases were filtrated through 0.2 µm nylon-membrane. Chromatography of lipophilic toxins under alkaline pH was validated in out laboratory and provided better sensitivity for cyclic imines than other chromatographic conditions [45].

The column oven temperature was set at 30 °C and the flow rate was 0.5 mL/min. The elution gradient was optimized [45] and started at 20% mobile phase B (mpB), reached 100% mpB in 8 minutes, held for one minute, then back to 20% mpB in 0.5 minutes and equilibrated for 2.5 minutes before the next run started. The diverter valve was programmed to deliver the eluent from column to waste for the first 1.5 min.

Injection volume was optimized at 10 µL in the Agilent LC system and 15 µL in the Accela LC system. The sample compartment was set at 4 °C. The needle was washed with methanol in the flush port of the autosampler before every injection to avoid carryover.

5.2.4 Mass spectrometry

For low resolution LC-MS/MS, a hybrid triple quadrupole linear ion trap 3200QTrap® mass spectrometer (MS) equipped with a TurboV™ electrospray ion source (Applied Biosystems, Foster City, CA) operating at atmospheric pressure and positive ionization mode with the following parameters: curtain gas 20 psi, collision gas 4 (arbitrary units), ion spray voltage 5500V, temperature 500 °C, nebulizer gas 50 psi, heater gas 50 psi, interface heater On. The MS was operated in the multiple reaction monitoring (MRM) mode. The precursor ions monitored $[M+H]^+$ were 692 *m/z* and 694 *m/z* for SPX-1 and PnTX-G respectively. Product ions monitored were 674 *m/z*, 444 *m/z* and 164 *m/z* for SPX-1 (MRM1, MRM2 and MRM3 respectively); and 676 *m/z*, 458 *m/z* and 164 *m/z* for PnTX-G (MRM1, MRM2 and MRM3 respectively). MRM1 was the quantifier while MRM2 and MRM3 were qualifiers; these ions were selected according to their diagnostic power [18, 35, 40] and included the cyclic imine (MRM3). Table 5-1 shows the precursor and product ions applied for the screening of analogs of PnTX-G and SPX-1. Resolution of the quadrupoles was set at unit and the rest of MS parameters were: dwell time 150 ms, declustering potential 86V, entrance potential 7V, collision cell entrance potential 30V and collisions energy 45eV. Analyst software v1.4.2 was used for the entire MS tune, instrument control, data acquisition and data analysis.

For high resolution LC-MS/MS, a hybrid high-resolution LTQ Orbitrap Discovery® FT-MS (Thermo Fisher Scientific, Hemel Hempstead, UK) operating in positive ionization mode with a heated electrospray interface (HESI) was used. The ion source tune method values were optimized and set at: capillary temperature 250 °C, capillary voltage 47.5 V, tube lens 90 V, sheath gas 50 (arbitrary units), auxiliary gas 10 (arbitrary units). The analysis was divided into

two experiments: first experiment was a full MS scan event from 100 to 800 *m/z*; second experiment involved full MS^2 scans from precursor ions previously isolated in the first-stage ion trap mass analyzer: 692 *m/z* (Isolation Width 4.0 Da) at 45.0% collision energy (CE) in the high collision dissociation (HCD) cell for SPX-1, and 694 *m/z* (Isolation Width 4.0 Da) with the same CE for PnTX-G. Resolution of 30,000 FWHM (at 400 *m/z*) was selected (the maximum provided by the instrument). To improve mass accuracy measurements, we used 453.34353 *m/z* as lock mass, a frequent and consistent background interference from the membrane nylon disks used for filtering the mobile phases [51, 52]). The lock mass offers real time recalibration of the mass spectral region. The tuning, control, data acquisition and data analysis were done with Xcalibur® software v2.0.7.

5.2.5 Method performance and quality control

A quality assessment of the quantification capabilities of the method on the triple quadrupole 3200QTrap® mass spectrometer was conducted. The single laboratory three days assessment relied on the concepts described in Taverniers et al. [53]; and the guidelines proposed by the Regulation (EC) 657/2002 [54] and the EU-Harmonized SOP for Lipophilic toxins [55]. The external standard calibration curves were prepared in methanol (LC-MS grade) from an initial multi-toxin stock solution of 100 ng/mL of NRC CRM 13-desmethyl SPX-C and NRC RM PnTX-G, with five levels in the range of 2.5 to 50 ng/mL. These concentrations would correspond to 25 to 500 µg/kg, thus in the range of concentrations found in other studies cited in the Introduction of this paper. Sensitivity of the method was evaluated as the slope of the calibration curves [56]. Linearity was assessed by two parameters: correlation coefficients of the quantification curves had to be greater than 0.98; and the deviation of the slopes between consecutive calibration curves had to be lower than 25%. The drift in the retention times (RT) corresponds to the variation of RT along the three days and was considered as acceptable below 3%. Product ion ratios were calculated as the relative area (in percentage) of the qualifier MRM2 compared to the area of the quantifier MRM1. Ion ratios were calculated in the external standards of the calibration curves, and variations in product ion ratios in mussels and oysters were measured as the difference (in percentage) between product ion rations measured in the external standards solutions and in spiked samples of mussels and oysters.

Recovery (ratio between quantified and spiked concentration in percentage, %R) and precision (intra-day relative standard deviation RSDr, inter-day RSDR) were calculated with blank homogenated samples of mussel and oyster, spiked at 50 µg/kg of NRC CRM SPX-1 and NRC RM PnTX-G. The spiked samples were analyzed in three consecutive days, three replicates per day, and quantified against the external standard calibration curves.

Limits of detection and quantification (LODs and LOQs) where calculated by the IUPAC method [57] considering the improves recommended in later studies [57, 58]:

$$[\, c_L = \frac{(k \cdot s_B)}{m} \,] \qquad (1)$$

Where c_L is the concentration that generates a signal equal to three times (k = 3 for LOD) or ten times (k = 10 for LOQ) the standard deviation of the noise in the blanks (s_B), divided by the analytical sensitivity (m), which is the slope of a matrix matched calibration curve in the concentration range of the limits. The spiked mussel and oyster where diluted in methanol five

times (1 to 25 µg/kg) to calculate *m*, and noise was calculated as the height of MRM2 for LODs and MRM1 for LOQs in the vicinity of RT of the toxins, with three injection replicates of the blank samples (not spiked). Average limits include one replicate per day (n=3).

After the quality assessment, the spiked samples were considered as "internal material" and used to correct the quantification of the shellfish samples with its recovery. Samples were injected in duplicate and quantified against the external standard calibration curves (less squared adjustment of the linear regression using peak area).

5.2.6 Identification and assessment of identification criteria

A two days single laboratory quality assessment of the identification criteria with a LTQ Orbitrap Discovery® (mass resolution FTWM 30,000) was performed. This brief assessment only included the standards (five dilutions from 2.5 to 40 ng/mL of SPX-1, 0.95 to 190 ng/mL of PnTX-G), not the spiked samples. We evaluated the RT and its drift along two days. The mass accuracy (Δ, in ppm) of the precursor ions (measured in the full MS scan) and the selected fragments (in the full MS^2 scan) was evaluated using the features provided by the qualitative browser of Xcalibur software. Ion ratios and their variation (relative standard deviation, in percentage) in the MS^2 spectra were calculated as the relative intensity of the fragment ions compared to the most intense one in the full MS^2 scan.

Identification was confirmed when the precursor ion was found in the full MS scan and the main fragments (Table 5-1) were found in the full MS^2 scan with a mass tolerance of 5 ppm. The retention times and product ion ratios compared to those obtained from reference standards were also used as confirmation criteria to unambiguously confirm the presence of SPX-1 and PnTX-G in the samples.

5.3 Results and Discussion

Two cyclic imines, PnTX-G and SPX-1, were found at low concentrations (2 to 60 µg PnTX-G/kg and 2 to 16 µg SPX-1/kg) in 13 samples of mussels and oysters (out of 22 samples analyzed, Table 5-2). Pinnatoxin G has also been detected in 17 seawater samples (out of 34) using solid phase adsorption toxin tracking devices (SPATTs, 0.3 to 0.9 µg/kg-resin, Table 5-3). The quality assessment of the methods of quantification and confirmation was satisfactory. We looked for other cyclic imines (Table 5-1) and acyl ester derivatives of cyclic imines (section 2.4), but we could not confirm their presence in the samples.

5.3.1 Unambiguous confirmation and quantification of PnTX-G and SPX-1

Figure 5-2 illustrates the unambiguous confirmation of PnTX-G and SPX-1 in a mussel sample from Fangar Bay collected in May, 2012 (MUS120523). Pinnatoxin-G and SPX-1 were confirmed by their retention time (RT) compared to that of the standards (<1% difference, Figure 5-2A and 2B), the mass accuracy of the precursor and of three diagnostic fragments (<2 ppm, Figure 5-2D, 2F and 2I) and one ion ratio. The final concentration in the sample was 60 ± 5 µg/kg PnTX-G and 16 ± 1 µg/kg SPX-1.

Table 5-2. Confirmation with LTQ Orbitrap Discovery® FT-MS and quantification with 3200QTrap® of SPX-1 and PnTX-G in shellfish. ND: Not detected, NC: Not confirmed; NQ: Not quantified. Δ ppm: mass error in ppm; $[M+H]^+$: Molecular Ion (SPX-1: 692.4521 m/z; PnTX-G: 694.4677 *m/z*); Fragment 1: 164.1434 *m/z* (both SPX-1 and PnTX-G); Fragment 2: 444.3108 (SPX-1) and 458.3265 *m/z* (PnX-G); Fragment 3: 674.4415 *m/z* (SPX-1) and 676.4572 *m/z* (PnTX-G).

Sample details	SPX-1 (Δ ppm)		SPX-1 (μg/kg)	PnTX-G (Δ ppm)		PnTX-G (μg/kg)
OYS110102	$[M+H]^+$	1.0		$[M+H]^+$	Δppm> 5 ppm	
Oyster	Frag 1	-0.2	3.6 ± 0.1	Frag 1	Δppm> 5 ppm	ND
Jan-2011	Frag 2	1.2		Frag 2	Δppm> 5 ppm	
Fangar Bay	Frag 3	-2.3		Frag 3	Δppm> 5 ppm	
OYS110103	$[M+H]^+$	-0.2		$[M+H]^+$	Δppm> 5 ppm	
Oyster	Frag 1	0.2	3.5 ± 0.8	Frag 1	Δppm> 5 ppm	ND
Jan-2011	Frag 2	-0.9		Frag 2	Δppm> 5 ppm	
Fangar Bay	Frag 3	-3.5		Frag 3	Δppm> 5 ppm	
OYS110105	$[M+H]^+$	5.0		$[M+H]^+$	40.6	
Mussel	Frag 1	-0.2	2.2± 0.6	Frag 1	-0.2	3.8 ± 0.6
Jan-2011	Frag 2	0.5		Frag 2	-2.6	
Fangar Bay	Frag 3	0.4		Frag 3	-0.7	
OYS110115	$[M+H]^+$	0.4		$[M+H]^+$	Δppm> 5 ppm	
Oyster	Frag 1	-0.2	5± 1	Frag 1	Δppm> 5 ppm	ND
Jan-2011	Frag 2	0.3		Frag 2	Δppm> 5 ppm	
Fangar Bay	Frag 3	2.3		Frag 3	Δppm> 5 ppm	
MUS110116	$[M+H]^+$	1.6		$[M+H]^+$	1.3	
Mussel	Frag 1	0.1	3.6 ± 0.18	Frag 1	0.5	3 ± 1
Jan-2011	Frag 2	-0.1		Frag 2	-0.2	
Fangar Bay	Frag 3	0.9		Frag 3	-0.1	
OYS110117	$[M+H]^+$	-0.1		$[M+H]^+$	Δppm> 5 ppm	
Oyster	Frag 1	0.1	6.6± 0.7	Frag 1	Δppm> 5 ppm	ND
Jan-2011	Frag 2	-0.1		Frag 2	Δppm> 5 ppm	
Fangar Bay	Frag 3	-0.9		Frag 3	Δppm> 5 ppm	
OYS110205	$[M+H]^+$	0.4		$[M+H]^+$	Δppm> 5 ppm	
Oyster	Frag 1	-0.1	5.8± 0.5	Frag 1	Δppm> 5 ppm	ND
Feb-2011	Frag 2	0.1		Frag 2	Δppm> 5 ppm	
Fangar	Frag 3	1.6		Frag 3	Δppm> 5 ppm	
MUS110205	$[M+H]^+$	-0.2		$[M+H]^+$	2.2	
Mussel	Frag 1	0.3	NQ	Frag 1	0.5	4.1 ± 0.1
Feb-2011	Frag 2	-0.2		Frag 2	-1.8	
Fangar Bay	Frag 3	0.9		Frag 3	0.4	
MUS1027	$[M+H]^+$	0.2		$[M+H]^+$	42.6	
Mussel	Frag 1	-0.6	3 ± 2	Frag 1	-0.5	2.2 ± 0.1
Feb-2011	Frag 2	-1.0		Frag 2	-1.9	
Fangar Bay	Frag 3	0.3		Frag 3	-2.00	
OYS110208	$[M+H]^+$	0.5		$[M+H]^+$	Δppm> 5 ppm	
Oyster	Frag 1	-0.2	4 ± 1	Frag 1	Δppm> 5 ppm	ND
Feb-2011	Frag 2	0.1		Frag 2	Δppm> 5 ppm	
Fangar	Frag 3	-1.0		Frag 3	Δppm> 5 ppm	
MUS120520	$[M+H]^+$	1.0		$[M+H]^+$	-1.1	
Mussel	Frag 1	-0.5	NC	Frag 1	-0.5	39± 6
May-2012	Frag 2	Δppm> 5 ppm		Frag 2	-0.7	
Fangar Bay	Frag 3	Δppm> 5 ppm		Frag 3	-0.9	
MUS120523	$[M+H]^+$	-2.1		$[M+H]^+$	0.2	
Mussel	Frag 1	-0.1	16 ± 1	Frag 1	-0.1	59 ± 5
May-2012	Frag 2	0.4		Frag 2	-0.1	
Retail market	Frag 3	-0.1		Frag 3	-0.1	
MUS120524	$[M+H]^+$	Δppm> 5 ppm		$[M+H]^+$	-1.1	
Mussel	Frag 1	-1.1	NC	Frag 1	-0.5	58 ± 2
May-2012	Frag 2	Δppm> 5 ppm		Frag 2	-0.9	
Fangar Bay	Frag 3	Δppm> 5 ppm		Frag 3	-0.9	

Table 5-3. Confirmation with LTQ Orbitrap Discovery® FTMS and quantification with 3200QTrap® of PnTX-G in SPATTs samples from Alfacs Bay. Δ ppm: mass error in ppm; $[M+H]^+$: Molecular Ion (PnTX-G: 694.4677 *m/z*); Fragment 1: 164.1434 *m/z*; Fragment 2: 458.3265 *m/z*; Fragment 3: 676.4572 *m/z*.

			PnTX-G (Δ ppm)	PnTX-G (µg/kg)
TB_1028		$[M+H]^+$	0.9	
	Jan-2007	Frag 1	0.3	0.47 ± 0.01
		Frag 2	-0.8	
		Frag 3	-0.1	
TB_1029		$[M+H]^+$	1.3	
	Jan-2007	Frag 1	0.6	0.65 ± 0.09
		Frag 2	-0.8	
		Frag 3	-0.1	
TB_1036		$[M+H]^+$	-1.1	
	Feb-2007	Frag 1	0.9	0.70 ± 0.05
		Frag 2	-0.1	
		Frag 3	0.4	
TB_1037		$[M+H]^+$	2.0	
	Feb-2007	Frag 1	-3.3	0.75 ± 0.03
		Frag 2	2.6	
		Frag 3	3.5	
TB_1359		$[M+H]^+$	1.9	
	Jun-2008	Frag 1	-2.6	0.48 ± 0.03
		Frag 2	-3.8	
		Frag 3	-3.1	
TB_1360		$[M+H]^+$	3.8	
	Jun-2008	Frag 1	-2.5	0.28 ± 0.02
		Frag 2	-3.7	
		Frag 3	-2.9	
TB_1363		$[M+H]^+$	1.9	
	Jun-2008	Frag 1	-2.7	0.93 ± 0.02
		Frag 2	-3.9	
		Frag 3	-3.2	
TB_1367		$[M+H]^+$	4.1	
	Jun-2008	Frag 1	-3.4	0.65 ± 0.06
		Frag 2	-4.7	
		Frag 3	-4.0	
TB_1374		$[M+H]^+$	-0.1	
	Jul-2008	Frag 1	-3.4	0.55 ± 0.01
		Frag 2	-4.3	
		Frag 3	-3.4	
TB_1378		$[M+H]^+$	-2.8	
	Jul-2008	Frag 1	-3.3	0.47 ± 0.07
		Frag 2	-4.1	
		Frag 3	-3.4	
TB_1379		$[M+H]^+$	-1.1	
	Jul-2008	Frag 1	-3.1	0.34 ± 0.02
		Frag 2	-4.8	
		Frag 3	-2.5	
TB_1381		$[M+H]^+$	8.7	
	Jul-2008	Frag 1	-3.3	0.33 ± 0.02
		Frag 2	-5.0	
		Frag 3	-4.0	
TB_1614		$[M+H]^+$	-0.8	
	Jun-2009	Frag 1	-2.9	0.58 ± 0.06
		Frag 2	-5.1	
		Frag 3	-1.0	

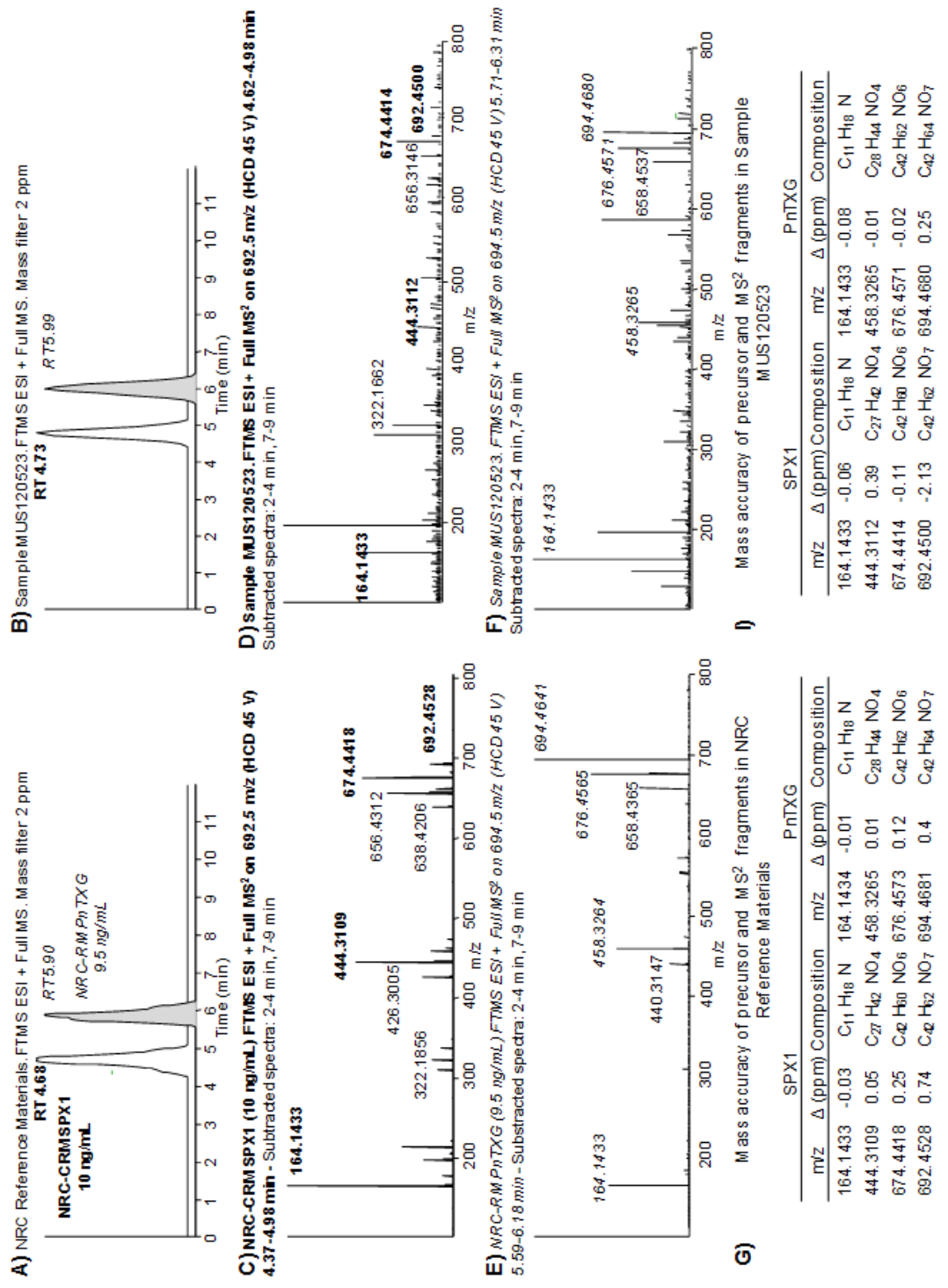

Figure 5-2. A and B) Chromatograms; C and D) MS^2 product scans; and G and I) assigned formulae and mass accuracy measurements (Δ in ppm) of the precursor ions and the diagnostic product ions of SPX-1 and PnTX-G in the reference standard materials (A, C and G) and sample MUS120523 (B, D and I).

Following the same approach, we analyzed 22 samples of shellfish (14 mussels and 8 oysters, Table 5-2) that were initially screened by triple quadrupole LC-MS/MS: 4 mussels samples from Alfacs Bay (Catalonia, Spain), 8 from Fangar Bay (Catalonia, Spain) and 2 mussels samples from retail market, one oyster sample from Alfacs Bay, and 7 from Fangar Bay. We confirmed the presence of PnTX-G in 6 mussels from Fangar Bay and one mussel from the retail market, with concentrations from 2 to 60 μg/kg (Table 5-2). SPX-1 was confirmed in 5 mussels samples and 6 oysters samples from Fangar Bay, and in one mussel samples from retail market. The SPX-1 concentrations ranged from 2 to 16 μg/kg. In summary, 13 samples were confirmed to contain one cyclic imine (PnTX-G or SPX-1), and 4 mussels samples from Fangar Bay and one from the retail market had both toxins. Nine samples showed characteristic transitions for PnTX-G and/or SPX-1 in the triple quadrupole LC-MS/MS at very low intensity, but could not meet the confirmation requirements in the LTQ Orbitrap method. Separately, a total of 34 SPATT samples immersed for a week in the seawater of Alfacs Bay (Table 5-3) were selected and analyzed from the period 2006-2009. Pinnatoxin G was present in 17 SPATT samples from 2007, 2008 and 2009 and its concentration was quantified in 13 SPATT samples, ranging from 0.28 to 0.93 μg/kg resin.

Although several SPATT samples showed some of the diagnostic fragments of SPX-1 in the MS^2 product scan of 692.5 *m/z*, the precursor ion for SPX-1 was not detected in the full MS scan in any SPATT sample using a 5 ppm mass window. This could be explained by the relative low abundance of the ion 692.4521 *m/z* in the presence of much more abundant ions present in the matrix. LTQ Orbitraps operate with a C-trap that storage the ions coming from the ion trap to be injected into the Orbitrap analyzer. The filling of the C-trap is controlled by the automatic gain control function of the instrument (based on a pre-scan in the ion trap that optimizes the number of ions stored in the C-trap [59]). In full MS experiments, the detection of low abundance ions in the presence of high abundance ions is therefore challenging for two reasons: 1) the space charge capacity of the C-trap may get saturated with ions present in high abundance and thus the sensitivity for low abundance ions gets limited; and 2) the high dynamic range of the ion population (the ratio of maximum signal to minimum signal) compromises the mass accuracy measurements of the ions with too low and too high intensity [60].

5.3.2 Study of PnTXs and SPXs analogs without reference standard materials

Pinnatoxins and SPX-1 comprise a long list of more than 20 analogs (Table 5-1), most of them without available reference standard materials. High resolution mass spectrometry (HRMS) suits these applications: it enables the screening of an unlimited list of precursor ions in full scan mode, and provides great selectivity thanks to its high resolving power and precision in mass accuracy measurements. Thus, HRMS reduces the dependence on reference standard materials to identify compounds [61, 62].

Two studies from 2011 explored the capabilities of the Orbitrap® mass analyzer to screen marine toxins in shellfish samples, and in 2014 Domènech et al. [63] validated a quantitative method for lipophilic toxins. The screening methods were very comprehensive: Gerssen et al.[64] created an exportable search library for 85 lipophilic marine toxins, and Blay et al. [61] included the most common lipophilic and hydrophilic marine toxins in shellfish. However, the screening methods had different approaches using the same instrumentation (LC-HR Orbitrap FT-MS 100,000

resolution at 400 *m/z* FWHM): while Blay et al. [61] relied only on the extraction of 5 ppm mass windows around the calculated mass of the precursor ions in full MS scans; Gerssen et al. [64] claimed that this approach is insufficient for confirmation, thus the study included criteria such as retention times of the analytes, spectral information, and blank samples to assess the potential false positives. Domènech et al. [63] also included those confirmation criteria, which could be potentially applied to real samples.

A suitable selection of the mass tolerance error is essential to provide optimum selectivity: the narrower the mass tolerance error, the less "false positives" (chromatographic peaks produced by compounds with an exact mass in the mass tolerance range). On the other hand, physical resolution and precision in mass accuracy measurements of the instrument determine the width of the mass error tolerance: setting a too narrow tolerance may lead to false negatives due to shifts in accurate mass measurements caused by hidden isobaric interferences and/or distortion of chromatographic peaks[62, 65]. Defining an appropriate mass error tolerance seems to be a fit-for-purpose task [62], thus taking into account the resolution of our LTQ Orbitrap Discovery® (resolution 30,000 at 400 *m/z* FWHM) and the good precision in mass accuracy measurements for PnTX-G and SPX-1 (<2 ppm, section 2.5.2.), we screened the samples for PnTXs and SPXs with a 10 ppm mass tolerance window. This tolerance widely accepted in HRMS applications led to a remarkable number of false positives, even in methanol blanks (Sup. Mat. Figure 5-1). Therefore we investigated the isotopic patterns and MS^2 full scans as additional confirmation tools.

Isotopic pattern and relative isotope abundance (RIA) can be used as confirmation criteria and facilitate elemental composition elucidation, also in retrospective analysis[66], but both can be affected by low ion abundance [67, 68]. According to our data, mass accuracy and RIA are not reliable when ion abundance is lower than 10^4 counts, which would correspond to 0.2 ng/mL PnTX-G in methanol in our conditions of analysis (**¡Error! No se encuentra el origen de la referencia.**, Sup. Mat. Table 5-1 and Sup. Mat. Table 5-2). We assessed the isotopic pattern of the protonated ion $[M+H]^+$ of PnTX-G in sample MUS120523 (694.4677 *m/z*; 5.9 ng/mL PnTX-G in the methanolic extract) and found that only the first isotope ($C_{41}{}^{13}CH_{64}NO_7$) was measured accurately (<10 ppm), thus the complexity of shellfish matrices negatively influenced the abundance threshold for isotopic pattern analysis (Sup. Mat. Table 5-3). Therefore the used of this confirmation criteria was not feasible in our study.

Product ion scans from previously isolated precursor ions can provide reliable information for confirmation, but they cannot be used as a post-run screening tool [66], unless the precursor ions had been isolated in the ion trap analyzer. The LTQ Orbitrap Discovery® can perform "data dependent MS^2 experiments" (i.e. the precursor ion found in the full MS scan triggers an MS^2 scan). However, the success of these experiments depend on the careful selection of an appropriate abundance threshold for the precursor ion in the full MS scan: too low thresholds lead to MS^2 scans even in methanol blanks, while higher thresholds did not trigger any scan even in positive control samples. Thus, for the samples analyzed in this study, the levels of cyclic imines around few parts-per-billion did not allow performing data dependant MS^2 experiments.
The comprehensive study of sample MUS120523 illustrates our strategy applied to identify PnTXs and SPXs. We searched for all PnTXs and SPXs listed in Table 5-1 using a 10 ppm filter around the exact mass of the precursor ions. Figure 5-3 shows that 9 out of 22 precursor ions

produced a chromatographic peak in the sample, although the ion abundances were too low to apply isotopic patterns and MS^2 products as confirmation criteria. We focused on the peak produced by 766.4889 *m/z* (PnTX-F, Figure 5-3J), since the abundance of this ion was in the same order of magnitude as the ion abundance of the confirmed PnTX-G. Figure 5-4 illustrates the extracted ion chromatograms (Figure 5-4A), evaluation of the isotopic pattern (Figure 5-4B and 4C) and the MS^2 full scan on 766.5 *m/z* (Figure 5-4D). We rejected the presence of PnTX-F in the sample, since: i) the fragment 164.1434 *m/z* (the actual cyclic imine in the structure) was not present in the MS^2 product ion scan scan (Figure 5-4A and 4D), ii) the diagnostic fragment 446.3265 *m/z* was present but not at the same retention time as the precursor ion (Figure 5-4A), iii) the isotopic pattern of the precursor ion did not correspond with the simulated isotopic pattern for PnTX-F formula: the isotopes A+1 ($C_{44}{}^{13}CH_{68}NO_9$) and A+2 ($C_{43}{}^{13}C_2H_{68}NO_9$) were not present (with 10 ppm mass tolerance) and the isotopic ion ratios of the present ions did not fit the expected pattern (Figure 5-4B and 4C), iv) the MS^2 product ion scan from the precursor ion $[M+H]^+$ of PnTX-F did not reveal any fragments that could have been related with toxins from the cyclic imine group (Figure 5-4D).

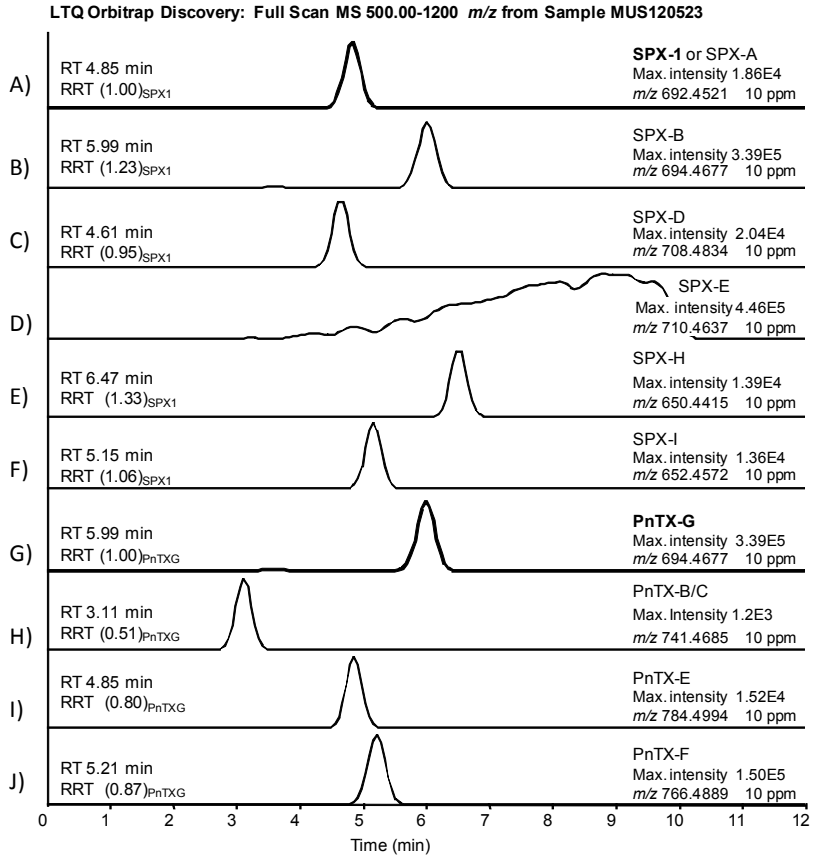

Figure 5-3. A to J) Extracted chromatograms of precursor ions of spirolides and pinnatoxins listed in Table 5-1 that produced a peak with 10 ppm mass window tolerance in sample MUS120523. Retention times (RT) in minutes; RRT in brackets is the RT relative to the main toxin in the group (SPX-1 or PnTX-G).

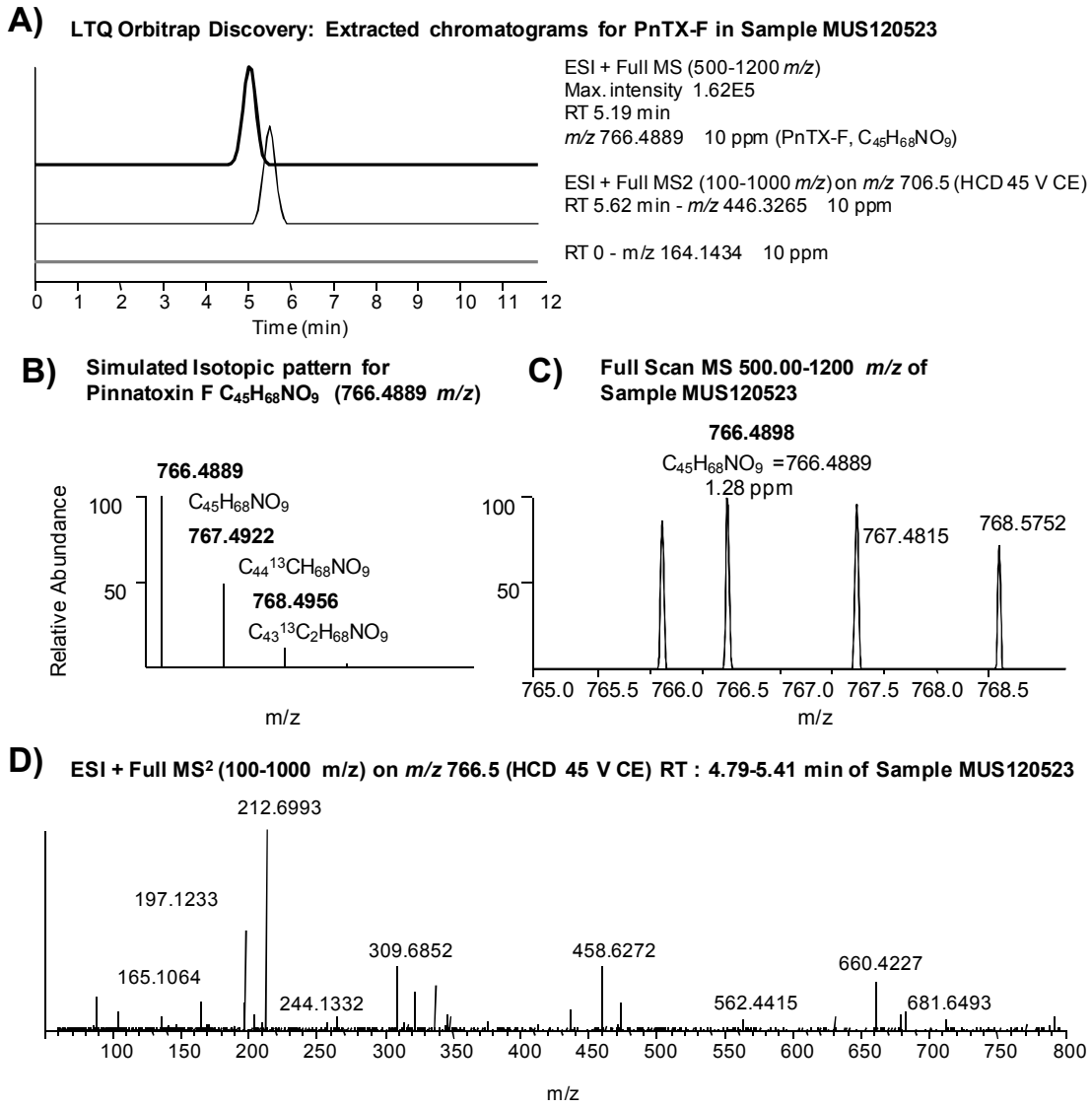

Figure 5-4. Study of a false positive of PnTX-F in sample MUS120523: A) extracted ion chromatogram of the precursor ion (766.4889 *m/z*) in the MS scan, and an extracted chromatogram of the diagnostic fragments (164.1434 *m/z* and 446.3265 *m/z*) in the MS² product scan (10 ppm mass window in both cases); B and C) isotopic pattern of the precursor ion (simulated and found, respectively); and D) MS² product scan on the precursor ion (766.5 *m/z*).

We confirmed that all peaks in Figure 5-3 (except peaks of PnTX-G and SPX-1, Figure 5-3A and 3G) were false positives. Before applying the confirmatory tests in HRMS in the rest of the samples, we screened them in the 3200QTrap® using the diagnostic fragments listed in Table 5-1. Some samples showed peaks in MRM that could correspond to diagnostic fragments of PnTXs and SPXs analogs, but they were proved to be false positives during the confirmatory analysis in HRMS. Therefore, according to our identification criteria, only PnTX-G and SPX-1 were present in the sample above the limits of detection.

5.3.3 Search for acyl ester derivatives of pinnatoxins and spirolides

Acyl ester derivatives have been found for toxin analogs belonging the three major types of cyclic imines (SPXs, PnTXs, GYMs) and described in shellfish samples from Tunisia, Canada and Norway [39, 41, 69]. Unlike SPXs and GYMs, PnTXs resist the alkaline hydrolysis protocol applied for the indirect determination of acyl ester analogs of the okadaic acid group of toxins. The presence of these shellfish metabolites can be evidenced by an increment in the concentration of free PnTXs after hydrolysis, compared to the concentration in the crude extract [41] However, acyl esters of SPXs cannot be assessed with this approach. We hydrolized the three mussel samples with the highest PnTX-G concentration to look for PnTX-G acyl derivates, but the concentration of PnTX-G only increased about 20%, much less than the 3-fold increase in PnTX-G concentration reported in Canadian shellfish [41]. Further investigation of the samples by precursor ion scans of the product 164.1 *m/z* in a 3200QTrap® did not provide evidences on the presence of PnTXs or SPXs acyl esters in the samples (Sup. Mat. Figure 5-3). Our results are in line with other studies that reported free PnTXs in mussels, oysters and sea hares with no significant levels of acyl ester metabolites of PnTXs being present [70-72]. Thus, metabolization of free toxins into acyl ester derivatives should always be studied in different shellfish species and/or in their physiological state.

5.3.4 Quality assessment of the methods

5.3.4.1 Low resolution MS with the triple quadrupole 3200QTrap®

Our method developed on the triple quadrupole 3200QTrap® provided the first hint of the presence of cyclic imines in samples of mussels, oysters and passive sampler devices from Catalonia (Spain). According to the Commission Decision 2002/657/EC [54], the confirmatory potential of the low resolution MS method is enough for PnTX-G and SPX-1 (one precursor ion, three product ions, ratio of abundance between product ions, and retention times). However, the method relying on the triple quadrupole mass analyzer constrained its applicability for the rest of toxin analogs lacking of reference standards. For them, the method was used as a screening tool in combination with high resolution MS as a confirmatory technique. The quantitative method presented comparable results for PnTX-G and SPX-1 (Table 5-4), showing good intra-day and inter-day precision (<3.1% RSDr and 7.1% RSDR, for SPX-1 in oysters), high sensitivity, good linearity, and small variation in retention time.

Matrix components might influence identification parameters, such as product ion ratio [73], but it was not the case in our study. Product ion ratios were very reproducible in the calibration curves prepared in methanol (<0.5% variation), and the influence of the matrices was completely negligible for PnTX-G ion ratios (<0.3% variation). Product ion ratios for SPX-1 where slightly different in spiked mussels compared to those in methanol (-1.0%), and especially in oysters (-4.9% variation), but these variations fell in the tolerance ranges proposed by the Commission Decision 2002/657/EC (±25% variation allowed) [54] .

The average recovery (Table 5-4) for SPX-1 was over 80% for mussels and oysters, but shellfish tissues may suppress the ion signal for PnTX-G quantification, since recoveries were below 80% (Table 5-4). We found negative matrix effects with mussels and oysters for GYM-A in a previous work [45], thus structurally related PnTX-G may suffer the same problem. We addressed this

issue by correcting the quantification of the samples with recovery values obtained for the spiked samples.

Limits of detection and quantification were very low for both toxins in oysters (<1.5 µg/kg), but unexpectedly high (up to 56.1 µg/kg for PnTX-G) in mussels (Table 5-4). This can be explained because the mussel tissue used as a blank had trace levels (below LOQ) of SPX-1 and PnTX-G. Carryover did not cause this problem since the methanol blanks analyzed after the most concentrated level of the calibration curves never showed signal for these toxins. We could not find any mussel sample (from n=12) with undetectable levels of PnTXs and SPXs at the time of the study. In 2014, we had access to a mussel sample collected in the same shellfish harvesting area with no traces of PnTXs. Since PnTX-G standard solution is not commercialized, its availability is extremely restricted. Thus we could not repeat the experiments to calculate LOQ and LOD using the same methodology. Nevertheless, we spiked a metanolic extract of a mussel sample at 38 µg PnTX-G/kg mussel tissue and estimated the LODs and LOQs with five injections. The new LOD and LOQ would be 0.2 and 0.3 µg PnTX-G/kg mussel, a much lower result that would fit better with the S/N ratios we observed in samples and in standard solutions. For instance, the same spiking in methanol yielded to LODs and LOQs of 0.08 and 0.19 µg PnTX-G/L.

Table 5-4. Quality assessment of the quantification on the triple quadrupole 3200QTrap® mass spectrometer (three days, single laboratory). $[M+H]^+$ ions were 692 *m/z* and 694 *m/z* for SPX-1 and PnTX-G respectively. Product ions monitored were 674 *m/z*, 444 *m/z* and 164 *m/z* for SPX1 (MRM1 as the quantifier, MRM2 and MRM3 as the qualifiers respectively); and 676 *m/z*, 458 *m/z* and 164 *m/z* for PnTX-G (MRM1, MRM2 and MRM3 respectively). Product ion ratios were calculated as the relative area (in percentage) of the qualifier MRM2 compared to the area of the quantifier MRM1. Variations in product ion ratios in mussels and oysters represent the difference (in percentage) between product ion rations measured in metanolic standard solutions and in spiked samples of mussels and oysters. LODs and LOQs in mussels were not trustable because the spiked sample was not completely blank. Later analysis on a PnTX-G free mussel sample had an LOD = 0.2 µg/kg and LOQ = 0.3 µg/kg (different methodology for limits calculation, see Results and Discussion and Experimental Section).

		SPX-1	PnTX-G
Linearity range (ng/mL) (n=15)		2.5-50	2.5-50
RT (average, n=75)		6.33	7.36
% drift		0.3	0.2
Product ion ratios (%) (n=30)	Area MRM2 / Area MRM1	40.7	77.1
	% variation in mussels	-1.0%	0.3%
	% variation in oysters	-4.9%	0.1%
Recovery (%) (n=9)	Mussel	91.6	77.6
	Oyster	81.0	66.6
Intra-day precision (RSDr)(%) (n=9)	Mussel	2.6	2.9
	Oyster	3.1	2.5
Inter-day precision (RSDR) (%) (n=9)	Mussel	7.0	6.8
	Oyster	7.1	6.2
LOQ (µg/kg) (n=3)	Mussel	19.6	56.1
	Oyster	0.7	0.9
LOD (µg/kg) (n=3)	Mussel	5.5	10.8
	Oyster	1.1	0.5

5.3.4.2 High resolution MS with the LTQ Orbitrap Discovery®

The confirmatory method with the LTQ Orbitrap Discovery® for PnTX-G and SPX-1 included the precursor and three product ions measured at high resolution (mass accuracy <2 ppm), in addition to one product ion ratio and retention times. Relative isotope abundances could not be applied to precursor ions due to lack of sensitivity.

High resolution MS reduces dependence on analytical standards for qualitative analysis. For instance, to confirm PnTXs and SPXs analogs without reference standards, the measurement of the precursor and three diagnostic product ions by HRMS would satisfy the guidelines of the Commission Decision 2002/657/EC[54].

Mass accuracy measurements for PnTX-G and SPX-1 were very reliable (<2 ppm in all cases, Table 5-5) for the precursor and product ions selected. Even for the lowest concentration analyzed of the standard solutions (2.5 ng/mL SPX-1 and 0.95 ng/mL PnTX-G), the mass accuracy was very good (<1 ppm). Thus, the method could reliably confirm the presence of SPX-1 and PnTX-G even at very low concentrations.

Variations in retention times were below 2%, but the variation in product ion ratios was about 20% in the methanolic solutions of the standards (concentrations 2.5 to 40 ng/mL SPX-1 and 0.95 to 190 ng/mL PnTX-G, see Experimental Section). The use of product ion ratios for identification and confirmation has been questioned in several studies due to their lack of robustness, especially at low concentrations [74-77], which seem to concur with the lack of reproducibility in our product spectra acquired with the LTQ Orbitrap Discovery®.

Table 5-5. Quality assessment of identification (LTQ Orbitrap Discovery®, mass resolution FTWM 30,000 at 400 *m/z*). RT: retention time. Averages of 13 injections in two days at five concentrations (2.5 to 40 ng SPX-1/mL; 0.95 to 190 ng PnTX-G/mL).

	NRC CRM SPX-1				NRC CRM PnTX-G			
RT (min)								
Average	4.75				5.92			
% drift	2				1			
	Frag 1	Frag 2	Frag 3	Prec.	Frag 1	Frag 2	Frag 3	Prec.
Exact mass	164.1434	444.3108	674.4415	692.4521	164.1434	458.3265	676.4572	694.4677
Mass accuracy (Δ ppm)								
Average	-0.3	0.1	0.4	0.5	-0.4	-0.5	-0.1	0.1
Max.	-2.0	-1.6	-0.9	0.7	-1.7	-1.8	-1.4	-1.6
Ion ratios								
% of Frag 1 intensity	100	53	50		94	69	100	
% difference		19	23		22	15		

5.4 Conclusions

We unequivocally confirmed and quantified PnTX-G and SPX-1 in shellfish and passive samplers (SPATTs) from Catalonia, Spain. This is the first report of pinnatoxins in Spain and the first time that spirolides have been detected in Catalonia. We developed and discussed a comprehensive strategy to avoid false positives of toxin analogs of PnTXs and SPXs by LC-MS/MS analysis, with applicability to other toxin groups and analogs, that consisted on:

1) Fast and sensitive screening in low resolution MS with a 3200QTrap® triple quadrupole using diagnostic transitions for all PnTXs and SPXs described up to date.
2) Confirmation analysis in high resolution MS with an LTQ Orbitrap Discovery® that included the inspection of isotopic patterns and MS^2 spectra, and the look for the precursor ion and three diagnostic product ions with a mass tolerance window selected accordingly to the method performance.

Evidences of acyl ester metabolites of PnTXs could not be obtained from mussel samples, neither after application of the alkaline hydrolysis procedure nor through precursor ion scan mass spectrometric experiments.

Cyclic imines should be included in the shellfish safety monitoring programs of lipophilic marine toxins by LC-MS methods, even if they are not regulated, to better assess their presence in shellfish and favor exposure studies that would enable a reliable risk analysis for consumers. The introduction of benchtop high resolution mass spectrometry instruments in research and control laboratories may enhance the capabilities to ensure unequivocal confirmation of emerging marine toxins, as shown in this work. However, a proper strategy should be applied combining isotopic patterns, MS and MS^2 accurate mass measurements, signal thresholds, and tolerances applied to mass filters in order to avoid potential false positives or negatives.

References

1. Guéret, S. and M. Brimble, *Spiroimine shellfish poisoning (SSP) and the spirolide family of shellfish toxins: Isolation, structure, biological activity and synthesis.* Natural Product Reports, 2010. **27**: p. 1350-1366.
2. Otero, A., et al., *Cyclic imines: chemistry and mechanism of action: a review.* Chemical Research in Toxicology, 2011. **24**: p. 1817-1829.
3. Kita, M., et al., *Symbioimine and neosymbioimine, amphoteric iminium metabolites from the symbiotic marine dinoflagellate Symbiodinium sp.* Bioorganic & Medicinal Chemistry, 2005. **13**(17): p. 5253-5258.
4. Selwood, A.I., et al., *Portimine: a bioactive metabolite from the benthic dinoflagellate Vulcanodinium rugosum.* Tetrahedron Letters, 2013. **54**(35): p. 4705-4707.
5. Duroure, L., et al., *6,6-Spiroimine analogs of (-)-gymnodimine A: Synthesis and biological evaluation on nicotinic acetylcholine receptors.* Organic and Biomolecular Chemistry, 2011. **9**(23): p. 8112-8118.
6. Hu, T., et al., *Spirolides B and D, two novel macrocycles isolated from the digestive glands of shellfish.* J. Chem. Soc. Chem. Commun., 1995: p. 2159-2161.
7. Hellyer, S., et al., *Marine algal pinnatoxins E and F cause neuromuscular block in an in vitro hemidiaphragm preparation.* Toxicon, 2011. **58**: p. 693-9.
8. Hauser, T.A., et al., *Comparison of acetylcholine receptor interactions of the marine toxins, 13-desmethylspirolide C and gymnodimine.* Neuropharmacology, 2012. **62**(7): p. 2239-2250.
9. EFSA Panel on Contaminants in the Food Chain (CONTAM), *Scientific Opinion on marine biotoxins in shellfish - Cyclic imines* - EFSA Journal, 2010. **8**(6): p. 1628.
10. Cembella, A., N. Lewis, and M. Quilliam, *The marine dinoflagellate Alexandrium ostenfeldii (Dinophyceae) as the causative organism of spirolide shellfish toxins.* Phycologia, 2000. **39**: p. 67-74.
11. Touzet, N., J.M. Franco, and R. Raine, *Morphogenetic diversity and biotoxin composition of Alexandrium (Dinophyceae) in Irish coastal waters.* Harmful Algae, 2008. **7**: p. 782-797.
12. Haywood, A., et al., *Comparative morphology and molecular phylogenetic analysis of three new species of the genus Karenia (Dinophyceae) from New Zealand.* Journal of Phycology, 2004. **40**(1): p. 165-179.
13. Rhodes, L., et al., *Dinoflagellate Vulcanodinium rugosum identified as the causative organism of pinnatoxins in Australia, New Zealand and Japan.* Phycologia, 2011. **50**: p. 624-628.
14. Tomas, C., et al., *Alexandrium peruvianum (Balech and Mendiola) Balech and Tangen a new toxic species for coastal North Carolina.* Harmful Algae, 2012. **17**: p. 54-63.
15. Van Wagoner, R.M., et al., *Occurrence of 12-methylgymnodimine in a spirolide-producing dinoflagellate Alexandrium peruvianum and the biogenetic implications.* Tetrahedron Letters, 2011. **52**: p. 4243-4246.
16. Zheng, S., et al., *The isolation and bioactivities of pinnatoxin.* Chin. J. Mar. Drugs, 1990. **33**: p. 33-35.
17. Rhodes, L., et al., *Production of pinnatoxins E, F and G by scrippsielloid dinoflagellates isolated from Franklin Harbour, South Australia.* New Zealand Journal of Marine and Freshwater Research, 2011. **45**: p. 703-709.
18. Rundberget, T., et al., *Pinnatoxins and spirolides in Norwegian blue mussels and seawater.* Toxicon, 2011. **58**: p. 700-711.

19. Hess, P., et al., *Pinnatoxin G is responsible for atypical toxicity in mussels (Mytilus galloprovincialis) and clams (Venerupis decussata) from Ingril, a French Mediterranean lagoon.* Toxicon, 2013.
20. Hu, T., et al., *Characterization of biologically inactive spirolides E and F: Identification of the spirolide pharmacophore.* Tetrahedron Lett., 1996. **37**: p. 7671-7674.
21. MacKinnon, S., et al., *Biosynthesis of 13-desmethyl spirolide C by the dinoflagellate Alexandrium ostenfeldii.* Journal of Organic Chemistry, 2006. **71**: p. 8724-8731.
22. Amzil, Z., et al., *Report on the first detection of pectenotoxin-2, spirolide-a and their derivatives in French shellfish.* Marine drugs, 2007. **5**: p. 168-79.
23. Ciminiello, P., et al., *Toxin profile of Alexandrium ostenfeldii (Dinophyceae) from the Northern Adriatic Sea revealed by liquid chromatography-mass spectrometry.* Toxicon, 2006. **47**: p. 597-604.
24. Villar-González, A., et al., *First evidence of spirolides in Spanish shellfish.* Toxicon, 2006. **48**: p. 1068-74.
25. Álvarez, G., et al., *First identification of azaspiracid and spirolides in Mesodesma donacium and Mulinia edulis from Northern Chile.* Toxicon, 2010. **55**: p. 638-641.
26. Gribble, K., et al., *Distribution and toxicity of Alexandrium ostenfeldii (Dinophyceae) in the Gulf of Maine, USA.* Deep-Sea Research Part II: Topical Studies in Oceanography, 2005. **52**: p. 2745-2763.
27. Biré, R., et al., *First evidence on occurrence of gymnodimine in clams from Tunisia.* Journal of Natural Toxins, 2002. **11**: p. 269-275.
28. Marrouchi, R., et al., *Quantitative Determination of Gymnodimine-A by High Performance Liquid Chromatography in Contaminated Clams from Tunisia Coastline.* Marine Biotechnology, 2010. **12**(5): p. 579-585.
29. Naila, I.B., et al., *Prevalence and persistence of gymnodimines in clams from the Gulf of Gabes (Tunisia) studied by mouse bioassay and LC–MS/MS.* Harmful Algae, 2012. **18**: p. 56-64.
30. Ciminiello, P., et al., *Spirolide toxin profile of adriatic Alexandrium ostenfeldii cultures and structure elucidation of 27-hydroxy-13,19-didesmethyl spirolide C.* Journal of Natural Products, 2007. **70**(J. Nat. Prod.): p. 1878-1883.
31. Ciminiello, P., et al., *Complex toxin profile of Mytilus galloprovincialis from the Adriatic sea revealed by LC-MS.* Toxicon, 2010. **55**: p. 280-288.
32. Ciminiello, P., et al., *Characterization of 27-hydroxy-13-desmethyl spirolide C and 27-oxo-13,19-didesmethyl spirolide C. Further insights into the complex Adriatic Alexandrium ostenfeldii toxin profile.* Toxicon, 2010. **56**: p. 1327-33.
33. Satta, C.T., et al., *Studies on dinoflagellate cyst assemblages in two estuarine Mediterranean bays: A useful tool for the discovery and mapping of harmful algal species.* Harmful Algae, 2013. **24**: p. 65-79.
34. Hu, T., et al., *Characterization of spirolides a, c, and 13-desmethyl c, new marine toxins isolated from toxic plankton and contaminated shellfish.* J. Nat. Prod., 2001. **64**: p. 308-12.
35. Sleno, L., A.J. Windust, and D.A. Volmer, *Structural study of spirolide marine toxins by mass spectrometry: Part I. Fragmentation pathways of 13-desmethyl spirolide C by collision-induced dissociation and infrared multiphoton dissociation mass spectrometry.* Anal. Bioanal. Chem., 2004. **378**: p. 969-976.
36. MacKinnon, S., et al., *Spirolides Isolated from Danish Strains of the Toxigenic Dinoflagellate Alexandrium o stenfeldii.* J. Nat. Prod., 2006. **69**: p. 8-12.
37. Roach, J.S., et al., *Characterization of a dispiroketal spirolide subclass from Alexandrium ostenfeldii.* Journal of Natural Products, 2009. **72**: p. 1237-1240.
38. Sleno, L., et al., *Structural study of spirolide marine toxins by mass spectrometry. Part II. Mass spectrometric characterization of unknown spirolides and related compounds in a cultured phytoplankton extract.* Anal. Bioanal. Chem., 2004. **378**: p. 977-986.

39. Aasen, J., et al., *Discovery of fatty acid ester metabolites of spirolide toxins in mussels from Norway using liquid chromatography/tandem mass spectrometry.* Rapid Communications in Mass Spectrometry, 2006. **20**: p. 1531-1537.
40. Selwood, A., et al., *Isolation, structural determination and acute toxicity of pinnatoxins E, F and G.* J. Agric. Food. Chem., 2010. **58**: p. 6532-6542.
41. McCarron, P., et al., *Identification of pinnatoxins and discovery of their fatty acid ester metabolites in mussels (mytilus edulis) from eastern Canada.* Journal of Agricultural and Food Chemistry, 2012. **60**: p. 1437-1446.
42. Uemura, D., et al., *Pinnatoxin A: A toxic amphoteric macrocycle from the Okinawan bivalve Pinna muricata*, in *J. Chem. Soc.* 1995. p. 1155-1156.
43. Takada, N., et al., *Pinnatoxins B and C, the most toxic components in the pinnatoxin series from the Okinawan bivalve Pinna muricata.* Tetrahedron Lett., 2001. **42**: p. 3491-3494.
44. Gerssen, A., et al., *Liquid chromatography-tandem mass spectrometry method for the detection of marine lipophilic toxins under alkaline conditions.* Journal of chromatography A, 2009. **1216**: p. 1421-1430.
45. García-Altares, M., J. Diogène, and P. de la Iglesia, *The implementation of liquid chromatography tandem mass spectrometry for the official control of lipophilic toxins in seafood: Single-laboratory validation under four chromatographic conditions.* Journal of Chromatography A, 2013. **1275**: p. 48-60.
46. Comunitary Reference Laboratory on Marine Biotoxines, *Interlaboratory Validation Study of the EU-Harmonised SOP-LIPO-LC-MS/MS v.4.* 2011.
47. Mountfort, D.O., T. Suzuki, and P. Truman, *Protein phosphatase inhibition assay adapted for determination of total DSP in contaminated mussels.* Toxicon, 2000. **39**(2-3): p. 383-390.
48. MacKenzie, L., et al., *Solid phase adsorption toxin tracking (SPATT): A new monitoring tool that simulates the biotoxin contamination of filter feeding bivalves.* Toxicon, 2004. **44**(8): p. 901-918.
49. Caillaud, A., et al., *Monitoring of dissolved ciguatoxin and maitotoxin using solid-phase adsorption toxin tracking devices: Application to Gambierdiscus pacificus in culture.* Harmful Algae, 2011. **10**(5): p. 433-446.
50. Gerssen, A., et al., *In-house validation of a liquid chromatography tandem mass spectrometry method for the analysis of lipophilic marine toxins in shellfish using matrix-matched calibration.* Analytical and Bioanalytical Chemistry, 2010. **397**: p. 3079-3088.
51. Tran, J.C. and A.A. Doucette, *Cyclic Polyamide Oligomers Extracted from Nylon 66 Membrane Filter Disks as a Source of Contamination in Liquid Chromatography/Mass Spectrometry.* Journal of the American Society for Mass Spectrometry, 2006. **17**(5): p. 652-656.
52. Keller, B.O., et al., *Interferences and contaminants encountered in modern mass spectrometry.* Analytica Chimica Acta, 2008. **627**(1): p. 71-81.
53. Taverniers, I., M. De Loose, and E. Van Bockstaele, *Trends in quality in the analytical laboratory. II. Analytical method validation and quality assurance.* TrAC - Trends in Analytical Chemistry, 2004. **23**(8): p. 535-552.
54. European Commission, *Commision Decission 2002/657/EC.* Official Journal of the European Union, 2002. **L 221**(8).
55. EURLMB, *Interlaboratory Validation Study of the EU-Harmonised SOP LIPO LC MS/MS.* 2011.
56. IUPAC, *Compendium of Chemical Terminology, 2nd ed. (the "Gold Book"). Compiled by A. D. McNaught and A. Wilkinson. Blackwell Scientific Publications, Oxford (1997). XML on-line corrected version: http://goldbook.iupac.org (2006-) created by M. Nic, J. Jirat, B. Kosata; updates compiled by A. Jenkins. ISBN 0-9678550-9-8. doi:10.1351/goldbook. Last update: 2012-08-19; version: 2.3.2.* 2012.
57. Fassel, V.A., *International Union of Pure and Applied Chemistry. Analytical Chemistry Division. Commission on Spectrochemical and Other Optical Procedures for Analysis. Nomenclature,*

symbols, units and their usage in spectrochemical analysis. II. Data interpretation. (Rules approved 1975). Analytical Chemistry, 1976. **48**(14): p. 2294-2294.

58. Corley, J., *Best practices in establishing detection and quantification limits for pesticide residues in foods.* Handbook of residue analytical methods for agrochemicals, 2003. **1**: p. 0471491942-4.
59. Perry, R.H., R.G. Cooks, and R.J. Noll, *Orbitrap mass spectrometry: instrumentation, ion motion and applications.* Mass spectrometry reviews, 2008. **27**(6): p. 661-699.
60. Makarov, A., E. Denisov, and O. Lange, *Dynamic Range of Mass Accuracy in LTQ Orbitrap Hybrid Mass Spectrometer.* Journal of the American Society for Mass Spectrometry, 2006. **17**(7): p. 977-982.
61. Blay, P., et al., *Screening for multiple classes of marine biotoxins by liquid chromatography-high-resolution mass spectrometry.* Analytical and Bioanalytical Chemistry, 2011. **400**: p. 577-585.
62. Kaufmann, A. and S. Walker, *Evaluation of the interrelationship between mass resolving power and mass error tolerances for targeted bioanalysis using liquid chromatography coupled to high-resolution mass spectrometry.* Rapid Communications in Mass Spectrometry, 2012. **27**(2): p. 347-356.
63. Domènech, A., et al., *Determination of lipophilic marine toxins in mussels. Quantification and confirmation criteria using high resolution mass spectrometry.* Journal of Chromatography A, 2014. **1328**: p. 16-25.
64. Gerssen, A., P.P.J. Mulder, and J. de Boer, *Screening of lipophilic marine toxins in shellfish and algae: development of a library using liquid chromatography coupled to orbitrap mass spectrometry.* Analytica chimica acta, 2011. **685**: p. 176-85.
65. van der Heeft, E., et al., *Full-Scan Accurate Mass Selectivity of Ultra-Performance Liquid Chromatography Combined with Time-of-Flight and Orbitrap Mass Spectrometry in Hormone and Veterinary Drug Residue Analysis.* J. American. Soc. Mass Spectrom., 2009. **20**(3): p. 451-463.
66. Kaufmann, A. and S. Walker, *Post-run target screening strategy for ultra high performance liquid chromatography coupled to Orbitrap based veterinary drug residue analysis in animal urine.* Journal of Chromatography A, 2012.
67. Kaufmann, A. and S. Walker, *Accuracy of relative isotopic abundance and mass measurements in a single-stage orbitrap mass spectrometer.* Rapid Communications in Mass Spectrometry, 2012. **26**(9): p. 1081-1090.
68. Xu, Y., et al., *Evaluation of accurate mass and relative isotopic abundance measurements in the LTQ-Orbitrap mass spectrometer for further metabolomics database building.* Anal. Chem., 2010. **82**(13): p. 5490-5501.
69. De La Iglesia, P., et al., *Discovery of gymnodimine fatty acid ester metabolites in shellfish using liquid chromatography/mass spectrometry.* Rapid Communications in Mass Spectrometry, 2013. **27**(5): p. 643-653.
70. MacKenzie, L.A., et al., *Benthic dinoflagellate toxins in two warm-temperate estuaries: Rangaunu and Parengarenga Harbours, Northland, New Zealand.* Harmful Algae, 2011. **10**: p. 559-566.
71. Miles, C.O., et al. *The presence of pinnatoxins in Norwegian mussels. National Veterinary Institute*. 2010. Oslo.
72. Selwood, A.I.A.I.a., et al., *Isolation, structural determination and acute toxicity of pinnatoxins E, F and G.* Journal of Agricultural and Food Chemistry, 2010. **58**: p. 6532-6542.
73. Stolker, A.A.M., et al., *Application of the revised EU criteria for the confirmation of anabolic steroids in meat using GC-MS.* Analytical and Bioanalytical Chemistry, 2004. **378**(5): p. 1313-1321.
74. De Zeeuw, R., *Substance identification: The weak link in analytical toxicology*. J. Chromatogr. B, 2004. **811**: p. 3-12.
75. Lehotay, S., et al., *Identification and confirmation of chemical residues in food by chromatography-mass spectrometry and other techniques.* TrAC - Trends in Analytical Chemistry, 2008. **27**: p. 1070-1090.

76. Mol, H., P. Zomer, and M. De Koning, *Qualitative aspects and validation of a screening method for pesticides in vegetables and fruits based on liquid chromatography coupled to full scan high resolution (Orbitrap) mass spectrometry.* Analytical and Bioanalytical Chemistry, 2012. **403**: p. 2891-2908.

77. Nielen, M.W.F., et al., *Screening and confirmation criteria for hormone residue analysis using liquid chromatography accurate mass time-of-flight, Fourier transform ion cyclotron resonance and orbitrap mass spectrometry techniques.* Analytica chimica acta, 2007. **586**: p. 122-9.

Supplementary Materials

Sup. Mat. Table 5-1. Assigned mass errors (Δ in ppm) to the molecular formula and theoretical *m/z*, and ion intensities on the precursor ion (A) and the first three isotopes (A+m) of PnTX-G (n=2 for 19 and 1.9 ng/mL; n=1 for 190 and 0.2 ng/mL). Mass errors larger than 5 ppm are in bold, also the intensities associated with the analysis that yielded these high mass errors. When intensity were below 1E4, mass accuracy dropped below 5 ppm.

		Concentration – PnTX-G (ng/mL)			
		190	19	1.9	0.2
Isotopes – PnTX-G (*m/z*)		Δ (ppm)			
A (Prec ion) $C_{42}H_{64}NO_7$	(*m/z* 694.4677)	-0.1	-0.4	-0.1	0.4
A+1 $C_{42}{}^{13}CH_{64}NO_7$	(*m/z* 695.4711)	-0.1	-0.5	-1.2	**-20.6**
A+2 $C_{42}{}^{13}C_2H_{64}NO_7$	(*m/z* 696.4744)	0.1	-0.1	-1.4	**-22.7**
A+3 $C_{42}{}^{13}C_3H_{64}NO_7$	(*m/z* 697.4778)	0.7	1.1	**-50.5**	**15.2**
		Intensity counts			
A (Prec ion) $C_{42}H_{64}NO_7$	(*m/z* 694.4677)	1.56E+07	1.95E+06	2.17E+05	1.74E+04
A+1 $C_{42}{}^{13}CH_{64}NO_7$	(*m/z* 695.4711)	7.24E+06	8.88E+05	1.01E+05	**9.36E+03**
A+2 $C_{42}{}^{13}C_2H_{64}NO_7$	(*m/z* 696.4744)	1.80E+06	2.18E+05	1.57E+04	**8.10E+02**
A+3 $C_{42}{}^{13}C_3H_{64}NO_7$	(*m/z* 697.4778)	3.13E+05	2.81E+04	**6.74E+03**	**7.24E+02**

Sup. Mat. Table 5-2. Differences in (%) in intensity ratios between the isotopes (A+m) and the precursor ion (A) compared to the simulated isotopic pattern for PnTX-G (n=2 for 19 and 1.9 ng/mL; n=1 for 190 and 0.2 ng/mL). For low concentrations (1.9 and 0.2 ng/mL PnTX-G) the difference between the simulated isotopic ratios and the measured isotopic ratios is very evident (over 35%).

	Concentration – PnTX-G (ng/mL)			
Isotopes – PnTXG *(m/z)*	*190*	*19*	*1.9*	*0.2*
A+1 / A (Prec ion)	-2	0	-2	-19
A+2 / A (Prec ion)	-15	-11	**38**	**54**
A+3 / A (Prec ion)	-39	0	**-175**	**-187**

Sup. Mat. Table 5-3. Isotopic pattern analysis in sample MUS120523. Assigned mass errors (in ppm) to the molecular formula and theoretical *m/z*, and ion intensities on the precursor ion (A) and the first three isotopes (A+m) of PnTX-G. Differences in (%) in intensity ratios between the isotopes (A+m) and the precursor ion (A) compared to the simulated isotopic pattern for PnTX-G. Only A+1 could be measured with appropriate mass accuracy, and its relative intensity compared to the precursor ion (A) similar to the simulated relative intensity between A+1 and A (12.5% difference). A+2 could not be measured accurately and A+3 was not found.

	Sample MUS120523			
Isotopes – PnTXG (m/z)	*m/z found*	*Intensity counts*	*Mass error (ppm)*	*% Diff. Int. ratios*
A (Prec ion) $C_{42}H_{64}NO_7$ (*m/z* 694.4677)	694.4669	1.63E+05	1.15	
A+1 $C_{42}{}^{13}CH_{64}NO_7$ (*m/z* 695.4711)	695.4702	6.46E+04	1.29	12.5
A+2 $C_{42}{}^{13}C_2H_{64}NO_7$ (*m/z* 696.4744)	696.4883	2.11E+04	**-19.96**	**-28.7**
A+3 $C_{42}{}^{13}C_3H_{64}NO_7$ (*m/z* 697.4778)	Not found	Not found	Not found	Not found

A)

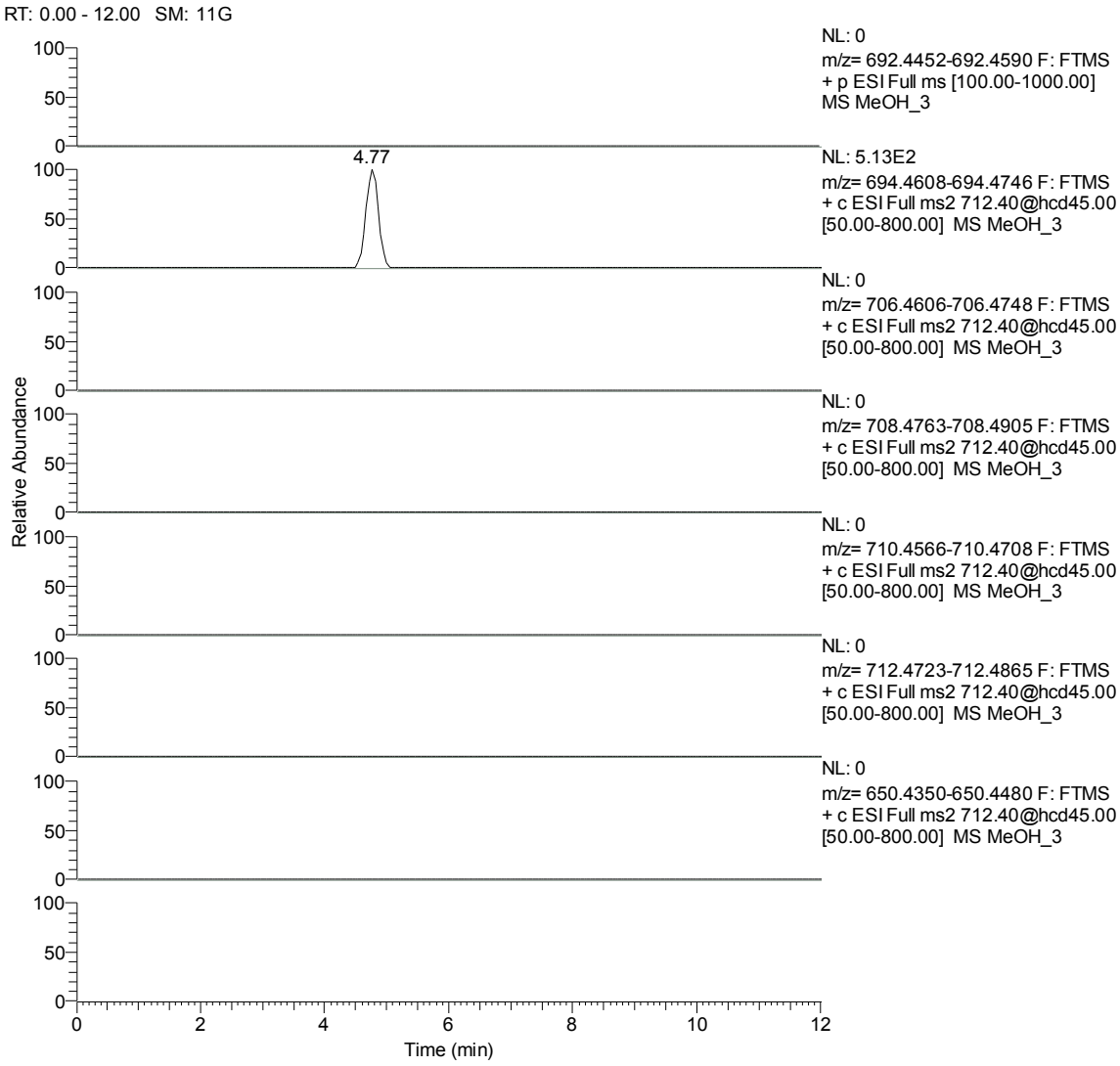

Sup. Mat. Figure 5-1. (A, B, and C): Three methanol blanks screened for spirolides (SPX-1 to SPX-I, see Table 1 in the main article) in the full MS scan at 10 ppm mass error tolerance. Blanks were included in a batch of sixty samples (shellfish and SPATT samples) every six samples. Blank A) First methanol blank; Blank B) Fifth methanol blank; Blank C) Tenth methanol blank. Carryover was discarded by checking the methanol blanks analyzed after the most concentrated level of the calibration curves, which never showed signal for PnTX-G of SPX-1 at their retention times. Peaks did not correlate with the expected relative retention time of the target analytes, but there are no standards available for PnTXs and SPXs other than PnTX-G and SPX-1.

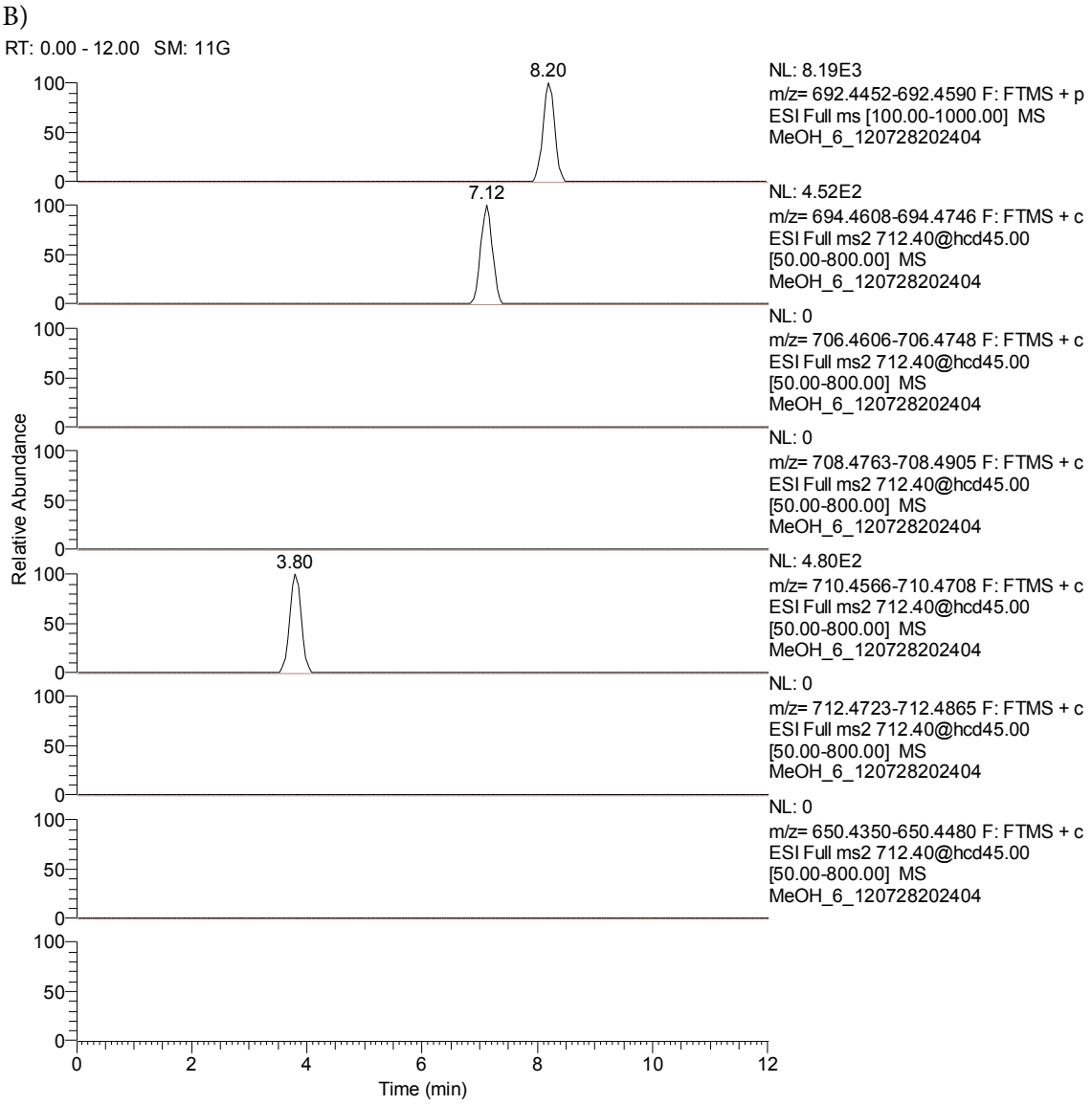

Sup. Mat. Figure 5-1. (A, B, and C): Three methanol blanks screened for spirolides (SPX-1 to SPX-I, see Table 1 in the main article) in the full MS scan at 10 ppm mass error tolerance. Blanks were included in a batch of sixty samples (shellfish and SPATT samples) every six samples. Blank A) First methanol blank; Blank B) Fifth methanol blank; Blank C) Tenth methanol blank. Carryover was discarded by checking the methanol blanks analyzed after the most concentrated level of the calibration curves, which never showed signal for PnTX-G of SPX-1 at their retention times. Peaks did not correlate with the expected relative retention time of the target analytes, but there are no standards available for PnTXs and SPXs other than PnTX-G and SPX-1.

C)

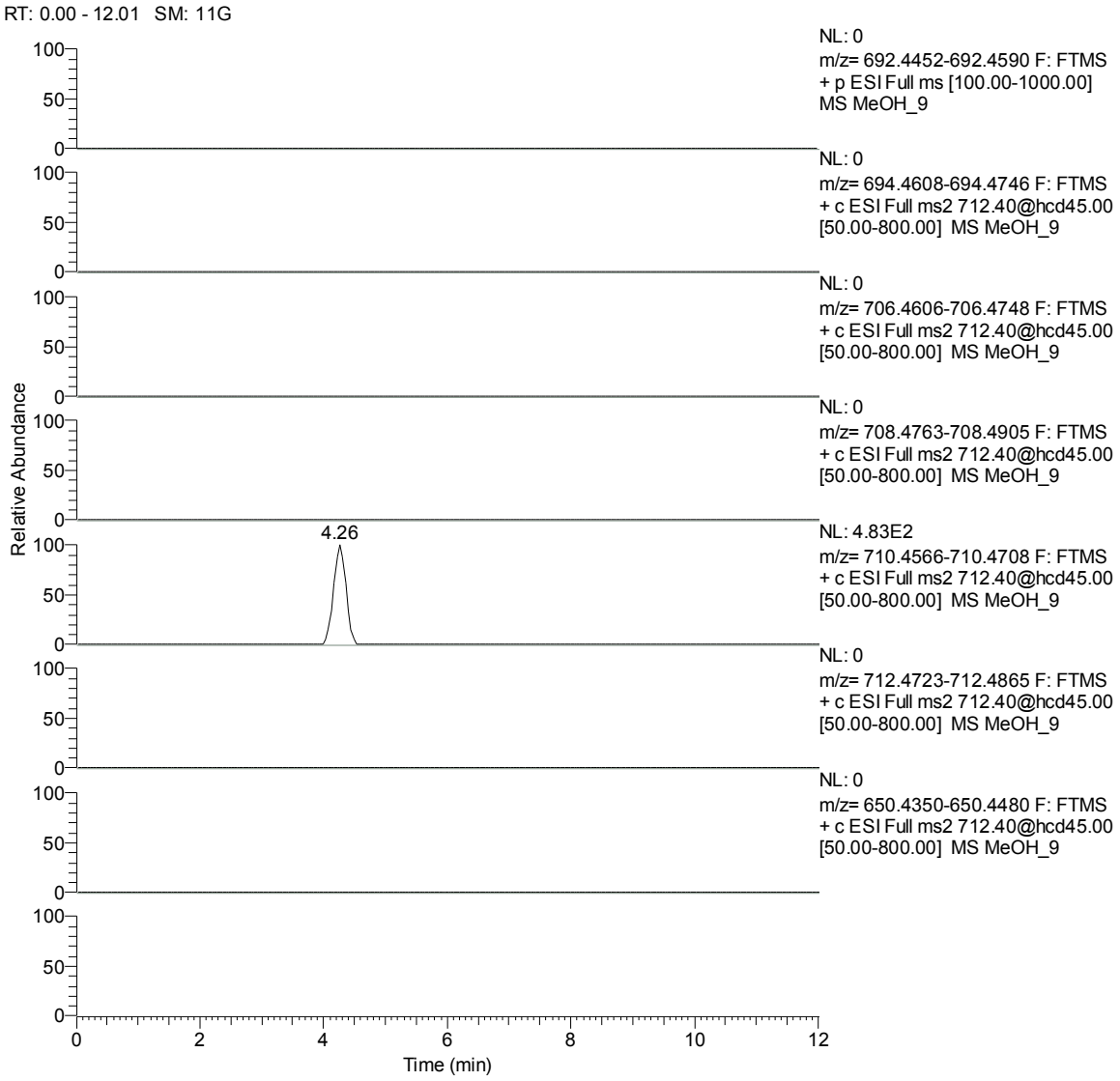

Sup. Mat. Figure 5-1. (A, B, and C): Three methanol blanks screened for spirolides (SPX-1 to SPX-I, see Table 1 in the main article) in the full MS scan at 10 ppm mass error tolerance. Blanks were included in a batch of sixty samples (shellfish and SPATT samples) every six samples. Blank A) First methanol blank; Blank B) Fifth methanol blank; Blank C) Tenth methanol blank. Carryover was discarded by checking the methanol blanks analyzed after the most concentrated level of the calibration curves, which never showed signal for PnTX-G of SPX-1 at their retention times. Peaks did not correlate with the expected relative retention time of the target analytes, but there are no standards available for PnTXs and SPXs other than PnTX-G and SPX-1.

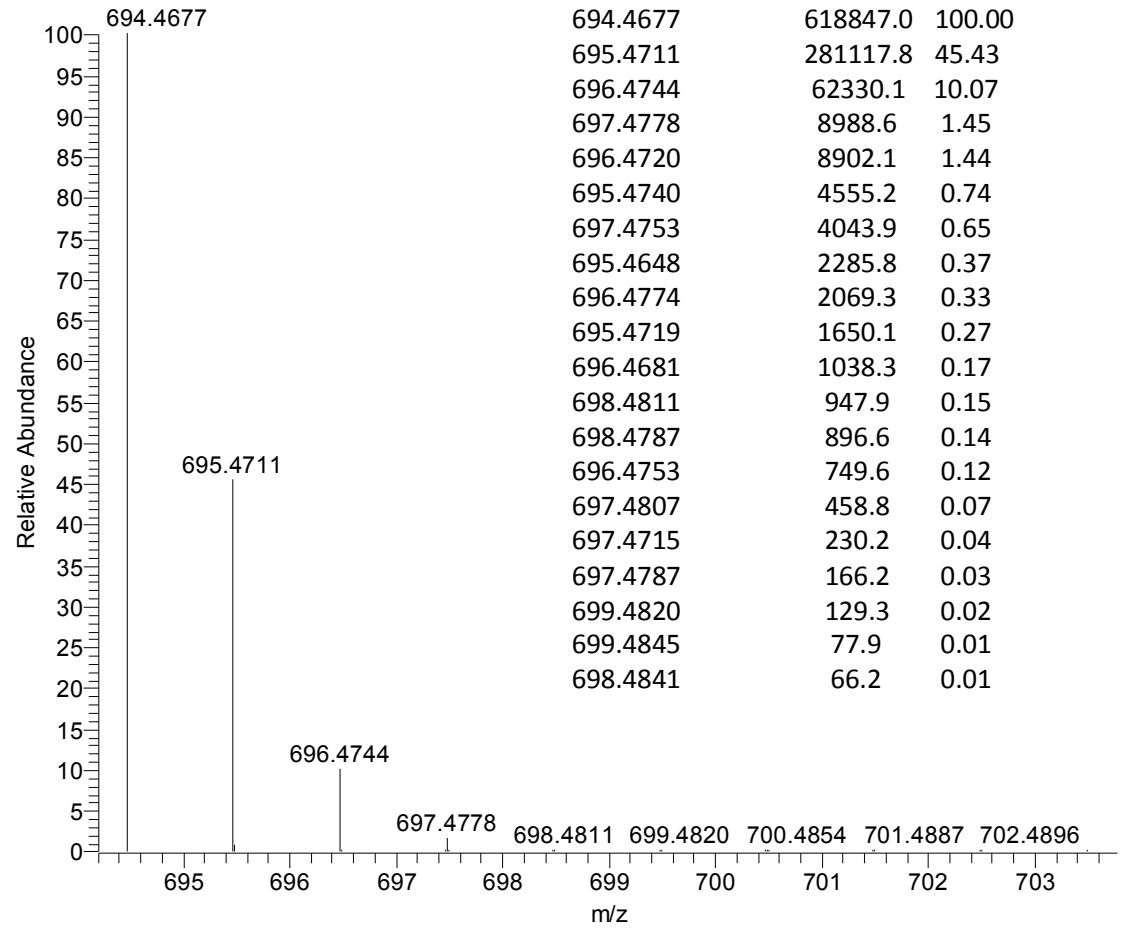

m/z	Intensity	Relative
694.4677	618847.0	100.00
695.4711	281117.8	45.43
696.4744	62330.1	10.07
697.4778	8988.6	1.45
696.4720	8902.1	1.44
695.4740	4555.2	0.74
697.4753	4043.9	0.65
695.4648	2285.8	0.37
696.4774	2069.3	0.33
695.4719	1650.1	0.27
696.4681	1038.3	0.17
698.4811	947.9	0.15
698.4787	896.6	0.14
696.4753	749.6	0.12
697.4807	458.8	0.07
697.4715	230.2	0.04
697.4787	166.2	0.03
699.4820	129.3	0.02
699.4845	77.9	0.01
698.4841	66.2	0.01

Sup. Mat. Figure 5-2. Isotopic pattern simulation for PnTX-G ($C_{42}H_{64}NO_7$) calculated by Xcalibur ® 2.07

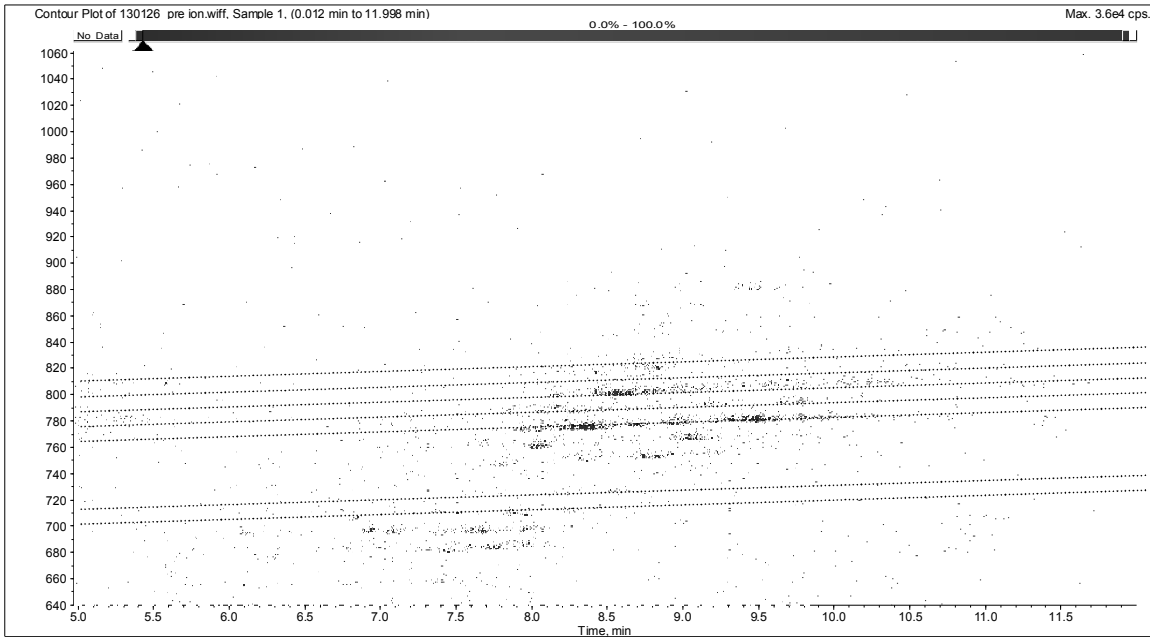

Sup. Mat. Figure 5-3. Contour Plot of LC-MS precursor scan for *m/z*164.2 (CE 45V) with a Triple Quadrupole QTRAP 3200 ®. Sample of mussel from Alfacs Bay (May 2012) with 60 µg/kg free PnTXG. The characteristic pattern with diagonal lines is evident in the figure, which could be consistent with an acylation of PnTXG with fatty acids; although PnTXG esters described in literature [1] were formed by longer chains with *m/z* values between *m/z* 904 (C14:0) and *m/z*1034. (C24:5). The low concentration of these compounds constrained their characterization by MS^2.

[1]McCarron, P.; Rourke, W. A. b. W. a.; Hardstaff, W. W. a.; Pooley, B. b. B.; Quilliam, M. A. a. M. a. *Journal of Agricultural and Food Chemistry* **2012**, *60*, 1437-1446.

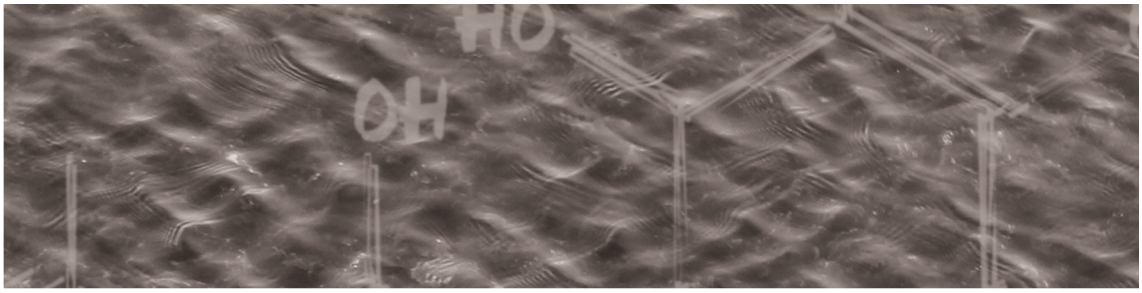

CHAPTER 6

The Novel Ovatoxin-g and Isobaric Palytoxin (so far Referred to as Putative Palytoxin) from *Ostreopsis* cf. *ovata* (NW Mediterranean Sea): Structural Insights by Liquid Chromatography-High Resolution Mass Spectrometry^n

Running Title: **Ovatoxin-g and isomeric palytoxin by LC-HRMS**

Published as:

García-Altares, M., L. Tartaglione, C. Dell'Aversano, O. Carnicer, P. de la Iglesia, M. Forino, J. Diogène, and P. Ciminiello, *The novel ovatoxin-g and isobaric palytoxin (so far referred to as putative palytoxin) from* Ostreopsis *cf.* ovata *(NW Mediterranean Sea): structural insights by LC-High Resolution MS^n*. Analytical and Bioanalytical Chemistry, 2015. 407(4): p. 1191-1204.

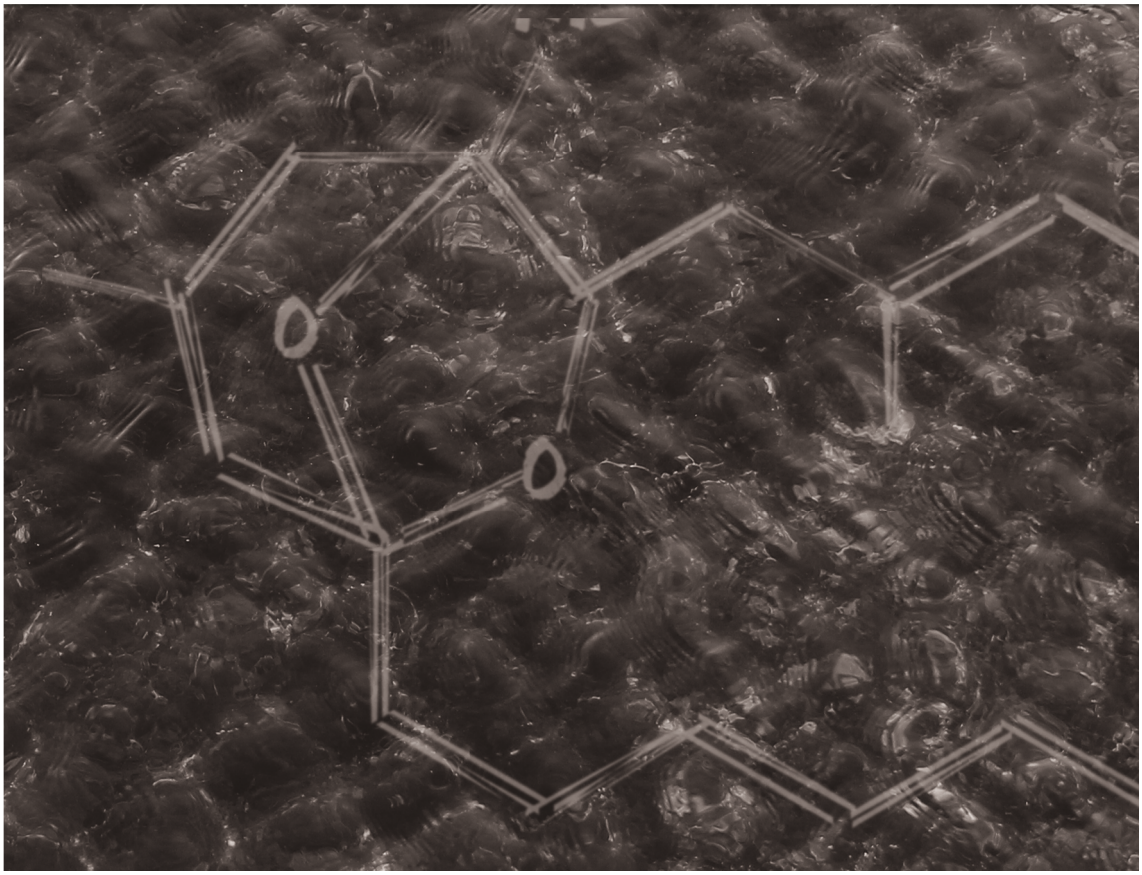

Abstract

Blooms of the benthic dinoflagellate *Ostreopsis* cf. *ovata* are a concern in the Mediterranean Sea, since this species produces a wide range of palytoxin-like compounds listed among the most potent marine toxins. This study focused on two analogs of palytoxin found in cultures of six strains of *Ostreopsis* cf. *ovata* isolated from the south of Catalonia (NW Mediterranean Sea). In addition to some already known ovatoxins, our strains produced two minor compounds, ovatoxin-g and an isomer of palytoxin (putative palytoxin), whose structures had not been elucidated before. Insufficient quantity of these compounds impeded a full NMR-based structural elucidation, thus we studied their structure in crude algal extracts through Liquid Chromatography Electro Spray Ionization High Resolution Mass Spectrometry^{n} (LC-ESI-HRMS^{n}) in positive ion mode. Under the used MS conditions, the molecules underwent fragmentation at many sites of their backbone and a large number of diagnostic fragment ions were identified. As a result, tentative structure was assigned to both ovatoxin-g and putative palytoxin.

Keywords

Putative palytoxin; Ovatoxin-g; *Ostreopsis* cf. *ovata*; High Resolution Mass Spectrometry; NW Mediterranean Sea

6.1 Introduction

Ovatoxins (OVTXs) are complex macromolecules produced by the benthic dinoflagellate *Ostreopsis* cf. *ovata* (Figure 6-1) [1-3]. Structurally, they are closely related to palytoxin (PLTX, $C_{129}H_{223}N_3O_{54}$), one of the most toxic non-peptidic marine compound (LD_{50} by intra-venous administration of 0.15 µg/kg in mouse) [4] first isolated from soft corals of the genus *Palythoa* [5, 6] (Figure 6-1).

Although little is known on their toxicity [7], ovatoxins have been frequently involved in several *Ostreopsis*-related toxic outbreaks following inhalation of marine aerosols in the Mediterranean basin [8-10]. The presence of ovatoxins and *O.* cf. *ovata* cells in the aerosols has been recently proved by chemical and biomolecular means [11, 12].

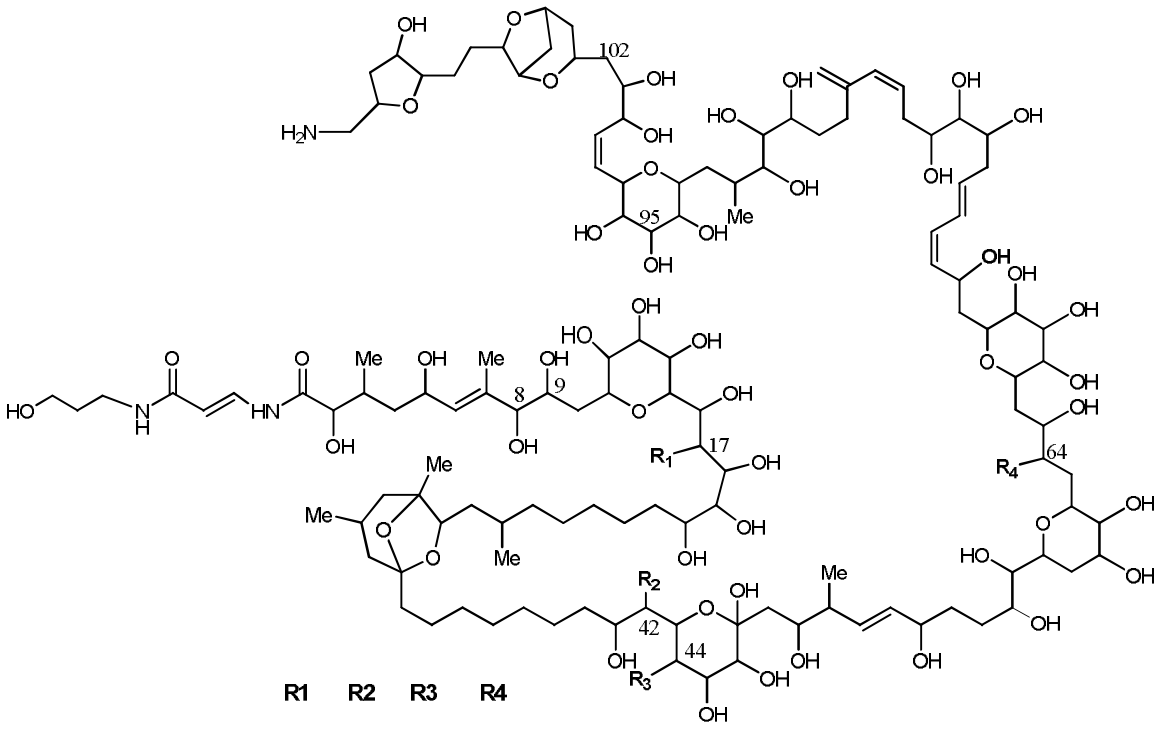

Figure 6-1. Planar structure of palytoxin ($C_{129}H_{223}N_3O_{54}$) from the soft coral *Palythoa tuberculosa* [5, 6] and ovatoxin-a ($C_{129}H_{223}N_3O_{52}$) from the Mediterranean dinoflagellate *Ostreopsis* cf. *ovata* [13, 14] Structure numbering and was performed according to Uemura et al. [6].

Within the complex pool of palytoxin-like compounds produced by Mediterranean *O.* cf. *ovata*, OVTX-a usually represents the major component of the toxin-profile, accounting for about 60% of the total toxin content [3]. In most of the analyzed strains, OVTX-a is followed by OVTX-b, OVTX-d and/or –e, OVTX-c, and a putative palytoxin (pPTLX), listed in decreasing order of abundance. Putative PLTX was the first analog of the toxin profile to be discovered [1] based on

liquid chromatography tandem mass spectrometry (LC-MS/MS) evidences. The term "putative" was added since, due to the complex stereo-structure of palytoxin molecule (Figure 6-1), the possibility that the detected compound was a structural- and/or a stereo-isomer of palytoxin itself could not be excluded.

O. cf. *ovata* toxin profiles have been proven to be strain-specific, since some strains lack some toxins and/or produce individual toxins with different relative abundances. For example, unlike most of the analyzed Italian *O.* cf. *ovata* strains presenting the typical toxin profile [2], some were found not to produce OVTX-b and –c [14]. In addition, OVTX-f was identified only in one strain, of which it also represented the major toxin [3]. Recently, a *O.* cf. *ovata* strain from the French Mediterranean coast has been reported to produce all the ovatoxins (OVTX-a to –f) and quite high levels of pPLTX (12% of the total toxin content) [15]. Toxins scenario becomes even more complicate considering toxin profiles of *Ostreopsis* spp. strains from Japan, that produce a number of different isomers of ovatoxins, namely ovatoxins AC [16] and ovatoxins IKA2 [17]. Such findings suggest that toxin profiles may be a valuable feature to characterize new strains of *O.* cf. *ovata* belonging to the same genetic clade.

Only ovatoxin-a has been isolated and stereo-structurally elucidated by NMR [13, 14]. For all the other ovatoxins, their quantity in *O.* cf. *ovata* extracts was not sufficient for a full NMR-based structural elucidation, and only high resolution (HR) LC-MS data have been provided [18]. They include (a) elution order of the toxins on reversed phase column, (b) molecular formulae of protonated and adduct ions of multiple charge states (1^+, 2^+ and 3^+) which are contained in their full HRMS spectra, and (c) preliminary structural information deriving from the favored cleavage between C-8 and C-9 in fragmentation spectra (Figure 6-1).

More detailed insights into the chemical structures of ovatoxins can be obtained through LC-MS/MS methods, especially when low concentrations of toxins hamper any NMR-based investigation. In 2012, Ciminiello et al. developed a LC-HRMS^n method on the LTQ-Orbitrap, highlighting that palytoxin-like compounds undergo characteristic fragmentations at several sites of their skeleton in positive ion mode [19]. The fragmentation behavior proved useful for gaining structural insights into ovatoxin-a in crude extract [19], that were all confirmed by an NMR-based study on pure compound [14] . The approach was successively used for a preliminary structural characterization of OVTX-f which turned out to differ from OVTX-a only in the C-95/C-102 region (Figure 6-1) [3]. In 2013, Uchida et al. [17] proposed a LC-QTOFMS method in both positive and negative ion modes for structural characterization of ovatoxins IKA2, it allowed to identify sites where such compounds are different from the Mediterranean OVTXs.

In this paper we report on the chemical analysis of *O.* cf. *ovata* strains from Spain where blooms of *Ostreopsis* spp. have been reported since 2001 [20]. *O.* cf. *ovata* was the dominant species but occasionally coexisted with *O.* cf. *siamensis* [9]. In some cases, blooms have caused respiratory distress in humans [9, 10, 21]. Although studies based on LC with fluorescence detection (LC-FLD) and LC-MS have highlighted the presence of palytoxin-like compounds in some Spanish strains [23], algal toxin profiles have not been detailed yet [9]

Since the summer of 2011, the presence of *O.* cf. *ovata* has been detected in the south of Catalonia at the Ebro River Delta (Carnicer et al., submitted). Several strains of *O.* cf. *ovata* were isolated from this area and included in the Mediterranean clade according to their genetic characterization.

We here report on LC-HRMS^n quali-quantitative investigation of the toxin profile of six cultured *O.* cf. *ovata* strains from the Ebro River Delta. Besides identifying the most common ovatoxins in the algal extracts, we gained structural insights into putative PLTX and the novel ovatoxin-g.

6.2 Materials and Methods

6.2.1 Chemicals and Materials

For extraction, methanol gradient grade for HPLC was purchased from Merck (Darmstadt, Germany) and ultrapure water was obtained through a Milli-Q purification system (resistivity >18 MW•cm) from Millipore (Bedford, MA). For LC-MS analyses, acetonitrile (HPLC grade) and water (HPLC grade) were purchased from Sigma Aldrich (Steinheim, Germany). Glacial acetic acid (laboratory grade) was purchased from Carlo Erba (Milan, Italy). Palytoxin standard (from *Palythoa tuberculosa*) was purchased from Wako Chemicals GmbH (Neuss, Germany). An Adriatic *O.* cf. *ovata* extract previously characterized (strain OOAN0601) [22] was used as reference for the Mediterranean ovatoxins.

6.2.2 Collection, Identification and Culturing of *Ostreopsis* cf. *ovata* strains

Six strains of *O.* cf. *ovata* (IRTA-SMM-11-10 from August 2011, IRTA-SMM-12-38, IRTA-SMM-12-46, IRTA-SMM-12-51, IRTA-SMM-12-57 and IRTA-SMM-12-62 from August 2012) were isolated from macroalgae samples (*Jania rubens*) collected in south Catalonia rocky coasts. Cells were isolated by the capillary method [23] and identified under an inverted microscope (Leica DM-IL). Full detailed description of the isolation, morphological and genetic characterization of the *O.* cf. *ovata* strains is described in Carnicer et al. 2014 (submitted). Cultures were made in 500 mL with autoclaved natural filtered seawater and one of them (IRTA-SMM-11-10) was scaled-up to 4 L. Salinity was set at 36, temperature at 24ºC, and illumination was set to 100 µmol photons $m^{-2}{\cdot}s^{-1}$ under 12:12-h light:dark photoperiod. Extraction of DNA was performed according to Andree et al. [24] and polymerase chain reaction (PCR) conditions were set as in Sato et al. [25]. Resulted fragments of rRNA were sequenced bidirectionally by Sistemas Genómicos LLC (Valencia, Spain). Molecular analyses confirmed the identity of *O.* cf. *ovata* in all the strains.
Cell counting was performed in aliquots of each culture using the Utermöhl method [26] as described in Carnicer et al. 2014 (submitted). Cultures were collected in the late stationary phase. Cell abundances where $3.6{\cdot}10^6$ cell/L in IRTA-SMM-11-10, $5.3{\cdot}10^5$ cell/L in IRTA-SMM-12-38, $9.0{\cdot}10^5$ cell/L in IRTA-SMM-12-46, $6.2{\cdot}10^5$ cell/L in IRTA-SMM-12-51, $7.1{\cdot}10^5$ cell/L in IRTA-SMM-12-57 and $5.2{\cdot}10^5$ cell/L in IRTA-SMM-12-62. The cultures were filtered under mild vacuum conditions thought 0.45 µm GF filters and stored at -80ºC until extraction.

6.2.3 Extraction

Cell pellets on filters were extracted with 5 mL of methanol/water solution (80:20, v/v), vortex-mixed for 30 seconds by MS2 Minishaker (IKA Labortechnik, Staufen, Germany) and sonicated

for 35 minutes in pulse mode at 37% amplitude with in an ultrasonic processor Vibra-CellTM (Sonics and Materials, Inc., Newton, CT, USA) while cooling in ice bath. The mixture was centrifuged at 2000 rpm for 10 minutes using Jouan MR 23i Centrifuge (Thermo Fisher Scientific Inc., Waltham, MA, USA) and the supernatant was decanted and then filtered by 0.45 µm nylon membrane syringe filters. This procedure was repeated thrice. The extracts were combined, evaporated and made up to a final volume of 10 mL with the extracting mixture. Extraction was slightly modified for strain IRTA-SMM-11-10 (scaled up culture), its filters were extracted thrice with 10 mL of methanol/water solution (80:20, v/v) and made up to a final volume of 20 mL. The extracts were stored at -20ºC until analyses.

6.2.4 Liquid Chromatography-High Resolution Mass Spectrometry (LC- HRMS)

The analysis were performed on a hybrid linear ion trap LTQ Orbitrap XL™ Fourier transform mass spectrometer (FTMS) equipped with an ESI ION MAX™ source (Thermo Fisher, San José, USA) coupled to an Agilent 1100 LC binary system (Palo Alto, CA, USA). The following LC-HRMS method developed by Ciminiello et al (submitted) was used, slightly modifying the gradient condition to achieve a complete chromatographic resolution of the new ovatoxins. A column of 2.7 µm Poroshell 120 EC-C18, 100 x 2.10 mm (Agilent), was kept at room temperature and eluted at 0.2 mL/min with water (eluent A) and 95% acetonitrile/water (eluent B), both containing 30 mM acetic acid. Gradient elution was 28-29% B in 10 min., 29-30% B in 10 min., 30-100% B in 1 min, and hold for 1 min. Re-equilibration time was 13 min. Injection volume was 5 µL.

High Resolution full MS experiments (positive ions) were acquired in the *m/z* 700-1600 range at a resolving power of 60,000. The following source settings were used: spray voltage = 4.8 kV, capillary temperature = 290 ºC, capillary voltage = 50 V, sheath gas flow = 32 and auxiliary gas flow = 4 (arbitrary units), tube lens voltage = 130 V.

High Resolution collision induced dissociation (CID) MS^2 experiments were acquired at a resolving power of 60,000 (FWHM at *m/z* 400) using a collision energy (CE) = 35%, isolation width (IW) = 4.0 Da, activation Q = 0.250 and activation time (at) = 30 msec. The precursors were $[M+H+Ca]^{3+}$ ions at *m/z* 906.8 (pPLTX and PLTX), *m/z* 896.1 (OVTX-a), *m/z* 910.8 (OVTX-b), *m/z* 916.1 (OVTX-c), *m/z* 901.4 (OVTX-d and -e) and *m/z* 890.8 (OVTX-g).

Calculation of elemental formulae was performed on the mono-isotopic peak of each ion cluster using Xcalibur software v2.0.7. with a mass tolerance of 3 to 5 ppm. The following constrains were used in assignment of molecular formulae: C 50 to 200, H 80 to 300, O 5 to 80, N 1 to 3, assorted cations (Ca, Mg, Na, K) 0 to 1. The isotopic pattern of each ion cluster was taken into consideration in assigning molecular formula.

An external standard calibration curve at four levels of concentration (25, 50, 100 and 1000 ng/mL) was prepared by serial dilution of the palytoxin standard 1000 ng/mL in methanol:water (1:1 v/v) and was used in quantitative analyses. The calibration curve was obtained from triplicate injections. Extracted ion chromatograms (XIC) for all palytoxin-like compounds were obtained by selecting the three most abundant ion peaks of both $[M+H+Ca]^{3+}$ and $[M+2H-H_2O]^{2+}$ ion clusters [2, 19]. Concentration was quantified against the external standard calibration curves by less squared adjustment of the linear regression (Area (cps) =

10147·[PLTX] (ng/mL) - 124714) using chromatographic peak area integrated manually. Instrumental limit of quantification was measured (ILQ= 6 ng/mL). Analytical standards for pPTLX and OVTXs are not available, thus quantification was performed assuming that these compounds would have the same molar response as PLTX.

6.3 Results and Discussion

Six batch-cultures of *O.* cf. *ovata* strains from the Ebro River Delta were extracted and their toxin profiles characterized by LC-HRMS experiments. A newly developed method for ovatoxins (Ciminiello et al., 2014 submitted) was used to analyze the crude extracts under very slow gradient elution. This allowed baseline chromatographic separation of all palytoxin-like compounds contained in the extracts (Figure 6-2). The analyses of the extracts were carried out in parallel with a palytoxin standard (from *P. tuberculosa*) and with an Adriatic *O.* cf. *ovata* extract previously characterized [22] that was used as reference for the Mediterranean ovatoxins. All the samples were analyzed under the same experimental conditions.

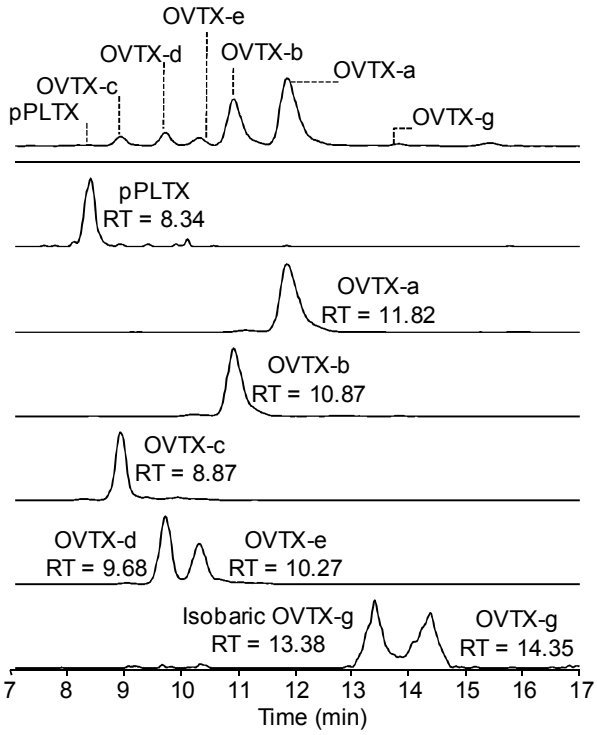

Figure 6-2. TIC of *O.* cf. *ovata* strain IRTA-SMM-11-10 (top trace) and XIC of the $[M+H+Ca]^{3+}$ ions of each toxin (mass tolerance 3 ppm). Analysis were carried out in full HRMS positive ion mode in the mass range *m/z* 700-1600. Under the same experimental conditions, PLTX standard eluted at 10.72 min.

All of the six analyzed *O.* cf. *ovata* extracts contained OVTX-a, -b, -c, -d, -e and pPLTX, whose presence was ascertained by:

a) comparison of retention times of individual compounds with those of toxins contained in the Adriatic extract,
b) ion profile of PLTX-like compounds in full HRMS spectra (mass range *m/z* 700-1600), which represents the fingerprint of this class of molecules [2]. It consists of triply-charged ions in the region *m/z* 830-950 and doubly-charged ions in the region *m/z* 1250-1400 (Table 6-1, Sup. Mat. Figure 6-1). Among them, $[M+H+Ca]^{3+}$ and $[M+2H-H_2O]^{2+}$ ions are the most intense,
c) elemental formula assigned to the mono-isotopic ion peak of each of the formed ions (mass tolerance <3ppm, Table 6-1),
d) consistency of the isotopic pattern of each ion with that simulated for the expected elemental formula,
e) fragmentation behavior of individual compounds in $LC\text{-}HRMS^2$ spectra compared to that of ovatoxins contained in the Adriatic extract used as reference. Results were interpreted according to the previous work on PLTX and OVTX-a [19].

Figure 6-2 shows the total ion chromatogram (TIC) of a representative *O.* cf. *ovata* extract of our strains (IRTA-SMM-11-10) and extracted ion chromatograms (XIC) of $[M+H+Ca]^{3+}$ ions of individual palytoxin-like compounds. Relative abundance of each toxin to the total toxin content was similar to that observed for most of the Mediterranean *O.* cf. *ovata* strains analyzed so far [2, 3, 27-29]. In particular, in this representative sample, OVTX-a accounted for 52% of the total toxin content, followed by OVTX -b (29%), OVTX -e (7%), OVTX -d (6%), OVTX -c (4%), and pPLTX (0.5%). The six *O.* cf. *ovata* strains presented the same toxin profile and similar relative abundance, but total toxin contents were quite different ranging from 50 to 250 pg/cell (Table 6-2). Toxin content on a per cell basis was in most cases higher than that reported for other Mediterranean *O.* cf. *ovata* strains (7.5 to 75 pg/cell) and quite similar to that recently reported for a strain from the French Mediterranean coast (up to 300 pg/cell) [2, 3, 15, 27, 29, 30].

Under the used conditions, pPLTX eluted about 2 min earlier than palytoxin standard, which indicated that pPLTX was indeed an isomer (either structural or stereo-isomer) of PLTX itself. In addition, the analysis of full HRMS spectra associated to the region of TIC nearby OVTX-a revealed the presence in all the extracts of two new isobaric ovatoxins eluting at 13.38 min and 14.35 min respectively, each of them accounting for 0.7% of the total toxin content. We referred to these compounds as ovatoxin-g (OVTX-g) and isobaric OVTX-g. This prompted us to further analyze these molecules on the basis of their full HRMS and collision-induced dissociation (CID) MS^n behavior. The obtained results were interpreted in the light of palytoxin and ovatoxin-a (17,44,64-trideoxy-42-hydroxypalytoxin) fragmentation behavior [19], whose structures had been confirmed by NMR [13]. The resulting structural hypotheses are reported below.

Table 6-1. HRMS data of putative palytoxin and ovatoxins acquired in full MS spectra in the mass range m/z 700-1600. Theoretical molecular (M) mass and elemental formulas assigned to the mono-isotopic ion peaks of triply charged and doubly charged ions, and relative double bonds equivalent (RDB). Mass errors were below 3 ppm in all cases. n.d. = not detected.

			Triply charged ions						Doubly charged ions					
		Theoretical [M]	$[M+H+Ca]^{3+}$	$[M+H+Mg]^{3+}$	$[M+3H-H_2O]^{3+}$	$[M+3H-2H_2O]^{3+}$	$[M+3H-3H_2O]^{3+}$	$[M+H+K]^{2+}$	$[M+H+Na]^{2+}$	$[M+2H]^{2+}$	$[M+2H-H_2O]^{2+}$	$[M+2H-2H_2O]^{2+}$	$[M+2H-3H_2O]^{2+}$
	m/z	2678.4790	906.4830	901.1579	887.8294	881.8268	875.8228	1359.2212	1351.2353	1340.2491	1331.2419	1322.2337	1313.2326
pPLTX	Formula	$C_{129}H_{223}O_{54}N_3$	$C_{129}H_{224}O_{54}N_3Ca$	$C_{129}H_{224}O_{54}N_3Mg$	$C_{129}H_{224}O_{53}N_3$	$C_{129}H_{222}O_{52}N_3$	$C_{129}H_{220}O_{51}N_3$	$C_{129}H_{224}O_{54}N_3K$	$C_{129}H_{224}O_{54}N_3Na$	$C_{129}H_{225}O_{54}N_3$	$C_{129}H_{223}O_{53}N_3$	$C_{129}H_{221}O_{52}N_3$	$C_{129}H_{219}O_{51}N_3$
	(RDB)	20.0	19.5	19.5	19.5	20.5	21.5	19.0	19.0	19.0	20.0	21.0	22.0
	m/z	2646.4892	895.8197	890.4941	877.1674	871.1640	865.1602	1343.2269	1335.2425	1324.2524	1315.2472	1306.2420	1297.2367
OVTX-a	Formula	$C_{129}H_{223}O_{52}N_3$	$C_{129}H_{224}O_{52}N_3Ca$	$C_{129}H_{224}O_{52}N_3Mg$	$C_{129}H_{224}O_{51}N_3$	$C_{129}H_{222}O_{50}N_3$	$C_{129}H_{220}O_{49}N_3$	$C_{129}H_{224}O_{52}N_3K$	$C_{129}H_{224}O_{52}N_3Na$	$C_{129}H_{225}O_{52}N_3$	$C_{129}H_{223}O_{51}N_3$	$C_{129}H_{221}O_{50}N_3$	$C_{129}H_{219}O_{49}N_3$
	(RDB)	20.0	19.5	19.5	19.5	20.5	21.5	19.0	19.0	19.0	20.0	21.0	22.0
	m/z	2690.5154	910.4950	905.1696	891.8431	885.8393	879.8358	1365.2400	1357.2557	1346.2658	1337.2606	1328.2553	1319.2494
OVTX-b	Formula	$C_{131}H_{227}O_{53}N_3$	$C_{131}H_{228}O_{53}N_3Ca$	$C_{131}H_{228}O_{53}N_3Mg$	$C_{131}H_{228}O_{52}N_3$	$C_{131}H_{226}O_{51}N_3$	$C_{131}H_{224}O_{50}N_3$	$C_{131}H_{228}O_{53}N_3K$	$C_{131}H_{228}O_{53}N_3Na$	$C_{131}H_{229}O_{53}N_3$	$C_{131}H_{227}O_{52}N_3$	$C_{131}H_{225}O_{51}N_3$	$C_{131}H_{223}O_{50}N_3$
	(RDB)	20.0	19.5	19.5	19.5	20.5	21.5	19.0	19.0	19.0	20.0	21.0	22.0
	m/z	2706.5103	915.8270	910.5015	897.1747	891.1713	885.1676	1373.2384	1365.2535	1354.2636	1345.2588	1336.2532	1327.2469
OVTX-c	Formula	$C_{131}H_{227}O_{54}N_3$	$C_{131}H_{228}O_{54}N_3Ca$	$C_{131}H_{228}O_{54}N_3Mg$	$C_{131}H_{228}O_{53}N_3$	$C_{131}H_{226}O_{52}N_3$	$C_{131}H_{224}O_{51}N_3$	$C_{131}H_{228}O_{54}N_3K$	$C_{131}H_{228}O_{54}N_3Na$	$C_{131}H_{229}O_{54}N_3$	$C_{131}H_{227}O_{53}N_3$	$C_{131}H_{225}O_{52}N_3$	$C_{131}H_{223}O_{51}N_3$
	(RDB)	20.0	19.5	19.5	19.5	20.5	21.5	19.0	19.0	19.0	20.0	21.0	22.0
	m/z	2662.4841	901.1512	895.8257	882.4988	876.4952	870.4917	1351.2244	1343.2399	1332.2501	1323.2449	1314.2393	1305.2344
OVTX-d	Formula	$C_{129}H_{223}O_{53}N_3$	$C_{129}H_{224}O_{53}N_3Ca$	$C_{129}H_{224}O_{53}N_3Mg$	$C_{129}H_{224}O_{52}N_3$	$C_{129}H_{222}O_{51}N_3$	$C_{129}H_{220}O_{50}N_3$	$C_{129}H_{224}O_{53}N_3K$	$C_{129}H_{224}O_{53}N_3Na$	$C_{129}H_{225}O_{53}N_3$	$C_{129}H_{223}O_{52}N_3$	$C_{129}H_{221}O_{51}N_3$	$C_{129}H_{219}O_{50}N_3$
	(RDB)	20.0	19.5	19.5	19.5	20.5	21.5	19.0	19.0	19.0	20.0	21.0	22.0
	m/z	2662.4841	901.1513	895.8259	882.4991	876.4953	870.4918	1351.2249	1343.2401	1332.2502	1323.2451	1314.2400	1305.2356
OVTX-e	Formula	$C_{129}H_{223}O_{53}N_3$	$C_{129}H_{224}O_{53}N_3Ca$	$C_{129}H_{224}O_{53}N_3Mg$	$C_{129}H_{224}O_{52}N_3$	$C_{129}H_{222}O_{51}N_3$	$C_{129}H_{220}O_{50}N_3$	$C_{129}H_{224}O_{53}N_3K$	$C_{129}H_{224}O_{53}N_3Na$	$C_{129}H_{225}O_{53}N_3$	$C_{129}H_{223}O_{52}N_3$	$C_{129}H_{221}O_{51}N_3$	$C_{129}H_{219}O_{50}N_3$
	(RDB)	20.0	19.5	19.5	19.5	20.5	21.5	19.0	19.0	19.0	20.0	21.0	22.0
	m/z	2630.4943	890.4870	885.1611	871.8343	865.8303	859.8275	n.d.	1327.2432	1316.2516	1307.2486	1298.2436	n.d.
OVTX-g	Formula	$C_{129}H_{223}O_{51}N_3$	$C_{129}H_{224}O_{51}N_3Ca$	$C_{129}H_{224}O_{51}N_3Mg$	$C_{129}H_{224}O_{50}N_3$	$C_{129}H_{222}O_{49}N_3$	$C_{129}H_{220}O_{48}N_3$	--	$C_{129}H_{224}O_{51}N_3Na$	$C_{129}H_{225}O_{51}N_3$	$C_{129}H_{223}O_{50}N_3$	$C_{129}H_{221}O_{49}N_3$	--
	(RDB)	20.0	19.5	19.5	19.5	20.5	21.5	--	19.0	19.0	20.0	21.0	--

Table 6-2. Total toxin content on a per cell basis (pg/cell) and relative abundance (%) of pPLTX and OVTXs in the 6 analyzed *O.* cf. *ovata* strains from south Catalonia rocky coasts (NW Mediterranean Sea).

Strain name	Total toxin content (pg/cell)	Relative abundances (%)						
		pPLTX	OVTX-a	OVTX-b	OVTX-c	OVTX-d	OVTX-e	OVTX-g
IRTA-SMM-11-10	50	0.5	52	29	4	7	6	0.7
IRTA-SMM-12-38	143	0.3	58	25	3	6	6	0.7
IRTA-SMM-12-46	140	0.6	53	26	5	8	6	0.9
IRTA-SMM-12-51	102	0.6	55	21	6	8	8	0.6
IRTA-SMM-12-57	104	0.7	55	22	6	8	7	0.6
IRTA-SMM-12-62	250	0.4	59	20	4	7	7	0.9

6.3.1 Putative palytoxin

Full HRMS spectra of pPLTX and PLTX appeared superimposable in terms of diagnostic ions and their relative intensities (Figure 6-3). Ion assignment (Table 6-1) indicated that pPLTX had the same molecular formula as palytoxin ($C_{129}H_{223}N_3O_{54}$, theoretical mass *m/z* 2678.4790, RBD 20.0) [5, 6].

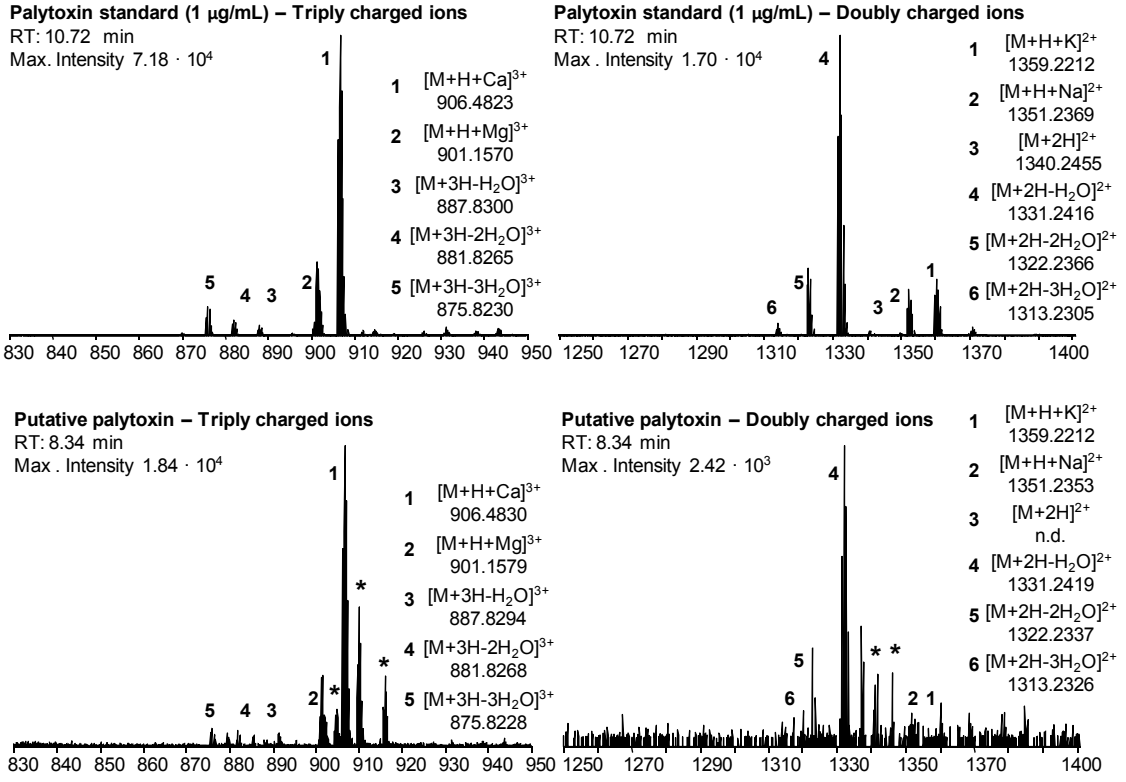

Figure 6-3. Full HRMS spectra of palytoxin standard and putative palytoxin (*m/z* 700-1600) zoomed in *m/z* 830-950 and *m/z* 1250-1400 ranges. Elemental formula assignment of triply and doubly charged ions. n.d. = not detected. * = ions corresponding to co-eluting palytoxin-like compounds, still under investigation.

Structural differences between PLTX and pPLTX have been assessed by interpretation of their full HRMS^n spectra of the $[M+H+Ca]^{3+}$ ion at *m/z* 906.8. Elemental formulae assigned to all the fragment ions are listed in Table 6-3. Figure 6-4 shows the structural hypotheses based on the observed cleavages.

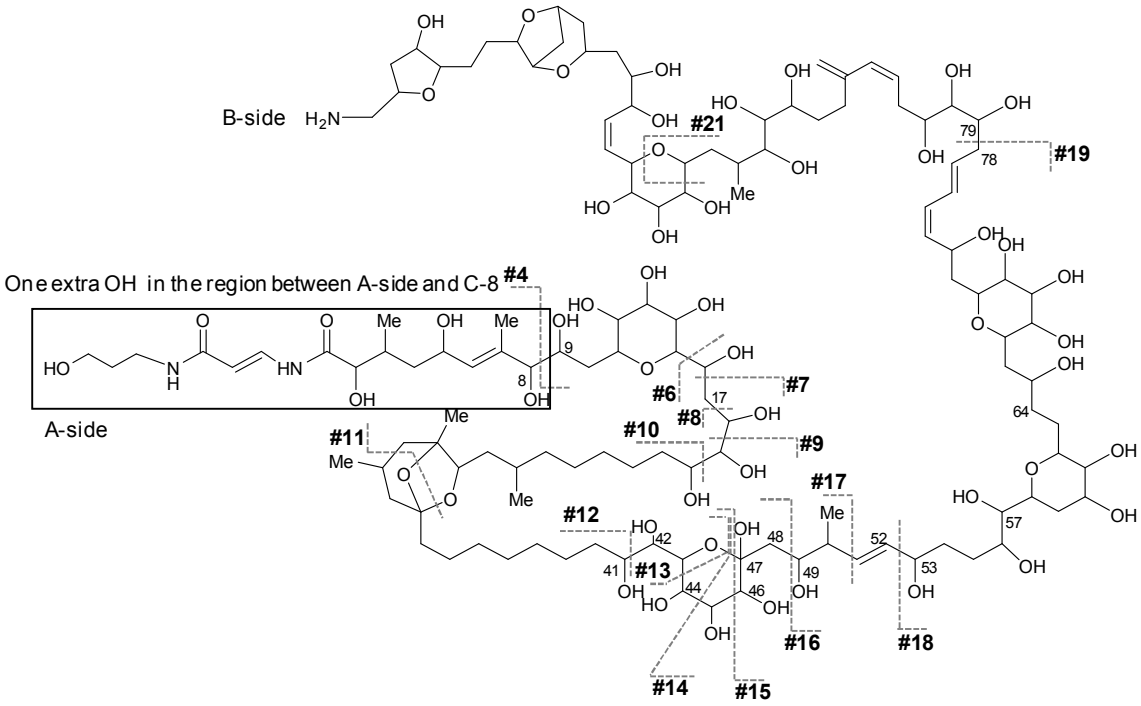

Figure 6-4. Tentative planar structure of putative palytoxin ($C_{129}H_{223}N_3O_{54}$) including all the cleavages emerging from its HRMS^2 spectrum. Assignment of fragment ions is reported in Table 6-3.

The key cleavages highlighting the structural differences between the two analogs are discussed below. The first such cleavage was #4 that produced an A-side fragment at *m/z* 343.1863 ($C_{16}H_{27}O_6N_2$) in pPLTX as opposed to that of PLTX at *m/z* 327.1910 ($C_{16}H_{27}O_5N_2$). Therefore, pPLTX was deduced to possess one oxygen more than PLTX in the region stretching from the A-side terminal to C-8. Consistently, the B-side moiety due to cleavage #4 yielded a fragment containing one O less than the relevant fragment in PLTX.

Unlike #4, cleavages #11 and #12 produced doubly-charged A-side fragments ($C_{40}H_{72}O_{17}N_2Ca$ and $C_{52}H_{92}O_{19}N_2Ca$) in pPLTX identical to the relevant fragments in PLTX. This suggested that pPLTX in comparison to PLTX lacked one O in the part structure stretching from C-9 to C-41. A cross interpretation of the internal fragments relevant to the part structures C-17 to C-41 (cleavage #7+#12) and C-18 to C-41 (cleavage #8+#12) provided insightful structural details. In fact, the fragment stretching from C-17 to C-41 possessed one oxygen less than PLTX, while the C-18 to C-41 fragment appeared identical to that of PLTX (Table 6-3). Hence, pPLTX turned out to lack the hydroxyl group at C-17, in analogy with OVTX-a.

Moving along the structural determination of pPLTX, cleavage #13 originated an A-side fragment featuring again an extra oxygen atom compared to PLTX. As cleavage #12 gave rise to an A-side fragment superimposable to that of PLTX, it was inferred that the additional oxygen was reasonably present at position 42. This was once again in accordance with the chemical structure of OVTX-a (Figure 6-1). Fragment ions deriving from cleavages #14 through #17 showed that the PLTX and pPLTX shared the same C-43 to C-50 part structure.

Further differences between the two toxins were deduced by a comparative analysis of the elemental formulae of fragments deriving from cleavages #18 (C-52/C53) and #19 (C-78/C-79). In particular, the pPLTX B-side fragment due to cleavage #18 lacked one oxygen with respect to PLTX, while the A-side fragment consequent to cleavage #19 matched again that of PLTX. Thus, one oxygen was missing in the region stretching from C-53 to C-78. As already observed for other palytoxin-like compounds further fragmentation does not occur in this region [19], thus preventing us to identify the exact position of the structural modification. However, by analogy with OVTX-a, it was reasonable to hypothesize that pPLTX was dehydroxylated at position 64. In order to more deeply investigate the C-53/C-78 segment, the Uchida et al. approach [17] was applied. This method is based on MS/MS analysis of conjugated polyenes produced from polyol structures through subsequent water losses. According to the authors, the serial loss of water molecules comes to an end when there are no more hydroxyl groups properly located to extend the conjugation process. Such a method was successfully applied to gain structural information on palytoxin analogs basing on the number of water losses observed in MS^2 spectra [17].

We successfully applied the Ukida et al. method to OVTX-a, contained at a concentration level of 6 μg/mL in the *O.* cf. *ovata* extract. In the part structure under investigation (C-53/C-78), the most favored cleavage #16 (C-48/C-49) was selected for this approach. The B-side fragment ion due to this cleavage in OVTX-a underwent six water losses (Sup. Mat. Figure 6-2), consistent with the dehydroxylation at C-64 of this molecule [13] (Figure 6-1).

On the contrary, in the case of pPLTX, cleavage #16 generated a B-side fragment ion accompanied by only three detectable water losses. Even if this apparently points to a dehydroxylation at C-57 for pPLTX, we don't feel like excluding that the low concentration of pPLTX in the extract (168 ng/mL) may have limited the detectable number of water losses.

It should be noted that putative palytoxin contained in the *O.* cf. *ovata* reference extract from the Adriatic Sea eluted practically at the same retention time (8.33 min) as pPLTX in the strain IRTA-SMM-11-10. However, concentration of pPLTX in the Adriatic sample impeded the acquisition of $HRMS^n$ spectra needed to fully confirm that both pPLTXs were actually the same compound.

Table 6-3. Assignment of A-side, B-side and internal fragments contained in HRMS² spectra of palytoxin standard and putative palytoxin to relevant cleavages (#Clv) reported in Figure 6-4. Elemental formulae of the monoisotopic ion peaks (*m/z*) are reported together with number of water losses (-nH_2O) and relative double bonds (RDB). Mass errors were below 5 ppm in all cases. n.d. = not detected.

	Palytoxin		Putative palytoxin	
	A-side	B-side	A-side	B-side
#Clv	*m/z* (-nH_2O) Formula (RDB)	*m/z* (-nH_2O) Formula (RDB)	*m/z* (-nH_2O) Formula (RDB)	*m/z* (-nH_2O) Formula (RDB)
#4	327.1910 (1+) (-1H_2O) $C_{16}H_{27}O_5N_2$ (4.5)	1187.1212 (2+) (-6H_2O) $C_{113}H_{195}O_{48}NCa$ (17.0) 791.7500 (3+)(-4H_2O) $C_{113}H_{196}O_{48}NCa$ (16.5)	343.1863 (1+) $C_{16}H_{27}O_6N_2$ (4.5)	1179.1206 (2+) (-4H_2O) $C_{113}H_{195}O_{47}NCa$ (17.0) n.d.
#11	446.2212 (2+) (-2H_2O) $C_{40}H_{72}O_{17}N_2$ Ca (6.0)		446.2221 (2+) $C_{40}H_{72}O_{17}N_2Ca$ (6.0)	
#12	544.2943 (2+) (-2H_2O) $C_{52}H_{92}O_{19}N_2Ca$ (8.0)	807.8890 (2+) (-1H_2O) $C_{77}H_{125}O_{32}NCa$ (16.0)	544.2945 (2+) $C_{52}H_{92}O_{19}N_2Ca$ (8.0)	n.d.
#13	566.3074 (2+) (-2H_2O) $C_{54}H_{96}O_{20}N_2Ca$ (8.0)	803.8863 (2+) (-1H_2O) $C_{75}H_{123}O_{33}NCa$ (14.0)	574.3051(2+) $C_{54}H_{96}O_{21}N_2Ca$ (8.0)	n.d.
#14	572.3074 (2+) (-1H_2O) $C_{55}H_{96}O_{20}N_2Ca$ (9.0)	797.8860 (2+) (-2H_2O) $C_{74}H_{125}O_{33}NCa$ (13.0)		762.8721(2+) (–H_2O) $C_{74}H_{119}O_{29}NCa$ (14.0)
#15	596.3179 (2+) (-3H_2O) $C_{56}H_{100}O_{22}N_2Ca$ (8.0)	782.8808 (2+)(-3H_2O) $C_{73}H_{123}O_{32}NCa$ (13.0) 1526.8077 (1+)(-3H_2O) $C_{73}H_{124}O_{32}N$ (12.5)	604.3157 (2+) (-2H_2O) $C_{56}H_{100}O_{23}N_2Ca$ (8.0)	n.d. 1510.8142 (1+)(-3H_2O) $C_{73}H_{124}O_{31}N$(12.5)
#16	633.3363 (2+) (-3H_2O) $C_{59}H_{106}O_{24}N_2Ca$ (8.0)	745.8624 (2+)(-5H_2O) $C_{70}H_{117}O_{30}NCa$ (13.0) 1452.7713 (1+)(-5H_2O) $C_{70}H_{118}O_{30}N$ (12.5)	641.3340 (2+) (-2H_2O) $C_{59}H_{106}O_{25}N_2Ca$ (8.0)	737.8661 (2+)(-3H_2O) $C_{70}H_{117}O_{29}NCa$ (13.0) 1436.7777 (1+) (-3H_2O) $C_{70}H_{118}O_{29}N$ (12.5)
#17	647.3337 (2+) (-2H_2O) $C_{60}H_{106}O_{25}N_2Ca$ (9.0)	1406.7658 (1+) (-3H_2O) $C_{69}H_{116}O_{28}N$ (12.5)	655.3317 (2+) (-1H_2O) $C_{60}H_{106}O_{26}N_2Ca$ (9.0)	n.d.
#18		694.8289 (2+) (-3H_2O) $C_{65}H_{107}O_{28}NCa$ (13.0)		686.8316 (2+) $C_{65}H_{107}O_{27}NCa$ (13.0)
#19	948.4986(2+) $C_{90}H_{156}O_{37}N_2Ca$ (14.0)	804.4366 (1+) (-1H_2O) $C_{39}H_{66}O_{16}N$ (7.5)	948.5029 (2+) $C_{90}H_{156}O_{37}N_2Ca$ (14.0)	n.d.
#20	n.d.	n.d.	n.d.	n.d.
#21	1129.5955 (2+) (-4H_2O) $C_{107}H_{186}O_{45}N_2Ca$ (16.0)	406.2217 (1+) (-1H_2O) $C_{22}H_{32}O_6N$ (7.5)	1129.5965 (2+) $C_{107}H_{186}O_{45}N_2Ca$ (16.0)	n.d.
#22	1144.6011 (2+) (-2H_2O) $C_{108}H_{188}O_{46}N_2Ca$ (16.0)		n.d.	
#23	1174.6123 (2+) (-4H_2O) $C_{110}H_{192}O_{48}N_2$ Ca (16.0)		n.d.	
#24	1215.6323 (2+) (-1H_2O) $C_{115}H_{198}O_{49}N_2Ca$ (18.0)		n.d.	
#25	1222.6411 (2+) (-3H_2O) $C_{116}H_{200}O_{49}N_2Ca$ (18.0)		n.d.	
#26	1235.6480 (2+) (-4H_2O) $C_{118}H_{202}O_{49}N_2Ca$ (19.0)		n.d.	
#27	1236.6335 (2+) (-4H_2O) $C_{117}H_{200}O_{50}N_2Ca$ (19.0)		n.d.	
#28	1321.6819 (2+) (-3H_2O) $C_{117}H_{200}O_{53}N_2Ca$ (21.0)		n.d.	

	Palytoxin Internal fragments	Putative palytoxin Internal fragments
#Clv	*m/z* (-nH_2O) Formula (RDB)	*m/z* (-nH_2O) Formula (RDB)
#4+#12	372.1975 (2+) $C_{36}H_{64}O_{13}Ca$ (5.0) 743.3878 (1+) $C_{36}H_{63}O_{13}Ca$ (5.5)	n.d. n.d.
#4+#13	394.2105 (2+) $C_{38}H_{68}O_{14}Ca$ (5.0)	n.d.
#4+#15	424.2210 (2+) (-1H_2O) $C_{40}H_{72}O_{16}Ca$ (5.0)	n.d.
#4+#16	461.2389 (2+) (-2H_2O) $C_{43}H_{78}O_{18}Ca$ (5.0)	n.d.
#5+#12	657.3511(1+) $C_{32}H_{57}O_{11}Ca$ (4.5)	n.d.
#6+#12	n.d.	567.3244 (1+) (-1H_2O) $C_{29}H_{51}O_8Ca$ (4.5)
#7+#12	537.3088 (1+) (-1H_2O) $C_{28}H_{49}O_7Ca$ (4.5)	521.3145 (1+) $C_{28}H_{49}O_6Ca$ (4.5)
#8+#12	507.2982 (1+) $C_{27}H_{47}O_6Ca$ (4.5)	507.2983(1+) $C_{27}H_{47}O_6Ca$ (4.5)
#9+#12	477.2877(1+) $C_{26}H_{45}O_5Ca$ (4.5)	477.2888 (1+) $C_{26}H_{45}O_5Ca$ (4.5)
#10+#12	447.2771 (1+) (-1H_2O) $C_{25}H_{43}O_4Ca$ (4.5)	447.2770 (1+) $C_{25}H_{43}O_4Ca$ (4.5)

6.3.2 Ovatoxin-g

The full HRMS spectrum of ovatoxin-g (Rt = 14.35 min) showed, the most intense triply- and doubly-charged ion at *m/z* 890.4870 and *m/z* 1307.2486 (mono-isotopic peaks). According to the expected ionization behavior of palytoxin-like compounds [2, 3, 18], these ions were assigned to $[M+H+Ca]^{3+}$ and $[M+2H-H_2O]^{2+}$, respectively. A cross-check of elemental formulae of all the ions contained in the spectrum (Table 6-1) pointed to an elemental formula for ovatoxin-g of $C_{129}H_{223}N_3O_{51}$ (theoretical mass *m/z* 2630.4943, RBD 20.0) displaying one O less than OVTX-a ($C_{129}H_{223}N_3O_{52}$). Figure 6-5 shows the full HRMS spectrum of OVTX-g in comparison with that of OVTX-a.

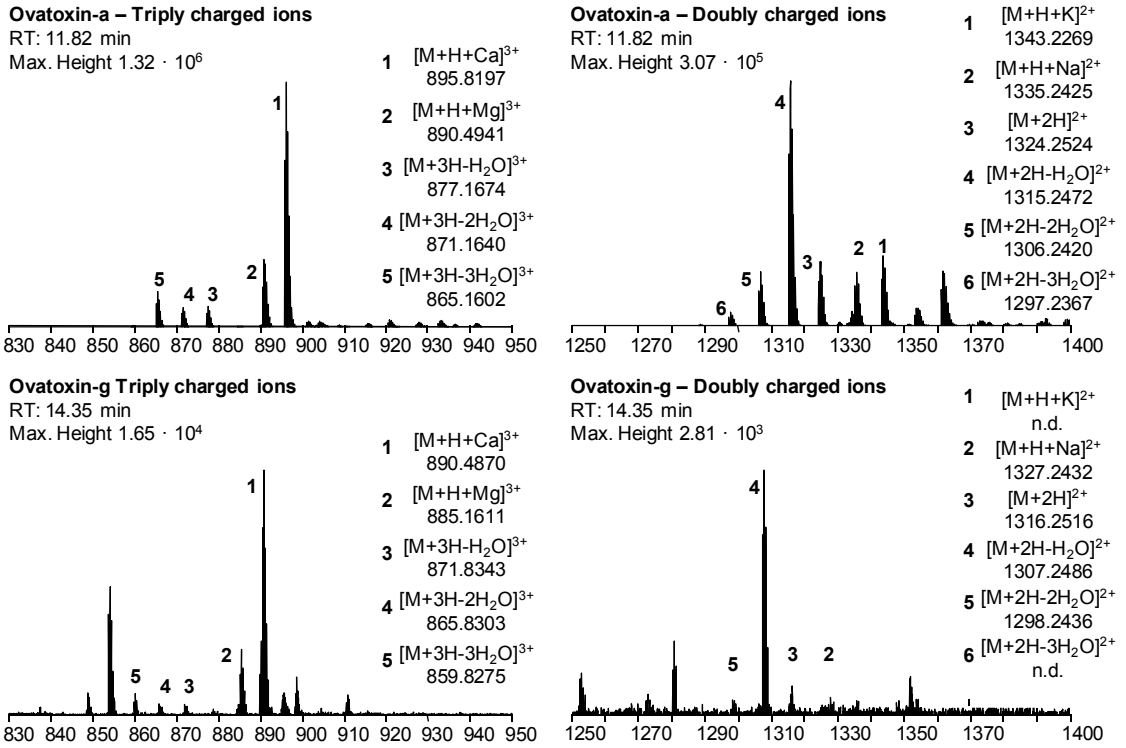

Figure 6-5. Full HRMS spectra of ovatoxin-a and ovatoxin-g (*m/z* 700-1600) zoomed in *m/z* 830-950 and *m/z* 1250-1400 ranges. Elemental formula assignment of triply and doubly charged ions. n.d. = not detected.

It is noteworthy that the $[M+H+Ca]^{3+}$ ion of OVTX-g (*m/z* 890.4870) is only 6.7 mDa lower than the $[M+H+Mg]^{3+}$ ion of OVTX-a (*m/z* 890.4937) and a resolving power of 150,000 (FWHM) would be needed to resolve ion peaks at 50% of peak width (Sup. Mat. Figure 6-3). Thus, quantification of OVTX-g based on XICs of the calcium adduct might be biased if chromatographic separation between OVTX-a and OVTX-g is not achieved.

Positive $HRMS^2$ spectrum of the *m/z* 890.8 was acquired to gain structural insights into ovatoxin-g and identify the specific site(s) of difference between OVTX-g and –a. Figure 6-6 shows the structural hypotheses for OVTX-g based on the observed fragmentations. Table 6-4 reports elemental formulae assigned to each fragment.

Table 6-4. Assignment of A-side, B-side and internal fragments contained in HRMS² spectra of ovatoxin-a and ovatoxin-g to relevant cleavages (#Clv) reported in Figure 6-6. Elemental formula of the monoisotopic ion peaks (*m/z*) are reported together with number of water losses observed in the spectra (-nH_2O) and relative double bonds (RDB). Mass errors were below 5 ppm in all cases. n.d. = not detected

	Ovatoxin-a		Ovatoxin-g	
	A-side	B-side	A-side	B-side
#Clv	*m/z* (-nH_2O) Formula (RDB)	*m/z* (-nH_2O) Formula (RDB)	*m/z* (-nH_2O) Formula (RDB)	*m/z* (-nH_2O) Formula (RDB)
#4	327.1906 (1+) (-1H_2O) $C_{16}H_{27}O_5N_2$ (4.5)	1171.1254 (2+)(-6H_2O) $C_{113}H_{195}O_{46}NCa$ (17.0) 781.0860 (3+)(-3H_2O) $C_{113}H_{196}O_{46}NCa$ (16.5)	327.1906 (1+) (-1H_2O) $C_{16}H_{27}O_5N_2$ (4.5)	1163.1261 (2+)(-5H_2O) $C_{113}H_{195}O_{45}NCa$ (17.0) 769.7508 (3+)(-1H_2O) $C_{113}H_{196}O_{46}NCa$ (17.5)
#11	438.2238 (2+) (-2H_2O) $C_{40}H_{72}O_{16}N_2$ Ca (6.0)		n.d.	
#12	536.2965 (2+) (-2H_2O) $C_{52}H_{92}O_{18}N_2Ca$ (8.0)	799.8905 (2+) (-1H_2O) $C_{77}H_{125}O_{31}NCa$ (16.0)	536.2958 (2+) (-1H_2O) $C_{52}H_{92}O_{18}N_2Ca$ (8.0)	n.d.
#13	566.3071(2+) (-2H_2O) $C_{54}H_{96}O_{20}N_2Ca$ (8.0)	778.8855 (2+) (-3H_2O) $C_{75}H_{123}O_{30}NCa$ (15.0)	n.d.	n.d.
#14		n.d.		n.d.
#15	588.3201 (2+) (-3H_2O) $C_{56}H_{100}O_{21}N_2Ca$ (8.0)	774.8829 (2+)(-3H_2O) $C_{73}H_{123}O_{31}NCa$ (13.0) 1510.8122 (1+)(-3H_2O) $C_{73}H_{124}O_{31}N$ (12.5)	588.3195 (2+) (-2H_2O) $C_{56}H_{100}O_{21}N_2Ca$ (8.0)	766.8841 (2+)(-2H_2O) $C_{73}H_{123}O_{30}NCa$ (13.0) 1494.8126 (1+)(-3H_2O) $C_{73}H_{124}O_{30}N$ (12.5)
#16	625.3385 (2+) (-3H_2O) $C_{59}H_{106}O_{23}N_2Ca$ (8.0)	737.8646 (2+)(-5H_2O) $C_{70}H_{117}O_{29}NCa$ (13.0) 1436.7757 (1+)(-6H_2O) $C_{70}H_{118}O_{29}N$ (12.5)	617.3406 (2+) (-2H_2O) $C_{59}H_{106}O_{22}N_2Ca$ (8.0)	737.8642 (2+)(-3H_2O) $C_{70}H_{117}O_{29}NCa$ (13.0) 1436.7749 (1+) (-3H_2O) $C_{70}H_{118}O_{29}N$ (12.5)
#17	639.3359 (2+) (-3H_2O) $C_{60}H_{106}O_{24}N_2Ca$ (9.0)	1390.7716 (1+) (-3H_2O) $C_{69}H_{116}O_{27}N$ (12.5)	631.3374 (2+) (-1H_2O) $C_{60}H_{106}O_{23}N_2Ca$ (9.0)	n.d.
#18		686.8308 (2+) (-2H_2O) $C_{65}H_{107}O_{27}NCa$ (13.0)		n.d.
#19	932.5032 (2+) $C_{90}H_{156}O_{35}N_2Ca$ (14.0)	804.4360 (1+) (-1H_2O) $C_{39}H_{66}O_{16}N$ (7.5)	924.50291 (2+) $C_{90}H_{156}O_{34}N_2Ca$ (14.0)	n.d.
#20	n.d.	n.d.	n.d.	n.d.
#21	1113.6005 (2+) (-3H_2O) $C_{107}H_{186}O_{43}N_2Ca$ (16.0)	406.2216 (1+) (-2H_2O) $C_{22}H_{32}O_6N$ (7.5)	1105.6007 (2+) (-2H_2O) $C_{107}H_{186}O_{42}N_2Ca$ (16.0)	n.d.
#22	1128.6053 (2+) (-2H_2O) $C_{108}H_{188}O_{44}N_2Ca$ (16.0)		n.d.	
#23	1158.6164 (2+) (-3H_2O) $C_{110}H_{192}O_{46}N_2$ Ca (16.0)		n.d.	
#24	1199.6367 (2+) (-1H_2O) $C_{115}H_{198}O_{47}N_2Ca$ (18.0)		n.d.	
#25	1206.6449 (2+) (-4H_2O) $C_{116}H_{200}O_{47}N_2Ca$ (18.0)		1190.1423 (2+) (-1H_2O) $C_{116}H_{200}O_{46}N_2Ca$ (18.0)	
#26	1219.6517 (2+) (-4H_2O) $C_{118}H_{202}O_{47}N_2Ca$ (19.0)		n.d.	
#27	1220.6386 (2+) (-5H_2O) $C_{117}H_{200}O_{48}N_2Ca$ (19.0)		n.d.	
#28	n.d.	n.d.	n.d.	n.d.

	Ovatoxin-a Internal fragments	Ovatoxin-g Internal fragments
#Clv	*m/z* (-nH_2O) Formula (RDB)	*m/z* (-nH_2O) Formula (RDB)
#4+#12	364.1999 (2+) $C_{36}H_{64}O_{12}Ca$ (5.0) 727.3924 (1+) $C_{36}H_{63}O_{12}Ca$ (5.5)	n.d. 727.3920 (1+) $C_{36}H_{63}O_{12}Ca$ (5.5)
#4+#13	394.2104 (2+) $C_{38}H_{68}O_{14}Ca$ (5.0)	n.d.
#4+#15	416.2234 (2+) (-2H_2O) $C_{40}H_{72}O_{15}Ca$ (5.0)	416.2224 (2+) (-1H_2O) $C_{40}H_{72}O_{15}Ca$ (5.0)
#4+#16	453.2415 (2+) (-1H_2O) $C_{43}H_{78}O_{17}Ca$ (5.0)	n.d.
#5+#12	641.3557 (1+) $C_{32}H_{57}O_{10}Ca$ (4.5)	641.3554 (1+) $C_{32}H_{57}O_{10}Ca$ (4.5)
#6+#12	n.d.	n.d.
#7+#12	521.3136 (1+) (-1H_2O) $C_{28}H_{49}O_6Ca$ (4.5)	521.3134 (1+) $C_{28}H_{49}O_6Ca$ (4.5)
#8+#12	507.2979 (1+) $C_{27}H_{47}O_6Ca$ (4.5)	507.2975 (1+) $C_{27}H_{47}O_6Ca$ (4.5)
#9+#12	477.2875 (1+) $C_{26}H_{45}O_5Ca$ (4.5)	477.2866 (1+) $C_{26}H_{45}O_5Ca$ (4.5)
#10+#12	447.2771 (1+) (-1H_2O) $C_{25}H_{43}O_4Ca$ (4.5)	447.2760 (1+) (-1H_2O) $C_{25}H_{43}O_4Ca$ (4.5)

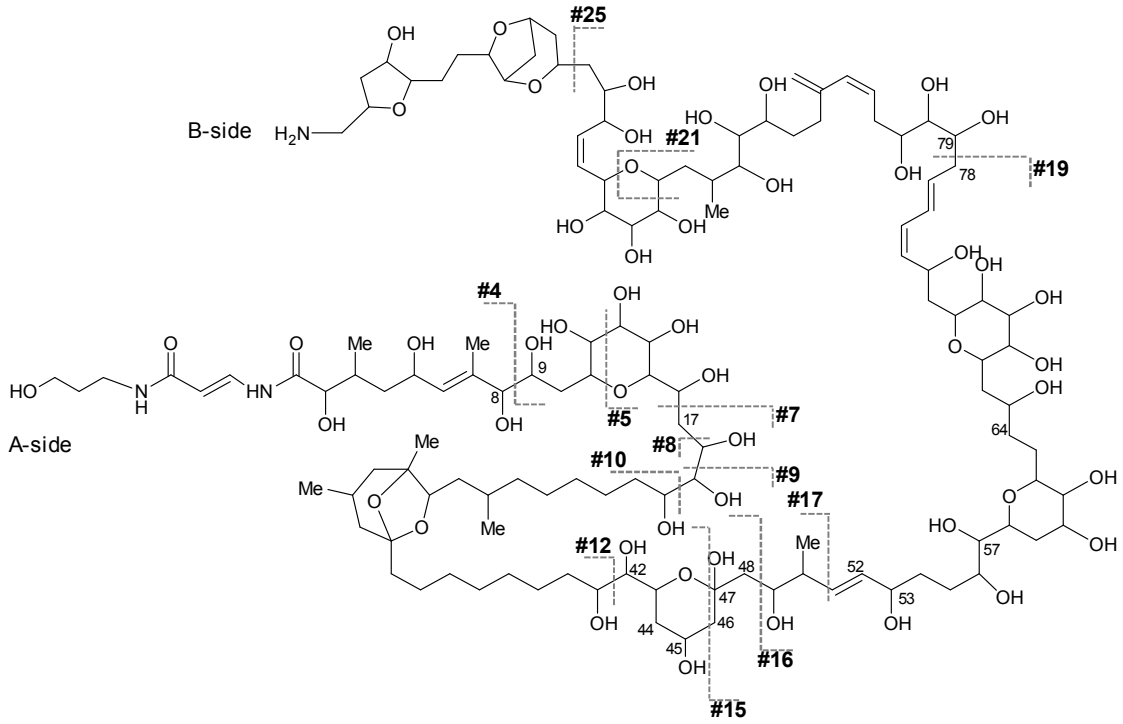

Figure 6-6. Tentative planar structure of ovatoxin-g ($C_{129}H_{223}N_3O_{51}$) including all the cleavages emerging from its HRMS² spectrum (Table 6-4). Assignment of fragment ions is reported in Table 6-4. Cleavage numbering was performed according to Ciminiello et al. [19]

The first crucial information on OVTX-g was provided by cleavage #4 that originated an A-side fragment ion (*m/z* 327.1906, $C_{16}H_{27}O_5N_2$) identical to that of OVTX-a and a B-side fragment ion ($C_{113}H_{195}O_{45}NCa$) with one O less than that observed for OVTX-a ($C_{113}H_{195}O_{46}NCa$). So, the two molecules shared the same A-side terminal-C-8 part structure. The structural analogy between the two OVTXs was extended up to C-45 in the light of cleavage #15 that still generated identical A-side fragment ions for both OVTXs. This was confirmed by internal fragments due to double cleavages that were the same for both compounds (Table 6-4).

The first difference in the elemental formulae of the A-side fragment ions of the two toxins appeared with cleavage #16, which generated an A-side fragment in OVTX-g displaying one O less ($C_{59}H_{106}O_{22}N_2Ca$) than OVTX-a ($C_{59}H_{106}O_{23}N_2Ca$) and B-side fragments with the same elemental formulae. This clearly indicated that the structural difference between OVTX-g and OVTX-a lied in the region stretching from C-46 to C-48. Reasonably, the missing oxygen atom is that belonging to the alcoholic functionality at C-46, as the other O is involved in a hemiketal functionality.

All the A-side fragments generated by cleavages #17, #19, #21 and #25 in OVTX-g presented one O less than in OVTX-a (Table 6-4), which was consistent with the hypothesis that the only structural difference between the two toxins was the missing O at C-46. So, by analogy with OVTX-a, OVTX-g would be dehydroxylated at C-64. However, isomerism in this region cannot be discarded. The already mentioned approach proposed by Uchida et al. was applied [17] also

to OVTX-g. The B-side fragment ion due to cleavage #16 underwent only three detectable water losses (Sup. Mat. Figure 6-2), so OVTX-g could lack the hydroxyl at C-57. However, such as for pPLTX, OVTX-g concentration in the crude extract (235 ng/mL) might be constraining the number of water losses detected.

Besides OVTX-g (Rt 14.35 min), XIC of $[M+H+Ca]^{3+}$ ion at *m/z* 890.4870 displayed another peak eluting about one minute earlier (Figure 6-2). Its full HRMS spectrum showed a similar ion profile as OVTX-g, which suggested that it was an OVTX-g isomer. However, the fragmentation behavior in the $HRMS^2$ spectrum of this compound was significantly different from that we have usually observed for palytoxins, thus preventing us from any reliable interpretation.

6.4 Conclusions

The LC-HRMS analyses of cultures of *O.* cf. *ovata* from the Ebro River Delta allowed to highlight the presence in the extracts of the novel ovatoxin-g. $HRMS^2$ studies provided insights into the structure of this new ovatoxin in addition to disclosing that putative palytoxin is indeed a structural isomer of palytoxin itself. Compared to palytoxin, putative palytoxin from the analyzed *O.* cf. *ovata* strains is hydroxylated at C-42 and dehydroxylated at C-17 and most likely at C-64 (like OVTX-a). In addition, an-extra oxygen is contained in the segment stretching from the A-side terminal to C-8. Compared to ovatoxin-a, ovatoxin-g is dehydroxylated at C-46.

Both pPLTX and OVTX-g were contained in algal extracts at levels too low for a full NMR-based study and $LC\text{-}HRMS^n$ structural investigation was carried out directly in crude extract at ng/mL levels, with no need for derivatization.

The ever growing number of palytoxins being discovered makes even more urgent the need of evaluating the toxicity on humans of this class of compounds. The study of mechanisms of action and potency of individual palytoxin-like compounds should be performed to ensure a correct risk assessment of *Ostreopsis*-related syndromes.

References

1. Ciminiello, P., et al., *Putative Palytoxin and Its New Analogue, Ovatoxin-a, in Ostreopsis ovata Collected Along the Ligurian Coasts During the 2006 Toxic Outbreak.* Journal of the American Society for Mass Spectrometry, 2008. **19**(1): p. 111-120.
2. Ciminiello, P., et al., *Complex palytoxin-like profile of Ostreopsis ovata. Identification of four new ovatoxins by high-resolution liquid chromatography/mass spectrometry.* Rapid Communications in Mass Spectrometry, 2010. **24**(18): p. 2735-2744.
3. Ciminiello, P., et al., *Unique toxin profile of a mediterranean Ostreopsis cf. ovata Strain: HR LC-MSn characterization of ovatoxin-f, a new palytoxin congener.* Chemical Research in Toxicology, 2012. **25**(6): p. 1243-1252.
4. Munday, R., *Palytoxin toxicology: Animal studies.* Toxicon, 2011. **57**(3): p. 470-477.
5. Moore, R.E. and G. Bartolini, *Structure of palytoxin.* Journal of the American Chemical Society, 1981. **103**(9): p. 2491-2494.
6. Uemura, D., et al., *Studies on palytoxins.* Tetrahedron, 1985. **41**(6): p. 1007-1017.
7. Crinelli, R., et al., *Palytoxin and an Ostreopsis toxin extract increase the levels of mRNAs encoding inflammation-related proteins in human macrophages via p38 MAPK and NF-kB.* PloS one, 2012. **7**(6): p. e38139.
8. Durando, P., et al., *Ostreopsis ovata and human health: epidemiological and clinical features of respiratory syndrome outbreaks from a two-year syndromic surveillance, 2005-06, in north-west Italy.* Euro surveillance, 2007. **12**(23): p. http://www.eurosurveillance.org/ViewArticle.aspx?ArticleId=3212 (accessed June 10, 2014).
9. Mangialajo, L., et al., *Trends in Ostreopsis proliferation along the Northern Mediterranean coasts.* Toxicon, 2011. **57**(3): p. 408-420.
10. Tubaro, A., et al., *Case definitions for human poisonings postulated to palytoxins exposure.* Toxicon, 2011. **57**(3): p. 478-495.
11. Casabianca, S., et al., *Quantification of the toxic dinoflagellate* Ostreopsis s*pp. by qPCR assay in marine aerosol.* Environmental science & technology, 2013. **47**(8): p. 3788-3795.
12. Ciminiello, P., et al., *First Finding of Ostreopsis cf. ovata Toxins in Marine Aerosols.* Environmental science & technology, 2014. **48**(6): p. 3532-3540.
13. Ciminiello, P., et al., *Stereochemical Studies on Ovatoxin-a.* Chemistry-A European Journal, 2012. **18**(52): p. 16836-16843.
14. Ciminiello, P., et al., *Isolation and structure elucidation of ovatoxin-a, the major toxin produced by Ostreopsis ovata.* Journal of the American Chemical Society, 2012. **134**(3): p. 1869-1875.
15. Brissard, C., et al., *Complex Toxin Profile of French Mediterranean Ostreopsis cf. ovata Strains, Seafood Accumulation and Ovatoxins Prepurification.* Marine Drugs, 2014. **12**(5): p. 2851-2876.
16. Suzuki, T., et al., *LC-MS/MS analysis of novel ovatoxin isomers in several Ostreopsis strains collected in Japan.* Harmful Algae, 2012. **20**: p. 81-91.
17. Uchida, H., Y. Taira, and T. Yasumoto, *Structural elucidation of palytoxin analogs produced by the dinoflagellate Ostreopsis ovata IK2 strain by complementary use of positive and negative ion liquid chromatography/quadrupole time of flight mass spectrometry.* Rapid Communications in Mass Spectrometry, 2013. **27**(17): p. 1999-2008.
18. Ciminiello, P., et al., *LC-MS of palytoxin and its analogues: State of the art and future perspectives.* Toxicon, 2011. **57**(3): p. 376-389.
19. Ciminiello, P., et al., *High resolution LC-MSn fragmentation pattern of palytoxin as template to gain new insights into ovatoxin-A structure. The key role of calcium in MS behavior of palytoxins.* Journal of the American Society for Mass Spectrometry, 2012. **23**(5): p. 952-963.
20. Vila, M., E. Garcés, and M. Masó, *Potentially toxic epiphytic dinoflagellate assemblages on macroalgae in the NW Mediterranean.* Aquatic microbial ecology, 2001. **26**(1): p. 51-60.

21. Barroso García, P., et al., *Brote con síntomas respiratorios en la provincia de Almería por una posible exposición a microalgas tóxicas.* Gaceta sanitaria, 2008. **22**(6): p. 578-584.
22. Pezzolesi, L., et al., *Influence of temperature and salinity on Ostreopsis cf. ovata growth and evaluation of toxin content through HR LC-MS and biological assays.* Water Research, 2012. **46**(1): p. 82-92.
23. Hoshaw, R.W. and J.R. Rosowski, *Methods for microscopic algae*, in *Handbook of phycological methods*, J.R. Stein, Editor. 1973, CUP Archive. p. 53-67.
24. Andree, K.B., et al., *Quantitative PCR coupled with melt curve analysis for detection of selected* Pseudo-nitzschia *spp.(Bacillariophyceae) from the northwestern Mediterranean Sea.* Applied and environmental microbiology, 2011. **77**(5): p. 1651-1659.
25. Sato, S., et al., *Phylogeography of Ostreopsis along west Pacific coast, with special reference to a novel clade from Japan.* PloS one, 2011. **6**(12): p. e27983.
26. Utermöhl, v.H., *Neue Wege in der quantitativen Erfassung des Planktons.* Verh. int. Verein. theor. angew. Limnol, 1931. **5**: p. 567-596.
27. Accoroni, S., et al., *Ostreopsis cf. ovata bloom in the northern Adriatic Sea during summer 2009: Ecology, molecular characterization and toxin profile.* Marine Pollution Bulletin, 2011. **62**(11): p. 2512-2519.
28. Guerrini, F., et al., *Comparative growth and toxin profile of cultured Ostreopsis ovata from the Tyrrhenian and Adriatic Seas.* Toxicon, 2010. **55**(2): p. 211-220.
29. Honsell, G., et al., *Harmful dinoflagellate Ostreopsis cf. ovata Fukuyo: detection of ovatoxins in field samples and cell immunolocalization using antipalytoxin antibodies.* Environmental science & technology, 2011. **45**(16): p. 7051-7059.
30. Rossi, R., et al., *New palytoxin-like molecules in Mediterranean Ostreopsis cf. ovata (dinoflagellates) and in Palythoa tuberculosa detected by liquid chromatography-electrospray ionization time-of-flight mass spectrometry.* Toxicon, 2010. **56**(8): p. 1381-1387.

Supplementary Materials

A) Ovatoxin-a

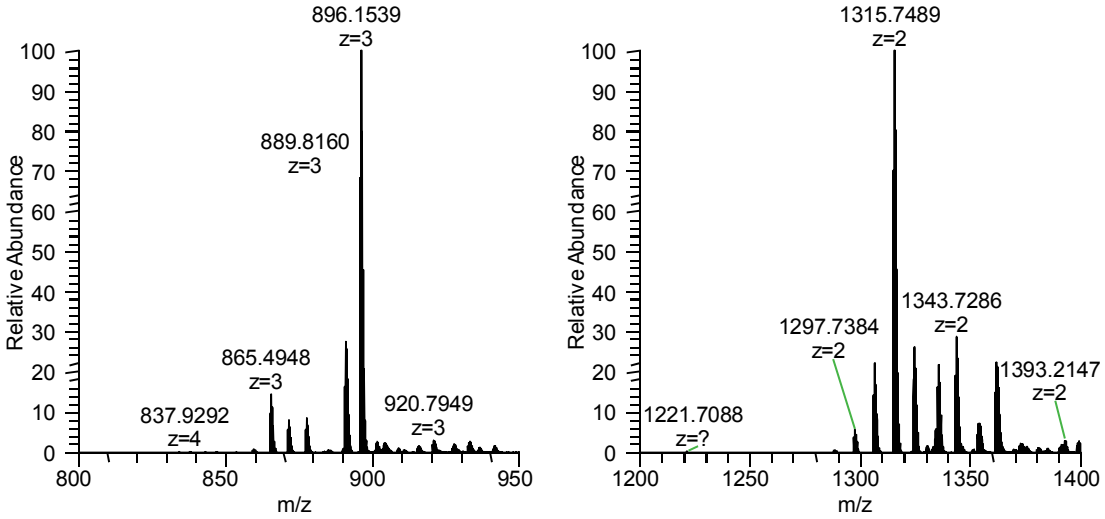

B) Ovatoxin-b

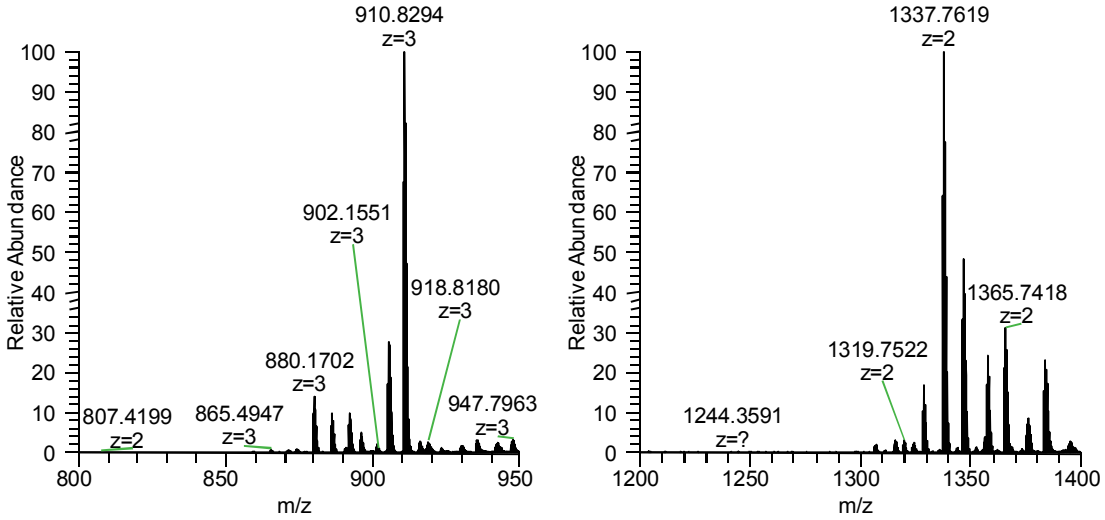

Sup. Mat. Figure 6-1 (A to H). Full HRMS spectra of ovatoxins —a to —e, ovatoxin-g, an isobaric compound of ovatoxin-g, and putative palytoxin, (*m/z* 700-1600) zoomed into the intervals *m/z* 830-950 and *m/z* 1250-1400.

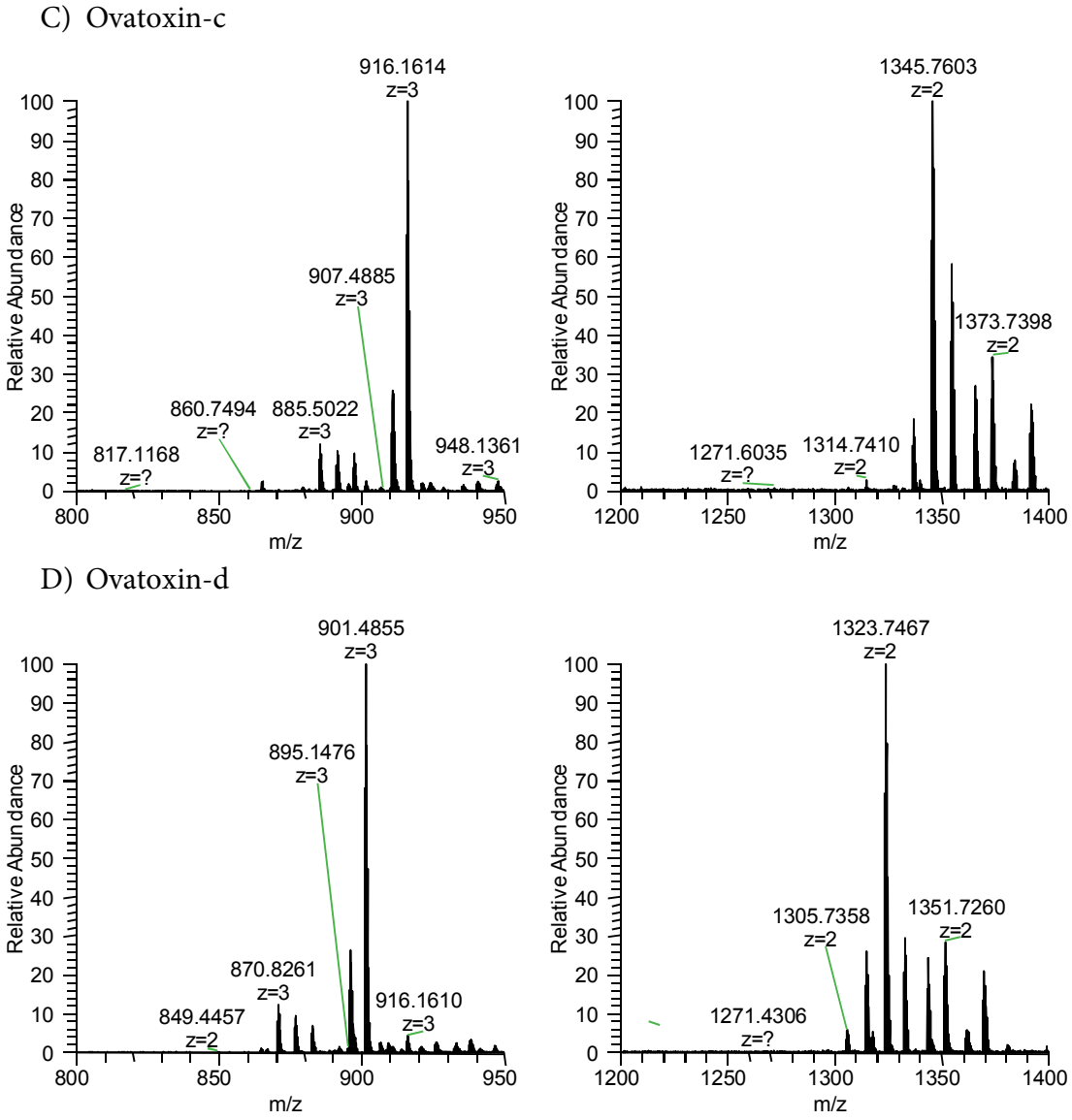

Sup. Mat. Figure 6-1 (A to H). Full HRMS spectra of ovatoxins —a to —e, ovatoxin-g, an isobaric compound of ovatoxin-g, and putative palytoxin, (m/z 700-1600) zoomed into the intervals m/z 830-950 and m/z 1250-1400.

E) Ovatoxin-e

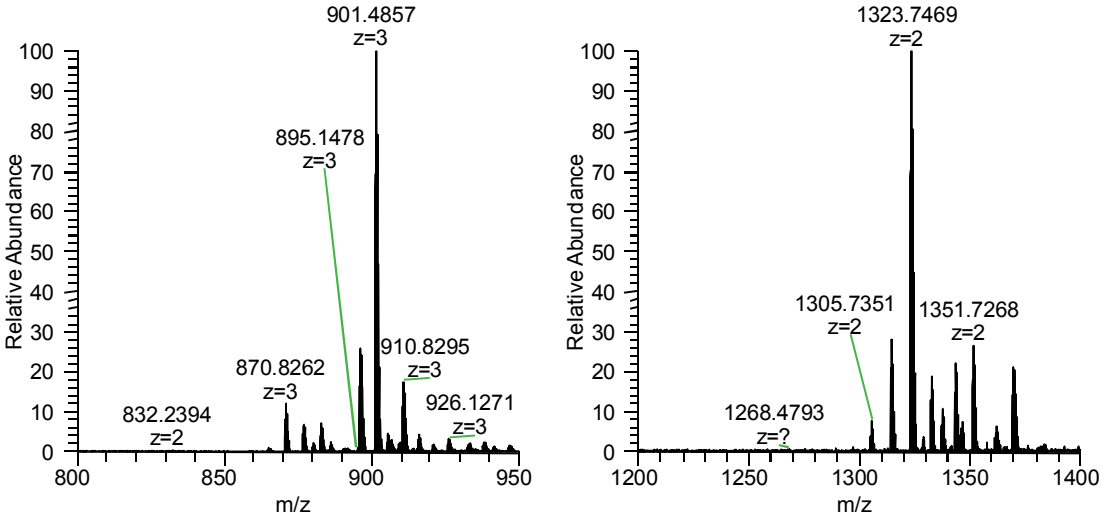

F) Isobaric of Ovatoxin-g

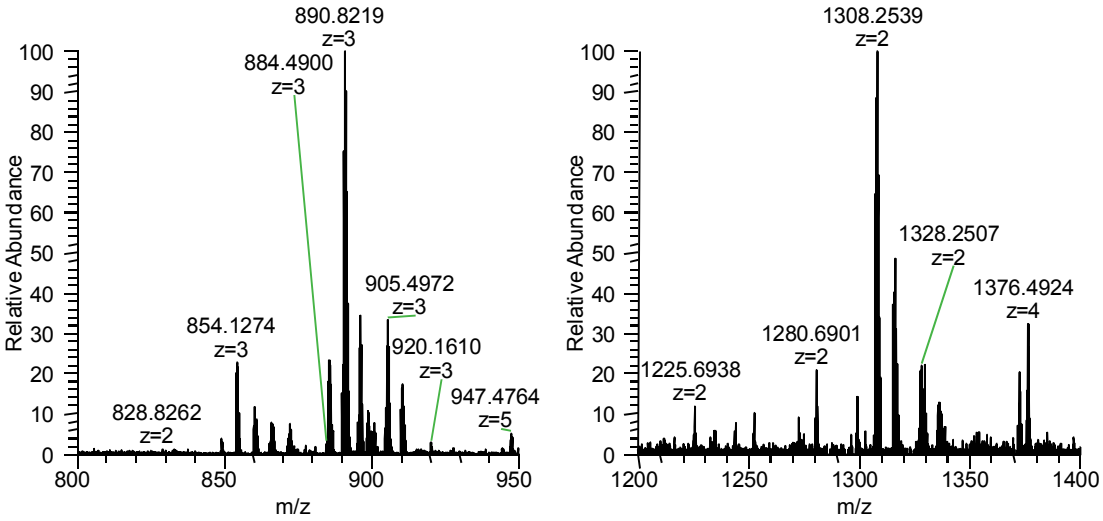

Sup. Mat. Figure 6-1 (A to H). Full HRMS spectra of ovatoxins —a to —e, ovatoxin-g, an isobaric compound of ovatoxin-g, and putative palytoxin, (m/z 700-1600) zoomed into the intervals m/z 830-950 and m/z 1250-1400.

G) Ovatoxin-g

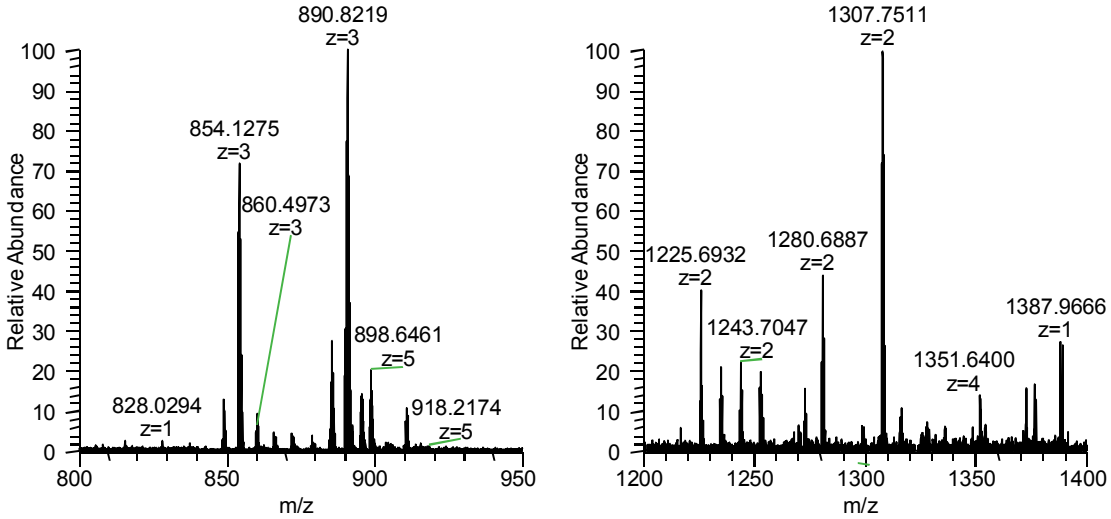

H) Putative palytoxin

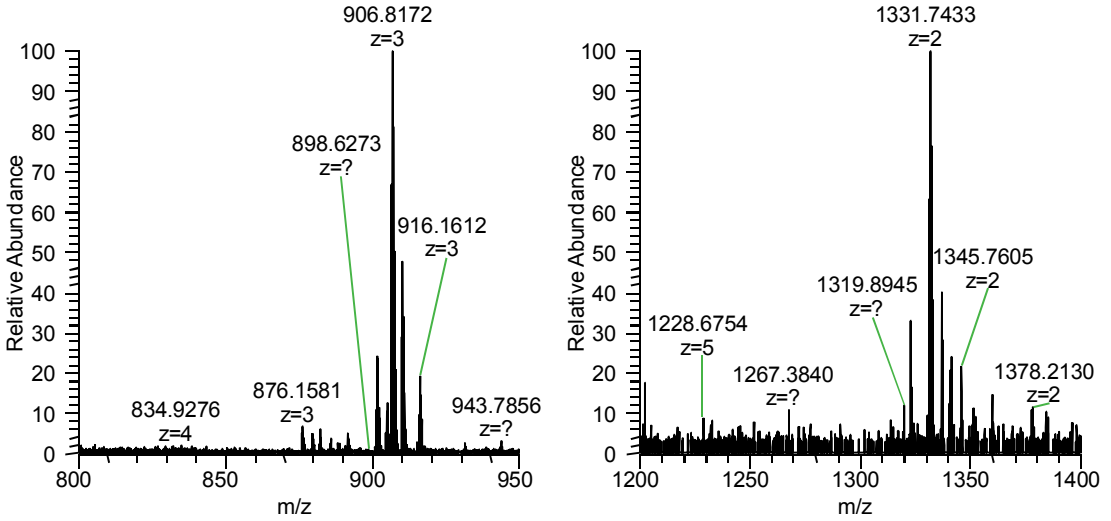

Sup. Mat. Figure 6-1 (A to H). Full HRMS spectra of ovatoxins —a to —e, ovatoxin-g, an isobaric compound of ovatoxin-g, and putative palytoxin, (m/z 700-1600) zoomed into the intervals m/z 830-950 and m/z 1250-1400.

A) Palytoxin standard 100 µg/mL (Maximum abundance $1.40 \cdot 10^5$ cps.)

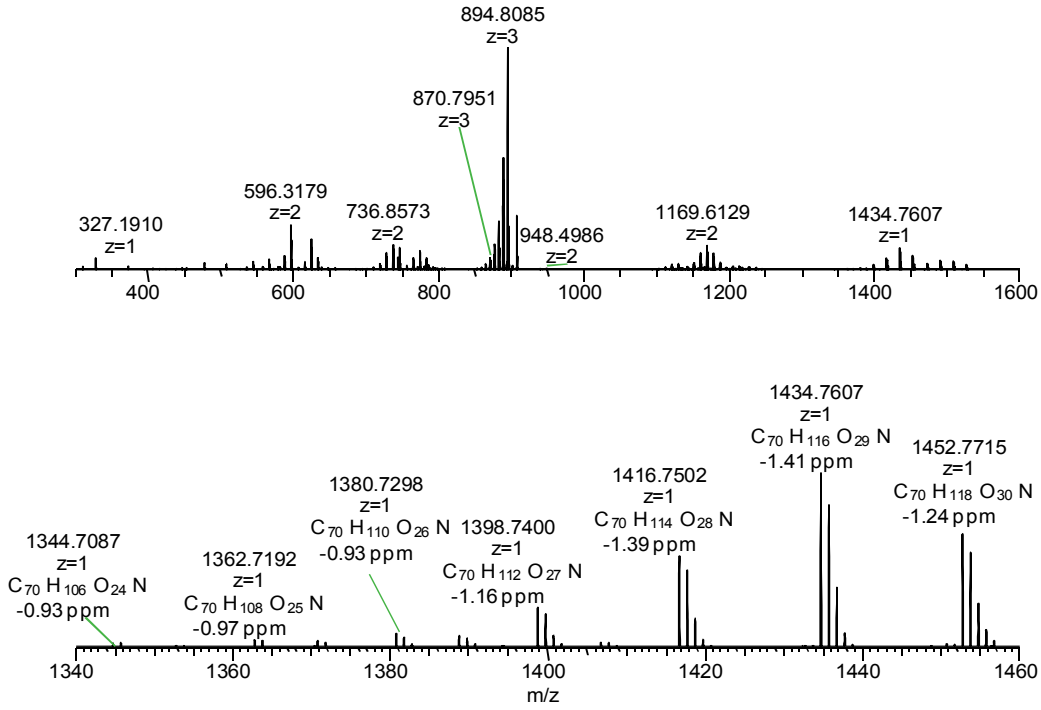

B) Ovatoxin-a (Maximum abundance $3.21 \cdot 10^4$ cps.)

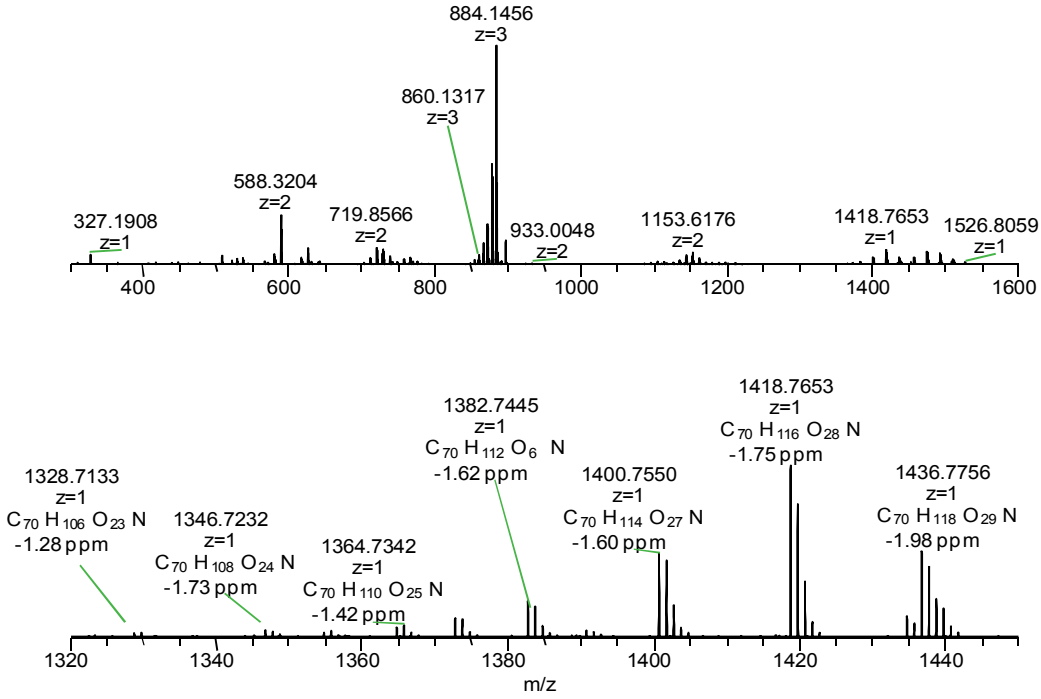

Sup. Mat. Figure 6-2 (A to D). HR CID MS^2 spectrum of $[M+H+Ca]^{3+}$ ion of palytoxin standard (*m/z* 906.8), ovatoxin-a (*m/z* 896.2), ovatoxin-g (*m/z* 890.8) and putative palytoxin (*m/z* 906.8). Zoom into the approx. *m/z* 1300-1500 region of the spectra to show the water losses produced by cleavage #16, B-side fragment.

C) Ovatoxin-g (Maximum abundance $1.60 \cdot 10^4$ cps.)

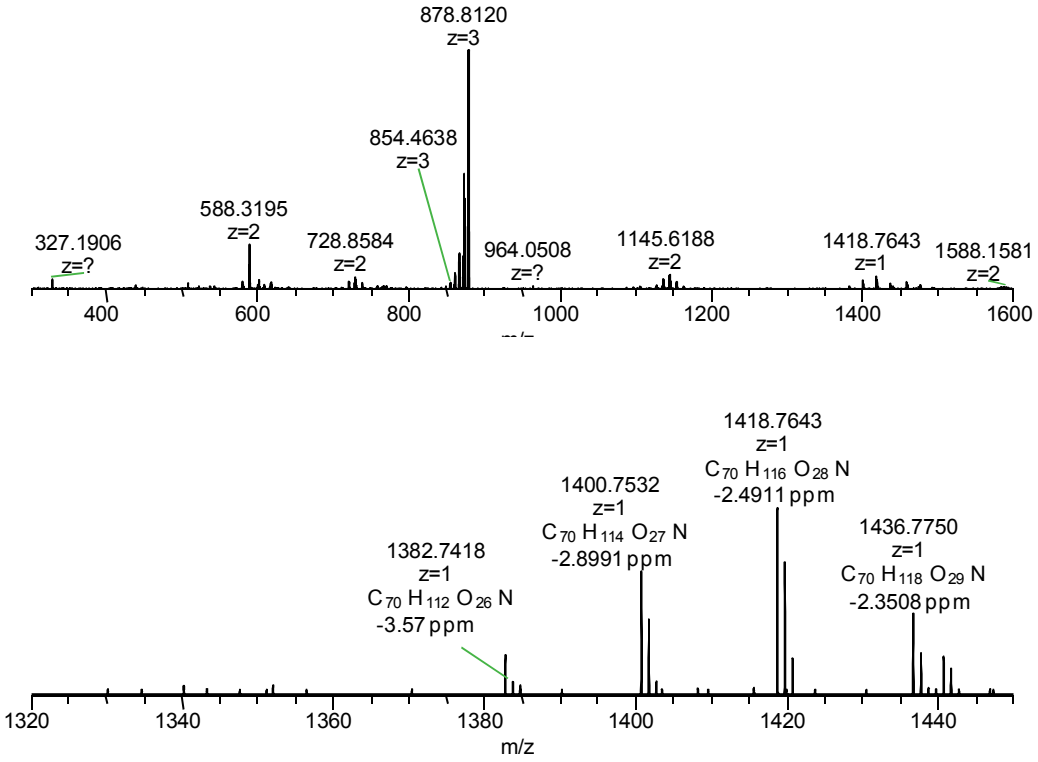

D) Putative palytoxin (Maximum abundance $8.84 \cdot 10^3$ cps.)

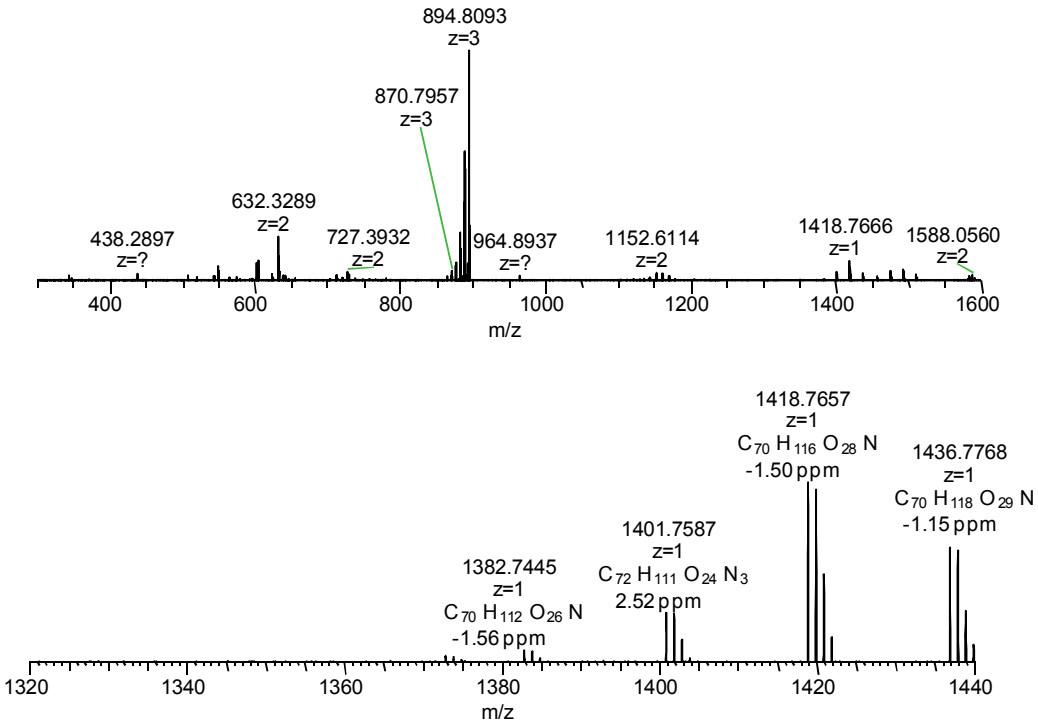

Sup. Mat. Figure 6-2 (A to D). HR CID MS2 spectrum of [M+H+Ca]3+ ion of palytoxin standard (m/z 906.8), ovatoxin-a (m/z 896.2), ovatoxin-g (m/z 890.8) and putative palytoxin (m/z 906.8). Zoom into the approx. m/z 1300-1500 region of the spectra to show the water losses produced by cleavage #16, B-side fragment.

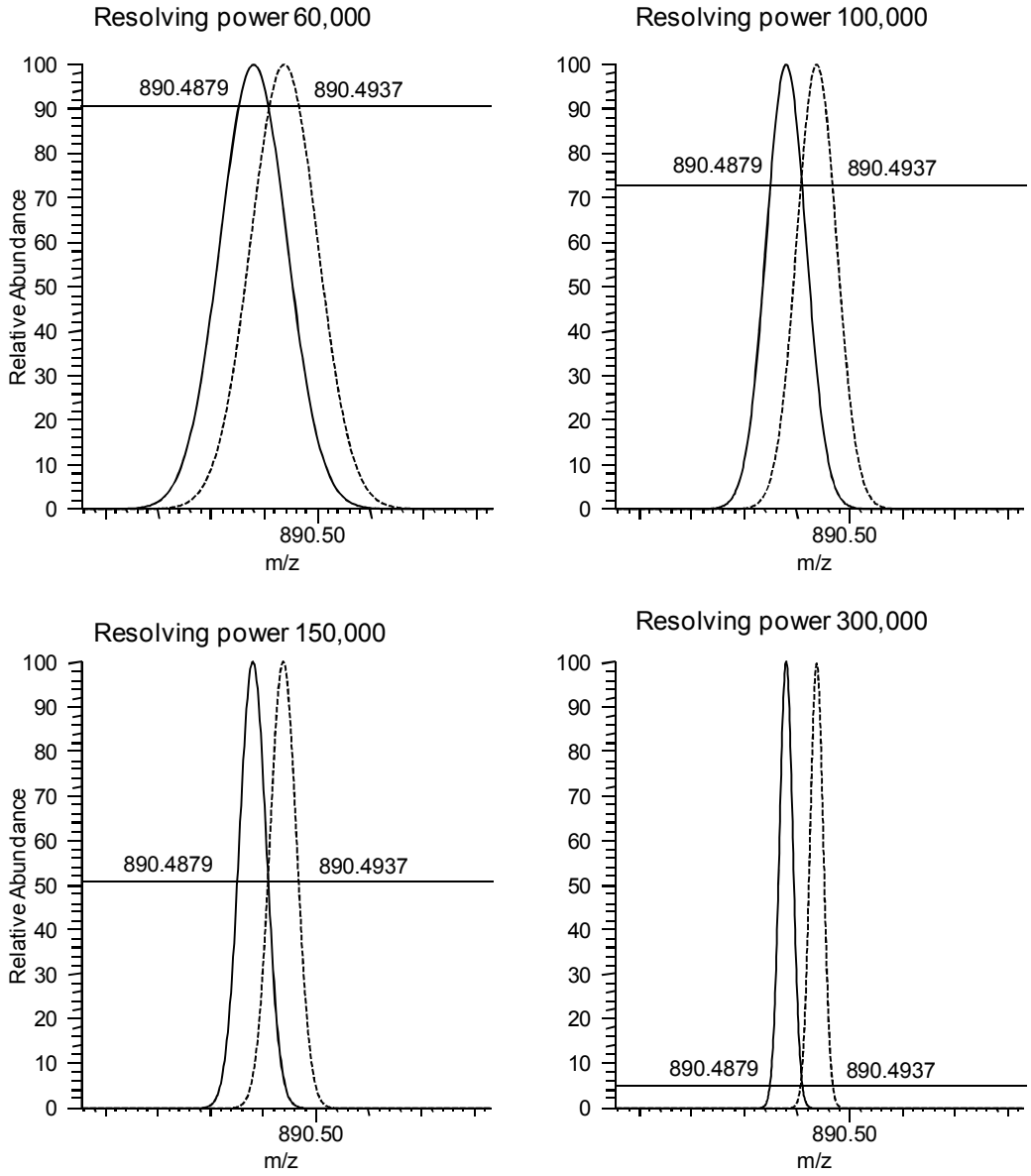

Sup. Mat. Figure 6-3. Simulated mass spectrometry resolution of peaks m/z 890.4870 and m/z 890.4937 (6.7 mDa difference) corresponding to the [M+H+Ca]3+ ion of OVTX-g and the [M+H+Mg]3+ ion of OVTX-a. Resolving power of 150,000 (FWHM) would be needed to resolve ion peaks at 50% of peak width.

7 General Discussion

This thesis aimed to improve the application of liquid chromatography coupled to mass spectrometry (LC-MS) methods for the study of lipophilic and emerging toxins in a Mediterranean coastal estuarine system, where toxic microalgae blooms are usually a great concern for shellfish aquaculture and public health. Ever-developing analytical technologies based on LC-MS are one of the most powerful mitigation tools against harmful algae blooms (HAB), which constitute a fascinating research field.

This study contributed to solve three current challenges of the study of toxic HABs by LC-MS:

The first scientific contribution (*Validation of LC-MS/MS chromatographic conditions for lipophilic toxins*, **Chapter 3)** investigated the implementation of the most suitable monitoring strategy by the validation and improvement of the decision-making process of the optimum LC-MS method for the determination of lipophilic marine toxins at IRTA, and assisted other laboratories in their own process.

The second scientific contribution (Dinophysis *bloom and DSP shellfish toxicity in Alfacs Bay*, **Chapter 4)** addressed the unpredictability of toxic Harmful Algae Blooms by the study of the dynamics of diharretic toxins during a spring bloom dominated by *Dinophysis sacculus* in Alfacs Bay, providing relevant information to improve management measures for future blooms.

The third and fourth scientific contributions (*Confirmation of pinnatoxins and spirolides by HRMS*, **Chapter 5,** and *Ovatoxin-g and isomeric palytoxin by LC-HRMS*, **Chapter 6)** reflected on the relevance of analytical techniques in the identification and confirmation of marine toxins by the study of emerging and new toxins using High Resolution MS technologies. **Chapter 5** showed the unambiguous confirmation for the first time of the emerging toxins cyclic imines (Pinnatoxin G and 13-desmethyl Spirolide C) in Catalonia. **Chapter 6** reported the discovery and some structural insights on two novel palytoxin-like compounds (ovatoxin-g and isobaric palytoxin) from a strain of *Ostreopsis* cf. *ovata* isolated for the first time in our study area.

Methods based on LC-MS were declared as the reference control method for lipophilic toxins in Regulation (European Commission) No. 15/2011, which references the Standard Operational Procedure written by the European Union Reference Laboratory for Marine Biotoxins (EURLMB) as guidelines for the rest of laboratories. However, this document leaves open the choice of the chromatographic conditions and the recovery correction approaches, although this selection is not trivial. Chromatographic conditions, characterized by pH and buffer system of the mobile phases, affect chromatographic selectivity, ionization yields, sensitivity elution order and matrix effects. Thus, the work described in **Chapter 3** (*Validation of LC-MS/MS chromatographic conditions for lipophilic toxins*) aimed to be a wide-scope study of the possible alternatives to guide laboratories in the implementation of the most suitable conditions for their LC-MS methods. The study included six groups of marine lipophilic toxins: okadaic acid (OA) and dinophysistoxins (DTX-1 and DTX-2), pectenotoxins (PTX-2), azaspiracids (AZA-1),

yessotoxins (YTX), gymnodimines (GYM-a) and spirolides (SPX-1). Three concentration levels were evaluated (0.5, 1 and 1.5 times the maximum permitted levels in Europe) with three relevant matrices for the seafood industry (mussels, pacific oysters, clams and sea urchin) plus another poorly studied matrix (sea urchin); at four chromatographic conditions (pH 2, pH 6.8, pH 7.9 and pH 11), besides the comparison of two quantification strategies (external standard and matrix-matched standard) under alkaline conditions.

Alkaline conditions with external calibration and recovery correction for OA were selected as the most proper conditions in the context of our laboratory. The performance of alkaline conditions in the intra-laboratory validation assessment met the quality criteria demanded by EURLMB, including acceptable limits of quantitation (LOQ) and manageable matrix effects. Moreover, alkaline conditions allowed detection windows with polarity switching in our 3200 QTrap mass spectrometer, since toxins clustered according to their preferential electro-spray (ESI) polarity: OA, DTX-1, DTX-2 and YTX (ESI -) eluted at the beginning of the chromatograph, while AZA-1, PTX-2, GYM-a and SPX-1 (ESI +) eluted at the end. Thus the analysis of all toxins can be accomplished in a single run of 12 min, increasing sample throughput. On the other hand, alkaline conditions almost tripled the sensitivity for cyclic imines (GYM-a and SPX-1), and kept LOQs below 1.5 μg/kg tissue for mussels and oysters.

The optimized and validated LC-MS method implemented at IRTA became an essential tool for the following studies. **Chapter 4 (**Dinophysis *bloom and DSP shellfish toxicity in Alfacs Bay***)** describes the comprehensive study of a diarrhetic shellfish poisoning outbreak in Alfacs Bay, that included several types of samples: shellfish samples (mussels and oysters), phytoplankton concentrates (filters and net-haul samples) and solid phase adsorbing toxin tracking (SPATT) devices. In total, 228 samples and about 4000 runs (including screening batches, calibration curves, quality controls, blank samples, double and triplicate injections, etc.) were needed to complete the study. This task could not have been approached without a fast, high sample throughput LC-MS method. Validation of the method described in **Chapter 3** supports the accuracy of analytical results in **Chapter 4**, including matrix effects considerations, since blank shellfish material for the accuracy assessments were taken from the same bay, thus avoiding a potential source of intra-species matrix effects. Linearity assessments were also very useful, since samples of the study described in **Chapter 4** had a wide range of toxin concentrations, thus calibration curves and samples could be properly organized in batches to fall into the dynamic range of the instrument.

The implemented LC-MS method described in **Chapter 3** has great sensitivity and low LOQs for cyclic imines, and in fact it allowed the detection of very low concentrations of spirolides in mussels from Alfacs Bay, which was the starting point of the study described in **Chapter 5 (***Confirmation of pinnatoxins and spirolides by HRMS***)**. Spirolides had been detected before in some shellfish samples from Catalonia, but the previous LC-MS method used at IRTA (based on acidic conditions), less sensitive, only showed punctual traces of this cyclic imine. The good performance of the method for SPX-1 and GYM-a prompted us to request collaboration with the National Research Council of Canada to obtain a sample of the non-comercial (uncertified) reference material of Pinnatoxin G (PnTX-G). **Chapter 5** shows the data of a preliminary validation process of the method for PnTX-G, including limits of detection below 1.5 μg/kg shellfish tissue (mussels and oysters) and great sensitivity. Thus, we include PnTX-G in the LC-

MS protocol to screen shellfish samples and SPATTs samples from the Ebro Delta bays for the presence of spirolides and pinnatoxins, and both SPX-1 and PnTX-G could be identified by Multiple Reaction Monitoring in several samples.

Cyclic imines are geographically wide spread, but **Chapter 5** is actually the first report of PnTX-G in Spain. Pinnatoxins and spirolides comprise a long list of more than 20 analogs, most of them without available reference standard materials, thus the most reliable technique to prove its presence for the first time in our study area was High Resolution MS (HRMS), since it provides great selectivity thanks to its high resolving power and precision in mass accuracy measurements. One of the crucial parameters in HRMS analysis is the selection of mass tolerance error to provide optimum selectivity: too wide mass tolerance errors produce false positives (the chance that the chromatographic peak is not caused by the analyte, but by a coeluting compound whose mass fits in the tolerance range), but too narrow mass tolerance errors can lead to false negatives due to shifts in accurate mass measurements caused by hidden isobaric interferences, and to distortion of the chromatographic peaks. Thus, we selected a mass tolerance error of 10 ppm, according to the performance of the method and the instrument. This tolerance range, widely used in HRMS applications, produced false positives even in blanks of methanol. Since marine microalgal toxins are usually found at trace concentrations in complex matrices, concentration thresholds are rarely applied to leave out false positives. We studied those false positives, and developed a comprehensive strategy based on orthogonal filters such as the inspection of isotopic patterns and MS^2 spectra to unambiguously confirm the present toxins (PnTX-G and SPX-1) and reject the false positives.

The experience with HRMS instruments and the investigation of strategies to ensure proper confirmation described in **Chapter 5** were very valuable for the determination of toxin profiles of a novel cultured strain of the dinoflagellate *Ostreopsis* cf. *ovata* isolated from the Ebro Delta area, shown in **Chapter 6 (***Ovatoxin-g and isomeric palytoxin by LC-HRMS***)**. Toxin profiles of *O.* cf. *ovata* have been proven to be strain-specific, and the list of new ovatoxins keeps on growing with every in-depth study. In this case, the strategy to prove the presence of known ovatoxins in the new isolated strain included comparison of retention times of individual compounds with a reference sample from the Adriatic sea, full HRMS spectra of the representative fingerprint of double and triple charged precursor ions and adducts, elemental formula assigned to the mono-isotopic ion peak with mass accuracy measurements below 3 ppm, consistency of the isotopic patterns, and fragmentation behavior of individual compounds compared to the reference sample. Thus, the HRMS method and data mining strategy described in **Chapter 6** allowed the unequivocal characterization of the toxin profile of a new strain of *O.* cf. *ovata*.

Moreover, **Chapter 6** shows the structural investigation of two unknown ovatoxins directly in crude extracts at nanogram per milliliter levels, which is an insufficient quantity to perform nuclear magnetic resonance (NMR)-based structural elucidation. First, an isobaric compound of palytoxin with the same full HRMS pattern was found to elute about two minutes before the palytoxin standard (from *Palythoa tuberculosa*). The study of its full $HRMS^n$ spectra of the most intense precursor ion ($[M+H+Ca]^{3+}$ ion at *m/z* 906.8) and its comparison with fragmentation behavior of standard palytoxin (confirmed by NMR in the literature) provided enough information to highlight the regions of structural differences between de isomers. **Chapter 6** concluded that, compared to palytoxin, isobaric palytoxin is hydroxylated at carbon-42 (C-42)

and dehydroxylated at C-17 and most likely at C-64, thus isomeric palytoxin would share structural characteristics with ovatoxin-a. However, the extra oxygen found to be contained in the segment from the A-side terminal to C-8 could not be unequivocally located. The second unknown ovatoxin, named ovatoxin-g, presented a full HRMS spectra that followed the expected ionization behavior of palytoxin-like compound, and its elemental formula calculated from a cross-check of all the ions contained in the spectrum concluded that ovatoxin-g had one oxygen less than ovatoxin-a. Further studies on its fragmentation spectra revealed that, compared to ovatoxin-a, ovatoxin-g is dehydroxylated at C-46. Therefore, structure elucidation by HRMS is a useful resource to point out structural differences among analogs of the same family, even if they are present at trace concentrations in complex samples, but it has its limitation. On one hand, it relies on previous studies on reference compounds confirmed by NMR to facilitate the interpretation of the spectra. On the other hand, structural regions of the molecule that do not fragment cannot be investigated by this technique, thus some functional groups cannot be always allocated. **Chapter 6** describes the application of a recent approach, proposed by Uchida et al. in 2013[1], to investigate the position of hydroxyl groups in polyol structures according to the number of water losses derived from conjugated polyenes in a fragment, but we proved that this approach is intensity-dependent and cannot provide unequivocal information. Thus, the regiochemistry and stereochemistry of microalgal toxins still needs NMR investigations.

Besides analytical chemists and physiologists researching toxic HABs, this work may be of interest for stakeholders of the aquaculture sector, including policy makers, laboratories that perform monitoring and control, producers and consumers. The contribution of this thesis also has a relevant impact on the study of HABs in the Ebro Delta, one of the most sensitive and complex wetlands of the Mediterranean basin, which still requires much attention from ecologist, phycologist, bio-informaticians, toxicologist and analytical chemists. For example, **Chapter 6** (*Ovatoxin-g and isomeric palytoxin by LC-HRMS*) illustrates the close collaboration with phycologist to study a novel strain of *O.* cf. *ovata* isolated in our study area. The analytical results of the study will complement the morphological and genetically characterization of the strain, which will be described in a paper that has been already sent to be considered for publication (see **Appendix**).

The thesis also strengthened the collaborations with other European research groups focused on HABs and microalgal toxins. Experiments in **Chapter 5** (*Confirmation of pinnatoxins and spirolides by HRMS*) with HRMS were carried out with Dr. Ambrose Furey's group (PROTEOBIO) at the Chemistry Department of Cork Institute of Technology, in Ireland, where the LC-MS/MS method and confirmation strategy were also applied to active water samplers from a marine reserve from West Cork. The samples contained two spirolides (SPX-1 and 20-methyl SPX-g) and PnTX-G, whose presence has never been reported in Ireland. These results will be considered for publication in the future. **Chapter 6** (*Ovatoxin-g and isomeric palytoxin by*

---

[1] Uchida, Hideaki, Yohsuke Taira, and Takeshi Yasumoto. "Structural elucidation of palytoxin analogs produced by the dinoflagellate *Ostreopsis ovata* IK2 strain by complementary use of positive and negative ion liquid chromatography/quadrupole time-of-flight mass spectrometry." *Rapid Communications in Mass Spectrometry* 27.17 (2013): 1999-2008.

LC-HRMS) was performed with Professor Patrizia Ciminiello's group at the Natural Products Department of the Pharmacy Faculty at University Federico II from Naples, Italy, the leading group in the research of palytoxins in the Mediterranean. Professor Patrizia Ciminiello's group proposed the term "putative palytoxin" when they discovered in samples from the Adriatic Sea a compound that was isomeric to the standard palytoxin from *Palythoa tuberculosa* with a different retention time, but the limited quantity of this compound hampered its structural study, even by HRMS means. The study of isomeric palytoxin from the Ebro Delta *O.* cf. *ovata* strain reconsidered this issue, and the current question is if both strains produce the same isomeric palytoxin compound, or if these compounds have structural differences that may even have physiological significance.

8 General Conclusion

The selection of chromatographic conditions and recovery correction approaches to implement the reference LC-MS/MS method in optimal conditions to control lipophilic toxins in shellfish is not a trivial decision and requires a careful study of the alternatives.

The comprehensive assessment of the different alternatives allowed the implementation at IRTA of a high sample throughput method that met the European Union Reference Laboratory for Marine Biotoxins requirements for all toxins studied with a middle-class mass spectrometer.

Other factors regarding the analysis context (equipment available, number of samples needed to analyze, and most common toxin profiles in the area of interest) also play a role in the decision-making process of choosing the optimum LC-MS/MS to implement.

The study of natural populations of toxic *Dinophysis* in stratified Mediterranean coastal embayments required the study of different compartments of the ecosystem (phytoplankton, shellfish and water column) to understand the dynamics of diarrhetic shellfish toxins that lead to shellfish toxicity.

The current monitoring strategies to control *Dinophysis* blooms and shellfish toxicity in Alfacs Bay (Catalonia, NW Mediterranean Sea) are protective enough to public health, but two issues must be reconsidered: 1) during the *Dinophysis* blooms in Alfacs Bay pacific oysters did not accumulate diarrhetic shellfish toxins over the European maximum permitted level, thus the protocols to manage the commercialization of this species could be reviewed; 2) total toxin content per *Dinophysis* cell seems to increase towards the end of blooms, thus the alert threshold of 500 *Dinophysis* cell/L may not always be protective against shellfish toxicity.

Cyclic imines are wide spread emerging toxins in the Mediterranean: Pinnatoxin G and 13-desmethyl Spirolide C were unequivocally confirmed in at low concentrations in shellfish and solid phase adsorption toxin tracking devices from Catalonia (first report of pinnatoxins in Spain and first detection of spirolides in Catalonia). The monitoring of the cyclic imine group is highly encouraged, even though they are not yet regulated, in order to gather information about the prevalence of these toxins in shellfish products and the levels of exposure to consumers.

False positives in the study of cyclic imines (and potentially other marine toxins) by High Resolution MS can be an issue when dealing with very complex matrices and require a proper strategy to be discarded, based on information from isotopic patterns, precursor and product scans with accurate mass measurements, signal thresholds, and proper tolerances applied to mass filters.

Mediterranean *Ostreopsis* cf. *ovata* presents toxin profiles that are strain-specific, and some strains have unique ovatoxins that are not found in other strains.

Toxin profile of strains of *O.* cf. *ovata* from the Ebro Delta contained ovatoxin-a, -b, -c, -d and –e, at concentrations per cell remarkably higher than toxin quotas reported for other Mediterranean strains.

Two new palytoxins were discovered in cultures of *Ostreopsis* cf. *ovata* from the Ebro Delta. The novel ovatoxin-g share most part of the structure with ovatoxin-a, but it dehydroxylated at position C-46. The formerly denominated “putative palytoxin” is indeed a structural isomer of palytoxin: it has one extra oxygen at position C-42, and between the A-side terminal to C-8; and it is dehydroxylated at C-17 and most likely at C-64.

List of publications

García-Altares, M., J. Diogène, and P. de la Iglesia, *The implementation of liquid chromatography tandem mass spectrometry for the official control of lipophilic toxins in seafood: Single-laboratory validation under four chromatographic conditions.* Journal of Chromatography A, 2013. **1275**: p. 48-60.

García-Altares, M., A. Casanova, V. Bane, J. Diogène, A. Furey, and P. de la Iglesia, *Confirmation of pinnatoxins and spirolides in shellfish and passive samplers from Catalonia (Spain) by Liquid Chromatography coupled with triple quadrupole and High-Resolution hybrid tandem Mass Spectrometry.* Marine Drugs, 2014. **12**(6): p. 3706-3732.

García-Altares, M., L. Tartaglione, C. Dell'Aversano, O. Carnicer, P. de la Iglesia, M. Forino, J. Diogène, and P. Ciminiello, *The novel ovatoxin-g and isobaric palytoxin (so far referred to as putative palytoxin) from* Ostreopsis *cf.* ovata *(NW Mediterranean Sea): structural insights by LC-High Resolution MS^n.* Analytical and Bioanalytical Chemistry, 2015. **407**(4): p. 1191–1204.

In preparation:

García-Altares, M., A. Casanova, M. Fernández, J. Diogène, and P. de la Iglesia, *Bloom of* Dinophysis *spp. dominated by* D. sacculus *and its related Diarrheic Shellfish Poisoning (DSP) outbreak in Alfacs Bay (Catalonia, NW Mediterranean Sea): identification of DSP toxins in phytoplankton, shellfish and passive samplers.* Submitted to Harmful Algae in February 2015.

Carnicer, O., García-Altares, M., Andree, K. B.; Tartaglione, L., Dell'Aversano, C., Ciminiello, P., de la Iglesia, P., Diogène, J., Fernández-Tejedor, M., Ostreopsis *cf.* ovata *from western Mediterranean Sea: Physiological responses under different temperature and salinity conditions.* Submitted to Harmful Algae in May 2014.

Soliño, L., García-Altares, M., Ciminiello, P., Diogène, J., Sureda, F. X., *Semi-purified ovatoxins-a and -b from a super-producer strain of Mediterranean* Ostreopsis *cf.* ovata *and palytoxin from* Palithoa toxica *exhibit similar toxicity on cerebella granular cells calcium influx.* In preparation for Journal of Pharmacology and Toxicology.

McCarthy, M., Bane, V., García-Altares, M., van Pelt, F., Furey, A., O'Halloran, J. *Detection of Pinnatoxin G and Spirolides in Irish Waters: assessment of emerging biotoxins at Lough Hyne Marine Reserve.* In preparation for Toxicon.

Appendix: Scientific contribution summited to *Harmful Algae* Journal

Elsevier Editorial System(tm) for Harmful Algae
Manuscript Draft

Manuscript Number: HARALG-D-14-00107

Title: Ostreopsis cf. ovata from western Mediterranean Sea: Physiological responses under different temperature and salinity conditions

Article Type: Original Research Article

Keywords: Ostreopsis cf. ovata; temperature; salinity; growth rate; cell size; palytoxin

Corresponding Author: Mrs. Margarita Fernández-Tejedor,

Corresponding Author's Institution:

First Author: Olga Carnicer

Order of Authors: Olga Carnicer; María García-Altares; Karl B Andree; Luciana Tartaglione; Carmela Dell'Aversano; Patrizia Ciminiello; Pablo de la Iglesia; Jorge Diogène; Margarita Fernández-Tejedor

Abstract: Ostreopsis cf. ovata causing seasonal proliferations in the Mediterranean Sea produces "putative palytoxin" and ovatoxins which are considered among the most potent marine toxins. Blooms have been related with several toxic events such as respiratory problems in humans and mortality of benthic marine organisms. In the coming decades, an increase in temperature and salinity is predicted in the Mediterranean Sea as a consequence of global warming that may provoke alterations in the dynamics of marine microorganisms.
In this study, we analyzed the physiological effects of water temperature and salinity, and their interaction through a multi-factorial experiment using two O. cf. ovata strains in culture that had been isolated from western Mediterranean Sea. In order to perform an accurate and reliable estimation of cell abundance, hydrochloric acid and sodium-ethylenediaminetetraacetic acid treatments were evaluated. Results of the physiological study showed that growth was inhibited at 19oC for all salinities. High growth rates were registered for higher temperatures; at 24oC, growth rates in all salinities were relatively stable, while at 28oC, a significant reduction of growth rates was recorded at salinities 32 and 38. Two groups were distinguished by cell size in all high temperature conditions and a positive correlation between the amount of small cells and growth rate was found. Palytoxin-like content increased with time; for 28oC, at the beginning of the stationary phase while at 24oC, a significant higher amount of toxin appeared latter, between the stationary and the decaying phase. Our results suggest that climate change may not affect frequency of blooms but their length and toxicity may be enhanced.

Suggested Reviewers: Magda Vila
CSIC
magda@icm.csic.es
expert in Ostreopsis

IRTA
RESEARCH & TECHNOLOGY FOOD & AGRICULTURE

Crta. Poble Nou Km 5,5
E-43540 Sant Carles de la Ràpita

Tel. +34 902 789 449
Fax +34 977 74 41 38

irta@irta.cat
www.irta.cat

Sant Carles de la Ràpita, 29 May 2013

Dear Editor,

Please find enclosed our article entitled " *Ostreopsis* cf. *ovata* from western Mediterranean Sea: Physiological responses under different temperature and salinity conditions " by Olga Carnicer, María Garcia-Altares, Karl. B. Andree, Luciana Tartaglione, Carmela Dell'Aversano, Patrizia Ciminiello; Pablo de la Iglesia, Jorge Diogène and Margarita Fernández-Tejedor. This is a new and original paper which has been neither published nor submitted anywhere else. All authors have read and approved the final version submitted.

Our first choice has been to submit our manuscript to Harmful Algae, taking into consideration the scope of the journal. This manuscript describes the physiological effects (growth rate, morphology and toxicity) of two strains of *O.* cf. *ovata* from western Mediterranean Sea. The experiments were performed under different conditions of temperature and salinity, analyzing their interaction through a multi-factorial analysis. Our results would increase the knowledge of this species response to environmental factors fluctuations and potential risks to humans and marine ecosystems. In addition to that, in this manuscript we performed the first analyses of different samples treatments in order to refine the Utermöhl method for accurate cell abundance estimation taking into account mucilaginous aggregates present in cultures. Therefore, we expect that this contribution will be of the interest of Harmful Algae readers.

We remain at your disposal for any clarification.

Sincerely yours,

Margarita Fernández Tejedor
Seguiment del Medi Marí

IRTA
Crta. Poble Nou, km. 5.5
43540 Sant Carles de la Ràpita (Tarragona, Spain)

Telf.: 00 34 902 789 449 (ext. 1851)
Fax: 00 34 977 744 138

margarita.fernandez@irta.cat

Ostreopsis cf. _ovata_ from western Mediterranean Sea: Physiological responses under different temperature and salinity conditions.

We analyzed the physiological effects through a multi-factorial experiment on *O*. cf. *ovata*.

Higher growth rates were registered for higher temperatures.

A significant reduction of growth rates was recorded at salinities 32 and 38 compare to 36.

Palytoxin-like content increased at the stationary phase at 28ºC and the decaying phase at 28ºC.

A positive correlation between the amount of small cells and growth rate was found.

Ostreopsis cf. *ovata* from western Mediterranean Sea: Physiological responses under different temperature and salinity conditions

Olga Carnicer[1], María Garcia-Altares[1], Karl. B. Andree[1], Luciana Tartaglione[2], Carmela Dell'Aversano[2], Patrizia Ciminiello[2]; Pablo de la Iglesia[1], Jorge Diogène[1], Margarita Fernández-Tejedor[1*]

[1] IRTA, Carretera de Poble Nou, km 5.5, 43540 Sant Carles de la Ràpita, Spain

[2] Dipartimento di Chimica delle Sostanze Naturali, Università degli Studi di Napoli Federico II, via D. Montesano 49, 80131 Napoli, Italy

Corresponding author: Margarita Fernández-Tejedor
IRTA
Carretera de Poble Nou, Km 5.5,
43540, Sant Carles de la Ràpita, Tarragona, Spain
Tel: ++34 902 789 449 (ext. 1842); Fax: +34 977 744 138
E-mail address: margarita.fernandez@irta.cat

Abstract.

Ostreopsis cf. *ovata* causing seasonal proliferations in the Mediterranean Sea produces "putative palytoxin" and ovatoxins which are considered among the most potent marine toxins. Blooms have been related with several toxic events such as respiratory problems in humans and mortality

of benthic marine organisms. In the coming decades, an increase in temperature and salinity is predicted in the Mediterranean Sea as a consequence of global warming that may provoke alterations in the dynamics of marine microorganisms.

In this study, we analyzed the physiological effects of water temperature and salinity, and their interaction through a multi-factorial experiment using two *O.* cf. *ovata* strains in culture that had been isolated from western Mediterranean Sea. In order to perform an accurate and reliable estimation of cell abundance, hydrochloric acid and sodium-ethylenediaminetetraacetic acid treatments were evaluated. Results of the physiological study showed that growth was inhibited at 19°C for all salinities. High growth rates were registered for higher temperatures; at 24°C, growth rates in all salinities were relatively stable, while at 28°C, a significant reduction of growth rates was recorded at salinities 32 and 38. Two groups were distinguished by cell size in all high temperature conditions and a positive correlation between the amount of small cells and growth rate was found. Palytoxin-like content increased with time; for 28°C, at the beginning of the stationary phase while at 24°C, a significant higher amount of toxin appeared latter, between the stationary and the decaying phase. Our results suggest that climate change may not affect frequency of blooms but their length and toxicity may be enhanced.

Keywords: *Ostreopsis* cf. *ovata*; temperature; salinity; growth rate; cell size; palytoxin

1 Introduction

The genus *Ostreopsis,* Schmidt (1901) is a harmful benthic marine dinoflagellate distributed widely in both subtropical and tropical marine coral reef ecosystems and temperate regions (Parsons *et al.,* 2012; Rhodes *et al.,* 2011; Pistocchi *et al.,* 2011). Nine species having very similar morphological features have been described and nowadays taxonomical identification is

under revision using molecular methods to clarify controversial issues (Penna *et al.,* 2010; Sato *et al.,* 2011; Penna *et al.,* 2012). It is characterized by forming massive proliferations that reach very high concentrations in benthic subtracts such as macroalgae, rocks, or invertebrates. These blooms are associated with abundant amounts of mucilage, in which cells are embedded. This mucilaginous net is composed by acidic polysaccharides and a high number of trichocysts (Honsell *et al.,* 2013). As well, cultures maintained in the laboratory produced these aggregates that constitute an impediment to perform accurate cell abundance estimations. Previous studies have used different strategies in order to dissolve mucilage to better homogenize the samples and facilitate cell counting. Two chemicals have been tested, sodium-ethylenediaminetetraacetic acid (Na-EDTA) (Scalco *et al.,* 2012; Pezzolesi *et al.,* 2012) and hydrochloric acid (HCl) (Guerrini *et al.,* 2010; Vanucci *et al.,* 2012b; Monti *et al.,* 2012) to counteract the interference of mucilages for cell abundance estimations. The addition of HCl liberates H^+ protons in aqueous medium that may neutralize negative electric charges present in cell walls and polysaccharides. The mechanism of action for the Na-EDTA treatment can consist in chelating Ca^{2+} and Mg^{2+} that bind polysaccharides together, and thereby disrupting the aggregation (Alldredge *et al.,* 1993).

O. cf. *ovata* has been extensively studied in the last decade regarding its morphology (Penna *et al.,* 2005; David *et al.,* 2013; Kang *et al.,* 2013), toxicity (Ciminiello *et al.,* 2006; Ciminiello *et al.,* 2008; Ciminiclllo *et al.,* 2011; Suzuki *et al.,* 2012; Hwang *et al.,* 2013), and distribution. It has been detected in tropical waters such as in the Atlantic Ocean, in Brazilian islands (Nascimento *et al.,* 2012b) and in the western Pacific Ocean, in the south China Sea (Pin *et al.,* 2001; Penna *et al.,* 2010) and in temperate areas such as the east Atlantic Ocean (David *et al.,* 2013), the China Sea (Sato *et al.,* 2011; Kang *et al.,* 2013), and especially in the Mediterranean Sea (e. g. Vila *et al.,* 2001; Aligizaki *et al.,* 2006; Monti *et al.,* 2007; Mangialajo *et al.,* 2008;

Totti *et al.,* 2010; Cohu *et al.,* 2011; Accoroni *et al.,* 2011; Pfakunnchen *et al.,* 2012; Ismael and Hamil, 2012). This species, with its widespread distribution, shows an adaptation to different environmental conditions that can lead to distinct physiological responses among strains from different origin. *O.* cf. *ovata* isolated from the Mediterranean and the Atlantic Sea belong to a genetic clade that presents a high degree of sequence homology (Penna *et al.,* 2010). While *O.* cf. *ovata* in tropical waters has been reported all year long (Pin *et al.,* 2001; Parsons and Preskitt, 2007; Parsons *et al.,* 2012), in the Mediterranean Sea, a seasonal pattern in bloom dynamics has been observed, coinciding with high temperatures in most cases. However, depending on the area, the threshold temperature for bloom formation varies, and correlation between temperature and *O.* cf. *ovata* outbreaks is not easy to determine, as other factors may also affect bloom dynamics (reviewed in Pistocchi *et al.,* 2011). But still, temperature ranges may or may not explain having *O.* cf. *ovata* at certain densities in a given location. Considering projections for seawater warming for the 21st century, which is expected to be more intensive in the Mediterranean Sea than in other areas (IPCC, 2013), it is necessary to intensify the efforts to understand how the growth and toxin production of *O.* cf. *ovata* is affected by high temperature regimes.

Several laboratory studies have been performed to characterize the optimal growth temperatures for *O.* cf. *ovata* strains from the Mediterranean Sea. Two experiments on Tyrrhenian strains were not consistent on the conditions where the highest growth rates were obtained: 22-26^{o}C (Scalco *et al.,* 2012) and 26-30^{o}C (Granéli *et al.,* 2011). Much lower optimal temperatures were found in an Adriatic strain that grew faster at 20^{o}C in relation to higher temperatures (Pezzolesi *et al.,* 2012). From these results, differential adaptation to temperature may be expected among *O.* cf. *ovata* populations. In addition, the response of marine microalgae to warming could differ

92 depending on other environmental factors. Coastal waters often present highly pronounced
93 fluctuations of physicochemical factors. The interaction of these factors with temperature may
94 have consequences in *O.* cf. *ovata* distributions. In recent studies multi-factorial experiments
95 have combined temperature with other environmental factors. Scalco *et al.,* (2012) studied day
96 length and irradiance, concluding that *O.* cf. *ovata* temperature and light preferences were in
97 accordance with natural conditions in late June and September in the Mediterranean Sea.
98 Nutrient availability was also examined by Vydiarathna and Granéli (2013) suggesting that
99 future nutrient enrichment could enhance *O.* cf. *ovata* proliferations. In the same way, Vanucci et
100 al., (2012b) observed a negative effect on growth rates and a reduction in cell abundances under
101 nitrogen and phosphorus limitation. Taking into account that changes in salinity are common in
102 coastal waters due to evaporation, rainfall and/or riverine flow fluctuations (Tanimoto et al
103 2013), it is very important to study the interactions of this factor with temperature to clarify the
104 possible repercussions to microalgae physiology due to salinity changes. *O.* cf. *ovata* from
105 Japanese coastal waters has been studied under a wide range of conditions, suggesting that high
106 salinities and temperatures would favor its growth (Yamaguchi *et al.,* 2012b).
107 Morphometric changes in *O.* cf. *ovata* have been described during growth phases. Two different
108 size classes are present in both Mediterranean waters (Penna *et al.,* 2005; Aligizaki *et al.,* 2006;
109 Accoroni *et al.,* 2012; Bravo *et al.,* 2012; Carnicer *et al.,* in preparation) and laboratory cultures
110 (Guerrini *et al.,* 2010; Scalco *et al.,* 2012; Vanucci *et al.,* 2012a; Vanucci *et al.,* 2012b; Pezzolesi
111 *et al.,* 2012; Bravo *et al.,* 2012). A high abundance of small cells can be attributed to an increase
112 in cell divisions (Silva and Faust, 1995) in accordance with favored conditions that stimulate
113 growth (Accoroni *et al.,* 2012). A higher abundance of small cells in a population may indicate
114 growth acceleration under certain environmental circumstances that favor a rapid proliferation.

Strains of *O.* cf. *ovata* from the Mediterranean clade produce palytoxin-like (PLTX-like) compounds, identified as putative palytoxin (pPLTX) (Ciminiello *et al.,* 2006), and 6 PLTX analogs named ovatoxins (OVTX), OVTX-a, being the major component in most cases (Ciminiello *et al.,* 2008), -b, -c, -d, -e (Ciminiello *et al.,* 2010) and -f (Ciminiello *et al.,* 2012). There is evidence of accumulation of PLTX-like compounds in seafood from the Mediterranean Sea (Aligizaki *et al.,* 2008; Aligizaki *et al.,* 2011; Amzil *et al.,* 2012; Biré *et al.,* 2013) but there is no record of human poisoning caused by consumption of contaminated seafood in this area. However, there have been many cases of human illness registered by inhalation or direct contact with cells or aerosols, as well as mass mortalities of invertebrates (reviewed in Mangialajo *et al.,* 2011). It has been observed that *O.* cf. *ovata* toxin content is inversely correlated with growth rate (Pezzolesi *et al.,* 2012; Granéli *et al.,* 2011), suggesting that under unfavorable conditions, a higher amount of toxin is produced. Both studies differ in temperatures determined for optimal growth performance, so there is no clear pattern on the possible effects that higher water temperature could have in cell toxin content, as found by Scalco *et al.,* (2012). There is no validated methodology (either assay or analytical method) for detection of PLTX-like compounds (Riobó *et al.,* 2011), but it would be necessary to determine its presence regarding future monitoring programs in coastal waters to detect possible human intoxications or marine ecosystem damage. Riobó *et al.,* 2008 described a rapid, sensitive and reliable method based on the delayed haemolytic action produced by PLTX-like compounds on mammalian red blood cells (RBCs). The specificity of the assay lies in the inhibition of toxin haemolytic effects on RBCs in the presence of ouabain, that binds to the Na^+/K^+-ATPase pump as do PLTX-like compounds (Habermann *et al.,* 1981). Analytical methods based on liquid chromatography coupled with mass spectrometry (LC-MS) have shown great potential for investigating toxin profiles, since

they allow accurate identification of known and unknown PLTX-like compounds. However, some limitations such as the lack of certified reference standards, may constrain their use as a routine method for monitoring programs (Ciminiello *et al.,* 2011). A combination of both biochemical assays, like the haemolytic assay, and instrumental analytical methods seem to be the most comprehensive strategy to assess toxicity due to PLTX-like compounds.

Studying the physiological responses of *O.* cf. *ovata* is of concern taking into consideration the potential hazard this species may represent due to the production of potent toxins. The aim of this work is on the one hand, to refine the Utermöhl method regarding sample pre-treatment for an accurate enumeration of cells of mucilage-producing microalgae like *Ostreopsis* and, on the other hand, to describe the physiological responses of *O.* cf. *ovata* strains coming from the western Mediterranean Sea that have not been studied before, under different conditions of temperature and salinity. More specifically, to determine: 1) growth performances and toxin content effects with the interaction of temperature and salinity and 2) characterization of the presence of small cells associated with growth phases and environmental conditions.

2 Materials and Methods

2.1 Ostrepsis cf. ovata cultures maintenance

Strains IRTA-SMM-11-09 and IRTA-SMM-11-10 of *O.* cf. *ovata* were isolated from macroalgae samples, *Jania rubens*, collected in the southern coast of Catalonia in August 2011 (40° 33' 15.7176" N; 0° 31' 58.242" E and 40° 50' 47.8242" N; 0° 45' 44.9532" E); both are rocky shore areas in the south and north of the Ebre Delta respectively. Cells were isolated with a glass pipette by the capillary method (Hoshaw and Rosowski, 1973) under an inverted microscope (Leica DM-IL). After an initial growth in a 24 well microplate, stock cultures were maintained in

25 cm^2 non-treated polystyrene sterile flasks (IWAKI) filled with autoclaved sterile filtered natural seawater containing a nutrient supplement of a five-fold dilution of f/2 media (Guillard, 1975) (Sigma). Salinity was adjusted to 36 by adding autoclaved MiliQ water and re-inoculations were performed every three weeks. Cultures were maintained at a constant temperature of 24°C and illumination was provided by fluorescent tubes with a photon irradiance of 100 µmol photons m^{-2} s^{-1}under 12:12-h light:dark photoperiod, which remained constant in all experimental conditions.

2.2 DNA extraction, polymerase chain reaction amplification and sequencing

The DNA extraction protocol followed Andree *et al.,* (2011). Polymerase Chain Reaction (PCR) conditions were those used in Sato *et al.,* (2011). ITS and 5.8S ribosomal RNA (rRNA) regions were obtained by using oligonucleotide primers ITSA (5'-GTAACACGGTHTCCGTAGGT-3') and ITSB (5'-AKATGCTTATRTTCAGCRGG-3'), performed in an Eppendorf™ MasterCycler Personal Thermal Cycler. Resulting fragments of rRNA were evaluated by agarose gel electrophoresis and were sent to be sequenced bidirectionally (Sistemas Genómicos, LLC; Valencia, Spain) using the same primers as those used in the initial amplification. Forward and reverse sequence reactions were aligned and manually edited using BioEdit, version 7.0.0 (Hall, T.A., 1999). Genetic distances were obtained by Kimura's two-parameter model (Kimura, 1980) with MEGA 5.1.

2.3 Subsampling and cell quantification experiment

O. cf. *ovata* produces mucilaginous aggregates difficult or impossible to disrupt even after vigorous mixing. Samples of non homogeneous cultures can lead to errors in the estimation of cell abundances. We evaluated enumeration accuracy performed by the Utermöhl method

(Utermöhl, 1931; Utermöhl, 1958). Two experiments with IRTA-SMM-11-10 strain were carried out in cultures grown in 600 mL, in 150 cm^2 non-treated polystyrene sterile flat bottom flasks (Nunc). Experiment 1 was performed in a late decaying phase culture (seven weeks, $4.0x10^3$ $cell.mL^{-1}$) in May 2012 and Experiment 2 in a late stationary phase culture (four weeks, $2.5x10^3$ $cell.mL^{-1}$) in December 2012. Six different sample volumes (0.5, 1, 3, 5, 12 and 20 mL) were taken per triplicate after vigorous shaking alterning horizontally rolling and vertical turning upside down of the sample for 100 times. Taking into consideration results of Experiment 1, samples with a volume of 0.5 and 1 mL were not used in Experiment 2. For each sample volume, two treatments were added, Na-EDTA (0.01 M final concentration) and HCl (4 mM final concentration) and then immediately fixed by adding 0.5 mL of neutral Lugol's solution per 100 mL of sample. In every case a sample without treatment was taken as a control. Each sample was settled per triplicate in counting cell chambers; 0.5 and 1 mL volume samples in a 100 µL Palmer-Maloney chamber, and the rest of the samples in a 0.5 mL Utermöhl chamber. For 20 mL volume samples an additional settlement per triplicate in 3 mL was performed in both experiments. In Experiment 2, samples with a volume of 12 mL were also settled in 3 mL. In Experiment 2 a treatment consisting of 10 seconds sonication in pulse mode with an ultrasonic processor Vibra-Cell™ (Sonics and Materials, Inc., Newton, CT, USA) was performed in all volume samples. A total of 189 settlings for Experiment 1 and 162 for Experiment 2 were analyzed. Based on Uthermöhl, 1958, the minimum number of cells counted per chamber was 100. Cell abundance per sample volume was calculated by the average from 9 settlings (3 settlings for each of the 3 samples per volume). We calculated the variability among triplicate sub-samples, calculating the difference between relative standard deviation (RSD) and Poisson distribution (λ) within the three counts. We considered high variability in enumeration when we

obtained positive results which mean that the measured error was higher compared with the expected random error based on Poisson statistics (CEN, 2006).

2.4 Multi-factorial experiment the effect of salinity and temperature on O. *cf.* ovata

We analyzed cell growth, size and toxicity in the two *O.* cf. *ovata* strains exposed to nine different conditions, combining three temperatures (19, 24 and 28°C) and three salinities (32, 36 and 38). Acclimatization period lasted one year in temperature regulated culture rooms. Cells were grown in 50 mL culture volume in 25 cm^2 non-treated polystyrene sterile flashes (IWAKI).

2.4.1 Cell growth

Multi-factorial experiments were performed in triplicate, in a controlled environment chamber (IBERCEX, LTD) in 650 mL volume cultures in 150 cm^2 non-treated polystyrene sterile flat bottom flasks (Nunc). Experimental cultures (in triplicate for each condition) were inoculated from late exponential phase cells and initial concentration was between 100 and 150 $cell.mL^{-1}$ for cultures at 28ºC, and between 50 and 100 $cell.mL^{-1}$ for cultures at 19ºC and 24ºC because cell concentration in the stock culture was lower. Cultures remained under experimental conditions for sixteen days. To determine an accurate growth curve, based on our previous experimental results, samples were taken per triplicate every 2-3 days. In the exponential phase, 5 mL volume samples were settled in 0.5 mL chamber per triplicate. In the stationary phase, samples had a volume of 10 mL and were treated with Na-EDTA at a final concentration of 0.01 M. Settling was performed in 3 mL chamber per triplicate. Cell abundance was obtained by calculating the average of three subsamples settled thrice from three cultures; twenty seven per condition and day, a total of 3888 settlings were analyzed. Average cell abundances are expressed by mean ± standard deviation (SD). The total culture volume removed from each flask at the end of the

227 experiment due to sampling did not surpass 30% of the total culture volume to interfere as little
228 as possible in cell growth. Growth rate (y, div.day^{-1}) was calculated using the following
229 equation:

$$y = \frac{\ln N1 - \ln N0}{t1 - t0}$$

230 where N0 and N1 are cell abundances at time t0 (day 3) and t1 (day 9), coinciding with the
231 exponential phase. We did not include growth from the two first days considering the latency
232 phase. For the 19°C treatments, t1 was day 9 and t2 was day 16 according to the growth pattern.

233 *2.4.2 Cell size*

234 We selected one culture for each condition and strain to measure cell size. A minimum of 40
235 cells were analyzed every 2-3 days along the growth curve. Dorso-ventral (DV) and width (W)
236 diameters were measured using an image capture system (Analysis) with a Olympus DP70
237 camera connected to a Nikon Eclipse TE2000-S inverted microscope at 400x magnification. Cell
238 dimensions were expressed by mean ± SD.

239 *2.4.3 Toxicity*

240 Toxin content was analyzed for 24 and 28°C temperature conditions. Three cultures of both *O.*
241 cf. *ovata* strains were grown in parallel under the same multi-factorial conditions. Cultures were
242 grown in 200 mL non-treated polystyrene sterile flasks (Thermo) inoculated from the same
243 initial acclimatized stock culture as for the multi-factorial experimental cultures. Cells were
244 collected at the late exponential phase (12 days), stationary phase (21 days) and during decaying
245 phase (28 days). Samples of 10 mL were taken and settled per triplicate in 3 mL Utermöhl

chambers. Samples from stationary and decaying phase were treated with Na-EDTA before fixation.

2.4.3.1 Toxin extraction

Cells were collected by filtration on 0.45 µm nylon filters and stored at -80°C. For toxin extraction, 5 mL methanol/water (80:20) solution was added to filters and these were sonicated for 35 minutes in pulse mode. The mixture was centrifuged at 2000 g for 10 minutes; the supernatant was decanted and filtered using 0.45 µm polytetrafluoroethylene membrane syringe filters. This procedure was repeated tree times and filtered supernatants were pooled. The final extract was evaporated and made up to a final volume of 10 mL.

2.4.3.2 Haemolytic assay

Haemolytic test of *O.* cf. *ovata* strains was analyzed following the method of Riobó et al, (2008) with slight modifications regarding concentration of reagents in order to adjust the working range and calibration curve. Heamoglobin released in presence of PLTX-like compounds after cell lysis, is quantified by a microplate Reader KC4 from BIO-TEK Instruments, Inc. (Vermont) at 405 nm absorbance. A calibration curve was done by using PLTX standard (Wako Chemicals GmbH, Germany) with 12 concentrations from 12.5 to 1250 $pg.mL^{-1}$ adjusted to an exponential regression using SigmaPlot 9.0. Working solution was prepared with washed sheep blood (OXOID), centrifuged (4000 g, 10°C, 10 min) twice and diluted with phosphate buffered saline solution (PBS) 0.01 M, pH 7.4 (Sigma), 0.1% bovine serum albumin (BSA), 1 mM calcium chloride ($CaCl_2$ $2H_2O$) and 1 mM boric acid (H_3BO_3) to a final concentration of 1.5 x 10^6 $cells.mL^{-1}$. The assay for PLTX specificity was verified by a blank assay with ouabain (2 mM final concentration). Toxin extracts and PLTX standard were evaporated and refilled with PBS

268 solution to eliminate methanol and water from the extraction. The assay was performed in two
269 non-treated 96 well microplates and samples were analyzed in triplicate. After 22 hours
270 incubation at 24°C, microplates were centrifuged (416 g, 10 min), 200 µL of the supernatant was
271 transferred to another microplate for absorbance reading. Total toxicity was expressed as
272 palytoxin equivalents per cell (pg PLTX eq.cell^{-1}) related to the number of cells contained in
273 culture.

274 *2.4.3.3 Toxin profile analysis by liquid chromatography–high resolution mass spectrometry*
275 *(LC-HRMS).*

276 From the extracts used in the haemolytic assay to quantify toxin content, we selected those
277 collected in the decaying phase (28 days) to analyze their toxin profile by liquid chromatography
278 – electrospray ionization – high resolution mass spectrometry (LC-ESI-HRMS) in both strains.
279 The analyses were performed on a hybrid linear ion trap LTQ Orbitrap XL Fourier transform
280 mass spectrometer (FTMS) equipped with an ESI ION MAX^{TM} source (Thermo Fisher, San
281 José, USA) coupled to an Agilent 1100 LC binary system (Palo Alto, CA, USA). Organic
282 solvents (HPLC grade quality) and glacial acetic acid used in the LC-MS analysis were
283 purchased from Carlo Erba (Milan, Italy), The analytical method was previously described in
284 Ciminiello *et al.,* 2010. A 3µm Gemini C18 column (150×2.00 mm; Phenomenex, Torrance, CA,
285 USA) was eluted at 0.2 mL/min with water (eluent A) and 95% acetonitrile/water (eluent B),
286 both containing 30 mM acetic acid (control conditions). A gradient elution (20–50% B over 20
287 min, 50–80% B over 10 min, 80–100% B in 1 min, and hold 5 min) was used. Injection volume
288 was 5 µl.

289 Palytoxin standard was dissolved in methanol/water (1:1, vol/vol) to a concentration of 1µg.mL^{-1}
290 . Strain OOAN0601 from the Adriatic Sea (Pezzolesi *et al.,* 2012) was used as reference to
291 check for retention times and ionization behavior of OVTX-a to -e.
292 HR full MS experiments (positive ionization) were acquired in the range of *m/z* 700-1400. The
293 following source settings were used: spray voltage = 4.8 (Source Voltage (kV): 4.80); capillary
294 temperature = 290 ºC; capillary voltage = 50 V; sheath gas flow = 32 and auxiliary gas flow = 4
295 (arbitrary units); tube lens voltage = 130 V. Resolving power was set at 60,000 (FWHM at 400
296 *m/z*).
297 Calculation of elemental formulae was performed on the mono-isotopic peak of the most intense
298 bi-charged ($[M+2H-H_2O]^{2+}$) and tri-charged ($[M+H+Ca]^{3+}$) ions, and the isotopic patter of each
299 ion cluster was taken into consideration for identification purposes. The tuning, control, data
300 acquisition and data analysis were done with Xcalibur® software v2.0.7.

301 *2.7 Data analysis*

302 Variation in cell abundance estimations among treatments, temperature and salinity effects on
303 specific growth rates and cell DV diameter, as well as PLTX eq content in different growth
304 phases were statistically studied by the analysis of variance (ANOVA). Results are reported as
305 follow: F(degrees of freedom) =F-value, *MSE*= mean-square error, p-value). For significant
306 differences (p<0.05), a multiple comparison Tukey's HSD test was performed. Pearson's
307 correlation test was computed to assess the relationship between growth rate and cell DV
308 diameter. To perform statistical analysis we used the software package IBM SPSS Statistics.

3 Results

3.1 Molecular biology

The *Ostreopsis* strains IRTA-SMM-11-09 and IRTA-SMM-11-10 were taxonomically identified based on ITS and 5.8S regions of the rRNA genes. A phylogenetic analysis was performed and demonstrated both strains group within the species *O.* cf. *ovata,* being part of the Mediterranean and West Atlantic clade.

3.2 sample sampling method

Mucilaginous matrix was present in both experiments. Post-hoc Tukey's HSD test showed that an underestimation in the number of cells ($1.81\pm0.76\text{x}10^{6}$cells.mL^{-1}) was significant ($p<0.001$) when counting was performed in 0.5 and 1 mL volume samples compared to the average cell abundance calculated with the other sample volumes ($4.57\pm0.66\text{x}10^{6}$ cells.mL^{-1}). For control and HCl treated samples we obtained high variation in cell counting within triplicates of settling enumerations, seven out of fifteen had negative results in the difference between RSD and λ (Table 1).The average of subsample triplicates for 0.5 mL settling volume was negative for sample volumes 3, 5 and 20 mL. In samples treated with Na-EDTA, negative results for settling triplicates were less abundant, and only two out of fifteen were negative. In Experiment 2, the culture contained $2.52\pm0.34\text{x}10^{6}$ cells.mL^{-1}, and 162 settlements were performed for cell counting. Cell enumeration was more accurate for all treatments and control; five out of fifty four replicates were negative in total (Table 1). Broken cells were found in sonicated samples, thus we decided not to include these results for cell abundance estimations in our analyses.

Abundance cell estimation in Experiment 1 was significantly different considering sample volume ($F(4)=9.4$ $MSE=2.19\text{x}10^{12}$; $p<0.001$), settling volume ($F(1)=19.3$ $MSE=4.51\text{x}10^{12}$;

$p<0.001$), and treatment ($F(2)=11.4$ $MSE=2.68\text{x}10^{12}$; $p<0.001$). For Experiment 2, abundance cell estimation was significantly different for sample volume ($F(3)=5.3$ $MSE=5.31\text{x}10^{11}$; $p<0.01$) and settlement volume ($F(1)=11.7$ $MSE=1.16\text{x}10^{12}$; $p<0.001$) but not according to treatment.

3.3 Cell growth, cell abundances and growth rate

Cell growth was observed for all multi-factorial experimental conditions. At 24 and 28°C a typical growth curve was obtained with differentiation between exponential and stationary phases as early as the seventh day. At 19°C, this trend was not observed, and stationary phase was not achieved (Figure 1). Maximal cell abundances at the end of the experiment were 9.48±2.20 x 10^3 cells mL^{-1} (28ºC; salinity 36) and 3.97±0.55 x 10^3 cells mL^{-1} (24°C, salinity 38) for IRTA-SMM-11-10 and IRTA-SMM-11-09 respectively. The lowest maximal cell abundances were found at 19ºC; 0.71±0.11 x 10^3 cells mL^{-1} for IRTA-SMM-11-10 at salinity 38. Maximal growth rate was found in IRTA-SMM-11-10 at 28°C, salinity 36 (0.61±0.05 $div.day^{-1}$). During the exponential phase, IRTA-SMM-11-10 presented a significant ($F(1)=36.2$; $MSE=0.017$; $p<0.001$) higher average growth rate, 0.38±0.17 $div.day^{-1}$ comparing with IRTA-SMM-11-09, 0.34±0.14 $div.day^{-1}$. Experimental conditions significantly influenced growth rates: temperature ($F(2)=1014.7$; $MSE=0.485$; $p<0.001$), salinity ($F(2)=85.7$; $MSE=0.041$; $p<0.001$) and the interaction of both ($F(4)=50.6$ $MSE=0.024$; $p<0.001$). At 28ºC, the highest growth rates were found at salinity 36, significantly different from the rest of salinities for both strains (Tukey test; $p<0.005$). At 24°C, growth rate was more stable between salinities, and ranged from 0.39±0.01 to 0.54±0.03 $div.day^{-1}$. The lowest growth rate was registered at 19°C (0.17±0.02 $div.day^{-1}$) and little variability was obtained for growth rates among salinities and strains, being significantly different from to the rest of temperatures (Tukey test, $p<0.001$) (Figure 2).

353 *3.4 Cell size*

354 Presence of cysts and aberrant cell shapes were observed at 19°C in all growth phases (Figure 3a)
355 and therefore it was difficult to recognize cell shapes to perform correct measurements.
356 Consequently we decided not to include cells measurements from 19°C cultures in the cell size
357 analysis. Average cell size was 38.40 ±9.03 in DV and 29.61±8.38 in W (n=3863). A variability
358 of cell dimensions was found in all experimental conditions that ranged from 14.34 to 62.03 µm
359 for the DV diameter, and from 14.27 to 44.73 µm for the W diameter, both found at 24°C,
360 salinity 36 in IRTA-SMM-11-09. We observed that cultured cells were rounded (Figure 3b)
361 rather than tear-drop shaped *O.* cf. *ovata,* as found in field samples (Figure 3c). In addition, a
362 difficulty can arise from the position of the cell in the counting chamber. It is sometimes difficult
363 to determine whether cells are in a planar orientation which may lead to false cell dimensions
364 being obtained. We chose the DV diameter as a representative feature to study cell dimensions.
365 Based on a DV diameter/frequency distribution histogram dividing DV diameter every 1 µm
366 (Figure 4), two different sizes of cells were distinguished, a group of small cells (DV≤35 µm;
367 *DV mean*=28.64±3.78 µm; *W mean*= 21.20±3.99 µm; n=1474) and another composed by large
368 cells (DV>35 µm; *DV mean*=44.43±5.29 µm; *W mean*=34.81±5.77 µm; n=2389) (Figure 3d). An
369 increase in the number of small cells during the exponential phase was observed, more evident at
370 24°C (Figure 5). This observation is more visible if the first day of sampling is not considered, as
371 we should take into account that cell size corresponds to a character of the cells from a late
372 exponential phase stock culture that was used as a source of inoculums. Small cells are more
373 abundant when growth rate is higher. The smallest average DV diameter was found for IRTA-
374 SMM-11-10 at 28°C, salinity 36 (31.61±6.02 µm) that corresponds with the highest growth rate.
375 The DV diameter was negatively correlated ($r= -0.785$; $n=12$; $p<0.01$) with growth rate.

Significant differences regarding the average DV diameter were found for different conditions temperature ($F(2)=66.5$; $MSE=3695.21$; $p<0.001$), salinity ($F(2)=45.2$; $MSE=2511.1$; $p<0.001$) and the interaction of both ($F(4)=80.1$; $MSE=4454.7$; $p<0.001$).

3.5 Cell toxicity and toxin profile

Toxin content was quantified for samples at 24 and 28°C as they had typical growth trends and marked differentiation between exponential and stationary phases. In addition, *O.* cf. *ovata* in the field is not observed at 19°C in the area where these were isolated, thus blooms at this temperatures do not occur. Using the haemolytic test, we calculated PLTX-like content between $\%H_{20}$ and $\%H_{60}$ obtained in the calibration curve, according to the equation: $y=0.0153e^{0.064x}$ ($R^2=$ 0.96). In the presence of ouabain, a non-specific haemolytic activity was registered for the highest standard concentration but it was lower than $\%H_7$ and did not interfere in the haemolysis specific response (see Figure 1 in Sup. Materials).

Haemolytic activity was registered in all analyzed samples. PLTX-like content increased significantly ($F(2)=491.45$; $MSE=29993$; $p<0.001$) with time for both strains and for all conditions. For IRTA-SMM-11-09 at 28°C, with salinity 38, elevated PLTX-like content was detected at the end of the exponential phase compared to the decaying phase (Figure 6). At 24°C, PLTX-like content increased significantly from the end of the stationary phase to the decaying phase (Tukey test) while at 28°C, a significant increase occurred from the end of the exponential phase to the end of stationary phase (Tukey test). No significant differences were found in PLTX-like content for both strains between different temperature and salinity conditions, being slightly lower at 24°C and salinity 32. No significant correlation was found between PLTX-like content and cell size. PLTX-like concentrations ranged from 7.60±0.60 pg PLTX eq.cell^{-1} (late

398 exponential phase, 24°C, salinity 32, IRTA-SMM-11-10) to 104.5±4.91 pg PLTX eq.cell^{-1}
399 (decaying phase; 24°C, salinity 36, IRTA-SMM-11-09).
400 The study of the toxin profile of the cultures harvested in the decaying phase revealed that
401 pPLTX and OVTX-a, -b, -c and –d&-e were present in all the extracts; their relative abundance
402 was practically the same in both the *O.* cf. *ovata* strains (IRTA-SMM-11-09 and IRTA-SMM-
403 11-10) and did not vary depending on either temperature or salinity (Figure 7). OVTX-a always
404 represented almost 60% of the total toxin content, and pPLTX was the minor toxin component,
405 accounting for less than 1% of the total PLTX-like compounds in the extracts. Ovatoxin-b
406 accounted for 30% of the total toxin content, while OVTX-c represented 4%. Ovatoxins-d and –e
407 are isomers and could not be fully separated by chromatographic means, thus their quantitation
408 was made as a sum of both compounds, which accounted for about 9%.
409 The identification of pPLTX and OVTX-a to -e in the extract was supported by the comparison
410 of retention times and full HRMS spectra with those obtained under the same experimental
411 conditions for a reference sample of *O.* cf. *ovata* from the Adriatic Sea previously characterized
412 (Pezzolesi *et al.,* 2012); ionization behavior of individual toxins, isotopic patterns, and elemental
413 formulae assigned to mono-isotopic ion peaks in full MS spectra were consistent with those
414 reported for OVTXs and pPLTX by Ciminiello *et al.,* 2010 (see Table S1 in Sup. Materials).

415 **4 Discussion**

416 *4.1 Counting methodology*

417 During *Ostreopsis* blooms in Mediterranean coasts, a brownish mucilage covering different
418 substrates such as macrophytes and rocks, has been observed (e.g. Vila *et al.,* 2001; Totti *et al.,*
419 2010; Aligizaki *et al.,* 2006; Mangialajo *et al.,* 2008). This mucilage plays an important role on

epi-benthic microalgae ecology, providing attachment to the substrate (Vidyaranthna and Granéli, 2013), working as a micropredation mechanism that traps small organisms (Barone, 2007), or as a protective coat (Bravo *et al.,* 2012). This mucilage is composed of acid polysaccharides and trichocysts sticking together (Honsell *et al.,* 2013). The formation of cell aggregates embedded in mucilage impedes the accurate estimations of cell abundance. Some studies have employed different strategies adding HCl or Na-EDTA to samples in order to obtain more accurate cell abundance estimations in their growth curves. Guerrini *et al* (2010) and Pezzolesi *et al* (2012) performed batch cultures inoculated with the same initial cell concentrations from a stock culture. Every 2-3 days two cultures were treated with HCl for counting and discarded afterwards. Scalco *et al.,* (2012), followed a similar methodology adding a solution of Na-EDTA. Vanucci *et al* (2012b) and Monti *et al* (2012) added solutions of HCl and Na-EDTA respectively to samples taken from the same culture every 2-3 days. Treatments with HCl and Na-EDTA can minimize ionic interactions produced in the mucilage that could help to disaggregate cells in culture (Allgredge *et al.,* 1993). In order to evaluate this fact, we compared cell enumeration variability obtained in samples treated with HCl or Na-EDTA. We decided to analyze sampling strategy considering the fact that inoculations from the same stock culture may contain cell aggregates that can lead to a different initial cell concentration among parallel cultures. In our study, we included sample and settling volumes as supplementary factors involved in accuracy of cell abundance estimations. Sample and settling volumes vary among studies; in some studies 1 mL (Scalco *et al.,* 2012; Monti *et al.,* 2012), or 5 mL (Nascimento *et al.,* 2012a), were used but both were settled in a 1 mL chamber, while in others 50-250 mL were used (Vanucci *et al* 2012b) with no specification in settlement volume. In the experiment performed in the decaying phase, cell enumeration from 0.5 and 1 mL sample volumes was

443 significantly lower than in other volumes. This result may be due to the large cell size of *O.* cf.
444 *ovata* for a Palmer-Maloney chamber. Another reason may be that cells stuck to the inside walls
445 of the pipette tip during pipetting for settlement while in bigger chambers settling is done
446 directly, and this reduces cell losses. Less error was obtained in counting performed in 3 mL
447 chambers for both treatments and control, showing that bigger settling volumes, and thus bigger
448 sample volumes, are more suitable to estimate *O.* cf. *ovata* cell concentration. Cell abundance
449 estimation in Na-EDTA treated samples was more accurate than in control and HCl treated
450 samples, suggesting a better aggregate disruption with Na-EDTA. In Experiment 2, less error
451 was registered in all cases meaning that in cultures where cell concentration is lower, no need of
452 treatment is required to obtain better cell abundance estimation.
453 Other ways of determining *O.* cf. *ovata* growth curves have to be cited. Granéli *et al* (2011)
454 performed cultures in 8 mL Petri dishes and cell enumeration was done directly in alive cells.
455 Chlorophyll a (chl. a) content has been used recently (Vyatathna and Granéli, 2011; Vyatathna
456 and Granéli, 2013; Tanimoto *et al.,* 2013; Yamaguchi *et al.,* 2012b) and constitutes a rapid and
457 simple method for cell abundance estimation. Yamaguchi *et al* (2012a) found a significantly
458 correlation with chlorophyll a fluorescence measurements and cell abundances in different
459 *Ostreopsis* spp strains. Nevertheless, fluorescence techniques have to be considered carefully
460 when performing growth rate curves as advised by Raven and Beardall (2006), and Kruskopf and
461 Flynn (2006), because of changes in fluorescence per cell under different nutrient condition
462 and/or daily cycle.
463 From our results, we suggest to use no treatment in samples obtained during the exponential
464 phase as cell aggregates are less abundant. Addition of Na-EDTA to samples is recommended
465 starting at stationary phase when mucilage production is high.

4.2 Growth performance under different temperature and salinity conditions

We performed a multi-factorial experiment combining different water temperatures (19, 24 and 28°C) and salinities (32, 36, 38) and measured responses in growth, cell size and toxicity in two *O.* cf. *ovata* strains isolated from the western Mediterranean Sea, and for which their physiology had not been studied before. Both strains presented growth in all experimental conditions, although at 19°C growth rate was lower. This is in agreement with other laboratory studies where *O.* cf. *ovata* from Mediterranean clade (Pezzolesi *et al.,* 2012) and from Japan (Yamaguchi *et al* 2012b) grew in a wide range of temperatures and salinities. Presence of *O.* cf. *ovata* has been reported by other authors in different regions of the world presenting a wide spectrum of water temperature and salinity conditions (Pistocchi *et al.,* 2011 and references herein). This growth tolerance could explain why *O.* cf. *ovata* is capable of inhabiting both tropical and temperate areas and can be adapt to highly variable environments in coastal waters (Tanimoto *et al.,* 2012). Growth curves obtained at 24 and 28°C followed the same pattern as other *O.* cf. *ovata* strains from the Mediterranean Sea (Pezzolesi *et al.,* 2012; Guerrini *et al.,* 2010; Vanucci *et al.,* 2012a; Vanucci *et al* 2012b), characterized by a rapid exponential phase during the first week.

Water temperature is considered the most important factor that affects growth of benthic dinoflagellates (Pistocchi *et al.,* 2011; Mangialajo *et al.,* 2011; Parsons *et al.,* 2012). Different optimal temperatures for the growth of *O.* cf. *ovata* from the Mediterranean Sea have been proposed from laboratory studies. Adriatic strains have presented high growth performance at 30°C, with a growth rate of 0.74±0.1 div.day^{-1}(Granéli *et al.,* 2011), while Tyrrhenian strains have shown optimal temperature of growth at 20°C, 0.49 div.day^{-1}(Pezzolesi *et al.,* 2012). However, Scalco *et al.,* (2012) studied strains from both Seas under the same conditions without finding differences in their optimal growth temperatures that ranged between 22 and 26°C, with

489 growth rates higher than 0.6 div.day^{-1}for both temperatures. Optimal growth rates from our
490 strains were situated within the range of 0.61±0.05 to 0.51±0.01 div.day^{-1} at 28°C and 24°C
491 respectively, which are in accordance with the rates mentioned before. However, in Nascimento
492 *et al.,* (2012a), *O.* cf. *ovata* from Brazilian waters grown at 24°C, achieved much lower growth
493 rates, 0.22 div.day^{-1}. By contrast, in a *O.* cf. *ovata* strain from Japan, Vidyarathna et Granéli,
494 (2011) and Yamaguchi *et al.,* (2012) found growth rates higher than those found in
495 Mediterranean strains, 1.03±0.03 day^{-1} between 25 and 30°C. Those results are in agreement with
496 field temperatures where cells were isolated, reflecting that populations from diverse
497 environments may present different optimal temperatures for growth. Nevertheless, those data
498 have to be analyzed with caution taking into account possible differences on cell culture
499 characteristics and counting methodology used in each study. Culture volume, recipient material,
500 initial cell concentration, acclimation period and medium components, among others, can affect
501 growth performances (Andersen, 2005).
502 Influence of salinity on cell growth in *O.* cf. *ovata* is not as well studied and conclusions about
503 its effects are not as robust (Pistocchi *et al.,* 2011; Parsons *et al.,* 2012). Blooms of *O.* cf. *ovata*
504 in Mediterranean waters occur normally between June and November when salinity values are
505 higher than 37 on average. This is in agreement with results found in Pezolessi *et al.,* 2011 where
506 maximal growth rates were obtained at salinities between 36 and 40. In addition, there is no
507 presence of cells in waters under direct influence of rivers (Pistocchi *et al.,* 2011), indicating that
508 this species does not grow in areas where salinity drops below 20 (Yamaguchi *et al.,* 2012b). We
509 observed that our strains were tolerant to salinities between 32 and 38 but different growth
510 performances were observed depending on temperature. Tanimoto *et al.,* (2013) provided the
511 first evidence for significant effects of temperature, salinity and their interaction on the growth of

two *Ostreopsis* strains. Average water temperature where our strains were isolated is 25.00±1.58°C and salinity 37.15±0.87 during the bloom period from 2011 to 2013, measured weekly (data not shown). Temperatures and salinities varied, exceeding 26°C during 23% of time and 37 during 53% of the time, respectively. In our multi-factorial experiment, where cells were acclimated for one year to experimental conditions, we found that at 24°C, growth rate was more uniform among salinities, while at 28°C, growth was significantly higher at salinity 36 than at salinity 38. We hypothesize that for short periods of time, as it happens during blooms, growth is stimulated by a rapid temperature increase and salinity does not play a crucial role in growth. In accordance with references cited above, temperature would be the predominant environmental factor that influences bloom formation. However, from our laboratory results, we suggest that for long periods of acclimation to high temperatures, salinity could be a limiting factor for growth. An exposure to higher temperatures and salinities is a possible scenario according to climate change predictions in the Mediterranean Sea (IPCC, 2013). We suggest that such an occurrence may not enhance *O.* cf. *ovata* bloom formation, although it may increment bloom duration. Nevertheless, the response of marine communities to warming is difficult to predict as many environmental factors are involved and are not possible to control in a laboratory setting. Experimental results obtained in our multi-factorial study cannot be directly extrapolated to future natural conditions.

4.3 Cell size

Cells in culture had a more rounded morphology and were smaller than field cells from the area where they had been isolated as reported in other studies (Aligizaki et al, 2006; Accoroni et al, 2012; Nascimento et al 2012a; Laza-Martinez et al, 2011; David et at, 2013). A relevant

heterogeneity in *O.* cf. *ovata* morphology has been observed, distinguishing two different cell types not overlapping in size. This representative diversity of *O.* cf. *ovata* population morphology has been detected both in field samples (Penna *et al.,* 2005; Aligizaki *et al.,* 2006; Accoroni *et al.,* 2012; Bravo *et al.,* 2012; Nascimento *et al.,* 2012b; David *et al.,* 2013; Carnicer et al, in preparation) and in cultures (Guerrini *et al.,* 2010; Scalco *et al.,* 2012; Vanucci *et al.,* 2012a; Vanucci *et al.,* 2012b; Pezzolesi *et al.,* 2012; Bravo *et al.,* 2012). Silva and Faust (1995), hypothesized that small cells, could be either gametes or vegetative cells that perform rapid divisions resulting in a rapid increase of cell populations. Nevertheless, Bravo et al (2012), questioned the explanation of small cells being gametes as they identified gametes from all sizes. Accoroni *et al.,* (2012) suggested that cell size could be related with bloom phases. In Scalco *et al.,* (2012), small cells with DV diameters below 20 µm were considered small while we defined small cells for DV diameters down to 35 µm. A significant positive correlation between the percentage of large cells and growth rate was found in the former study, but as cell size ranges were determined differently, an overlap in cell size with our study could have been produced and comparisons may not be consistent. In our study, at 24 and 28°C, in general, the number of small cells increased from early to late exponential phase. High amounts of small cells during the exponential growth phase are significantly correlated with high growth rates. This is in agreement with the approach that small cells can act as vegetative cells that rapidly divide. In our experiments, at 19°C, the majority of cells were morphologically deformed from the beginning of the growth curve while at 24 and 28°C, the percentage of anomalous cells increased with time. This is in accordance with results in Scalco *et al.,* (2012), where it was observed the presence of cells of different sizes at 22, 26 and 30°C but not at 18°C where the percentage of anomalous cells increased. The appearance of these cells has been attributed with non optimal conditions of

growth (Bravo *et al.,* 2012) and more specifically at the end of stationary phase (Aligizaki *et al.,* 2008; Guerrini *et al.,* 2010, Accoroni *et al.,* 2012). A possible additional explanation is the genes responsible for cell size, or their protein products may be temperature sensitive in some way, but such an explanation requires deep investigations. Seasonal variations of *O.* cf. *ovata* have been reported by numerous field observations in Mediterranean waters (reviewed in Pistocchi *et al.,* 2011), populations not being observed from around late fall to early summer. Since aberrant cells with granulated cytoplasm can constitute the precursors of cyst formation described as described previously, these forms could represent the overwinter populations (Bravo *et al.,* 2012).

4.4 Toxicity

Under all tested conditions, the estimation of PLTX-like compounds per cell increased from late exponential phase to decaying phase. These results are in agreement with other studies on toxin content of *O.* cf. *ovata* strains from the Mediterranean area (Vanucci *et al.,* 2012a; Vanucci *et al.,* 2012b; Scalco *et al.,* 2012; Pezzolesi *et al.,* 2012; Guerrini *et al.,* 2010) and from Japan (Granéli et al, 2011; Vidyarathna and Granéli, 2011; Vidyarathna and Granéli, 2013). A similar response has been observed also in other phytoplankton species (Bates, 1998; Grzebyk, *et al.,* 2003) and it has been related to the fact that toxins are secondary metabolites that probably accumulate in cells after growth. The only exception was found in *Ostreopsis* cf. *ovata* strains from Brazilian waters that belong to the same Mediterranean/Atlantic clade, which did not follow this trend in toxin content progress over time (Nascimento *et al.,* 2012a).

It is not clear which are the environmental conditions that favor toxin production, though a negative correlation with PLTX-like content and growth in *O.* cf. *ovata* has been observed (Pezzolesi *et al.,* 2012; Granéli *et al.,* 2010 and references herein; Vidyarathna and Granéli,

2011; Guerrini et al, 2010). Our PLTX-like content study was focused on tolerable temperature growth conditions which limited the range of temperatures tested, and no correlation between toxin content and growth in our strains was observed. At 24°C, an increase in PLTX-like production occurred during the late stationary phase, while at 28°C, it occurred in the early stationary phase. The mechanisms that take place in the biosynthesis of PLTX-like components is still unknown. From our results we hypothesize that gene transcription related with toxin production could be increased at higher temperatures independently of growth rate.

Toxin profiles of the two analyzed *O.* cf. *ovata* strains (IRTA-SMM-11-09 and IRTA-SMM-11-10) were almost identical, and relative abundance of individual toxins was not affected by temperature and/or salinity: OVTX-a dominated the profile (about 60%, Figure 8), and OVTX-b, -c and –d&-e represented around 40% of total toxin content. Putative PLTX was the least abundant compound in all the analyzed samples and accounted for less than 1%. Such a toxin profile is similar to that reported for most of the Mediterranean strains reported so far (Ciminiello *et al.,* 2010; Pezzolesi *et al.,* 2012; Scalco *et al.,* 2012; Vanucci *et al.,* 2012a; Accoroni *et al.,* 2011; Sechet *et al.,* 2012), in which OVTX-a is the major toxin produced. In both the *O.* cf. *ovata* strains that were analyzed, OVTX-f was not detected; this PLTX-like compound represented the major component (50% of the total toxin content) of an Adriatic strain producing all the ovatoxins described so far, including OVTX-a (23%), OVTX-b (17%), OVTX-c (2.4%), OVTX-d+e (6.7%) and pPLTX (0.3%) (Ciminiello *et al.,* 2012). *O.* cf. *ovata* from other geographical origins have different toxin compositions as well. Brazilian strains had approximately the same amount of OVTX-a and -b (Nascimento *et al.,* 2012a). In several Japanese strains, new OVTX isomers were identified (Suzuki *et al.,* 2012), as well as Ostreol A was structurally elucidated in strains isolated from Jeju Island in Korea (Hwang *et al.,* 2013).

Differences in toxin profile occurred not only among species but also among strains belonging to the same genetic clade. This physiological feature represents an additional factor that contributes to the characterization of *O.* cf. *ovata* geographical distribution (Penna *et al.,* 2005).

According to the haemolytic assay, total toxicity reached its maximum at the decaying phase for both strains and all conditions (except for one single case, IRTA-SMM-11-09 at temperature 28º and salinity 38). Therefore, we selected these samples to obtain the best accuracy in the toxin profile analysis (García-Altares et al. 2014, in preparation).

5 Conclusions

In our experiment we found that big sample and settlement volumes seem to improve accuracy in cell abundance estimations, as well as the addition of Na-EDTA to samples to help disrupt aggregates in *O.* cf. *ovata* cultures, and thus, obtain a higher homogeneity. Different strategies to calculate the number of cells in cultures have been reported in different studies. This fact can lead to errors when comparing growth rates or toxin content per cell. A similar methodology for estimation of cell abundance and culturing may help to obtain more reliable conclusions between comparisons among different strain studies performed around the world.

It was demonstrated *O.* cf. *ovata* from the north western Mediterranean Sea is tolerant to a wide range of temperatures and salinities, in agreement with other strains which could explain the colonization of widely different climates and regions. The optimal growth temperatures for strains could differ depending on the environmental conditions of their origin. Growth rate is enhanced at high temperatures though a growth inhibition at salinities 32 and 38 was observed at 28°C. Variation in salinity values may act as a limiting factor in high temperature conditions such as is predicted for the coming years.

624 Small cells may be a result of an acceleration of cell division, as we found a correlation between
625 growth rate and an increase in the amount of this group of cells. The question whether these cells
626 act as gametes or vegetative cells is still unsolved.
627 An increase of toxin content with time was observed throughout the growth phases. We cannot
628 draw conclusions about the effect of environmental conditions on toxicity, though we raise the
629 hypothesis that the synthesis of PLTX-like toxins may increase at high temperatures
630 independently of growth. Toxin profiles did not change with different conditions of temperature,
631 or salinity, and it was similar to the majority found in the Mediterranean clade, representing a
632 characteristic feature of this clade.
633 From our results, a simultaneous increase on sea water temperature and salinity, as predicted in
634 global warming projections for the Mediterranean may not result in higher intensity of *O.* cf.
635 *ovata* bloom formations, though it might enhance their toxicity.

636 *Acknowledgements*

637 We thank Marta Biarnau, Idoia Remón and Jerome Massebiau for their help in the laboratory
638 work. This work has been funded by EU Seventh Framework Programme through the project
639 583 "ECsafeSEAFOOD, grant agreement Nº: 311820 (http://www.ecsafeseafood.eu/). María
640 García-Altares acknowledges the pre-doctoral FPI-INIA nº 27 (2010) scholarship.

641 *References*

642 Accoroni, S., Romagnoli, T., Pichierri, S., Colombo, F., Totti, C., 2012. Morphometric analysis
643 of Ostreopsis cf. ovata cells in relation to environmental conditions and bloom phases.
644 Harmful Algae 19, 15-22.

645 Accoroni, S., Romagnoli, T., Colombo, F., Pennesi, C., Di Camillo, C.G., Marini, M., Battocchi,
646 C., Ciminiello, P., Dell'Aversano, C., Dello Iacovo, E., Fattorusso, E., Tartaglione, L., Penna,
647 A., Totti, C., 2011. Ostreopsis cf. ovata bloom in the northern Adriatic Sea during summer
648 2009: Ecology, molecular characterization and toxin profile. Marine Pollution Bulletin 62,
649 2512-2519.
650 Aligizaki, K., Katikou, P., Milandri, A., Diogène, J., 2011. Occurrence of palytoxin-group toxins
651 in seafood and future strategies to complement the present state of the art. Toxicon 57, 390-
652 399.
653 Aligizaki, K., Katikou, P., Nikolaidis, G., Panou, A., 2008. First episode of shellfish
654 contamination by palytoxin-like compounds from Ostreopsis species (Aegean Sea, Greece).
655 Toxicon 51, 418-427.
656 Aligizaki, K., Nikolaidis, G., 2006. The presence of the potentially toxic genera Ostreopsis and
657 Coolia (Dinophyceae) in the North Aegean Sea, Greece. Harmful Algae 5, 717-730.
658 Alldredge, A.L., Passow, U., Logan, B.E., 1993. The Abundance and Significance of a Class of
659 Large, Transparent Organic Particles in the Ocean. Deep-Sea Research Part I-Oceanographic
660 Research Papers 40, 1131-1140.
661 Amzil, Z., Sibat, M., Chomerat, N., Grossel, H., Marco-Miralles, F., Lemee, R., Nezan, E.,
662 Sechet, V., 2012. Ovatoxin-a and Palytoxin Accumulation in Seafood in Relation to
663 Ostreopsis cf. ovata Blooms on the French Mediterranean Coast. Marine Drugs 10, 477-496.
664 Andersen, R.A., 2005, Algal Culturing Techniques. Elsevier/Academic Press.
665 Andree, K.B., Fernandez-Tejedor, M., Elandaloussi, L.M., Quijano-Scheggia, S., Sampedro, N.,
666 Garces, E., Camp, J., Diogene, J., 2011. Quantitative PCR Coupled with Melt Curve Analysis

667 for Detection of Selected Pseudo-nitzschia spp. (Bacillariophyceae) from the Northwestern
668 Mediterranean Sea. Applied and Environmental Microbiology 77, 1651-1659.
669 Bates, S. S. 1998. Ecophysiology and metabolism of ASP toxin production, p. 405–426. In D. M.
670 Anderson, A. D. Cembella and G. M. Hallegraeff [eds.], Physiological ecology of harmful
671 algal blooms. Springer-Verlag.
672 Barone, R., 2007. Behavioural trait of Ostreopsis ovata (Dinophyceae) in Mediterranean rock
673 pools: the spider's strategy. Harmful Algae News 33: 1–3. 25.
674 Biré, R., Trotereau, S., Lemee, R., Delpont, C., Chabot, B., Aumond, Y., Krys, S., 2013.
675 Occurrence of palytoxins in marine organisms from different trophic levels of the French
676 Mediterranean coast harvested in 2009. Harmful Algae 28, 10-22.
677 Bravo, I., Vila, M., Casablanca, S., Rodriguez, F., Rial, P., Riobo, P., Penna, A., 2012. Life cycle
678 stages of the benthic palytoxin-producing dinoflagellate Ostreopsis cf. ovata (Dinophyceae).
679 Harmful Algae 18, 24-34.
680 Ciminiello, P., Dell'Aversano, C., Dello Iacovo, E., Fattorusso, E., Forino, M., Tartaglione, L.,
681 Battocchi, C., Crinelli, R., Carloni, E., Magnani, M., Penna, A., 2012. Unique Toxin Profile
682 of a Mediterranean Ostreopsis cf. ovata Strain: HR LC-MSn Characterization of Ovatoxin-f, a
683 New Palytoxin Congener. Chemical Research in Toxicology 25, 1243-1252.
684 Ciminiello, P., Dell'Aversano, C., Dello Iacovo, E., Fattorusso, E., Forino, M., Tartaglione, L.,
685 2011. LC-MS of palytoxin and its analogues: State of the art and future perspectives. Toxicon
686 57, 376-389.
687 Ciminiello, P., Dell'Aversano,C., Dello Iacovo, E., Fatturosso, E., Forino, M., Grauso, L.,
688 Targlione, L., Guerrini, F., Pistocchi, R., 2010. Complex palytoxin-like profile of Ostreopsis

689 ovata. Identification of four new ovatoxins by high-resolution liquid chromatography/mass
690 spectrometry. Rapid Commun. Mass Spectrom. 24, 2735-2744.
691 Ciminiello, P., Dell'Aversano, C., Fattorusso, E., Forino, M., Tartaglione, L., Grillo, C.,
692 Melchiorre, N., 2008. Putative palytoxin and its new analogue, ovatoxin-a, in Ostreopsis
693 ovata collected along the Ligurian coasts during the 2006 toxic outbreak. J. Am. Soc. Mass
694 Spectrom. 19, 111-120.
695 Ciminiello, P., Dell'Aversano, C., Fattorusso, E., Forino, M., Magno, G.S., Tartaglione, L.,
696 Grillo, C., Melchiorre, N., 2006. The Genoa 2005 outbreak. Determination of putative
697 palytoxin in Mediterranean Ostreopsis ovata by a new liquid chromatography tandem mass
698 spectrometry method. Analytical Chemistry 78, 6153-6159.
699 Cohu, S., Thibaut, T., Mangialajo, L., Labat, J.P., Passafiume, O., Blanfune, A., Simon, N.,
700 Cottalorda, J.M., Lemee, R., 2011. Occurrence of the toxic dinoflagellate Ostreopsis cf. ovata
701 in relation with environmental factors in Monaco (NW Mediterranean). Marine Pollution
702 Bulletin 62, 2681-2691.
703 David, H., Laza-Martinez, A., Miguel, I., Orive, E., 2013. Ostreopsis cf. siamensis and
704 Ostreopsis cf. ovata from the Atlantic Iberian Peninsula: Morphological and phylogenetic
705 characterization. Harmful Algae 30, 44-55.
706 Granćli, E., Vidyarathna, N.K., Funari, E., Cumaranatunga, P.R.T., Sccnati, R., 2011. Can
707 increases in temperature stimulate blooms of the toxic benthic dinoflagellate Ostreopsis
708 ovata? Harmful Algae In Press, Corrected Proof.
709 Grzebyk, D., Bechemin, C., Ward, C.J., Verite, C., Codd, G.A., Maestrini, S.Y., 2003. Effects of
710 salinity and two coastal waters on the growth and toxin content of the dinoflagellate
711 Alexandrium minutum. Journal of Plankton Research 25, 1185-1199.

712 Guerrini, F., Pezzolesi, L., Feller, A., Riccardi, M., Ciminiello, P., Dell'Aversano, C.,
713 Tartaglione, L., Dello Iacovo, E., Fattorusso, E., Forino, M., Pistocchi, R., 2010. Comparative
714 growth and toxin profile of cultured Ostreopsis ovata from the Tyrrhenian and Adriatic Seas.
715 Toxicon 55, 211-220.
716 Guillard, R.R.L., 1975, Culture of Phyto Plankton for Feeding Marine Invertebrates. Smith,
717 Walter L. and Matoira H. Chanley, pp. 29-60.
718 Habermann, E., Ahnerthilger, G., Chhatwal, G.S., Beress, L., 1981. Delayed Hemolytic Action
719 of Palytoxin General-Characteristics. Biochimica Et Biophysica Acta 649, 481-486.
720 Hall TA., 1999. BioEdit, a user-friendly biological sequence alignment editor and analysis
721 program for Windows 95/98/NT. Nucleic Acids Symposium Series 41, 95-98.
722 Honsell, G., Bonifacio, A., De Bortoli, M., Penna, A., Battocchi, C., Ciminiello, P.,
723 Dell'Aversano, C., Fattorusso, E., Sosa, S., Yasumoto, T., Tubaro, A., 2013. New Insights on
724 Cytological and Metabolic Features of Ostreopsis cf. ovata Fukuyo (Dinophyceae): A
725 Multidisciplinary Approach. Plos One 8.
726 Hoshaw, R.W., Rosowski, J.R., 1973, Methods for Microscopic Algae. Stein, Janet R., pp. 53-
727 67.
728 Hwang, B.S., Yoon, E.Y., Kim, H.S., Yih, W., Park, J.Y., Jeong, H.J., Rho, J.-R., 2013. Ostreol
729 A: A new cytotoxic compound isolated from the epiphytic dinoflagellate Ostreopsis cf. ovata
730 from the coastal waters of Jeju Island, Korea. Bioorganic & Medicinal Chemistry Letters 23,
731 3023-3027.
732 IPCC. Intergovernmental Panel on Climate Change 2013. Fifth Assessment Report: Cambridge
733 University Press. New York. http:// www.ipcc.ch.

734 Ismael, A., Halim, Y., 2012. Potentially harmful Ostreopsis spp. in the coastal waters of
735 Alexandria - Egypt. Mediterranean Marine Science 13, 208-212.
736 Kang, N.S., Jeong, H.J., Lee, S.Y., Lim, A.S., Lee, M.J., Kim, H.S., Yih, W., 2013. Morphology
737 and molecular characterization of the epiphytic benthic dinoflagellate Ostreopsis cf. ovata in
738 the temperate waters off Jeju Island, Korea. Harmful Algae 27, 98-112. e57291
739 Kimura, M. 1980., A simple method for estimating evolutionary rates of base substitutions
740 through comparative studies of nucleotide sequences. J Mol Evol 16, 111-120.
741 Kruskopf, M., Flynn, K.J., 2006. Chlorophyll content and fluorescence responses cannot be used
742 to gauge reliably phytoplankton biomass, nutrient status or growth rate. New Phytologist 169,
743 525-536.
744 Laza-Martinez, A., Orive, E., Miguel, I., 2011. Morphological and genetic characterization of
745 benthic dinoflagellates of the genera Coolia, Ostreopsis and Prorocentrum from the south-
746 eastern Bay of Biscay. European Journal of Phycology 46, 45-65.
747 Mangialajo, L., Ganzin, N., Accoroni, S., Asnaghi, V., Blanfuné, A., Cabrini, M., Cattaneo-
748 Vietti, R., Chavanon, F., Chiantore, M., Cohu, S., Costa, E., Fornasaro, D., Grossel, H.,
749 Marco-Miralles, F., Masó, M., Reñé, A., Rossi, A.M., Sala, M.M., Thibaut, T., Totti, C., Vila,
750 M., Lemée, R., 2011. Trends in Ostreopsis proliferation along the Northern Mediterranean
751 coasts. Toxicon 57, 408-420.
752 Mangialajo, L., Bertolotto, R., Cattaneo-Vietti, R., Chiantore, M., Grillo, C., Lemee, R.,
753 Melchiorre, N., Moretto, P., Povero, P., Ruggieri, N., 2008. The toxic benthic dinoflagellate
754 Ostreopsis ovata: Quantification of proliferation along the coastline of Genoa, Italy. Marine
755 Pollution Bulletin 56, 1209-1214.

Monti, M., Cecchin, E., 2012. Comparative growth of three strains of Ostreopsis ovata at different light intensities with focus on inter-specific allelopathic interactions. Cryptogamie Algologie 33, 113-119.

Monti, M., Minocci, M., Beran, A., Ivesa, L., 2007. First record of Ostreopsis cfr. ovata on macroalgae in the Northern Adriatic Sea. Marine Pollution Bulletin 54, 598-601.

Nascimento, S.M., Correa, E.V., Menezes, M.n., Varela, D., Paredes, J., Morris, S., 2012a. Growth and toxin profile of Ostreopsis cf. ovata (Dinophyta) from Rio de Janeiro, Brazil. Harmful Algae 13, 1-9.

Nascimento, S.M., Franca, J.V., Goncalves, J.E.A., Ferreira, C.E.L., 2012b. Ostreopsis cf. ovata (Dinophyta) bloom in an equatorial island of the Atlantic Ocean. Marine Pollution Bulletin 64, 1074-1078.

Parsons, M.L., Aligizaki, K., Bottein, M.-Y.D., Fraga, S., Morton, S.L., Penna, A., Rhodes, L., 2012. Gambierdiscus and Ostreopsis: Reassessment of the state of knowledge of their taxonomy, geography, ecophysiology, and toxicology. Harmful Algae 14, 107-129.

Parsons, M.L., Preskitt, L.B., 2007. A survey of epiphytic dinoflagellates from the coastal waters of the island of Hawai'i. Harmful Algae 6, 658-669.

Penna, A., Fraga, S., Battocchi, C., Casabianca, S., Perini, F., Capellacci, S., Casabianca, A., Riobo, P., Giacobbe, M.G., Totti, C., Accoroni, S., Vila, M., Rene, A., Scardi, M., Aligizaki, K., Nguyen-Ngoc, L., Vernesi, C., 2012. Genetic diversity of the genus Ostreopsis Schmidt: phylogeographical considerations and molecular methodology applications for field detection in the Mediterranean Sea. Cryptogamie Algologie 33, 153-163.

777 Penna, A., Fraga, S., Battocchi, C., Casabianca, S., Giacobbe, M.G., Riobo, P., Vernesi, C.,
778 2010. A phylogeographical study of the toxic benthic dinoflagellate genus Ostreopsis
779 Schmidt. Journal of Biogeography 37, 830-841.
780 Penna, A., Vila, M., Fraga, S., Giacobbe, M.G., Andreoni, F., Riobo, P., Vernesi, C., 2005.
781 Characterization of Ostreopsis and Coolia (Dinophyceae) isolates in the western
782 Mediterranean Sea based on morphology, toxicity and internal transcribed spacer 5.8s rDNA
783 sequences. Journal of Phycology 41, 212-225.
784 Pezzolesi, L., Guerrini, F., Ciminiello, P., Dell'Aversano, C., Dello Iacovo, E., Fattorusso, E.,
785 Forino, M., Tartaglione, L., Pistocchi, R., 2012. Influence of temperature and salinity on
786 Ostreopsis cf. ovata growth and evaluation of toxin content through HR LC-MS and
787 biological assays. Water Research 46, 82-92.
788 Pfannkuchen, M., Godrijan, J., Pfannkuchen, D.M., Ivesa, L., Kruzic, P., Ciminiello, P.,
789 Dell'Aversano, C., Dello Iacovo, E., Fattorusso, E., Forino, M., Tartaglione, L., Godrijan, M.,
790 2012. Toxin-Producing Ostreopsis cf. ovata are Likely to Bloom Undetected along Coastal
791 Areas. Environmental Science & Technology 46, 5574-5582.
792 Pin, L.C., Teen, L.P., Ahmad, A., Usup, G., 2001. Genetic diversity of Ostreopsis ovata
793 (Dinophyceae) from Malaysia. Marine Biotechnology 3, 246-255.
794 Pistocchi, R., Pezzolesi, L., Guerrini, F., Vanucci, S., Dell'Aversano, C., Fattorusso, E., 2011. A
795 review on the effects of environmental conditions on growth and toxin production of
796 Ostreopsis ovata. Toxicon 57, 421-428.
797 Raven, J.A., Beardall, J., 2006. Chlorophyll fluorescence and ecophysiology: seeing red? New
798 Phytologist 169, 449-451.

799 Rhodes, L.L., Smith, K.F., Munday, R., Selwood, A.I., McNabb, P.S., Holland, P.T., Bottein,
800 M.-Y., 2011. Toxic dinoflagellates (Dinophyceae) from Rarotonga, Cook Islands. Toxicon 56,
801 751-758.
802 Riobo, P., Franco, J.M., 2011. Palytoxins: Biological and chemical determination. Toxicon 57,
803 368-375.
804 Riobo, P., Paz, B., Franco, J.M., Vazquez, J.A., Murado, M.A., 2008. Proposal for a simple and
805 sensitive haemolytic assay for palytoxin Toxicological dynamics, kinetics, ouabain inhibition
806 and thermal stability. Harmful Algae 7, 415-429.
807 Sato, S., Nishimura, T., Uehara, K., Sakanari, H., Tawong, W., Hariganeya, N., Smith, K.,
808 Rhodes, L., Yasumoto, T., Taira, Y., Suda, S., Yamaguchi, H., Adachi, M., 2011.
809 Phylogeography of Ostreopsis along West Pacific Coast, with Special Reference to a Novel
810 Clade from Japan. Plos One 6, e27983.
811 Scalco, E., Brunet, C., Marino, F., Rossi, R., Soprano, V., Zingone, A., Montresor, M., 2012.
812 Growth and toxicity responses of Mediterranean Ostreopsis cf. ovata to seasonal irradiance
813 and temperature conditions. Harmful Algae 17, 25-34.
814 Schmidt, I., 1901. Flora of Koh Chang, contributions to the knowledge of the vegetation in the
815 Gulf of Siam Peridinales. Botanisk Tidkrift 24, 212-221.
816 Silva, E.S., Faust, M.A., 1995. Small-Cells in the Life-History of Dinoflagellates (Dinophyceae)
817 - a Review. Phycologia 34, 396-408.
818 Suzuki, T., Watanabe, R., Uchida, H., Matsushima, R., Nagai, H., Yasumoto, T., Yoshimatsu, T.,
819 Sato, S., Adachi, M., 2012. LC-MS/MS analysis of novel ovatoxin isomers in several
820 Ostreopsis strains collected in Japan. Harmful Algae 20, 81-91.

821 Tanimoto, Y., Yamaguchi, H., Yoshimatsu, T., Sato, S., Adachi, M., 2013. Effects of
822 temperature, salinity and their interaction on growth of toxic Ostreopsis sp 1 and Ostreopsis
823 sp 6 (Dinophyceae) isolated from Japanese coastal waters. Fisheries Science 79, 285-291.
824 Totti, C., Accoroni, S., Cerino, F., Cucchiari, E., Romagnoli, T., 2010. Ostreopsis ovata bloom
825 along the Conero Riviera (northern Adriatic Sea): Relationships with environmental
826 conditions and substrata. Harmful Algae 9, 233-239.
827 Utermöhl H., 1958. Zur Vervollkomnung der quantitativen Phytoplankton-Methodik. Mitt. int.
828 Ver. ther. angew. Limnol 9, 1-38.
829 Utermöhl. H., 1931. Neue Wege in der quantitativen Erfassung des Planktons (mit besonderer
830 Berücksichtigung des Ultraplanktons). Verh. int. Ver. theor. angew. Limnol 5, 567-596.
831 Vanucci, S., Guerrini, F., Pezzolesi, L., Dell'Aversano, C., Ciminiello, P., Pistocchi, R., 2012a.
832 Cell growth and toxins' content of Ostreopsis cf. ovata in presence and absence of associated
833 bacteria. Cryptogamie Algologie 33, 105-112.
834 Vanucci, S., Pezzolesi, L., Pistocchi, R., Ciminiello, P., Dell'Aversano, C., Dello Iacovo, E.,
835 Fattorusso, E., Tartaglione, L., Guerrini, F., 2012b. Nitrogen and phosphorus limitation
836 effects on cell growth, biovolume, and toxin production in Ostreopsis cf. ovata. Harmful
837 Algae 15, 78-90.
838 Vidyarathna, N.K., Grancli, E., 2013. Physiological rcsponscs of Ostrcopsis ovata to changcs in
839 N and P availability and temperature increase. Harmful Algae 21-22, 54-63.
840 Vidyarathna, N.K., Granéli, E., 2011. Influence of temperature on growth, toxicity and
841 carbohydrate production of a Japanese Ostreopsis ovata strain, a toxic-bloom-forming
842 dinoflagellate. Aquatic Microbial Ecology 65, 261-270.

Vila, M., Garces, E., Maso, M., 2001. Potentially toxic epiphytic dinoflagellate assemblages on macroalgae in the NW Mediterranean. Aquatic Microbial Ecology 26, 51-60.

Yamaguchi, H., Tanimoto, Y., Yoshimatsu, T., Sato, S., Nishimura, T., Uehara, K., Adachi, M., 2012a. Culture method and growth characteristics of marine benthic dinoflagellate Ostreopsis spp. isolated from Japanese coastal waters. Fisheries Science 78, 993-1000.

Yamaguchi, H., Yoshimatsu, T., Tanimoto, Y., Sato, S., Nishimura, T., Uehara, K., Adachi, M., 2012b. Effects of temperature, salinity and their interaction on growth of the benthic dinoflagellate Ostreopsis cf. ovata (Dinophyceae) from Japanese coastal waters. Phycological Research 60, 297-304.

853 **Caption List**

854

855 **Table 1** Results obtained from the difference between the relative standard deviation (RSD) and
856 Poisson distribution (λ) of three settlement countings. Bold values indicate negative results, thus
857 not an acceptable enumeration estimation by the Utermöhl method.

858 **Fig. 1** Growth curves of *O.* cf. *ovata* strains IRTA-SMM-11-09 and IRTA-SMM-11-10 grown at
859 nine different conditions of temperature (A. 19°C; B. 24°C; C. 28°C) and salinity during sixteen
860 days. Error bars represent two standard deviation, n=9.

861 **Fig. 2** Growth rate (div.day^{-1}) of *O.* cf. *ovata* strains IRTA-SMM-11-09 and IRTA-SMM-11-10
862 grown at nine different conditions of temperature and salinity during sixteen days. Error bars
863 represent two standard deviation, n=3

864 **Fig 3 a**. Morphology of *O.* cf. *ovata*. **a**. Aberrant cell from IRTA-SMM-11-09 in exponential
865 phase at 19°C salinity 36 culture; **b**. Cell with wide W diameter from IRTA-SMM-11-09 in
866 stationary phase at 24°C, salinity 36 culture; **c**. Field *O.* cf. *ovata* cell from 40° 50' 47.8242" N;
867 0° 45' 44.9532" E in August 2013; **d**.. Example of large and small cells from IRTA-SMM-11-10
868 in exponential phase at 28°C, salinity 38 culture.

869 **Fig 4.** Size variability of *O.* cf. *ovata* for cultures at 24 and 28ºC (n=3863). Histogram every 1
870 µm in **A.** dorsoventral (DV) diameter and **B**. width (W) diameter for all condition at 24 and
871 28°C for both strains.

872 **Fig 5.** Percentage of number of small cells, DV≤35 µm, (bright grey) and big cells, DV>35µm
873 (dark grey) during growth phases in a all conditions for **A**. IRTA-SMM-11-09 and **B**. IRTA-
874 SMM-11-09

875 **Fig. 6** PLTX-like content (pg PLTX eq.cell^{-1}) of *O.* cf. *ovata* IRTA-SMM-11-09 (dark grey) and
876 IRTA-SMM-11-10 (bright grey) strains grown under different conditions of temperature and

877 salinity estimated with haemolytic assay. Error bars represent one standard deviation from the
878 average of three wells result from haemolytic assay.

879 **Fig. 7** Relative abundance (in percentage) of the palytoxin-like compounds produced by two
880 strains of *Ostreopsis cf. ovata* in the post-exponential growth phase. Average of six cultures
881 (n=6) under two temperatures (24ºC and 28ºC) and three salinities (32, 36, 38). Temperature and
882 salinity did not have any effect on the toxin profile. pPLTX = putative palytoxin; OVTX-a =
883 ovatoxin-a; OVTX-b = ovatoxin-b; OVTX-c = ovatoxin-c; OVTX-d&-e = sum of ovatoxin-d
884 and ovatxin-e (these last two compounds did not achieve complete chromatographic separation).

885

886 **Supplementary materials**

887 **Table S1** HRMS data of putative palytoxin (pPLTX), and ovatoxins –a to –e (OVTX-a, -b, -c, -
888 d&-e) obtained from full MS spectra in the mass range m/z 700-1400 on a LTQ Orbitrap XL® (Resolution 60,000 FWHM). Retention times (RT), molecular formulae and relative double bonds equivalents (RDB) of the mono-isotopic peak of the most intense bi-charged ($[M+2H-H_2O]^{2+}$) and tri-charged ($[M+H+Ca]^{3+}$) ions in the full MS spectra of the samples of the *multi-factorial* experiment (temperatures 24 and 28ºC; salinity 32, 36 and 36) with two strains of *Ostreopsis* cf. *ovata* (IRTA-SMM-11-09 and IRTA-SMM-11-10) collected in the post-exponential phase. Found *m/z* related to those ions and mass error (in ppm) associated with the molecular formulae are provided.

896 **Fig 1 S1** Haemolytic assay exponential calibration curve without ouabain (dotted line) and with
897 ouabain (crosses).

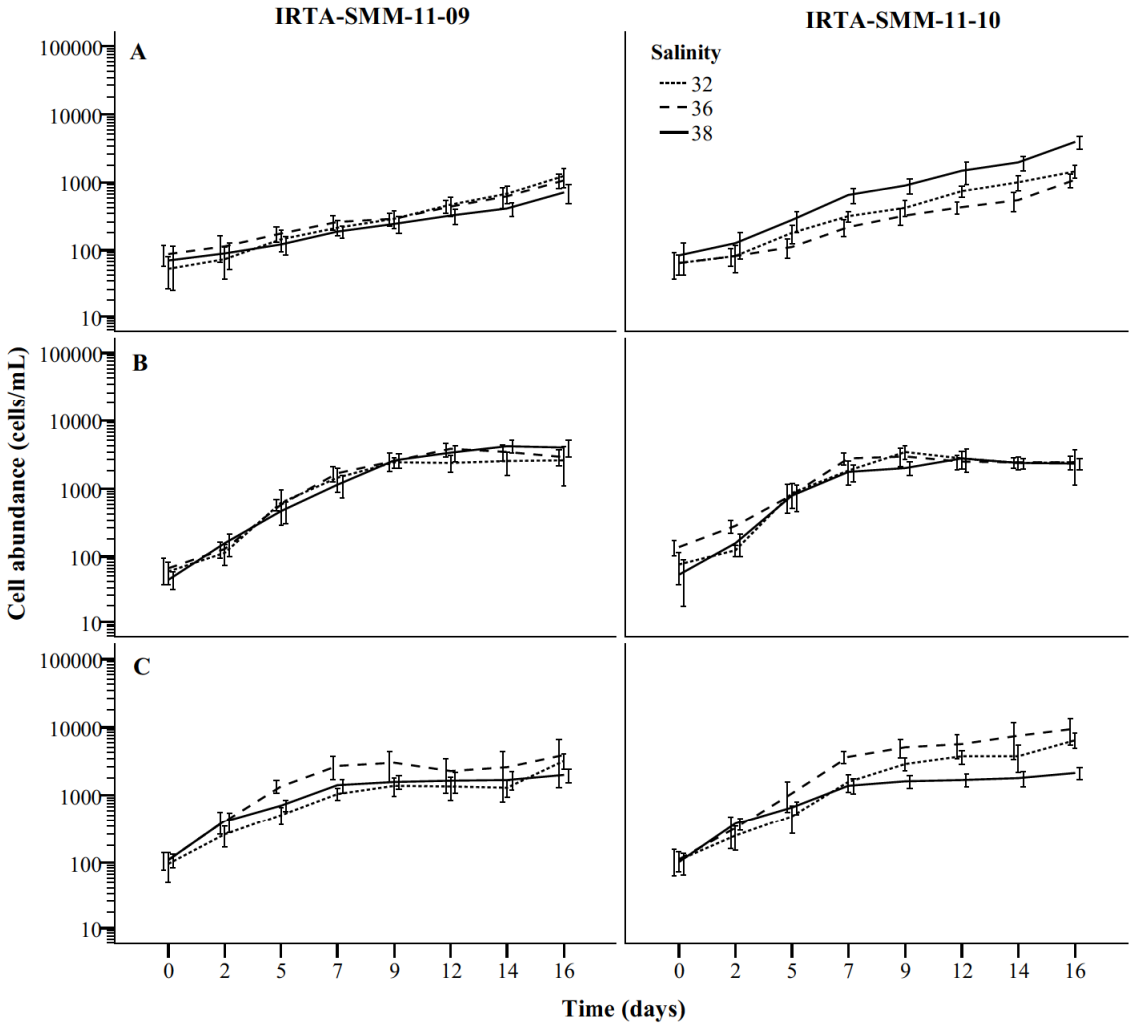
IRTA-SMM-11-09
IRTA-SMM-11-10
Salinity
32
36
38
A
B
C
Cell abundance (cells/mL)
100000
10000
1000
100
10
0
2
5
7
9
12
14
16
Time (days)

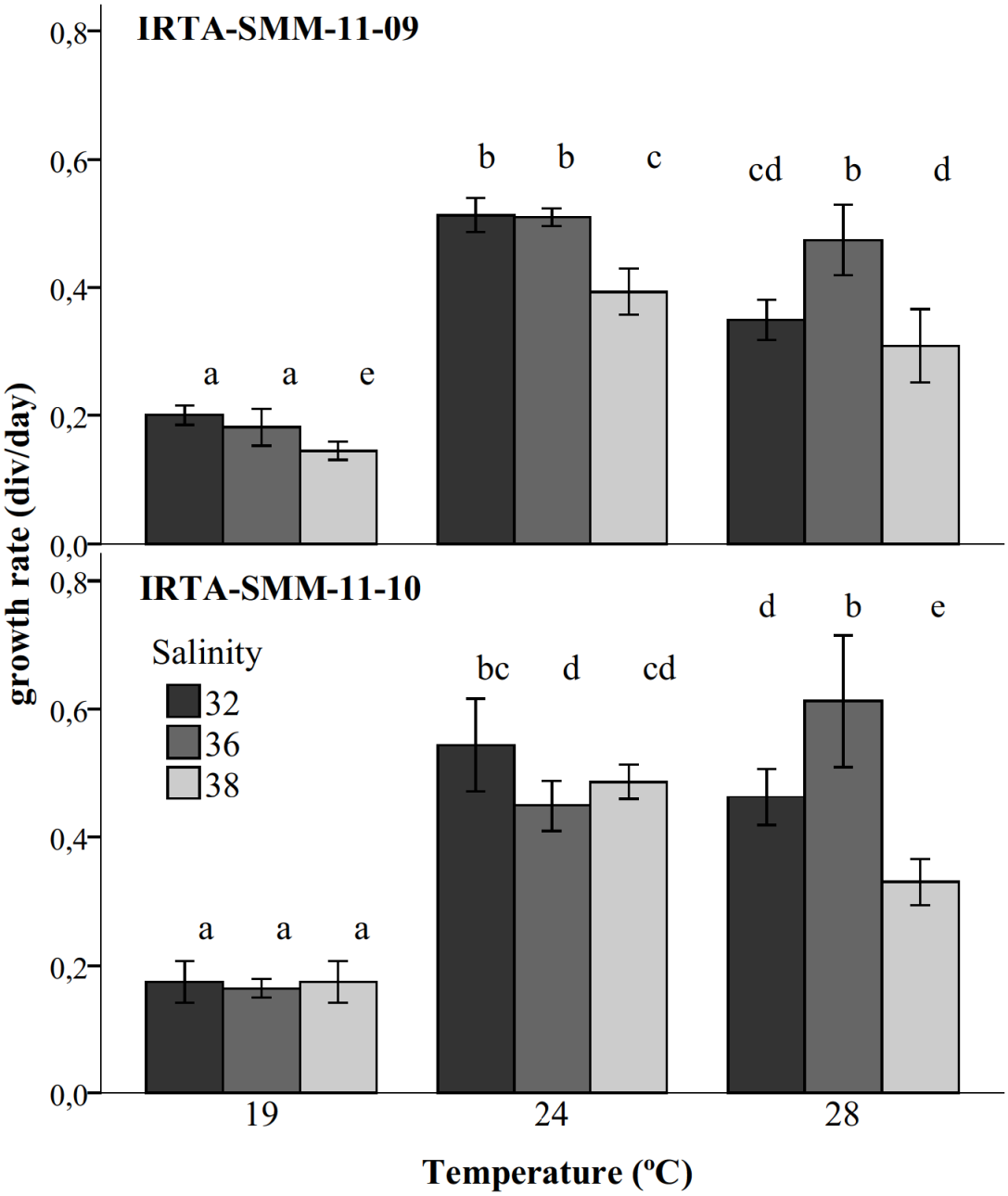
IRTA-SMM-11-09
IRTA-SMM-11-10
growth rate (div/day)
0,0
0,2
0,4
0,6
0,8
a a e
b b c
cd b d
a a a
bc d cd
d b e
Salinity
32
36
38
19
24
28
Temperature (ºC)

UNIVERSITAT ROVIRA I VIRGILI
IMPROVEMENTS IN LIQUID CHROMATOGRAPHY COUPLED TO MASS SPECTROMETRY METHODS FOR THE DETERMINATION OF LEGISLATED AND EMERGING MARINE TOXINS IN THE NORTHWEST MEDITERRANEAN COAST
María García Altares Pérez
Dipòsit Legal: T 330-2016

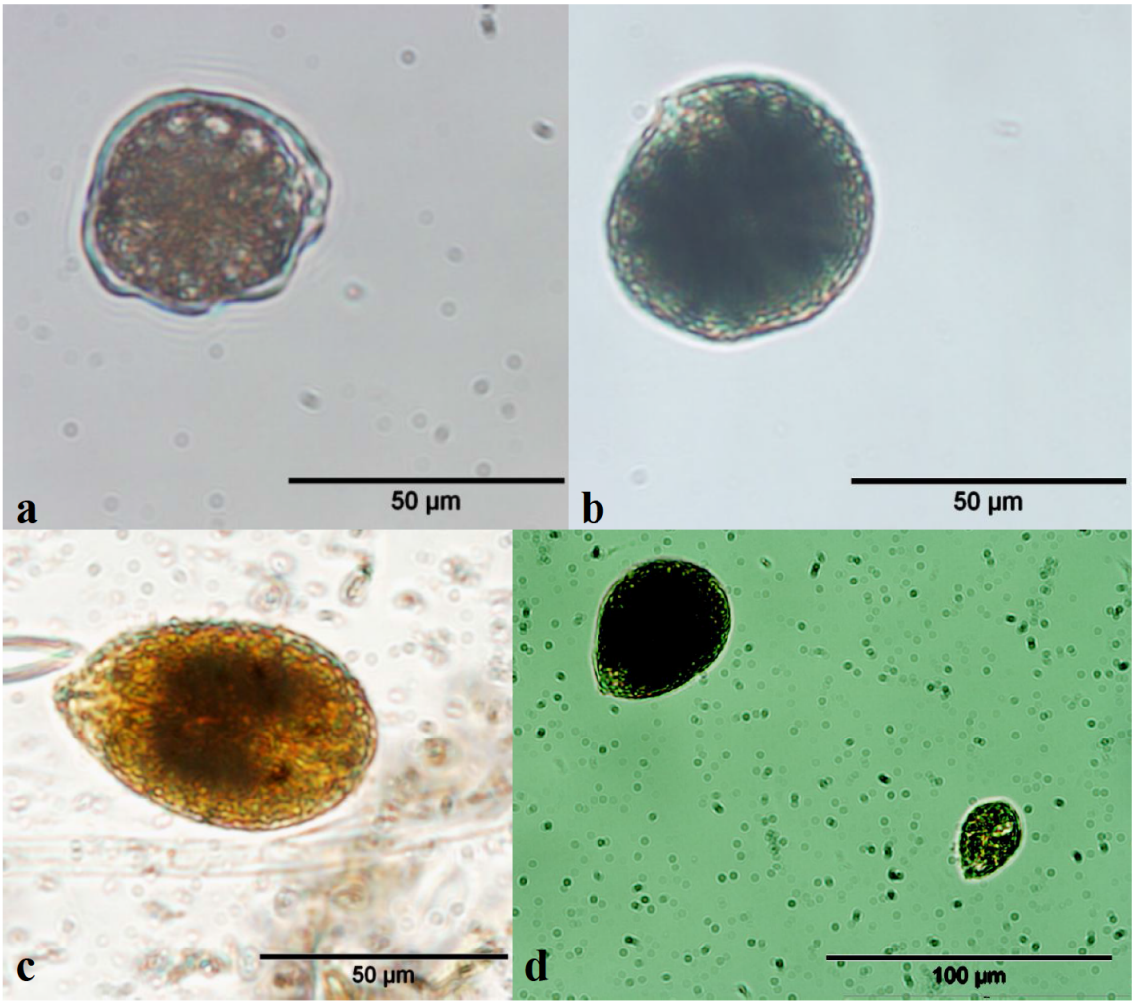

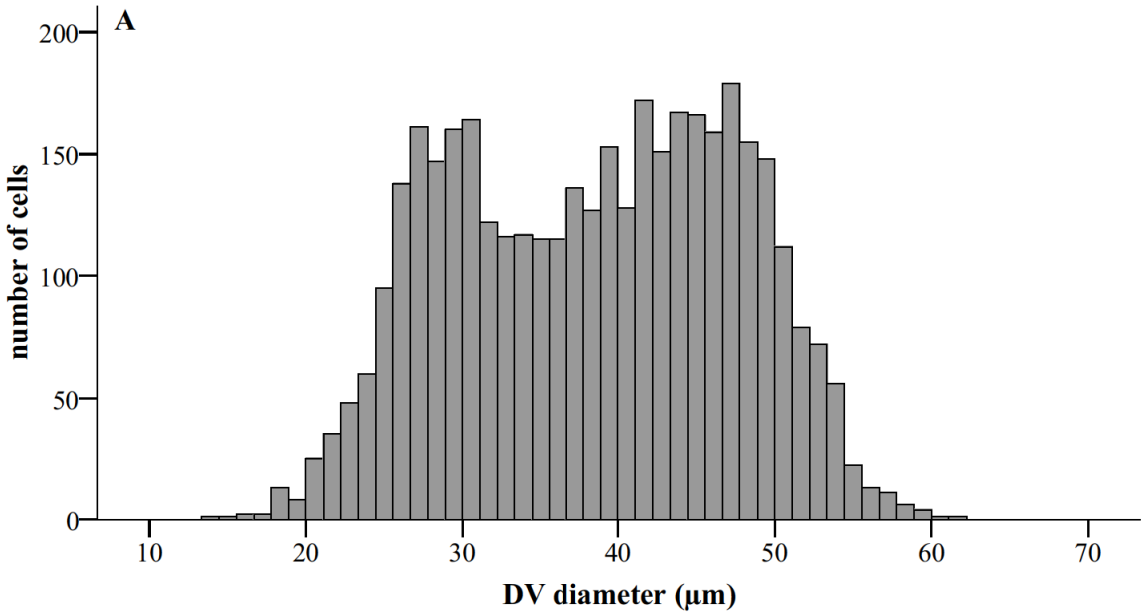
A
number of cells
DV diameter (µm)

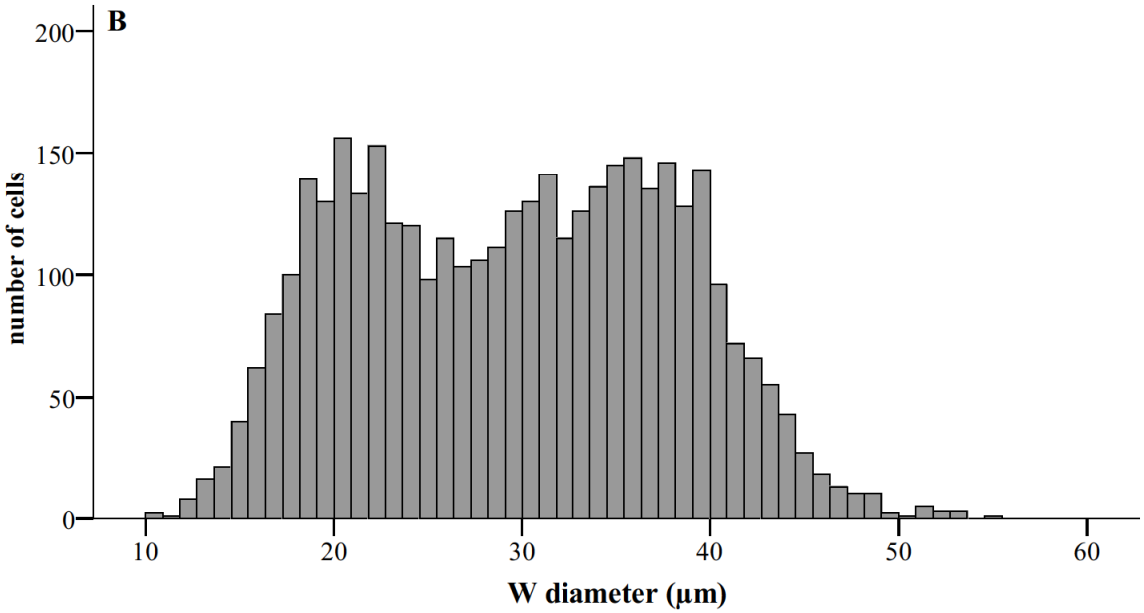
B
number of cells
W diameter (µm)

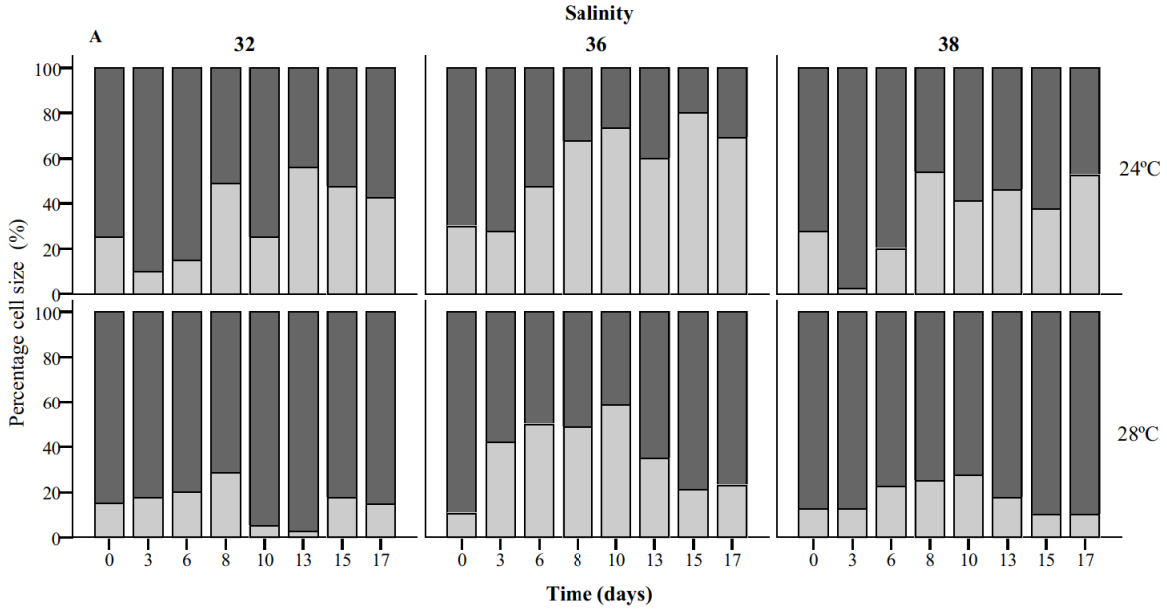

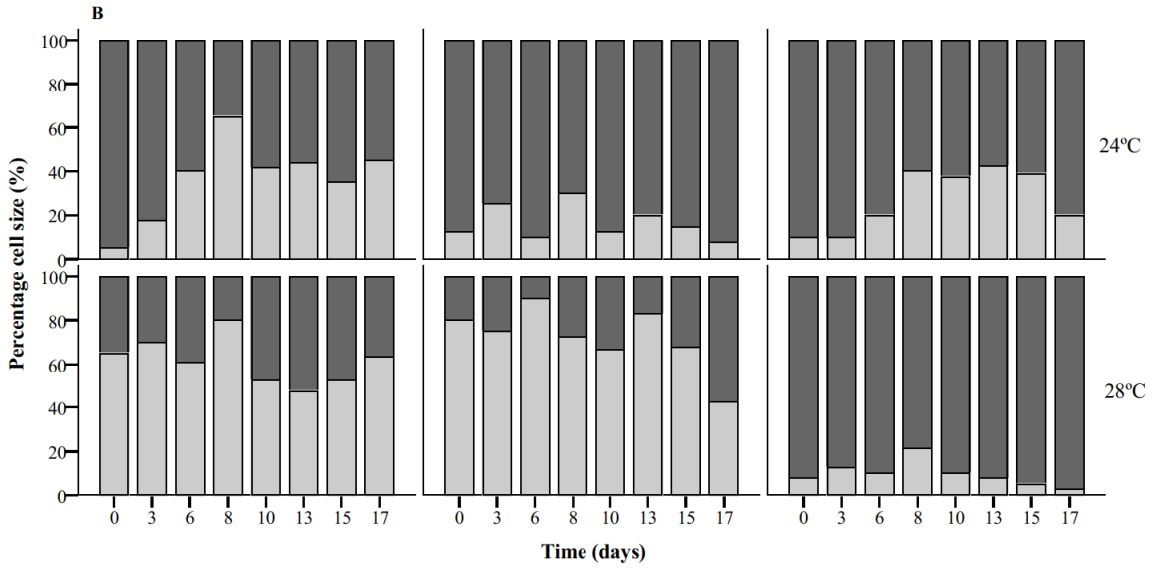

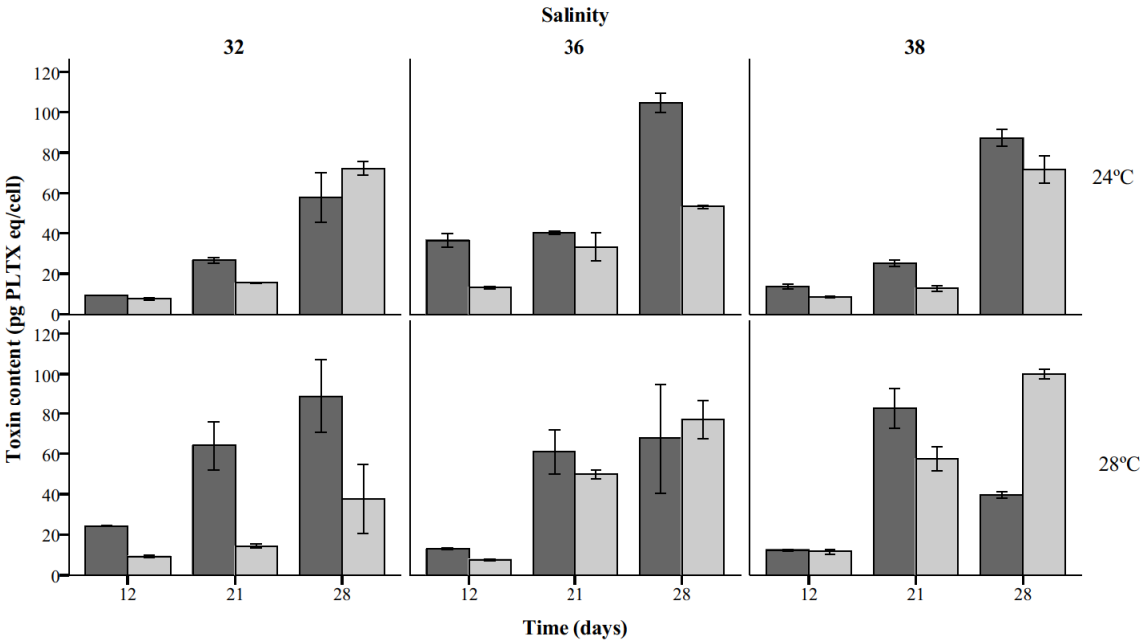

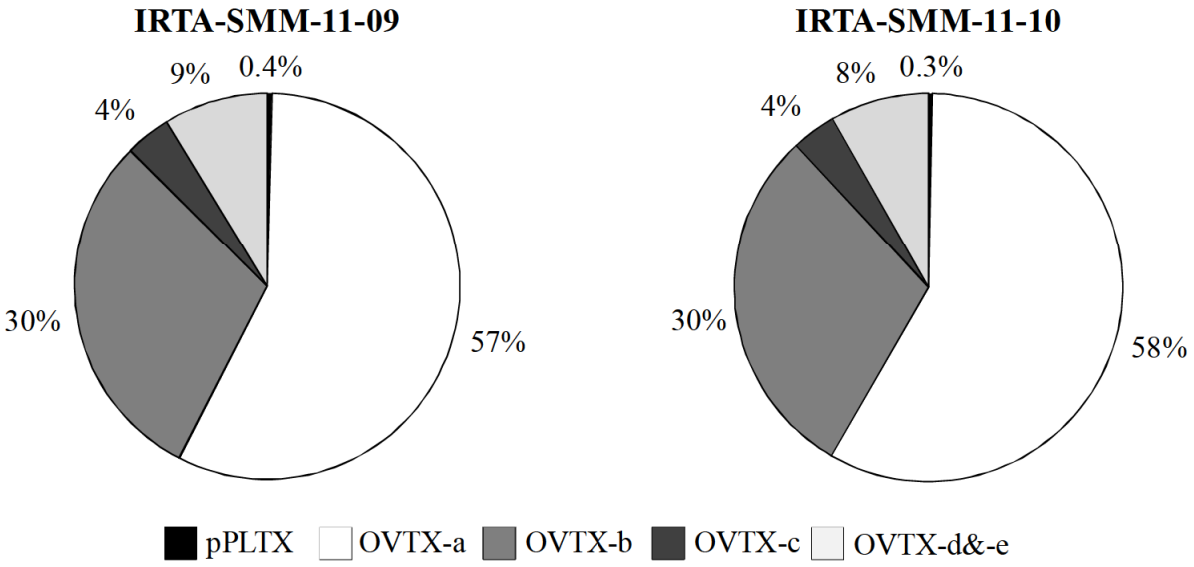

UNIVERSITAT ROVIRA I VIRGILI
IMPROVEMENTS IN LIQUID CHROMATOGRAPHY COUPLED TO MASS SPECTROMETRY METHODS FOR THE DETERMINATION OF LEGISLATED AND EMERGING MARINE TOXINS IN THE NORTHWEST MEDITERRANEAN COAST
María García Altares Pérez
Dipòsit Legal: T 330-2016

	Sample volume (mL)	Settling volume (mL)	Control				HCl treatment				Na-EDTA treatment			
			Average	Triplicates			Average	Triplicates			Average	Triplicates		
Exp 1	3	0.5	***-3.3***	**-2.8**	**-0.1**	**-6.0**	***-6.5***	0.8	3.6	**-9.8**	*1.4*	3.2	6.4	**-0.9**
	5	0.5	***-2.1***	1.9	1.3	**-4.2**	***-3.3***	**-1.8**	2.2	**-7.3**	***-2.1***	0.9	5.6	4.9
	20	0.5	***-6.5***	5.3	**-7.8**	**-4.2**	***-0.1***	**-0.6**	**-6.3**	**-2.8**	*0.9*	3.2	8.2	5.9
	12	3	*1.6*	9.0	6.8	0.3	***-0.2***	6.8	**-2.5**	1.4	*2.4*	2.5	5.8	**-1.0**
	20	3	*3.6*	5.9	**-0.2**	2.0	*4.8*	0.4	9.5	6.5	*4.2*	9.5	2.5	6.0
Exp 2	3	0.5	*9*	10.5	6.9	12.2	*9.6*	13.0	12.0	11.6	*4.5*	11.2	8.6	12.2
	5	0.5	*5.2*	3.3	11.6	3.4	*3.2*	**-5.1**	8.9	13.5	*4*	2.2	6.1	8.3
	12	0.5	***-0.2***	7.7	0.0	**-1.5**	*7.1*	**-0.2**	10.6	12.2	*0*	4.2	9.4	5.7
	20	0.5	***-0.9***	2.4	9.4	9.6	*4.2*	9.0	8.6	9.8	*7.6*	15.4	2.0	8.2
	12	3	*0.8*	2.0	2.3	**-4.7**	*2.5*	6.1	2.6	2.3	*0.6*	7.3	4.2	1.5
	20	3	*3.2*	5.6	4.0	7.9	*3.4*	3.7	0.0	6.0	*3.6*	6.8	**-1.1**	6.1

	pPLTX RT=8.6-8.9 min		OVTX-a RT=11.2-11.7 min		OVTX-b RT=10.56-10.95		OVTX-c RT=9.11-9.46		OVTX-d&-e RT=9.77-10.35	
	$[M+H+Ca]^{2+}$ $C_{129}H_{224}O_{54}N_3Ca$ RDB 19.5	$[M+2H-H_2O]^{2+}$ $C_{129}H_{223}O_{53}N_3$ RDB 20	$[M+H+Ca]^{2+}$ $C_{129}H_{224}O_{52}N_3Ca$ RDB 19.5	$[M+2H-H_2O]^{2+}$ $C_{129}H_{223}O_{51}N_3$ RDB 20	$[M+H+Ca]^{2+}$ $C_{131}H_{228}O_{53}N_3$ Ca RDB 19.5	$[M+2H-H_2O]^{2+}$ $C_{131}H_{227}O_{52}N_3$ RDB 20	$[M+H+Ca]^{2+}$ $C_{131}H_{228}O_{54}N_3$ Ca RDB 19.5	$[M+2H-H_2O]^{2+}$ $C_{131}H_{227}O_{53}N_3$ RDB 20	$[M+H+Ca]^{2+}$ $C_{129}H_{224}O_{53}N_3Ca$ RDB 19.5	$[M+2H-H_2O]^{2+}$ $C_{129}H_{223}O_{52}N_3$ RDB 20
	m/z found Δ (ppm)	*m/z* found Δ (ppm)	*m/z* found Δ (ppm)	*m/z* found Δ (ppm)	*m/z* found Δ (ppm)	*m/z* found Δ (ppm)	*m/z* found Δ (ppm)	*m/z* found Δ (ppm)	*m/z* found Δ (ppm)	*m/z* found Δ (ppm)
IRTA-SMM-11-09										
Tª 24 Salinity 32	906.4831	Not found	895.8197	1315.2479	910.4953	1337.2612	915.8269	1345.2581	901.1510	1323.2451
	0.32		0.23	0.74	0.37	0.92	0.37	0.46	-0.18	0.56
Tª 24 Salinity 36	906.4837	Not found	895.8197	1315.2474	910.4953	1337.2690	915.8269	1345.2582	901.1513	1323.2452
	1.04		0.199	0.38	0.45	0.61	0.42	0.59	0.13	0.69
Tª 24 Salinity 38	906.4826	Not found	895.8197	1315.2479	910.4952	1337.2608	915.8266	1345.2584	901.1517	1323.2452
	-0.21		0.26	0.77	0.29	0.63	0.04	0.74	0.01	0.63
Tª 28 Salinity 32	906.4826	1331.2426	895.8204	1315.2485	910.4954	1337.2612	915.8269	1345.2567	901.1516	1323.245
	-0.26	0.61	0.96	1.21	0.61	0.92	0.33	-0.53	0.46	0.88
Tª 28 Salinity 36	906.4829	Not found	895.8198	1315.2478	910.4950	1337.2611	915.8273	1345.2593	901.1516	1323.2456
	0.17		0.30	0.71	0.42	0.86	0.83	1.34	0.52	0.97
Tª 28 Salinity 38	906.4823	Not found	895.8194	1315.2473	910.4951	1337.2610	915.8268	1345.2577	901.1508	1323.2444
	-0.51		-0.16	0.35	0.21	0.72	0.24	0.22	-0.41	0.07
IRTA-SMM-11-10										
Tª 24 Salinity 32	906.4831	Not found	895.8196	1315.2474	910.4950	1337.2603	915.8268	1345.2571	901.1515	1323.2452
	0.26		0.12	0.56	0.04	0.35	0.23	-0.35	0.31	0.89
Tª 24 Salinity 36	906.4823	Not found	895.8198	1315.2479	910.4952	1337.2605	915.8268	1345.2579	901.1513	1323.2446
	-0.51		0.28	0.99	0.23	0.52	0.23	0.49	0.14	0.31
Tª 24 Salinity 38	906.4834	Not found	895.8197	1315.2475	910.4953	1337.2610	915.8267	1345.2594	901.1510	1323.2446
	0.57		0.15	0.59	0.35	0.100	0.18	1.98	-0.14	0.23
Tª 28 Salinity 32	906.4830	1331.2423	895.8195	1315.2472	910.4950	1337.2604	915.8268	1345.2581	901.1509	1323.2445
	0.24	0.60	-0.03	0.33	0.08	0.38	0.27	0.67	-0.26	0.19
Tª 28 Salinity 36	906.4826	Not found	895.4871	1315.2481	910.4950	1337.2607	915.8263	1345.2572	901.1510	1323.2451
	-0.20		0.29	1.20	0.10	0.75	-0.21	-0.22	-0.12	0.74
Tª 28 Salinity 38	906.4824	Not found	895.8192	1315.2468	910.4947	1337.2601	915.8264	1345.2590	901.1510	1323.2447
	-0.44		-0.33	-0.05	-0.21	0.16	-0.18	1.55	-0.14	0.39

UNIVERSITAT ROVIRA I VIRGILI
IMPROVEMENTS IN LIQUID CHROMATOGRAPHY COUPLED TO MASS SPECTROMETRY METHODS FOR THE DETERMINATION OF LEGISLATED AND EMERGING MARINE TOXINS IN THE NORTHWEST MEDITERRANEAN COAST
María García Altares Pérez
Dipòsit Legal: T 330-2016

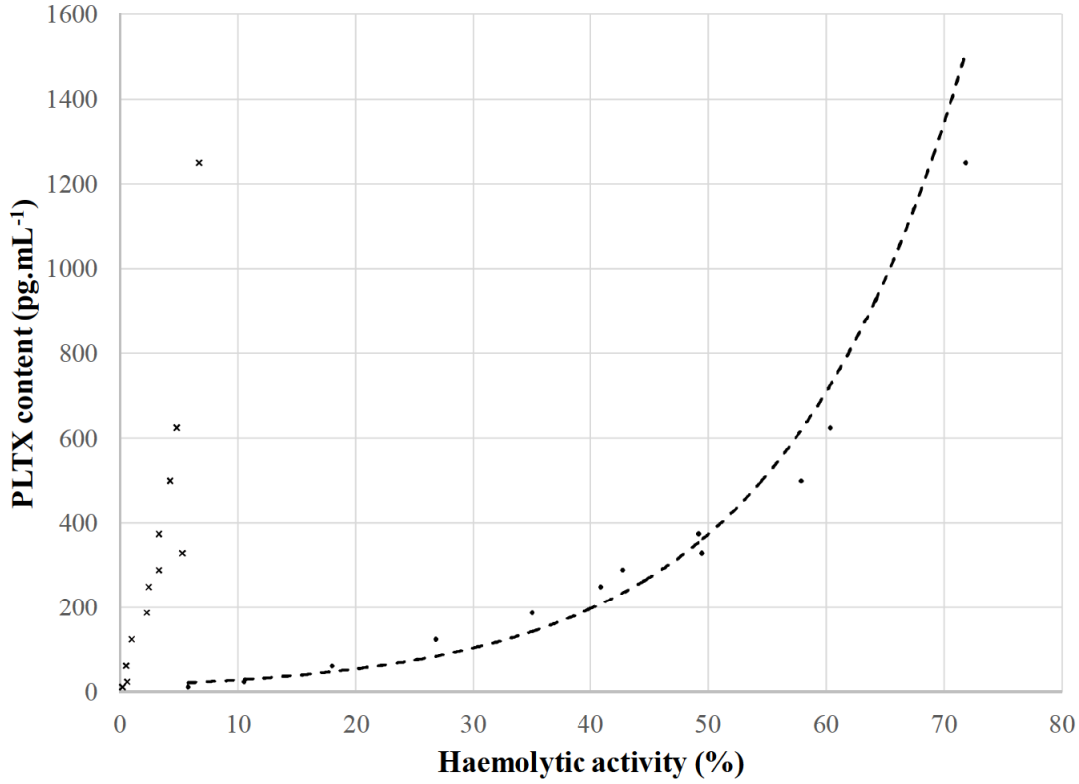

HARMFUL ALGAE

AUTHOR DECLARATION

Submission of an article implies that the work described has not been published previously (except in the form of an abstract or as part of a published lecture or academic thesis), that it is not under consideration for publication elsewhere, that its publication is approved by all authors and tacitly or explicitly by the responsible authorities where the work was carried out, and that, if accepted, it will not be published elsewhere in the same form, in English or in any other language, without the written consent of the copyright-holder.

By attaching this Declaration to the submission, the corresponding author certifies that:

- The manuscript represents original and valid work and that neither this manuscript nor one with substantially similar content under the same authorship has been published or is being considered for publication elsewhere.

- Every author has agreed to allow the corresponding author to serve as the primary correspondent with the editorial office, and to review the edited typescript and proof.

- Each author has given final approval of the submitted manuscript and order of authors. Any subsequent change to authorship will be approved by all authors.

- Each author has participated sufficiently in the work to take public responsibility for all the content.

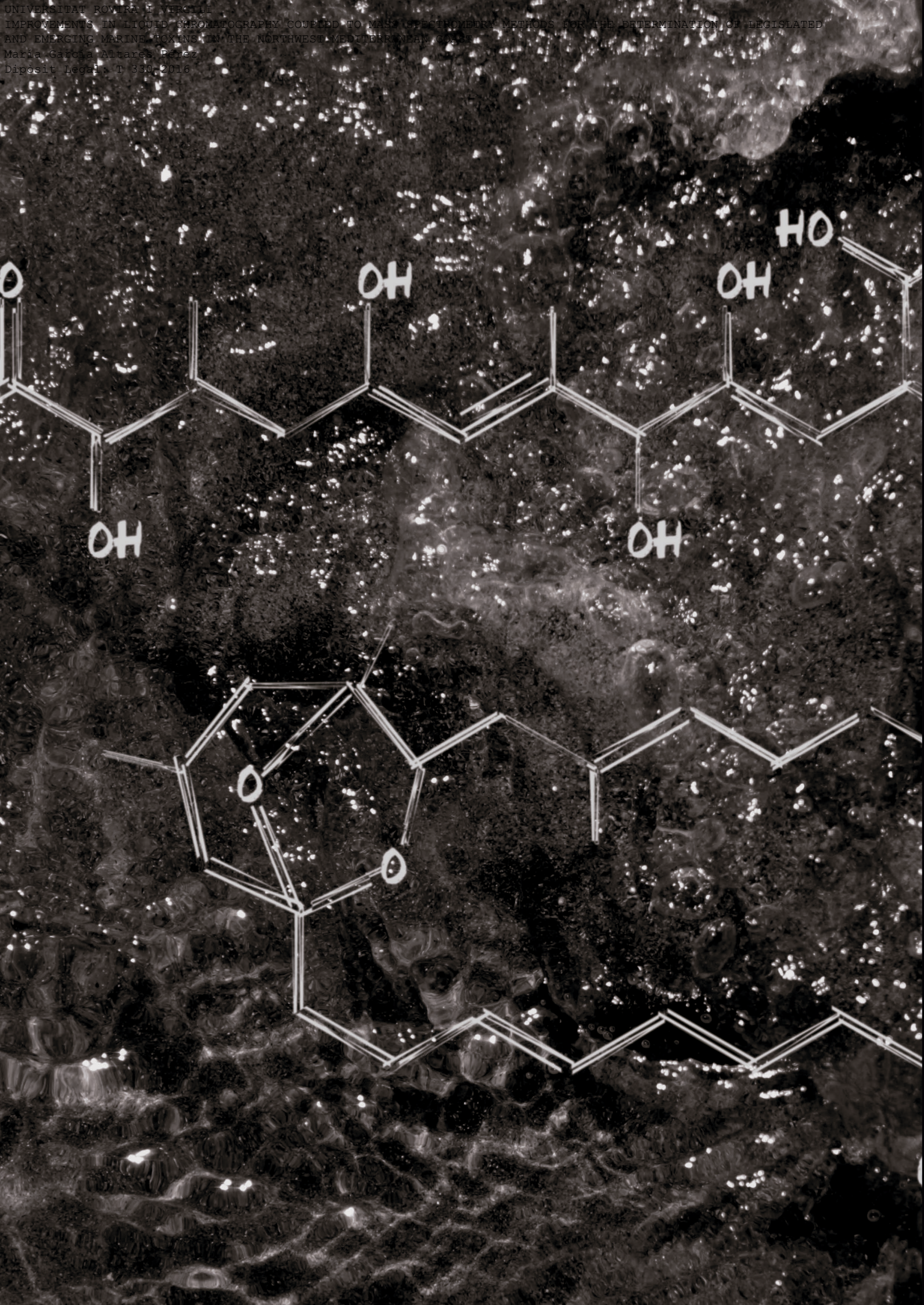

UNIVERSITAT ROVIRA I VIRGILI
IMPROVEMENTS IN LIQUID CHROMATOGRAPHY COUPLED TO MASS SPECTROMETRY METHODS FOR THE DETERMINATION OF LEGISLATED AND EMERGING MARINE TOXINS IN THE NORTHWEST MEDITERRANEAN COAST
María García Altares Pérez
Dipòsit Legal: T 330-2016

Errata

1. Section **Acknowledgements** (page I) should have included the following paragraph:

We also acknowledge the following projects and institutions: the Spanish National Institute for Agriculture and Food Research and Technology (INIA; project code RTA2009-000127-00-00); the ECsafeSEAFOOD: Priority environmental contaminants in seafood: safety assessment, impact and public perception' EU-funded project, Seventh Framework Programme (FP7), KBBE.2012.2.4-01: Contaminants in seafood and their impact on public health (The Ocean of Tomorrow), grant agreement Nº: 311820.2013-2016; INTERREG SUDOE IVB and FEDER through the SOE1/P1/E129 (ALARMTOX project), for covering travel expenses. Moreover, we thank the shellfish monitoring program of Catalonia (Departament d'Agricultura, Ramaderia, Pesca, Alimentació i Medi Natural, Generalitat de Catalunya), and both Drs. P. McCarron and M. A. Quilliam from the National Research Council of Canada for kindly providing ampoules of pre-released Pinnatoxin G standards. The CIT partners would like to acknowledge funding from the EU/INTERREG IIIB Atlantic Area Programme European "PHARMATLANTIC" project 'Knowledge Transfer Network for Prevention of Mental Diseases and Cancer in the Atlantic Area' and the Higher Education Authority (Programme for Research in Third-Level Institutions, Cycle 4 (PRTLI IV) National Collaboration Programme on Environment and Climate Changes: Impacts and Responses for funding the Orbitrap FT-MS instrumentation used in this study. The partners from Federico II di Napoli thank the frame of Programme STAR Linea 1, financially supported by UniNA and Compagnia di San Paolo.

2. Page 56 (Chapter 4) should have included the following figure properly printed:

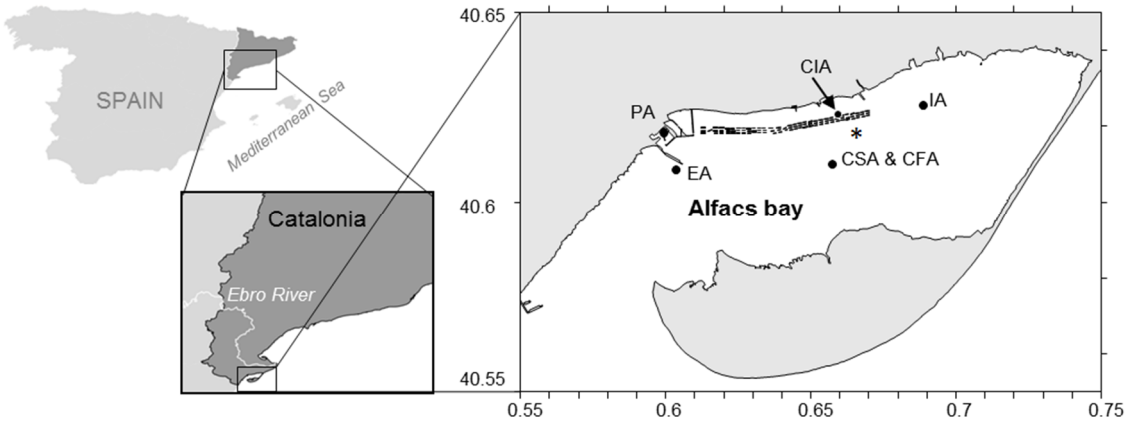

Figure 4-1. Map of Alfacs Bay in the Ebro River Delta (NW Mediterranean). Dots represent sampling stations (PA: Port Alfacs, EA: Exterior Alfacs, CIA: Central Interior Alfacs, CSA & CFA: Central Alfacs, surface (S) and bottom (F), IA: Interior Alfacs, BA: Buoy Alfacs). The star symbol (*) indicates the location of the buoy.

3. Page 36, 37, 64, 65, the symbol Ŷ should have been an μ.
4. Page 96 (Chapter 5), the missing reference should have been Sup. Mat. Table 5-1 and Sup. Mat. Table 5-2.

5. Page 118 (Chapter 6) should have included the following figure properly printed:

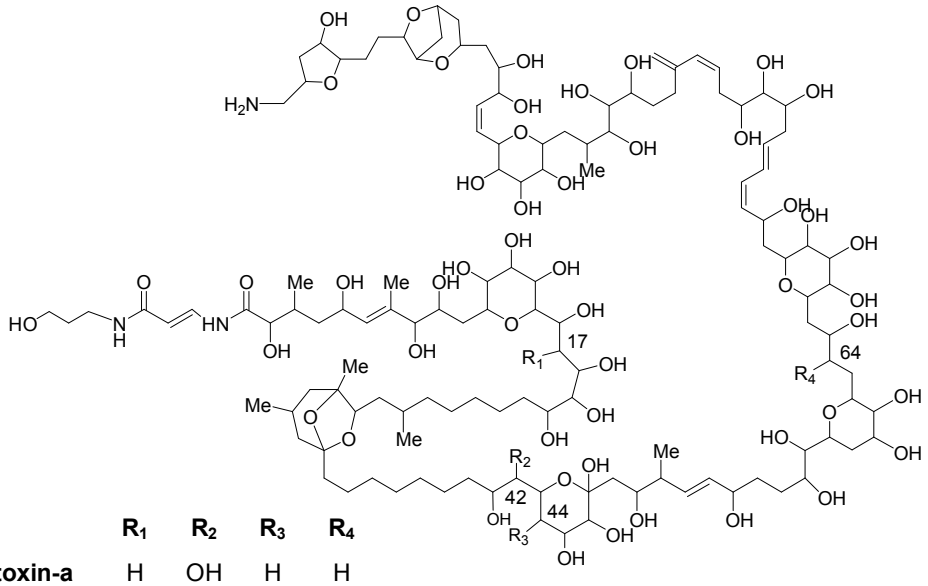

	R_1	R_2	R_3	R_4
Ovatoxin-a	H	OH	H	H
Palytoxin	OH	H	OH	OH

Figure 6-1. Planar structure of palytoxin ($C_{129}H_{223}N_3O_{54}$) from the soft coral *Palythoa tuberculosa* [5, 6] and ovatoxin-a ($C_{129}H_{223}N_3O_{52}$) from the Mediterranean dinoflagellate *Ostreopsis* cf. *ovata* [13, 14] Structure numbering and was performed according to Uemura et al. [6].

6. Page 96 (Chapter 5), the missing reference should have been Sup. Mat. Table 5-1 and Sup. Mat. Table 5-2.